Ultrasonically controlled preparation of functionalised styrene polymers and copolymers

Smith, Paul

Award date:
1991

Awarding institution:
University of Bath

Ultrasonically Controlled Preparation of

Functionalised Styrene Polymers and Copolymers

Submitted by PAUL SMITH

for the degree of PhD

at the University of Bath

1991

Paul Smith.

ProQuest LLC
789 East Eisenhower Parkway
P.O. Box 1346
Ann Arbor, MI 48106-1346

DEDICATION

This thesis is dedicated to the memory of
a very lovely mother, who died 17 March 1991

ACKNOWLEDGEMENTS

I would like to thank Dr G J Price for being not just a superb and omniscient supervisor and bringing chemistry to life, but also for being a really good friend throughout my PhD.

My special thanks go to Peter West - friends like this are hard to find.

To Kevin, Mark and Jane who all gave me more support and friendship over this year than I could ever repay. Thanks for being great.

Julia - thank you for being so understanding and giving me so much help and love.

To all of the research group and technicians who made my life at Bath University so memorable, especially Nick, Andy, Emma and Joe - thanks.

I would like to thank Jenny for smiling no matter what typing tasks I put before her and for her very close attention to this manuscript.

Finally to my Father who has given me so much encouragement, help and support and who was always there when I needed him - THANK YOU.

CONTENTS

SUMMARY

The work described in this thesis is concerned with the control of polymer and copolymer structure using high intensity ultrasound.

Solutions of polystyrene were degraded under a range of conditions, including various concentrations and temperatures. Eleven solvents and a range of dissolved gases were also employed and the results were correlated with the gas solubility, the critical overlap concentration of the solution and the physical properties of the solvents. Polymer-solvent interaction parameters were calculated viscometrically and the degradation results also correlated with this property. The extent of chain branching during the degradation of both a concentrated and dilute solution of polystyrene in toluene was examined using static light scattering and GPC-viscometry, the results indicating that chain branching does occur during the reaction.

A number of kinetic schemes were applied to the degradation results and it was found that the rate constants obtained from some models did not correlate with observed trends.

Similarities between ultrasonic and shear degradation were found, such as the existence of centre cleavage and an apparent negative activation energy, although the rates calculated from a pure shear rate model did not correlate with the observed degradations.

Production of radicals from the homolytic cleavage of the polymer was used to prepare both functionalised polystyrenes and copolymers. Control of the size of the polystyrene macroradical was achieved by use of the degradation results and copolymers were formed by addition of methyl methacrylate. Copolymer compositions measured during the reactions suggested that the copolymer degraded once it had formed, so making control of the monomer addition more difficult than expected.

CHAPTER ONE

INTRODUCTION

1.1 Nomenclature of Polymers

A polymer is a very large molecule comprising hundreds or thousands of units, known as monomers, held together by covalent bonds. When the polymer is made of only one type of monomer, the polymer is known as a homopolymer. If two or more types of monomer are used, the polymer is known as a copolymer. Varieties of copolymers can be formed and these are shown in Fig. 1.1.

Polymers can be linear, branched or in the form of a network. The type of structure which they possess controls the properties of the material. The nomenclature used for the block copolymers formed in this thesis will be that discussed by Ceresa[1] and defined by IUPAC. A block copolymer of monomer M_1 and monomer M_2 will be written as poly (M_1-b-M_2).

It is difficult to place polymers in categories, but three classes tend to be used; rubbers, thermosets and thermoplastics.

Rubbers display elastomeric properties due to the polymer being lightly crosslinked preventing any permanent relative movement of the chains when the polymer is deformed. Rubbers are impossible to melt and only degrade on the application of heat.

Thermosets are very rigid due to heavy crosslinking and normally consist of a 3D network. These polymers, as with rubbers, do not melt on heating.

Thermoplastics are the largest group of polymers and are the ones that will be studied in this thesis. This group consists of linear and branched polymers that melt on the application of heat.

1.1.1 Uses of polymers

The use of polymers has increased massively in recent years. This is due to the enormous variety of properties that can be obtained, which has been partially due to the emergence of block copolymers[2]. By varying the ratios of monomers and their positions in the polymer chain, it has been possible to obtain polymers with better properties than those available from a homopolymer. In order to obtain copolymers

(i) Random Copolymers.- formed when there is a random arrangement of A and B units along the polymer molecule.

-A-B-A-A-B-B-B-B-B-A-B-A-A-B-A-B-B-B-A-A-

(ii) Alternating Copolymers.

-A-B-A-B-A-B-A-B-A-B-A-B-A-B-A-B-A-B-A-B-

(iii) Block Copolymers.- contain sequences of monomer units in a linear copolymer.

-A-A-A-A-B-B-B-B-A-A-A-A-B-B-B-B-A-A-A-A-

(iv) Graft Copolymers.- consist of a main homopolymer chain with branches of another type of homopolymer.

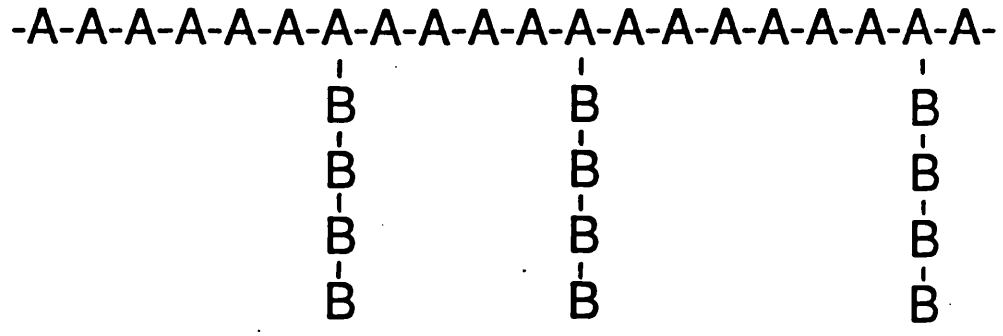

FIGURE 1.1. Varieties of block copolymers.

with the desired properties, it is necessary to prepare the constituent homopolymers with well defined block lengths and molecular weight distributions[3].

1.2 Molecular Weight Averages of Polymers

In natural polymers, such as DNA, the chains may all have the same number of repeat units, known as the degree of polymerisation, P. However, due to the statistical nature of laboratory preparative methods, a distribution of degrees of polymerisation is obtained as shown in Figure 1.2.

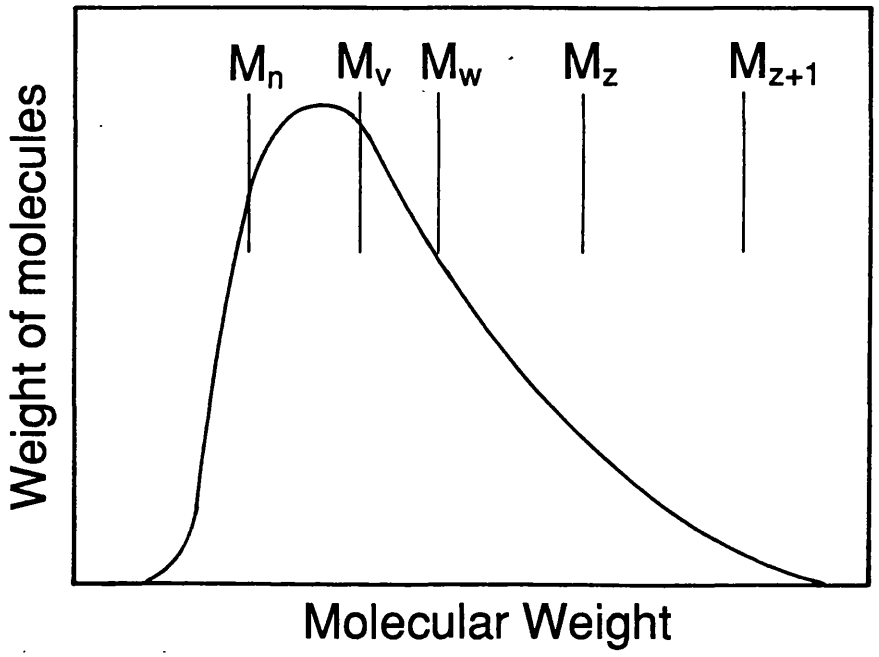

FIGURE 1.2. Molecular weight distribution of a polymer showing the locations of the molecular weight averages.

Hence, a unique molecular weight cannot be assigned and an average value is quoted. This average value can be defined in a number of ways:

i) Number average, M_n.

This is defined as[4]:

$$M_n = \frac{\Sigma_i n_i M_i}{\Sigma n_i} \qquad 1.1$$

where n_i is the number of molecules of length i.

It is possible to define a number average degree of polymerisation as:

$$X_n = \frac{M_n}{M_o} \qquad 1.2$$

where M_o is the molecular weight of the monomer.

This number average molecular weight determines the properties such as the brittleness and tensile strength of the polymer. For typical polymers, this average lies near the peak of the weight distribution curve.

ii) Weight average, M_w

This average depends on the weight of polymer, W_i, having a particular molecular weight

$$M_w = \frac{\Sigma_i W_i M_i}{\Sigma_i W_i} = \frac{\Sigma n_i M_i^2}{\Sigma n_i M_i} \qquad 1.3$$

As in the case of the number average degree of polymerisation, it is possible to define a weight average degree of polymerisation as:

$$X_w = \frac{M_w}{M_o} \qquad 1.4$$

In the weight average molecular weight, each molecule contributes to M_w in

proportion to the square of its mass and hence M_w is greatly influenced by high molecular weight species.

Due to the heavier molecules contributing more to M_w than M_n, M_w is always greater than M_n except for a monodisperse polymer.

iii) "Z" and "Z + 1" weight averages, M_z, M_{z+1}

These are not commonly used averages. They are normally used to correlate properties such as sedimentation and diffusion

$$M_z = \frac{\Sigma_i n_i M_i^3}{\Sigma_i n_i M_i^2} \qquad 1.5$$

$$M_{z+1} = \frac{\Sigma_i n_i M_i^4}{\Sigma_i n_i M_i^3} \qquad 1.6$$

As can be seen from Figure 1.2, M_z and M_{z+1} are always greater than M_n and M_w.

Quoting one of these values does not completely characterise a polymer. Polymers may have the same value of a molecular weight average, but have a different distribution of chain lengths. To overcome this, a polydispersity, γ, is defined, such that:

$$\gamma = \frac{M_w}{M_n} \qquad 1.7$$

Hence $\gamma = 1$ for a monodisperse polymer and has larger values for wider distributions. Most common synthetic methods give values around 2.0 although in some cases materials with γ greater than 20 are known. The lowest values are in the range 1.02 - 1.05 produced by anionic polymerisation[4].

1.3 Molecular Weight Determination

Various methods are available for the determination of molecular weight averages such as end group analysis, light scattering, viscometry, ultracentrifugation, gel permeation chromatography and measurement of the polymers colligative properties by ebulliometry, cryoscopy and osmometry. In this thesis gel permeation chromatography was the main method used to calculate molecular weights, however other methods such as viscometry and light scattering were used to correlate other properties of polymers such as their conformation in solution and the level of chain branching. The theory of these will be discussed in Section 1.8.

1.3.1 Gel permeation chromatography, GPC

A schematic of a GPC is shown in Figure 1.3. It consists of a pump giving an accurately known flow of eluent into which the polymer sample is injected. Separation occurs in the columns which are packed with beads with a range of pore sizes. Typical column packings are cross-linked styrene-divinyl benzene copolymers for organic solvents and Sephadex for aqueous systems.

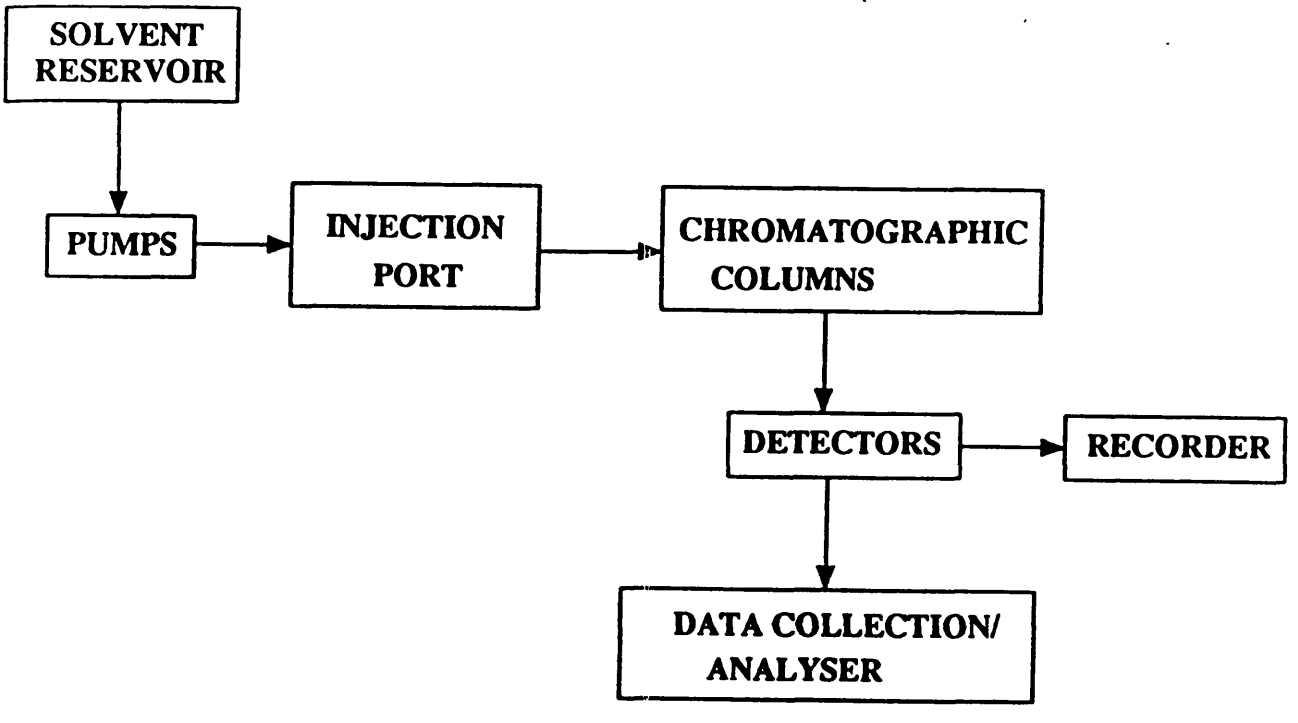

FIGURE 1.3. Schematic representation of a Gel Permeation Chromatograph.

While the dissolved polymer molecules flow over the porous beads, the smaller polymer chains are able to enter the pores, retarding their flow through the column. Larger polymer chains will be excluded and flow directly through the column. Hence the polymer chains are separated according to their size as shown in Figure 1.4.

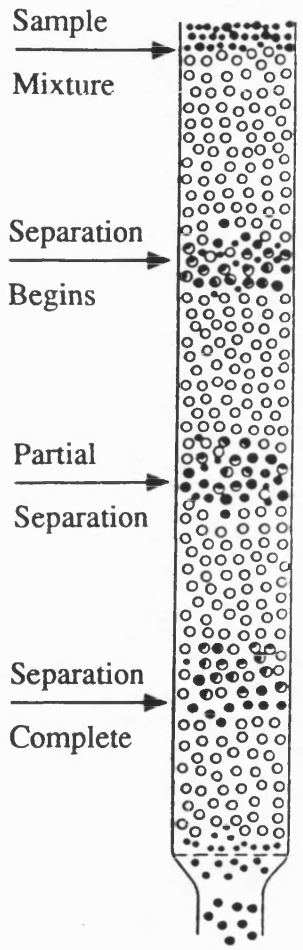

FIGURE 1.4. Separation of molecules according to their size by Gel Permeation Chromatography

After separation, the concentration of all the species are measured by either a differential refractometer which compares the refractive index of the column eluent, containing the separated polymer and a reference of pure eluent, or an ultraviolet photometer which is appropriate for a polymer with a significant UV absorbance with a non-absorbing eluent. The detectors used are normally non-destructive so that the

eluting component may be collected if necessary. A typical chromatogram of a polymer detected by a differential refractometer is shown in Figure 1.5.

The elution volume, V_R, is proportional to the logarithm of the molecular weight.

$$V_R = f(\log M) \qquad 1.8$$

GPC is a secondary method of analysis, in that it requires calibration with a series of known standards, i.e. the form of $f(\log M)$. There are three main methods for establishing a calibration curve[5]. Calibration standards with very narrow molecular weight distributions, a polydisperse reference material or a universal calibration requiring a relation between molecular size in solution and molecular weight can be used.

When using the narrow distribution standards, the retention time of each standard of known molecular weight is measured and a calibration curve of log M against V_R is plotted. This can be seen in Figure 1.6. Calibration standards are available for a range of polymers such as polystyrene, poly(methyl methacrylate) and poly(ethylene oxide).

The universal calibration arises from the work of Benoit[6], who suggested that a plot of log $[\eta]M$ against V_R is the same for all polymers where $[\eta]$ is the intrinsic viscosity. The hydrodynamic volume, H.V., is related to the product of $[\eta]$ and M and hence is known as the universal calibration parameter

$$H.V. = [\eta]M \qquad 1.9$$

It has been found that

$$\log M_P - \log M_{PS} = \log \frac{[\eta]_{PS}}{[\eta]_P} \qquad 1.10$$

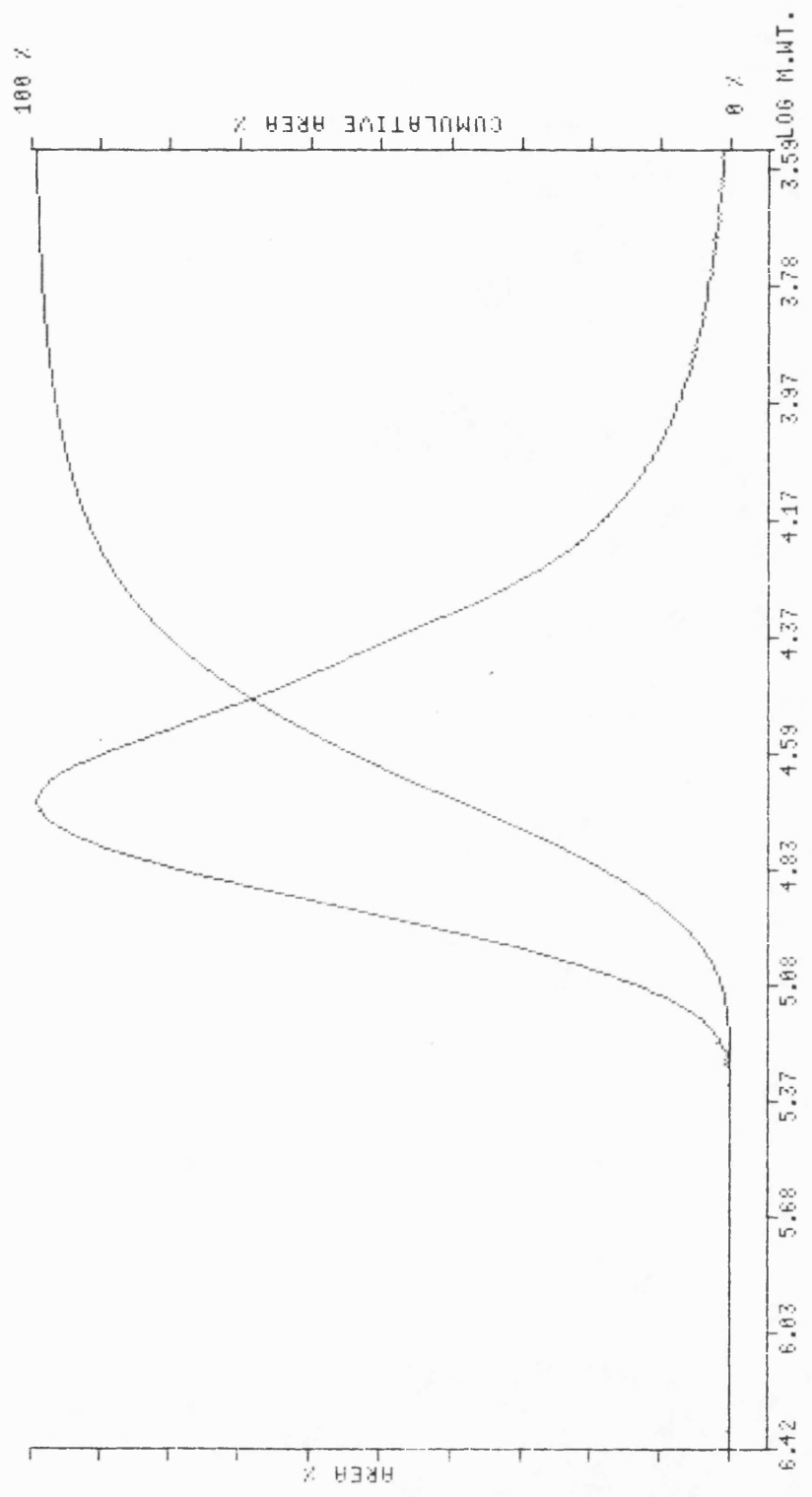

FIGURE 1.5. Typical G.P.C. Refractive Index trace.

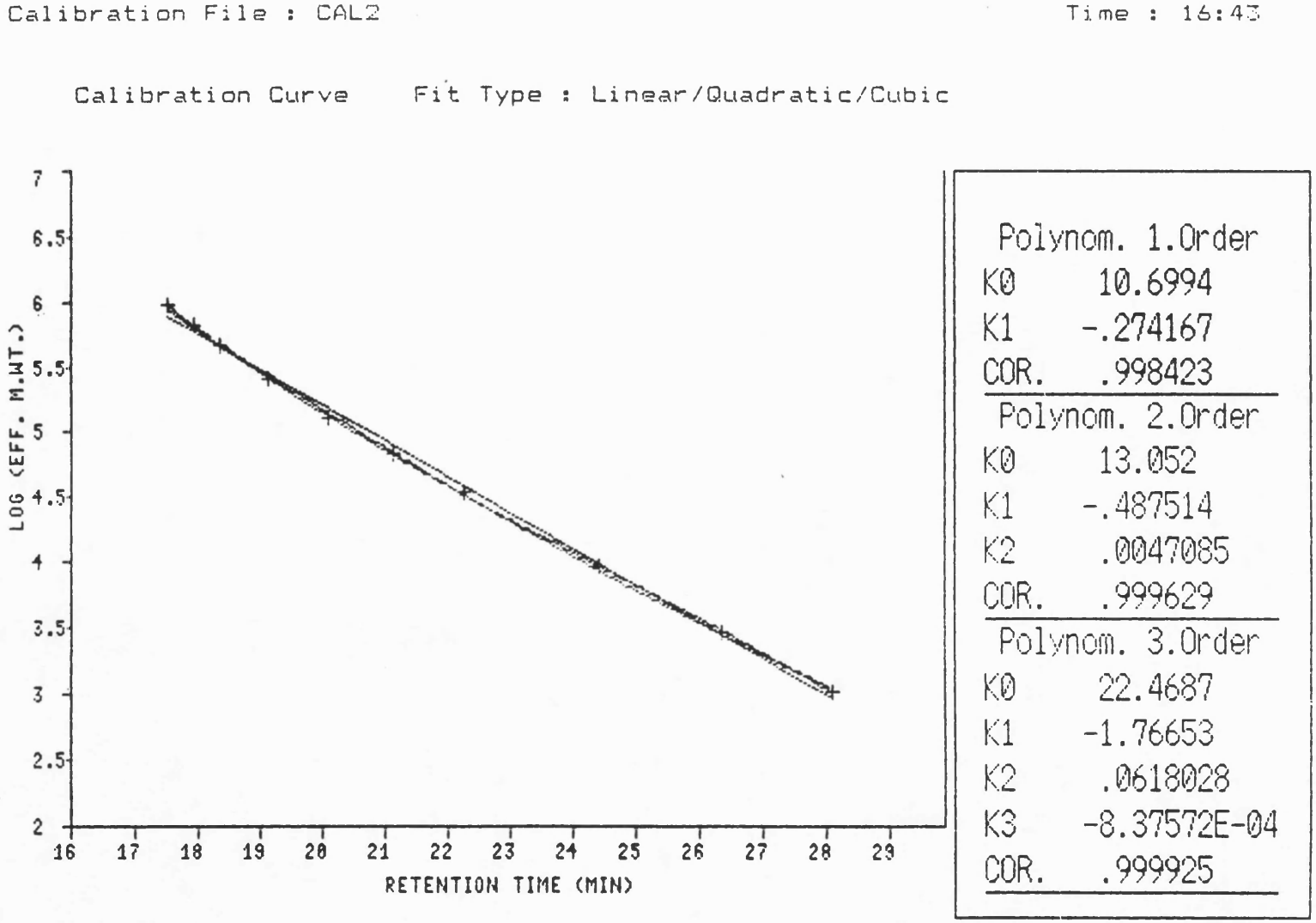

FIGURE 1.6. Calibration curve obtained from G.P.C.

where the subscript P refers to the polymer to be analysed and PS to the polystyrene standards used.

Equation 1.7 can be converted to a relation between M_P and M_{PS} using the Mark-Houwink constants for the standards and the polymer to be analysed. Substitution of the well-known Mark-Houwink viscosity equation[4]

$$[\eta] = KM_v^{\alpha} \qquad 1.11$$

into equation 1.10 gives

$$\log M_P - \frac{1+\alpha_{PS}}{1+\alpha_P} \log M_{PS} = \frac{1}{1+\alpha_P} \log \frac{K_{PS}}{K_P} \qquad 1.12$$

Analysis of the polymers during this study was undertaken using calibrations with polystyrene standards.

1.4 General Principles of Ultrasound

Ultrasound is defined as sound which has a frequency higher than the limit of human hearing, usually taken as 16 kHz. The upper limit of ultrasonic frequency is not sharply defined but is usually taken to be 5 MHz for gases and 500 MHz for liquids. The uses of ultrasound within this frequency range can be divided into two areas.

i) High frequency, low power ultrasound. This area has frequencies higher than 2MHz and is used for non-destructive testing and diagnostics since it gives high resolution.

ii) High power ultrasound. This area has frequencies between 20 and 100 kHz and is the area associated with chemical reactivity. It is this type of ultrasound that will be used throughout the studies in this thesis.

1.4.1 Propagation of ultrasound

Sound waves can be transmitted through any substance that has elastic properties. Ultrasound is concerned with sinusoidal motion and in the case of liquids, with longitudinal waves only. At these frequencies, Transverse waves are propagated in liquids but as their attenuation with distance is very high they need not be considered. Longitudinal waves are waves in which the vibration of the particle takes place in the direction of propagation of the wave. The passage of sound can thus be regarded as an alternating series of compressions and rarefactions of the medium as can be seen in Figure 1.7.

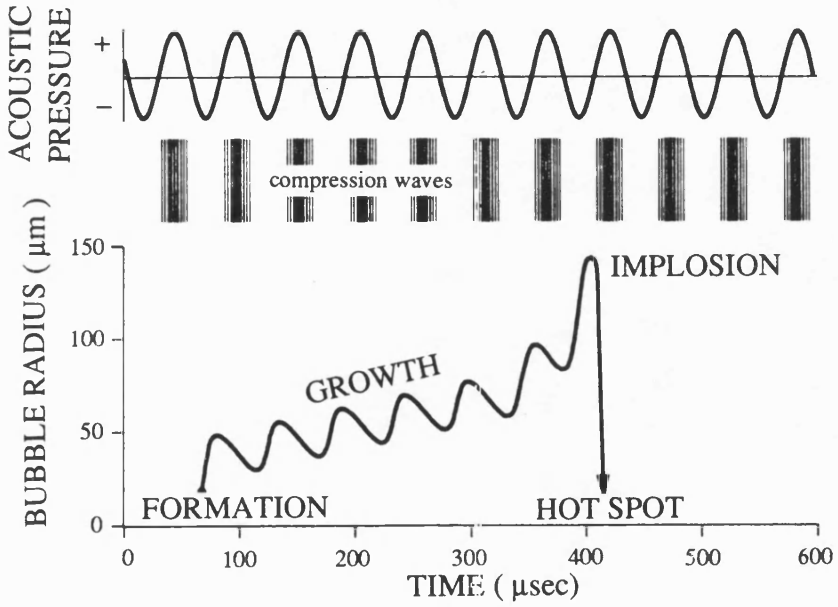

FIGURE 1.7. Representation of the growth and collapse of a cavitation bubble

A qualitative view of ultrasound is required to appreciate the processes occurring when ultrasound passes through a liquid, but more mathematical treatments can be found in the literature[7-9].

The succession of compressions and rarefactions may be represented as an acoustic pressure, P_A, which varies with time t;

$$P_A = P_{max} \sin (2\pi ft) \qquad 1.13$$

where P_{max} is the maximum acoustic pressure generated and f is the frequency of the ultrasound.

The intensity, I, of the wave is defined as the energy transmitted through unit area of the medium in unit time and is given by:

$$I = \frac{P_{max}^2}{2\rho c} \qquad 1.14$$

where c is the velocity of sound in the medium and ρ is its density.

During the propagation of the sound the intensity is attenuated due to the transfer of energy to the medium. As the molecules of the liquid vibrate they experience viscous interactions and some energy is lost in the form of heat. This can be seen by a small bulk temperature rise during sonication. The attenuation can be represented as:

$$I_d = I_o \exp(-2\alpha d) \qquad 1.15$$

where I_d is the intensity of sound at a distance d from a source radiating with an intensity I_o. The term α is the absorption coefficient and depends on factors such as the thermal conductivity, specific heat capacity, the density and velocity of sound in the medium[10].

At any temperature and in a given medium, the value of α/f^2 must be constant and so any increase in the frequency results in an increase in α, so causing more rapid attenuation of the sound intensity with distance.

This indicates one of the problems associated with building variable frequency transducers. For higher frequency transducers, a much higher initial power will be

required to produce equivalent effects at the same distance.

1.5 The Production of Cavitation by Ultrasound

Cavitation is the most important phenomenon produced by ultrasound when considering ultrasonic polymerisation and degradation.

As the sound wave passes through the medium, the distance between the molecules will vary as they oscillate about their mean position. If, during the rarefaction period of the wave, a sufficiently large negative pressure is applied to the liquid, which exceeds the force required to hold the liquid intact, the liquid will break down, forming voids. These are cavitation bubbles[11]. This has been found to occur at acoustic pressures much lower than that required to break the tensile strength of a liquid[12]. The pressure required to overcome the tensile strength of homogeneous liquids is of the order of hundreds of bar, whereas the reduction in pressure caused by the ultrasonic wave is only of a few bar.

The reason for the lower pressure required for the production of cavitation has been attributed to the presence of "weak spots" in the liquid lowering its tensile strength. One source of these weak spots could be the presence of particulate matter and the occurrence of trapped gas nuclei in the recesses of these particles[13,14]. Nucleation from these sites can be visualised in Figure 1.8.

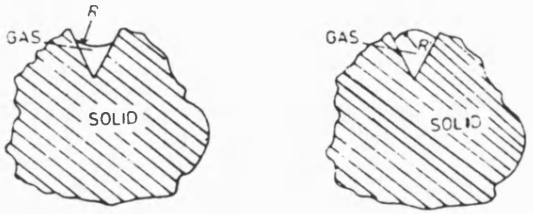

FIGURE 1.8. Cavitation from a suspended particle.

As the pressure decreases during the rarefaction period of the wave, the liquid-gas interface becomes more convex until at sufficiently low pressure, the gas breaks away to form a bubble. This idea has been confirmed by removing particles through

ultrafiltration[15] which was found to raise the cavitational threshold. (The value of applied acoustic pressure necessary before cavitation occurred). The cavitation threshold was also raised in rigorously degassed solutions[16,17] which led to the conclusion that gas bubbles could act as a source of cavitation nuclei.

There are several different types of cavity in a liquid, these being empty cavities, vapour-filled cavities and gas-filled cavities and it is these that are thought to cause the sonochemical effects.

It is possible to classify cavitation bubbles into two types, transient and stable cavities[11]:

i) Transient cavitation

These exist for one, or at most two acoustic cycles, expanding to a radius of at least twice their initial size before collapsing violently on compression. They can disintegrate into smaller bubbles which could act as nuclei for further bubbles. The lifetime of these bubbles is assumed to be too short to allow any diffusion of gas into the bubble although evaporation of the liquid can occur freely. Hence these are either voids or vapour-filled cavities.

On collapse, as there is no gas to cushion the implosion, a violent collapse occurs. Theoretical considerations by Neppiras[18,19] and Flynn[8] showed that during the adiabatic collapse of a cavitation bubble very high temperatures, of the order of 10^4 K, and pressures of thousands of atmospheres occur. These violent conditions have formed the basis of the explanation of radical production by bond cleavage.

ii) Stable cavitation

These are bubbles that oscillate about an equilibrium size for many acoustic cycles. They are thought to contain mainly gas and some vapour. As the bubble grows, it may transform into a transient cavity but the violence of its collapse will be less than that of a normal transient cavity due to the gas

cushioning its collapse.

The oscillation can cause great disruption and movement of adjacent liquid molecules[20,21] and these can be responsible for some mechanical effects associated with cavitation.

1.5.1 Factors affecting cavitation

There is now a large amount of experimental evidence[22-25] to suggest that cavitation effects play a major role in both the degradation and polymerisation of polymers. Due to cavitation being so important, in order to adequately understand the results it is necessary to discuss those factors which affect cavitation as it will be those factors that influence the degradation and polymerisation characteristics.

a) Solvents

The formation of cavities in a liquid requires that the negative pressure during the rarefaction period must overcome the cohesive forces acting within the liquid and hence cavitation should be more difficult to produce in more viscous fluids. It has been shown[26] that such an effect, though small, does occur. Conversely, the use of solvents with low surface tensions should lead to a reduction in the cavitational threshold[27]. The overall effect of surface tension and viscosity tends to be disregarded in most cases.

The vapour pressure of the solvent appears to be of greatest importance in the cavitation process[28]. When the volatility of the solvent is high, the amount of vapour entering the cavitation bubbles is also high, causing a cushioning effect when the bubbles collapse[8]. Therefore the intensity of the shock wave produced is reduced.

b) Frequency

It has been found that increasing the ultrasonic frequency decreases the amount of cavitation[29]. This was explained by Eyring[30]. At a high frequency, the time between compression and rarefaction cycles is too short to allow cavitation

bubbles to grow.

c) Intensity

From equation 1.14, it can be seen that $I \alpha P_{max}^2$ and from[8]

$$T_{max} = T_o \left[\frac{P_{max}(\gamma-1)}{P} \right] \qquad 1.16$$

where T_{max} is the temperature on bubble collapse, P is the pressure in the bubble at the maximum size, P_{max} is the maximum acoustic pressure generated, T_o is ambient temperature and γ is the ratio of specific heats of the gas or vapour, the temperatures and pressures produced on bubble collapse will increase with increasing intensity. However, it has been shown that intensity cannot be increased indefinitely[18,31] due to the bubble growing so large on rarefaction, that the time available for collapse will be insufficient. The increase in intensity will also cause an increase in the number of cavitation events.

d) Temperature

Raising the temperature increases the vapour pressure over the liquid and lowers the surface tension and therefore the cavitation bubble formed contains more vapour. Hence the bubble collapse will be cushioned.

e) Applied Pressure

Increasing the applied pressure increases both the cavitational threshold and the intensity of the bubble collapse. As the pressure is increased, the cavities will become progressively smaller due to surface tension forces and hence cavitation will be reduced.

f) Effect of Dissolved Gases

Gases with high solubility will reduce both the intensity of the cavitation and the cavitational threshold. The greater the gas solubility, the greater the amount of gas that penetrates into the cavitation bubble and hence the smaller the

intensity of the shock wave on bubble collapse[32]. This can be seen more quantitatively by considering the equation 1.16 and

$$P_{max} = P\left[\frac{P_m(\gamma-1)}{P}\right]^{\frac{\gamma}{(\gamma-1)}} \qquad 1.17$$

where P is the pressure in the bubble at maximum size, P_m is the pressure in the liquid at the moment of collapse, T_o is the ambient temperature, γ is the ratio of specific heats of the gas and P_{max} and T_{max} are the maximum pressure and temperature generated respectively.

P can be replaced by $(P_v + P_g)$ where P_v is the pressure of vapour in the bubble and P_g the pressure of gas in the bubble. Increasing the gas content of the liquid increases P_g and hence decreases both P_{max} and T_{max}. Another factor may be that the greater the gas solubility, the more likely it is to redissolve in the medium during the compression phase of the acoustic cycle.

Using gases with higher solubilities provides a larger number of cavitation nuclei in the solvent and hence lowers the cavitational threshold[33].

1.6 Generation of Ultrasound

The generation of ultrasound was first established in 1880 with the discovery of the piezoelectric effect by Curie[34,35]. The earliest form of ultrasonic transducer was a whistle developed by Galton[36] in 1883 to investigate the threshold of human hearing. However, it is only since 1945 with significant developments made in electronic circuitry and transducer design that ultrasonic equipment has become readily available.

1.6.1 The piezoelectric effect

The most common method employed for the generation of ultrasound uses the piezoelectric effect of crystals such as quartz and more recently ceramics such as barium titanate and lead zirconate titanate[37].

The piezoelectric effect is the production of charges on the faces of a crystal as a result of applying pressure. An inverse of this effect, of applying charges to the faces of a crystal, to force the crystal to expand and contract is the effect used in the generation of ultrasound. This fluctuation in dimensions can be harnessed to transmit the vibrations from the crystal through whatever medium it is attached to.

1.6.2 Ultrasonic apparatus

There are three main methods of production of ultrasound found on a laboratory scale:

i) Ultrasonic Bath (Fig. 1.9)

This is the most accessible and simplest equipment. It consists of a stainless steel tank with transducers clamped to its base. However there are limitations to this equipment, i.e.

(a) The efficiency and overall power generated by the bath are governed by the size and position of the reaction vessel in the bath.

(b) Control of temperature is a problem as most baths warm up during use. Ice may be added to the water but this will alter the power being transmitted to the reaction vessel.

(c) Baths do not all operate at the same frequency, hence results from different baths cannot easily be compared.

ii) Direct Immersion Sonic Horn (Fig. 1.11)

This is the most efficient method of transmitting ultrasonic energy into liquids. The main advantages over the cleaning bath are that it can be tuned to give optimum cavitation in the reaction and higher powers can be used since the ultrasound is introduced directly into the reaction vessel. However, during prolonged use, erosion of the probe tip is believed to cause contamination of the reaction mixture with metallic particles.

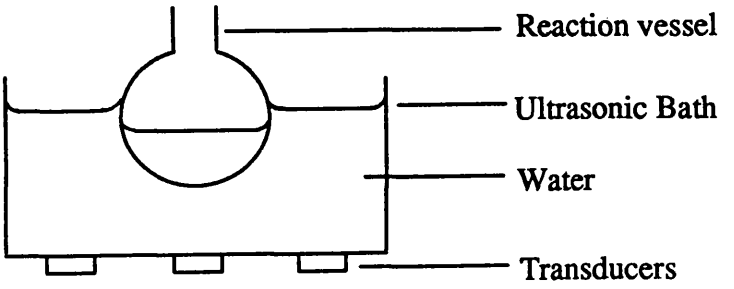

FIGURE 1.9. Ultrasonic Bath

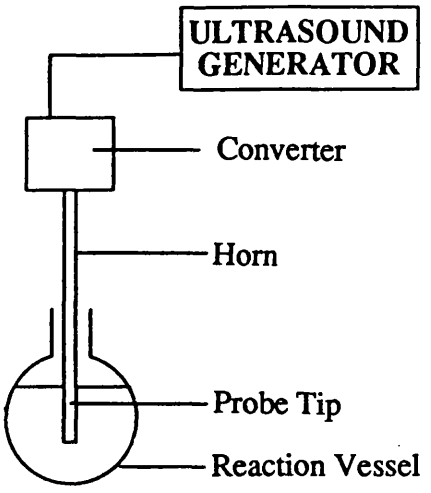

FIGURE 1.10. Ultrasonic Probe.

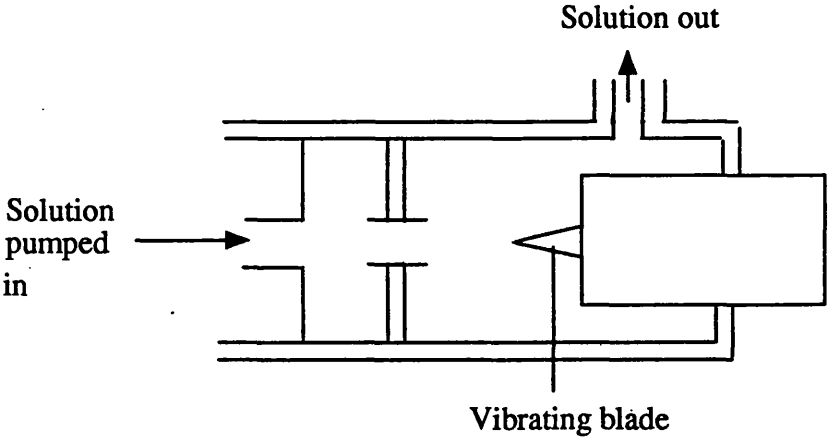

FIGURE 1.11. Whistle Reactor

The piezoelectric crystal is directly coupled to a horn, normally made of titanium alloy. The length of the horn is very important and needs to be an exact number of half wavelengths, producing an anti-node on the probe tip. It is this that produces the vibration.

An ultrasonic probe was used throughout the experiments in this thesis.

iii) Whistle Reactor (Fig. 1.11)

The whistle reactor relies on mechanical generation of ultrasonic power. It derives its power from the mechanical flow of the medium across the blade. The majority of the chemical effects observed when using whistle reactors for the sonication of heterogeneous reactions can be attributed mainly to the generation of very fine emulsions rather than the ultrasound itself.

1.7 Ultrasonic Degradation of Polymers

In 1933, Flosdorf and Chambers[38], Gyorgi[39] and Szalay[40] reduced the viscosity of solutions of natural polymers, such as starch, gum arabic and gelatin, by treatment with ultrasound. Szalay attributed this to a breakdown of the polymer molecule.

In 1938, however, Freundlich and Gillings[41], investigating the action of ultrasonic waves on aqueous solutions of gelatin and toluene solutions of rubber, found that the viscosity reduction was not permanent. They therefore concluded that the reduction was a thixotropic effect and not due to molecular degradation. This idea was compounded by previous work by Heyman[42] who had shown that viscosity was also reduced by vigorous shaking.

Freundlich had previously found[43] that the liquefaction of thixotropic gels could only be accomplished if the experiments were carried out at atmospheric pressure. Application of any external pressure prevented the liquefaction. Freundlich concluded that the liquefaction was not caused by the ultrasonic waves directly but by the mechanism of cavitation. Since all of the earlier experiments had been undertaken at atmospheric pressure, it was possible that the effects noted were also due to cavitation.

The presence of bond breakage was firmly established by Brohult[44] studying the effect of ultrasound on haemocyanin. He used an ultracentrifugation technique and found that the molecule fragmented into monodisperse fragments. This was further confirmed with work by Schmid and Rommel[44,45] who found permanent reductions in the viscosities of solutions of polystyrene and poly(acrylates) under ultrasonic irradiation. It was noted that the decrease in viscosity was initially quite rapid but slowed with time and reached a limiting value below which no further reaction occurred.

Schmid and Rommel investigated the possibility of the degradation being due to either oxidative fission or cavitation. They excluded the oxidative fission by working in an atmosphere of nitrogen and obtaining the same rate of breakdown as that found under air. In order to investigate the cavitation, the solutions were sonicated under sufficient pressure to prevent the formation of cavities. An increased pressure did cause a decreased degradation, however some degradation was still noted. Hence it was concluded that cavitation was mainly responsible for the degradation but other factors were involved. The increased pressure in the experiments was exerted by increasing the gaseous pressure over the solutions. This varied two factors simultaneously, the pressure over the solution, and more gas would be present in the solution due to increased solubility with increased pressure[18,31]. The increase in pressure suppressed the cavitation while the increased concentration of gas counteracted this effect.

In order to investigate these effects, Brett and Jellinek[47,48] carried out the ultrasonic degradation of solutions of polystyrene in benzene by exerting first gaseous pressure and then pressure via a mercury column. With increased nitrogen pressure the decrease in degradation rate was relatively small and reached a constant value. When the pressure was increased with the mercury column, the rate of degradation rapidly decreased to zero. The initial rapid degradation and the existence of a limiting degree of polymerisation (M_{LIM}) below which no further degradation occurs has since been noted by a number of workers and has been regarded as characteristic of ultrasonic

degradation[9].

1.7.1 Formation of macroradicals by chain cleavage

There are two possibilities for cleavage of a covalent bond in the degradation[49,50]:

i) Homolytic Cleavage. Two macroradicals are formed[50]:

$$P_{n+m} \rightarrow P_n^{\cdot} + P_m^{\cdot}$$

ii) Heterolytic Cleavage. Two macromolecular ions are formed:

$$P_{n+m} \rightarrow P_n^{+} + P_m^{-}$$

The most common cleavage seen during ultrasonic degradation is the homolytic cleavage. The first evidence for this was obtained by Melville and Murray[51] who sonicated polymers in the presence of vinyl monomers, and by Henglein[50] using 2,2'-diphenyl picryl hydrazyl, DPPH, as a radical scavenger.

More recently, evidence for the presence of radicals during the sonication of polystyrene, poly(methyl methacrylate), polypropylene and poly(vinyl acetate) solutions in benzene has been found by Tabata et al[52,53] using Electron Spin Resonance Spectroscopy (ESR). Spin trapping using pentamethyl nitrosobenzene was used to trap the primary radicals.

The production of ions through heterolytic bond fission has been detected by Thomas and de Vries[54] studying solutions of poly(dimethyl siloxane) (PDMS):

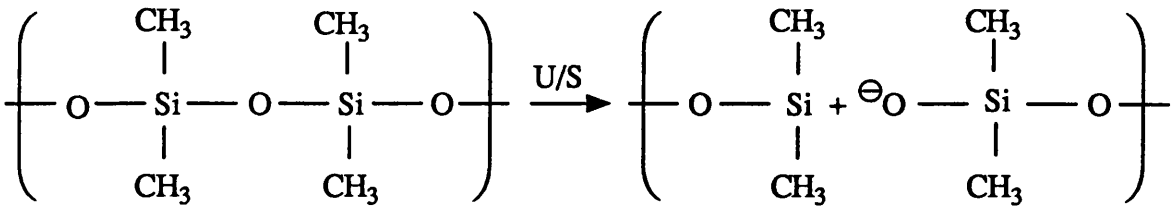

No presence of radicals was detected with DPPH. When the sonication was carried out in the presence of ^{14}C methanol, they found that the radioactivity was incorporated into the polymer. This did not occur on the sonication of polystyrene or on refluxing of PDMS solutions. Thomas and de Vries postulated the formation of an ion pair on sonication followed by stabilization with the strong nucleophile such as methanol.

1.7.2 Effect of sonication on the polydispersity of polymers

During the early studies comparatively few workers studied the alteration of the molecular weight distribution during the degradation[24,55]. This was due to the small variety of techniques available for studying the distribution. The methods available were tedious using fractional precipitation or turbimetric titrations of the polymer. The first study of this type was by Jellinek and White[24], who calculated the distribution of ultrasonically degraded polystyrene by fractional precipitation from methyl ethyl ketone using methanol. The molecular weight of each fraction was determined viscometrically.

Schmid *et al*[56] looked at the degradation of initially narrow distribution polymer samples. They found that the polydispersity initially broadened before narrowing as the limiting molecular weight was approached.

Studies by Gooberman and Lamb[57,58] on the degradation of polystyrene, examining the distribution using turbimetric titrations, revealed secondary peaks at lower molecular weights, suggesting a non-random degradation.

The advent of GPC by Moore in 1964[59] allowed changes in polydispersity during sonication to be measured more easily and with a much greater degree of

accuracy[60-62].

Shaw and Rodriguez[62] used GPC to study degraded poly(dimethyl siloxanes) with initial molecular weights of 1300000 and 240000 and found that the samples, despite having different initial polydispersities, approached the same distribution after long sonication times. Later similar findings were reported[63] studying poly(alkyl methacrylates). The polydispersities approached a value of 1.5 as the limiting chain length was reached.

Wu et al[64] used GPC to measure the polydispersities of sonicated poly(methyl methacrylate) solutions in tetrahydrofuran. It was found that narrow polydispersity fractions broadened their distribution before narrowing at long sonication times. This was in agreement with previous work by Schmid[56]. The wider distribution samples only narrowed their polydispersity.

GPC has also been used to study the degradation of narrow distribution polystyrene (γ = 1.02 - 1.12) in tetrahydrofuran[65]. The chromatograms obtained showed secondary peaks at approximately half the molecular weight of the original polymer. This suggested that bond cleavage was occurring near the centre of the chain. The results were compared with a sample degraded by benzoyl peroxide. In this case random cleavage took place and no secondary GPC peaks were observed. The preferential cleavage at the centre of the chain appears to be a general characteristic of ultrasonic degradation.

Glynn et al[66-68] used computer models to simulate the distributions of degraded polymers and found that centre cleavage best fitted their experimental results.

1.7.3 Parameters affecting the degradation

The effect of the frequency and intensity of ultrasound on the degradation is thought to be due to their effect on cavitation, not due to any direct effect on the polymers. The fundamental vibration frequency of chemical bonds lies in the 10^{12}-10^{14} Hz range[69] considerably above the frequency of the applied ultrasound (20 kHz), hence there would be no direct effect.

Mostafa[70] found that the degradation rate was frequency dependent. The rate and extent of degradation increased with frequency and reached a maximum around 1 MHz, whereafter the rate decreased. At frequencies above 2 MHz, cavitation is almost suppressed and hence there would be no degradation. However, as was explained in Section 1.4, an increase in frequency requires increased intensity to obtain equivalent effects and the results may have been due to a decrease in intensity rather than a frequency effect.

Theoretical work[71] showed that the degradation rate constant should be independent of frequency up to 500 kHz. This was confirmed experimentally[72] for solutions of poly(methyl methacrylate) in benzene irradiated at 10 kHz, 175 kHz and 300 kHz at an intensity of 1 W cm^{-2}.

The effect of the intensity on ultrasonic degradation has been more widely studied than the effect of frequency.

The first study was undertaken by Mostafa[73] on polystyrene in benzene. The degradation was found to be faster at higher intensities, as predicted from theory. Jellinek[71] used these results to show that the degradation rate constant was a linear function of intensity. Since these early studies the effect of intensity has been studied on many systems, such as poly(methyl methacrylate)[74], hydroxyethylcellulose and poly(ethylene oxide) in aqueous solutions[75], poly(dimethyl siloxane)[76] and poly(acrylamide)[77].

Okuyama[78] predicted that M_{LIM} should be independent of intensity as the strength of bubble collapse was not affected by the intensity. This is in direct contrast to the theoretical effect of intensity described in Section 1.5.1 which predicts that the strength of bubble collapse is affected by the ultrasonic intensity. Most workers agree that M_{LIM} is affected by ultrasonic intensity and decreases with an increase in intensity. However, Schoon and Rieber[79] working on poly(dimethyl siloxane) and natural rubber found results that agreed with Okuyama in that M_{LIM} was independent of the intensity.

The effect of the polymer molecular weight on the degradation has been studied by several workers[47,80,81]. As described earlier the degradation proceeded faster at

higher molecular weights. It was also noted that the limiting molecular weight obtained was independent of the initial molecular weight[82].

Attempts have been made to correlate the limiting molecular weight obtained with the nature of the polymer. Schoon and Rieber[83,84] studied the degradation of a range of polymers such as polystyrene, polybutadiene and poly(vinyl acetate) and found very similar values for M_{LIM}, suggesting that the chemical nature of the polymer was unimportant.

Malhotra[63] found similar results when degrading a series of poly(alkyl methacrylates) with side chains ranging between methyl and octadecyl. It was postulated that the size of the substituents was unimportant and the factors determining the kinetics of the degradation were chain structure and monomer molecular weight.

Thomas[85] also found that polystyrene, poly(methyl methacrylate) and polybutene degraded at similar rates but poly(lauryl methacrylate) degraded 3.5 times faster.

Grassie and Melville[86] showed that during the thermal degradation of copolymers of poly(methyl methacrylate-b-acrylonitrile) with methacrylate to acrylonitrile ratios of 40:1 and 411:1, the chains broke at the acrylonitrile units. This contrasted with results by Melville and Murray[51] looking at the ultrasonic degradation of the same copolymers. The degradation produced the same rates of degradation and limiting molecular weights for both polymers with no preferential cleavage at the acrylonitrile block. Encina *et al*[87] showed that weak links in the polymer backbone could be important in the degradation. They found that poly(vinyl pyrollidone) with peroxide linkages at a ratio of 1:250 in the chain degraded ten times faster and gave a lower limiting molecular weight than the homopolymer. The polymer recovered after sonication, had the molecular weight expected if all of the peroxide linkages had broken.

This evidence suggests that the polymers are not degraded through thermal effects. Many workers ascribed the effects to mechanical processes or shock waves as will be discussed in Section 1.7.4. If this is the case, then the nature of the solvent will

play a large part in the degradation.

The size and shape that a polymer adopts in solution should be an important factor. Schmid and Beuttenmuller[88] found that there was no degradation of polystyrene when sonicated as a suspension in water. They also noted that when a non-solvent (acetone) was added to solutions of polystyrene in benzene, the rate of degradation decreased.

Several workers have found no dependence of the degradation on the solvent. Thomas and Alexander[89] found similar rate constants for the degradation of cellulose nitrate in mixtures of ethyl acetate and ethanol (solvent and non-solvent respectively). Nelkenbaum[90] found the same kinetics for polyisobutylene dissolved in a range of solvents such as benzene, toluene, isopropylbenzene and chlorobenzene. However, results of the degradation being solvent independent are very much in the minority and most workers have found that their results are solvent dependent.

An attempt has been made to correlate the degradation with the thermodynamic quality of the solvent, described by the Flory-Huggins interaction parameter[48,91]. (This parameter is described in detail in Section 1.8.1).

Golubev et al[92] studied the degradation of a range of poly(alkyl methacrylates) including methyl-, lauryl- and octyl-. They found an acceleration in the rate with systems having higher Huggins constants. This constant is found from solution viscometry and higher values indicate uncoiling of the chain. Similar results were found by Malhotra[93] studying hydroxypropyl cellulose dissolved in water, ethanol and tetrahydrofuran. Other polymers have been studied including poly(ethylene glycol)[94] and dextran[80].

The effect of a number of physical factors concerning the solvent on the degradation have also been studied mainly to elucidate the degradation mechanism.

If thermal effects were responsible for the degradation then it would be expected that at higher temperatures more degradation should occur. It was found that this was not the case. Malhotra *et al* found increased degradation for polystyrene in tetrahydrofuran[95] and for a series of poly(alkyl methacrylates) in toluene and

tetrahydrofuran[63] all at -20° C . This effect was explained by considering the cavitation process. At higher temperatures, the solvent will have a higher vapour pressure, hence more vapour will enter the cavitation bubble and it will be cushioned on collapse, reducing the forces in the liquid and hence the degradation.

Other workers have also investigated the effect of solution temperature on the degradation. Schmid and Beuttenmuller[96] studied the degradation of polystyrene in toluene over the temperature range 40°C to 120°C and Thomas and Alexander[89] studied cellulose nitrate in a series of acetate solvents betwen 0°C and 25°C. All of the results showed that the degradation proceeded more slowly and yielded higher limiting molecular weights at higher temperatures. In addition to the cushioning effect Malhotra also suggested that the increase in viscosity at low temperatures led to a better energy transfer from the transducer to the solution and also decreased the polymer chain mobility leading to increased degradation.

The effect of surface tension and viscosity had been studied theoretically by Jellinek[27] who found that the two properties would have opposing effects on the degradation. It is normally considered that the viscosity and surface tension effects are very small compared to the effects contributed by other factors. This conclusion was supported by Basedow and Ebert[80] who found that the rate of degradation of dextran in water was unaltered on the addition of a surfactant.

The lower the heat of vaporisation, ΔH_v, the more vapour will be inside the cavitation bubble and hence the greater the cushioning effect on bubble collapse. Basedow and Ebert[80] found a linear relationship between the rate constant of degradation and the heat of vaporisation of the solvent for dextran in a range of solvents, such as water, dimethyl sulphoxide, ethylene glycol and glycerol.

Dissolved gases can also enter the cavitation bubble and cushion its collapse. Hence gases with a high solubility should lower the shock wave from the cavitation bubble and so lower the degradation. Melville and Murray[51] found that the degradation rate for polystyrene and poly(methyl methacrylate) in toluene were the same whether saturated with air or nitrogen. Very little work has been described on the effect of

dissolved gases on the degradation process.

The effect of solution concentration on the degradation has been studied by several workers[58,60,97,98]. All of the results showed that the degradation rate decreased with increasing concentration.

Gooberman and Lamb and Jellinek and White studied polystyrene solutions in benzene and found that the rate constant displayed a maximum in the region 0.01 - 0.03% (w/v) and fell at higher concentrations. The decrease in rate at higher concentrations was attributed to a reduction in cavitation efficiency as the chains began to overlap. Other systems that have demonstrated this decrease in rate with an increase in concentration are poly(α-methylstyrene) in toluene[99], poly(methyl methacrylate) in benzene[100] and hydroxypropyl cellulose in water[93].

1.7.4 Mechanism of ultrasonic degradation

In order to fully explain the results obtained from the degradation studies, the mechanisms proposed for the degradation must be discussed.

The early mechanisms proposed that cavitation did not play an appreciable role during the degradation[45,46]. They assumed that frictional and impact forces between the polymer chain and solvent molecules are developed in the liquid on ultrasonic exposure of sufficient magnitude to rupture carbon-carbon bonds. However, some of the experimental results could not be explained by this mechanism[88]. The degradation should cease when the solvent and solute are of the same density since the solute molecules would then move completely with the oscillating liquid. However, on studying the degradation of polystyrene in carbon-tetrachloride-toluene mixtures no differences in the degradations were observed[88,96].

Schmid calculated that if the polymer was rigidly fixed, an oscillating solvent would exert a frictional force on a polymer of degree of polymerisation 3000 of 5.37×10^{-4} dynes (1 dyne = 1×10^{-5} N). The force required to break a carbon-carbon bond[101] is 5.64×10^{-4} dyne and so the frictional force is of the right order of magnitude for rupture. Schmid also proposed a formula for the case of the chains not being rigidly

fixed. However this showed that the force produced in this case would only be 8.0×10^{-11} dyne, insufficient to break a C-C bond. In order to account for this, Schmid suggested that in practice the polymer chains were neither rigidly fixed nor freely mobile, but were entangled, so that the frictional forces were considerably increased.

Jellinek and White[102] suggested that the macromolecules were broken by the impact forces when the solvent molecules collide with them. It was assumed that the time of impact was so short that the chain molecule appeared to be rigid. In this case, the force acting on a polymer chain which is fixed at both ends, would be proportional to the momentum destroyed by the impact. However, calculations showed that the force produced was only 1.875×10^{-5} dynes, considerably less than that required to break a C-C bond.

Thieme[103], in another attempt to explain the mechanism of degradation, suggested that collisions between macromolecules were strong enough, due to their increased kinetic energies in the presence of ultrasonic waves, to cause degradation. However, if the molecules were free to move, they would follow the wave motion without collision. If the molecules are constrained from motion, their response will depend on the way that they are constrained, but in no case will there be a possibility of collisions.

There is now overwhelming evidence that degradation occurs as a result of cavitation. However, which effect caused by cavitation is responsible for the degradation has been the object of considerable discussion. The possibilities studied have been (i) thermal effects due to the hot spot created in the bubble[20], (ii) shock waves produced from transient bubble collapse[85] and (iii) shear forces from pulsating stable cavitation[109,110].

The thermal effect has now been discounted owing to thermal degradation producing a reverse polymerisation (i.e. with monomer loss from the chain end) whereas the degradation observed using ultrasound is a non-random cleavage.

A) Shock wave degradation

Thomas[85] proposed a mechanism whereby the collapse of a cavity produces large hydrodynamic pressures and velocity gradients in the surrounding fluid[18,31]. Since a polymer molecule occupies a relatively large volume in solution, it is apparent that with sufficiently large velocity gradients, the side of the polymer coil near a collapsing cavity will move at a higher velocity than the side away from the collapsing cavity. Assuming that the relaxation time of the polymer is short, the velocity gradient existing over the volume of the polymer will distort it from its initial spherical shape along a radius of the collapsing cavity. The unfolding of the coil will continue until a geometry is reached which is incapable of further relaxation. At this time a force operates on the polymer chain due to the relative motion of the polymer segments and solvents.

The model assumed that the polymer resembled a string of spherical beads as assumed by Flory[104], and that the polymer concentrations were moderately low and hence molecular entanglements between polymer molecules did not occur. The treatment gave a linear dependence of degradation rate on the degree of polymerisation and predicted centre cleavage of the polymer chain. The calculations from the model showed that there would be sufficient force to rupture a polymer chain with a degree of polymerisation of 2000 at a distance of 1×10^6 Å from the collapsing cavity.

This model was not rigorous in that, together with the previous assumptions mentioned, it assumed that each monomer unit behaved as a sphere and that all the cavities were of uniform size. However attempts to improve the accuracy of this model gave serious mathematical problems

Okuyama and Hirose[105] extended the treatment to include the fact that the stress forces only acted on parts of the chain. Thus one part of the chain would become extended and the remainder would be static. The collapse of both transient and stable cavities were examined in the model. The calculations showed that the collapse of stable gas-filled cavities would produce a degree of polymerisation

much higher than that obtained experimentally whereas, collapse of a transient cavity would produce a degree of polymerisation of approximately 100. Hence it was concluded that the degradation was due to transient cavity collapse.

Gooberman[106] explained the degradation as being due to the shock wave produced during the collapse of a transient cavity. The stresses in the polymer were due to the shock wave radiated from the cavity when it reached its minimum radius. The shock wave is pictured as a rapid pressure rise followed by an exponential pressure drop. During the pressure rise, the solvent will be compressed and, assuming, as demonstrated by Alexander and Fox[107] that a macromolecule does not change its configuration to a large extent during this time, the number of solvent molecules within the volume enclosed by a macromolecule when the pressure reaches its peak value will be greater than at atmospheric pressure. During the subsequent pressure drop, the entrained solvent molecules will flow out of the macromolecule and this flow sets up stresses in the macromolecule. Calculations showed that the stresses generated were of the right order to cause bond rupture.

This shock wave mechanism was extended by Schoon and Rieber[108] on examination of the degradation of poly(dimethyl siloxane) and poly(chloroprene). Examination of the polymers by electron microscopy showed that they were coiled into a series of structures that resembled a 'string of pearls'. The molecular weight of these structures corresponded to the limiting molecular weight obtained.

B) Shear degradation

When a polymer is subjected to hydrodynamic shear, such as being forced through a narrow capillary or being stirred very rapidly, centre cleavage is known to occur[109]. This has been a very difficult mechanism to quantify but several workers have attempted a treatment.

Harrington and Zimm[110] degraded polystyrene in a range of solvents and calculated that the forces generated in good solvents were 3.5×10^{-6} dyne and 4.0×10^{-7} dynes in poor solvents. Although this is not enough force to break the C-C bond, it agrees qualitatively with the results obtained.

The shear stresses during cavitation are thought to arise from the rapid movement around pulsating stable cavitation bubbles. Pritchard *et al*[111,112] studied this by using an apparatus devised by Hughes and Nyborg[113] employing a needle vibrating at a very high frequency, but at low power it was found that shearing effects were produced in the eddy currents around the needle tip. Studying the effects on calf thymus DNA, they found that a limiting molecular weight was reached and there was a very high probability of centre cleavage.

Although there is no clear agreement as to which mechanism best describes the degradation, it is generally accepted that the degradation is caused by a combination of the effects described[21].

1.7.5 Formation of copolymers

Ultrasonic chain scission of polymers results in the formation of macromolecular radicals. If this occurs in the presence of a polymerisable monomer, and in the absence of radical traps, then these macromolecular radicals can initiate the polymerisation of the monomer[114]. This leads to a block copolymer in which one segment is derived from the original polymer and another segment is obtained from the additional monomer.

This effect was first used by Melville and Murray[51] in an attempt to prove the presence of macromolecular radicals, during ultrasonic degradation. The method was also used by Henglein[50,115] to polymerise acrylonitrile in the presence of polyacrylamide in an aqueous solution.

Another possibility for the formation of copolymers is the irradiation of solutions containing a mixture of homopolymers. In this case both homopolymers must

have a degree of polymerisation greater than the limiting degree of polymerisation found from ultrasonic degradation[116]. A majority of the initial work on block copolymers looked at poly(styrene-b-methyl methacrylate) polymers[117,118]. Fujiwara *et al*[119] degraded polystyrene dissolved in methyl methacrylate monomers and established the rate of copolymer formation. Poly(methyl methacrylate) was isolated which was attributed to degradation of the copolymer. This work was extended to the copolymerisation of poly(vinyl chloride) with styrene[120] and methyl methacrylate[121] as well as poly(vinyl alcohol) with methyl methacrylate in an aqueous medium[122]. It was calculated that in the poly(vinyl chloride) copolymers consisted of approximately 80% poly(vinyl chloride).

Most of the poly(styrene-b-methyl methacrylate) copolymers have been prepared by the sonication of the two homopolymers[118]. Nakagawa et al[123] sonicated a mixture of polystyrene and poly(methyl methacrylate) dissolved in toluene. A copolymer was produced with molecular weights lower than either of the starting polymers.

Malhotra[116,124] has studied the degradation of polystyrene in the presence of a range of poly(alkyl methacrylates), dissolved in toluene. The copolymers were isolated and purified by selective solvents[1]. When the side chains on the methacrylate were methyl, ethyl, isopropyl, n-butyl or phenyl, "scrambled sequence copolymers" were obtained. When the substituents were hexyl, isodecyl, hexadecyl, octadecyl, lauryl and isobornyl, no copolymers were formed. It was found that the homopolymers did degrade but did not recombine. The results were attributed to differing chain "stiffness" of the poly(alkyl methacrylates).

Recently more complex copolymers have been prepared using ultrasound[125-129], including water soluble copolymers[128,129]. It was found that copolymers of poly(ethylene oxide) and poly(acrylamide) could be prepared in a reasonable yield by ultrasound.

1.7.6 Polymerisation of homopolymers from monomers

In 1964 El'Piner[130] stated in a review of the chemical effects of ultrasound that: "polymerisation of monomers in an ultrasonic field does not occur if these monomers are thoroughly dried and do not contain substances in the polymerised state". However, polymers have now been formed from monomers without the initial presence of polymers, originally thought necessary for the production of initiating radicals (obtained from the breakdown of the polymer).

Ultrasonic polymerisation was reported in 1951 by Lindstrom and Lamm[131] for acrylonitrile in an aqueous medium saturated with nitrogen. The initiating species was said to be HO· radicals from the decomposition of water. Berlin confirmed this opinion in his investigation of the polymerisation of polystyrene in the presence of styrene monomer since addition of water to the reaction enhanced the yield of polymer[132].

El'Piner's statement was disproved by Kruus in 1983 when initiation of polymerisation in styrene monomer by intense ultrasound was reported[133]. Since this discovery, it has been found possible to polymerise other purified monomers such as vinyl acetate and methyl methacrylate[134-136].

Kopina[137] compared the characteristics of polystyrene prepared by ultrasound and by thermal initiation. It was found that the use of ultrasound shortened the rate of polymerisation by approximately three times. More importantly, the impurity content in the polystyrene increased with increasing temperature of polymerisation and was lower in ultrasonically initiated polystyrene. Stilbene was said to be the main impurity in each case. Molecular weights of ultrasonically initiated polystyrene were lower than those of thermally initiated polystyrene.

Kruus *et al*[134] reported polymerisation of methyl methacrylate and styrene under several conditions. Whilst looking at the homopolymerisation of methyl methacrylate and of styrene by ultrasound over a large range of temperatures, it was found that the poly(methyl methacrylate) produced was a clear polymer but the polystyrene produced had a temperature dependent dark colour to it. It was found that the polystyrene produced at lower temperatures was much darker and this colouration

was attributed to the fusion of aromatic rings[138]. Obviously this reaction would compete with the initiation of polymerisation via the vinyl group. It would be expected that at lower temperatures cavity collapse would produce higher localised temperatures and a greater possibility of breaking bonds in the aromatic rings.

Miyata et al[139] studied the effects of frequency and intensity on the bulk polymerisation of styrene under ultrasonic irradiation. Azo-iso-butyronitrile (AIBN) was added to the reaction prior to sonication in order to initiate the polymerisation. It was found that the mechanism of polymerisation was not affected by the ultrasound, but the overall rate constant decreased linearly with increase in the intensity whilst the average molecular weight increased slightly. A range of frequencies was used, 200, 400, 600 and 800 kHz. A maximum for the rate of polymerisation was found at 400 kHz. However, it must be noted that the same intensity was used for all frequencies, and as was discussed in Section 1.4.1, to obtain equivalent effects at higher frequencies, greater intensities are required.

Activation energies have been obtained for the bulk polymerisation of methyl methacrylate in the presence of ultrasound[140]. The value obtained was approximately 19 kJ mol^{-1}, very close to that observed for bulk thermal polymerisation, provided that the initiation step is excluded. This suggests that the activation energy for the initiation step is 0 kJ mol^{-1}, as found in photopolymerisation.

Kruus[141] also studied the effect of dissolved gas on the polymerisation of nitrobenzene. It was found that the rate decreased in the presence of gases with high solubility. This could be predicted from equations 1.16 and 1.17.

1.8 Polymers in Solution

Many techniques of polymer characterisation are performed when the polymer is in solution. This, together with the fact that some of the results are linked with the properties of polymers in solution, has made it necessary to discuss some of the thermodynamics of polymer solutions.

A polymer can take up a very large number of conformations in solution. A

major influence on the conformation is the degree of interaction between the polymer and the solvent. In a thermodynamically 'good' solvent, contacts between polymer segments and solvent molecules are energetically favourable so that the coil expands to maximise these interactions. Conversely, if the contacts are unfavourable, the polymer chain will minimise the interactions by adopting a tightly coiled conformation in a thermodynamically 'poor' solvent. The intermediate stage where the polymer adopts an undisturbed conformation is termed a "theta" solvent.

These effects may be quantified in a number of ways. They include the root mean square end-to-end distance or more usually the "radius of gyration", S, which is the root mean square distance of the polymer segments from the centre of gravity[142]. This is shown in Figure 1.12

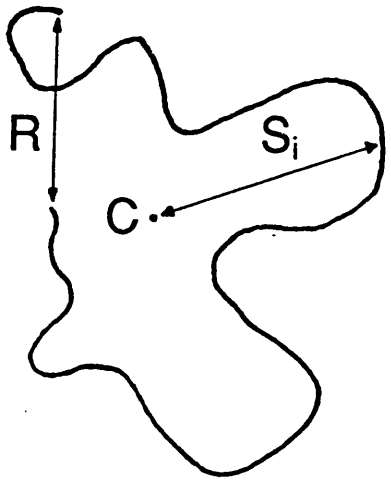

FIGURE 1.12. Representation of a polymer chain in solution. R is the "end to end " distance, S is the distance of a segment. i, from the centre of gravity, C, of the polymer.

An alternative approach to defining the polymer conformation is to use a thermodynamic property derived from the Flory-Huggins theory of polymer solutions. This was derived independently by P J Flory[143,144] and M L Huggins[145,146]. The theory

is based on a statistical mechanical treatment of a lattice model of polymer solutions. The theory predicts the free energy of mixing of a polymer solution from the equation.

$$\Delta G_m = RT(n_1 \ln \varnothing_1 + n_2 \ln \varnothing_2 + \chi n_1 \varnothing_2)$$

where ΔG_m is the free energy of mixing, R is the molar gas constant, T is the temperature, n_1 and n_2 are the number of moles of solvent and polymer respectively, $\varnothing_1$ and $\varnothing_2$ are the volume fraction of solvent and polymer respectively and χ is the Flory-Huggins interaction parameter, which quantifies the polymer/solvent interactions. A polymer in a theta solvent such as polystyrene in cyclohexane at 34°C will have an interaction parameter of 0.5. Polymers in 'good' solvents will have lower interaction parameters. In good solvents, contacts between polymer segments and solvent molecules are energetically favourable so that the coil expands to maximise these interactions. In a poor solvent, the polymer chain minimises the interactions by adopting a tightly coiled conformation. This can be seen in Figure 1.13

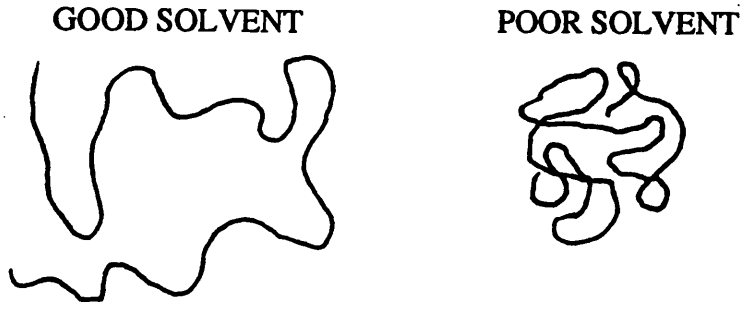

FIGURE 1.13. Polymer conformations in solution.

There are many different ways of measuring the interaction parameter, such as by osmometry, vapour sorption[147], gas-liquid chromatography [148,149], freezing-point depression of a polymer[150], light scattering[151,152] and viscometry[153-155].

Owing to the fact that the concentration of the polymer in the solvent during viscometric analysis would be approximately equivalent to that in the degradation experiments, and the availability of a viscometer, a viscometric approach was used to calculate χ in this thesis. This is discussed in the following section.

1.8.1 Solution viscometry and the Flory-Huggins interaction parameters

Solution viscometry has been recognised as a technique for the measurement of the molecular weight of polymers since the work of Staudinger in the 1930's[156]. The value of molecular weight obtained is a viscosity average, M_v. This is closer to M_w than M_n. The technique gives no indication of the polydispersity of the polymer.

Although in this thesis viscometry was not used to measure molecular weights, the technique enabled measurement of the Flory-Huggins interaction parameter, χ.

Due to the time consuming nature of solution viscometry, a comparison of two single point methods to calculate $[\eta]$ with the normal extrapolation procedure was undertaken. This single point intrinsic viscosity was then used to calculate χ and this value was compared to χ calculated using the extrapolated intrinsic viscosity in order to examine whether it is possible to obtain χ with single point measurements, without introducing large errors.

i) Theory of solution viscometry

Polymers dissolved in solvents markedly increase the solution viscosity. This is calculated by measuring the flow times of the solution and pure solvent through a capillary tube. The relative viscosity can be calculated from

$$\eta_{rel} = \frac{t_s \rho_s}{t_o \rho_o} \qquad 1.19$$

where t_s and t_o are the flow times of the solution and solvent respectively and ρ_s and ρ_o are their corresponding densities. Since dilute solutions are used, it is assumed that $\rho_s = \rho_o$.

Dilute solution viscosity data are normally plotted according to one of three equations:

$$\frac{\eta_{sp}}{c} = [\eta] + K'_H [\eta]^2 c \qquad 1.20$$

$$\frac{\ln \eta_{rel}}{c} = [\eta] - \beta [\eta]^2 c \qquad 1.21$$

$$\log \frac{\eta_{sp}}{c} = \log [\eta] + K'_M [\eta] c \qquad 1.22$$

where $\eta_{sp} = \eta_{rel} - 1$

Equation 1.20 is the Huggins equation[157] and K_H, the Huggins constant related to the size and shape of polymer molecules in solution[158,159].

Equation 1.20 is the Staudinger Equation, sometimes preferred to the Huggins equation due to it having a smaller slope and hence allows extrapolation of the data to infinite dilution with greater accuracy. Equations 1.20 and 1.21 have the same intercept and hence to obtain [η], the intrinsic viscosity, with greater accuracy, the data is often plotted in both forms.

Equation 1.22 is the Martin equation[160] which was designed to account for any upward curvature in the experimental plots of equation 1.20.

Extrapolation of the plots to infinite dilution gives a value for [η]. This is related to the molecular weight of the polymer by the Mark-Houwink

equation[161] (Equation 1.11). The Mark-Houwink constants, K and α are obtained by measuring $[\eta]$ as a function of M for a series of monodisperse samples and plotting log $[\eta]$ against log M from which a straight line is obtained and log K and α are the intercept and slope respectively. The value of α varies between 0.5 and 1.0 depending on the structure of the polymer and nature of the solvent. This semi-empirical relationship is valid only for linear polymers.

ii) Single point determination of the intrinsic viscosity.

The main drawback of the use of solution viscometry is that the measurements of η_{rel} are made at a series of concentrations and so is very time-consuming. A much easier method would be to determine the relative viscosity at a single concentration and from this estimate $[\eta]$. A number of workers have proposed such methods[162-167]. However, most of these have referred to a particular polymer system, and were not proposed for general applicability. During this study two single point methods that were more generally applicable were examined by calculating the single point $[\eta]$ and comparing this with the usual method of extrapolating results from a series of concentrations.

Soloman and Ciuta[162], by combining the Huggins[157] and Kraemer[168] equations, suggested that $[\eta]$ could be found using the equation

$$[\eta] = \frac{\sqrt{2}}{C}\sqrt{\eta_{sp} - \ln \eta_{rel}} \qquad 1.23$$

This equation was valid for polymer-solvent systems where the solution concentration of 0.2% was used.

Rudin[166,167,169] proposed a method that would have a wider applicability for slightly more concentrated solutions. The model assumed the existence of non-interpenetrating solvated spherical polymer molecules. A relation between

the volume fraction of solvated polymer molecules and relative viscosity was derived.

The volume fraction, $\varnothing$, of swollen polymer molecules in solution at a concentration, C, (g cm^{-3}), is given by

$$\varnothing = \frac{0.524\, C\, \epsilon_o}{0.524\rho + C(\epsilon_o - 1)} \qquad 1.24$$

where ρ is the density of the polymer at the solution temperature (g cm^{-3}) and ϵ_o is the infinite dilution swelling factor, given by

$$\epsilon_o = \rho \frac{[\eta]}{2.5} \qquad 1.25$$

Equation 1.24 is confined to concentrations such that

$$0 \leq C \leq 0.524\,\rho \qquad 1.26$$

Using $\varnothing$ from equation 1.23 it was shown that

$$\eta_o/\eta = \eta_{rel}^{-1} = 1 - 2.5\varnothing + 11\varnothing^5 - 11.5\varnothing^7 \qquad 1.27$$

where η_o and η are the solvent and solution viscosities respectively.

It was further shown that for concentrations in the appropriate range

$$[\eta] = \frac{\varnothing(1.31\rho - 2.5C)}{(C\rho)(0.524 - \varnothing)} \qquad 1.28$$

Thus from a single measurement of η_r, $\varnothing$ and hence $[\eta]$ can be calculated.

The value for $\varnothing$ was calculated from equation 1.27 using a Newton-Raphson

type iterative procedure, where only one root is real, positive and in the range

$$0 \leq \varnothing \leq 0.524 \qquad 1.29$$

iii) Calculation of the Interaction Parameter.

The interaction parameter, χ, is often used as a parameter describing the thermodynamic quality of a solvent for a polymer. As such, it determines the conformation adopted by chains in solution due to interaction with solvent molecules and hence affects the viscosity.

Kok and Rudin[153-155] developed a model showing that χ could be calculated from knowledge of the second-virial coefficient. The second virial coefficient could be calculated from

$$A_2 = \frac{16\pi N_o [\eta]}{M(9.3x10^{24} + 4\pi N_o C([\eta] - [\eta]_\theta))} \left\{ 1 - \frac{[\eta]_\theta}{[\eta]} \right\} \qquad 1.30$$

where M = polymer molecular weight

N_o = Avogadros number

C = concentration in g cm^{-3}

$[\eta]$ = intrinsic viscosity ($cm^3\ g^{-1}$)

$[\eta]_\theta$ = intrinsic viscosity under theta conditions

The value for $[\eta]_\theta$ can be calculated from

$$[\eta]_\theta = K_\theta M^{0.5} \qquad 1.31$$

In equation 1.32, K_θ = 72.03 $dm^3\ g^{-1}$ for polystyrene[170]. The value of χ can then be calculated from

$$\chi = 0.5 - A_2\rho_2V_1 \qquad 1.32$$

where ρ_2 is the density of the polymer (g cm^{-3}) and V_1 is the molar volume of the solvent (cm^3 mol^{-1}). The values for χ can be obtained up to a concentration of $0.5c_x$, where

$$c_x = \frac{9.3 \times 10^{24}}{4\pi N_o[\eta]_\theta} \qquad 1.33$$

Concentration dependence of χ could not be handled by this method, however, it did account for its molecular weight dependence.

Tseng and Lloyd[171] employed an alternative approach for calculating χ from $[\eta]$. They showed that by combining the Flory-Huggins lattice model of polymer solutions with the Flory-Fox treatment of solution viscosity[172,173], the interaction parameter was given by

$$\chi = \frac{1}{2} - \frac{V_1}{2C'_mkM}\left\{\frac{[\eta]^{1.66}}{[\eta]_\theta^{0.66}} - [\eta]\right\} \qquad 1.34$$

where V_1 is the molar volume of the solvent and C'_mk is a constant dependent only on the specific volume of the polymer at a given temperature and is equal to 2.4×10^{-3} for polystyrene[172].

A similar equation was also derived, using a modified viscosity treatment proposed by Kurata, Stockmayer and Riog[174] designed to account for the non-Gaussian shape of the polymer chains in solution.

$$\chi = \frac{1}{2} - \frac{V_1}{2C'_mkM}\left\{\left(\frac{[\eta]^5}{[\eta]_\theta^{2.57}}\right)^{\frac{1}{2.43}} - \left(\frac{[\eta]^3}{[\eta]_\theta^{0.57}}\right)^{\frac{1}{2.43}}\right\} \qquad 1.35$$

Other methods are available for deriving χ from $[\eta]$ such as those of Chee[175,176]. However, these require knowledge of Mark-Houwink constants which were not available for all of the solvents investigated. These can be predicted by a method derived by Chee[175] or by using group contribution methods as described by Van Krevelen[177].

1.8.2 Light Scattering

Light scattering is an absolute method of calculating the weight average molecular weight of polymers, together with their radius of gyration and second virial coefficient. In this study the technique was used to examine the amount of branching obtained during the polymer degradation. This is examined by studying the variation in the second virial coefficient during the reaction[178] and will be discussed in more detail in Section 3.8.

The theory of light scattering was first developed by Lord Rayleigh in 1871 during his studies on the properties of gases. He discovered that the quantity of light scattered, for particles small compared to the wavelength of light was inversely proportional to the number of scattering particles per unit volume and to the fourth power of the wavelength. The theory was adapted by Debye[179] and Zimm[180] and the following equation (overleaf) derived:

$$\frac{k^*c}{R_\theta} = \left(\frac{1}{\overline{M}_w}\right)\left[1 + \left(\frac{16\pi^2}{3\lambda^2}\right)\langle S^2\rangle_z \sin^2\left(\frac{\theta}{2}\right) + 2A_2c\right] \qquad 1.36$$

where:

k^* = optical constant for a particular system

$= 2\pi^2 n_o^2 \left(\frac{dn}{dc}\right)^2 \lambda_o^{-4} N_o^{-1}$

n_o = refractive index of solvent

$\frac{dn_o}{dc}$ = specific refractive index increment

λ_o = wavelength of light in vacuo

N_o = Avogadro's number

R_θ = measured excess scattering intensity of solution over that of pure solvent (Rayleigh ratio)

c = concentration (mg/ml)

M_w = weight average molecular weight

A_2 = second virial coefficient

λ = wavelength of light in the medium

θ = angle at which scattering is measured

$\langle S^2\rangle_z$ = mean square radius of gyration

This equation describes the light scattering from a polymer solution of low concentration and at low angles.

The value of (dn/dc) can be calculated experimentally[181], however, the value for polystyrene in toluene is well documented[182] and the value of 0.1065 ml g^{-1} was used throughout these experiments.

The Zimm treatment gives the most accurate graphical procedure for the derivation of light scattering parameters and was the method used in these experiments. In this treatment, measurements are made at a series of angles for different concentrations. A double extrapolation procedure is employed by plotting k^*c/R_θ

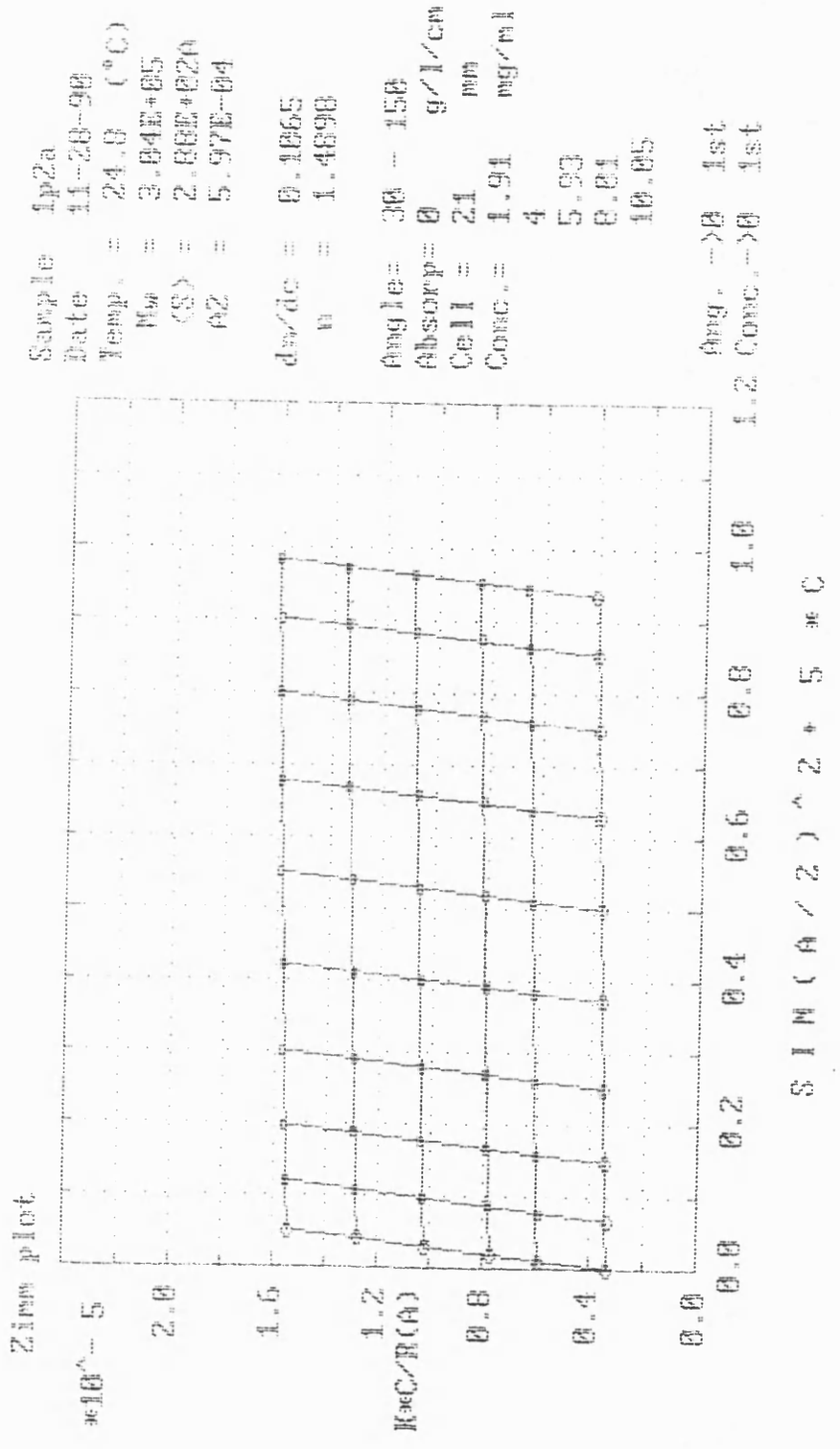

FIGURE 1.14. Zimm Plot obtained from Static Light Scattering.

against $\sin^2(\theta/2)$ + kc and extrapolating at constant concentration and constant angle to obtain a Zimm Plot as shown in Figure 1.14. The extrapolated points at different angles for the zero concentrations are extrapolated to zero angle, to cut the k^*c/R_θ axis, and similarly the points of zero angle at different concentrations are extrapolated to zero concentration. The two extrapolations should cut the k^*c/R_θ axis at the same point.

The reciprocal of the intercept, $[k^*c/R_\theta]_{\theta=0}^{c=0}$ is equal to the weight average molecular weight of the polymer. The gradient of the graph at zero angle gives a measure of the second virial coefficient, A_2. The mean square radius of gyration $\langle S^2 \rangle_z$ is given by the intercept and the initial slope of the line c=0

$$\langle S^2 \rangle_z = \left(\frac{3\lambda^2}{16\pi^2} \right) \left[\frac{\text{Initial slope of line c=0}}{\text{Intercept } [k^*c/R_\theta]_{\theta=0}^{c=0}} \right] \qquad 1.37$$

CHAPTER TWO

EXPERIMENTAL

2.1 Materials

The toluene (BDH Ltd), HiPerSolv, HPLC Grade (purity 99.9%) and tetrahydrofuran (Aldrich Ltd) (purity 99%), used as GPC eluents were used as received. The tetrahydrofuran was inhibited with butylated hydroxytoluene (0.025%). This was necessary to avoid peroxide formation in the tetrahydrofuran as the peroxides can change the surface of the column packing.

The solvents used for the ultrasonic degradations and the viscometric measurements, obtained from Aldrich Ltd were as follows, the purity being shown in parentheses:

Benzene, HPLC grade (99.9%), carbon tetrachloride, HPLC grade (99%), chloroform, ACS reagent, HPLC grade (99.9%), cyclohexane, ACS reagent (99%), dichloromethane, ACS reagent (99.6%), ethyl acetate, ACS reagent (99.5%), ethyl benzene (99%), methyl butyrate (99%), 3-methyl-2-butanone (99%), propyl benzene (98%), tetrahydrofuran, HPLC grade (99%), toluene, ACS reagent (99%), *o*-xylene (97%).

These were all used as received for the degradations but were filtered using 0.2 μm Nylaflo filters (Gelman Sciences) as described in Section 2.3.1 for use in the viscometric experiments. The solvents used for the polymer and copolymer purification were reagent grade from Aldrich Ltd.

The monomer used for the polymerisation studies was methyl methacrylate (Aldrich Ltd) (99%) inhibited with 10 ppm hydroquinone monomethyl ether. Before polymerisation could be achieved it was necessary to remove the inhibitor from the monomer.

2.1.1 Purification of the monomer

The monomer was purified using the method of Kruus and Patraboy[140]. The monomer (100 cm^3) was washed twice with equal volumes of 10% w/v sodium hydroxide solution and washed with distilled water until neutral. The monomer was then dried by washing twice with equal volumes of saturated aqueous sodium chloride

and allowing it to stand over anhydrous sodium sulphate for six hours. It was then stored in a dark bottle in the refrigerator over activated molecular sieves (type 3A) which had been dried at 110°C overnight. The monomer was then distilled under vacuum before use. Gas liquid chromatographic analysis showed the procedure to give the methyl methacrylate a purity in excess of 99.5%[122].

2.2 Sonication Experiments

The ultrasound was introduced into the reaction using a Sonic System VC50 ultrasonic probe. This was used in preference to an ultrasonic bath due to it providing a higher intensity of ultrasound in the reaction. There was only a very small amount of polymer degradation obtained when an ultrasonic bath was used.

2.2.1 Reaction cell design

It has been found that the shape of the reaction cell can affect ultrasonic reactions[37]. For both the degradation and polymerisation experiments a specially designed cell was used (Fig. 2.1).

A significant amount of heat is produced during sonication with an ultrasonic probe and so a water jacket was incorporated in the design. This enabled the temperature in the reaction cell to be controlled to ± 0.5°C. It was necessary to keep the reaction temperature constant to avoid any possible thermal polymerisation and because the kinetics of the reactions were being measured.

The internal flask had a modified bottom directly under the probe tip. This provided very efficient mass transfer during the sonication, so ensuring that all the contents were sonicated to the same degree.

The probe was inserted into the reactants to the same depth and in the same position for each experiment. This was ensured by leveling the top of the probe with the top of the reaction cell neck.

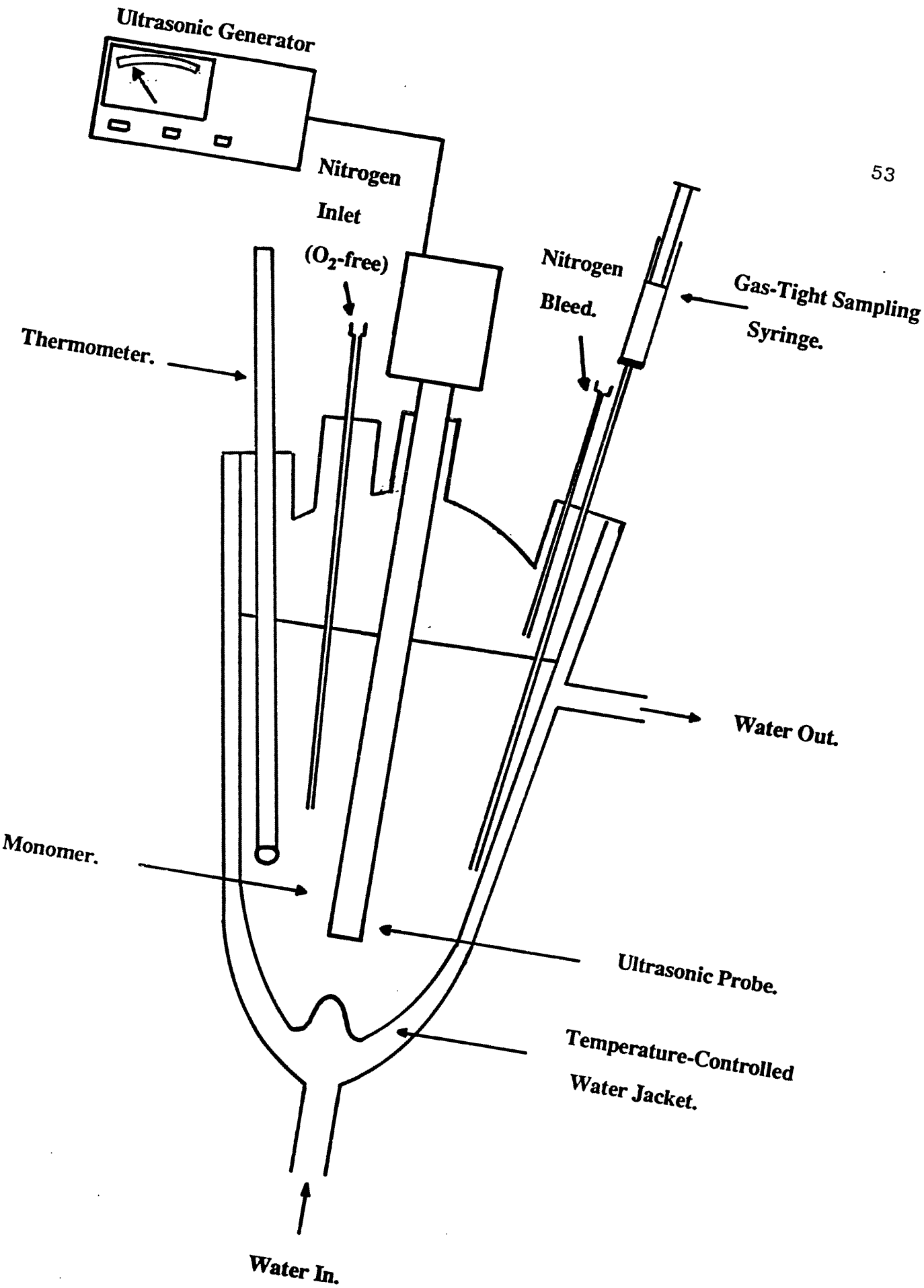

FIGURE 2.1. Ultrasonic Reaction Vessel. (Total volume = 100ml)

2.2.2 Calibration of probe intensity

There are various methods of stating the intensity used during sonication. Some workers report the nominal output as stated by the equipment manufacturers[37]. This has the disadvantage that the manufacturers' value is normally related to the amount of energy being supplied to the transducer and bears no relationship to the amount of energy being transferred to the reaction. To overcome this problem El'tsefon and Berlin[183,184] have suggested that the total energy input into the system should be used. A new parameter, q, was suggested

$$q = \frac{Ut}{Vc} \qquad 2.1$$

where U is the intensity, t, is the irradiation time, V is the volume of the solution and c is the polymer concentration.

Due to the reaction set-up being identical each time in this study, it was decided that a calorimetric approach would give the most reliable measurement. A value is stated for the time taken to heat a known volume of distilled water through a measured temperature rise. This accounts for the fact that in other studies various reaction cells are used which absorb differing amounts of energy and so should enable other workers to compare results with the ones presented here. In order for a value to be given to the intensities used during the experiments, the temperature rise was converted to an absolute value as follows.

The ultrasonic reaction vessel was set up as for the polymerisation and depolymerisation experiments. The water jacket was filled with water (non-circulating) and 50 cm^3 of distilled water was pipetted into the vessel. The system was allowed to equilibrate at room temperature and a heater switched on. The voltage and current through the heater were recorded using a Thandar TS3021S multimeter and the initial temperature was noted. The temperature rise was monitored at regular intervals.

The energy supplied to the heater was calculated from

$$E = VIt \qquad 2.2$$

where V is the voltage, I is the current and t is the time in seconds.

A total heat capacity, C, of the system was calculated from the temperature rise obtained.

The procedure was then repeated substituting the ultrasonic probe for the electrical heater, enabling the ultrasonic energy supplied by the probe to be calculated. The initial temperature of the water was noted and the ultrasonic probe turned on. The temperature rise was monitored. The ultrasonic power was calculated using

$$P = \frac{C\Delta\Theta}{t} \qquad 2.3$$

where C is the total heat capacity of the system, $\Delta\Theta$ is the temperature rise and t is the time in seconds.

This value was then converted to power per unit area by dividing by the diameter of the probe tip obtained from the manufacturers' specifications.

Results for the Intensity Calibration

Volume of distilled water = 50 cm^3 ($\pm$ 0.005%)

A) Electrical Heater

Time(s)	Temp. (°C)	Time(s)	Temp. (°C)
0	22.8	360	24.7
60	23.0	420	25.0
120	23.6	480	25.2
180	24.0	600	25.5
240	24.3	900	26.3
300	24.5	1200	27.0

Temperature rise was 4.2°C over 1200 seconds.

Current, I, = 137.57 mA

Voltage, V, = 11.93 V

Therefore, total heat capacity, C, = 468.9 JK^{-1}

B) Ultrasonic Probe

Time(s)	Temp. (°C)	Time(s)	Temp. (°C)
0	25.2	360	31.0
60	26.4	420	31.8
120	27.7	480	32.4
180	28.7	600	33.8
240	29.6	900	26.6
300	30.4	1200	39.2

Temperature rise was 14.0°C over 1200 seconds.

The power supplied, P = 5.47W.

The diameter of the probe tip = 6.4 mm.

Therefore, the area of the tip = 0.3217 cm^2

Intensity of the ultrasound = 17.0 W cm^{-2}

C) Estimation of the Errors in the Intensity Calibration:

The main errors arise from the thermometer and stop clock readings. Each thermometer reading is subject to ± 0.2°C.

For electrical heating, $\Delta\Theta = T_2 - T_1$, where $T_2 > T_1$

$$\text{Error} = \pm \left\{ \frac{0.2}{27.0} + \frac{0.2}{22.8} \right\} \times 100 = \pm 1.6\%$$

For ultrasonic heading, $\Delta\Theta$,

$$\text{Error} = \pm \left\{ \frac{0.2}{39.2} + \frac{0.2}{25.2} \right\} \times 100 = \pm 1.3\%$$

Therefore the total error = ± 2.9%.

The error in timing is estimated at ± 1 second. Therefore the error in timing of electrical heating and ultrasonic heating

$$= \pm \left\{ \frac{1}{1200} + \frac{1}{1200} \right\} \times 100 = \pm 0.17\%$$

Taking these errors into consideration, the total error is ± 3% or ± 0.16 W.

Other errors do occur such as heat loss to the surroundings and non-efficient heat transfer especially during the electrical heating and these are very difficult to quantify.

2.2.3 Ultrasonic polymerisation

i) Polymerisation of methyl methacrylate

The purified methyl methacrylate (50 cm^3) was introduced by pipette into the reaction cell which had previously been cleaned with tetrahydrofuran, chromic acid, distilled water and acetone and dried. The monomer was degassed by bubbling nitrogen (oxygen free) through for 45 minutes. It had been found in initial experiments that insufficient degassing either totally prevented polymer formation or caused a very large induction period. This was attributed to oxygen in the system reacting with the methyl methacrylate radicals before they could combine with other monomer radicals.

During the sonication a steady flow of nitrogen was maintained over the monomer, which acted as a 'nitrogen blanket', preventing any oxygen re-entering the system.

Nine 1 cm^3 sample vials were labelled and weighed to ± 0.1 mg using a Sartorius balance. At regular intervals during the sonication 1.00 cm^3 samples were removed using a Hamilton gas-tight syringe. The sonication was

continued while the sample was removed. The sample was very carefully injected into one of the weighed sample bottles. The reaction was undertaken for six hours. After the last sample had been removed, all of the sample bottles were placed in a vacuum desiccator and the unreacted monomer was carefully removed under a low vacuum. It was very important that a low vacuum was used to avoid the sample 'bumping' and the polymer spilling.

ii) Copolymer formation

The same procedure was used for degassing the solution and the sampling techniques as in the case of the polymerisation of the monomer. The polystyrene used in all of the copolymerisations was a secondary standard (Aldrich Ltd), Mn=145000, γ = 2.1. The volume of reactant solution was kept constant at 50 cm^3 for all of the experiments.

Two sets of copolymerisation reactions were investigated. In the first, the concentration of polystyrene dissolved in the methyl methacrylate monomer was varied between 0.5% w/v and 20% w/v. In order to obtain the copolymer composition throughout the sonication, the reaction was quenched by precipitating the solution in a ten-fold excess of ice cold methanol after 1 hr, 2 hr, 4 hr and 6 hr.

In the second set of experiments, the effect of reducing the monomer concentration on the copolymerisation reaction was investigated. This was performed by the addition of methyl butyrate to the methyl methacrylate. This is a solvent with similar physical properties to methyl methacrylate, as shown in Table 2.1.

The concentration of the polystyrene in the solutions was 0.5% w/v in each experiment.

Table 2.1 Physical Properties of methyl methacrylate and methyl butyrate

PROPERTY	METHYL BUTYRATE	MMA
STRUCTURE	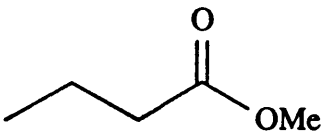	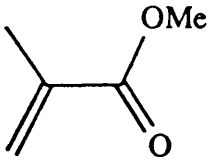
MOLECULAR WEIGHT	102.13	100.13
BOILING POINT	102.3°C	100-101°C
MELTING POINT	-84.8°C	-48°C
DENSITY AT 25°C	$0.8984gcm^{-3}$	$0.944gcm^{-3}$
SATURATED VAPOUR PRESSURE AT 298K	30.23 Torr	36.62 Torr

The series of experiments performed were as follows:

Table 2.2 Schedule for experiment to prepare copolymers

Weight % PS	Vol MMA (cm^3)	Vol Methyl Butyrate (cm^3)	Sonication Time (hrs)
0.5	50	0	6
1	50	0	6
5	50	0	6
10	50	0	6
20	50	0	6
0.5	50	0	1
0.5	50	0	2
0.5	50	0	4
0.5	50	0	6
0.5	37.5	12.5	6
0.5	25	12	6
0.5	12.5	37.5	6
0.5	25	25	1
0.5	25	25	2
0.5	25	25	4

PS = Polystyrene
MMA = Methyl methacrylate

In all cases the copolymers were precipitated and purified. They were then analysed using GPC and the copolymer composition determined using NMR.

2.2.4 Purification of block copolymers

The poly(styrene-b-methyl methacrylate) copolymers were purified according to the method of Malhotra[124]. It was important that any homopolymers were separated from the copolymer before analysis.

The solution containing the homopolymers and copolymers was precipitated into a ten-fold excess of methanol and filtered. The polymer was washed with methanol and dried at 100°C in a vacuum oven.

The polymer was extracted twice with cyclohexane at 34°C, a theta solvent for polystyrene but a non-solvent for poly(methyl methacrylate). The insoluble product was then filtered off, washed with cyclohexane at 34°C and dried in a vacuum oven at 100°C. The product was then extracted twice with acetonitrile, a selective solvent for poly(methyl methacrylate) but a precipitant for polystyrene. The insoluble product was filtered off and washed with acetonitrile and dried in a vacuum oven at 100°C.

This leaves only the block copolymer of poly(styrene-b-methyl methacrylate) containing no homopolymers.

2.2.5 Ultrasonic degradation

The degradation of polystyrene in solution was performed using the same procedure in each experiment. The required amount of polymer was weighed into a beaker previously cleaned with chromic acid, distilled water and acetone. To this was added 50 cm^3 of the solvent at 25°C. When dissolution was complete the mixture was placed in the reaction vessel.

In order to obtain temperatures of -10°C and 0°C, a Grant circulating bath containing ethylene glycol solution was used.

A range of gases from monatomic to polyatomic was used to study the effect of dissolved gases on the degradation. The solution was degassed for 45 minutes by bubbling the appropriate gas through the solution. During the reaction the gas flow was maintained over the solution to keep a positive pressure of gas in the reaction cell.

At regular intervals during the reaction 0.5 cm^3 was removed for GPC analysis.

All of the sonications were carried out for 6 hours.

2.2.6 Production of Telechelic Polystyrene

Polystyrene dissolved in tetrahydrofuran (1% w/v) was sonicated as described in Section 2.2.5, in the presence of 0.5% w/v

a) 9-Bromoanthracene

b) 1-amino-4-bromonaphthalene

Before sonication the solution was degassed and blanketed with nitrogen (oxygen free) as described previously.

After 6 hours sonication the resulting polymers were precipitated into a 10-fold excess of methanol and rigorously purified by redissolving in toluene and precipitating into methanol four times. The resulting polymer was then washed with methanol and dried throughly in a vacuum oven at 110°C.

The polymer was analysed by ultraviolet spectroscopy using a Pye Unicam SP6-250 spectrometer.

2.3 Polymer Analysis

2.3.1 Viscometric measurement of the interaction parameter

The viscometer used for the measurement of the interaction parameters, χ, and the absolute solvent viscosities was a calibrated Ubbelohde viscometer, size Oa. Flow times of at least 200 seconds were obtained to reduce drainage errors[160].

The viscometer had the advantage over ordinary capillary viscometers in that the volume of the liquid in the viscometer could be varied as the position of the suspended liquid level at the bottom of the capillary was always constant.

The polystyrene used was a secondary standard (Aldrich Ltd), with a number average molecular weight of 145000, a viscosity average molecular weight of 245000 and a polydispersity of 2.1, measured by GPC, as described in Section 2.3.4

Before the solvents were used, they were filtered using 0.2 μm Nylaflo filters (Gelman Sciences Ltd). Solutions had concentrations between 2 and 12 g dm^{-3} prepared by weighing the polystyrene into 25 ml volumetric flasks that had been cleaned with tetrahydrofuran, chromic acid, distilled water and acetone. The volumetric flask was then partially filled with the required solvent. When the solvation was complete, the volume was adjusted at 25°C ± 0.1°C. This procedure of independent weighings was less subject to a systematic error than that of dilution of a stock solution.

These solutions were filtered again, using 0.2 μm Nylaflo filters, into the

viscometer and their flow times measured. The viscometer was held in a thermostatted bath at 25°C ± 0.1°C (controlled by a Tempunit TU14 temperature controller), so that both the measurement lines were beneath the surface of the water. In the case of the cyclohexane, a temperature of 34°C ± 0.1°C was used to obtain a theta solvent.

The variation in temperature that can be tolerated in viscometry is very small due to the viscosities of most solvents decreasing rapidly with increasing temperature[185].

It was very important during the measurements that the viscometer was vertical[186] and this was ensured by lining-up the viscometer with a plumb-line dropped into the bath.

The sample was drawn into the upper bulb, after allowing the temperature of the solution to equilibrate, and allowed to flow out under gravity. The flow times were recorded for the solution to flow between the two measurement lines using a Stadion stopwatch. The times were recorded to an accuracy of ± 0.1 second. An average of three readings that had a variation of no more than 0.2 seconds for each concentration was used.

The intrinsic viscosities were measured by the conventional extrapolation techniques as described in Section 1.8.1.

The values of η_{rel}, the relative viscosity from the least concentrated solutions were used in the Rudin and the Soloman-Ciuta single point calculation of intrinsic viscosities.

The calibration constant, B, supplied with the viscometer allowed the viscosity of a solution in centistokes to be calculated by

$$\eta = Bt \qquad 2.4$$

where t is the flow time in seconds.

2.3.2 Sample preparation for light scattering

All of the light scattering experiments were undertaken at Polymer Laboratories Ltd, Church Stretton under the guidance of Dr S. O'Donohue.

The light scattering system used was a Photal DLS-700, shown diagramatically in Figure 2.2.

The polystyrene, a secondary standard (Aldrich Ltd), Mn = 120000, $\gamma = 2.7$ was degraded ultrasonically in toluene at two concentrations, 1% w/v and 15% w/v. Samples were taken at 10 minutes, 60 minutes and 360 minutes. These were precipitated into ice cold methanol, filtered and dried in a vacuum oven at 100°C.

All of the solvents used throughout the sample preparation were filtered four times using 0.02 μm Antop filters (Gelman Sciences Ltd). Presence of dust particles disturb the optical stability of the system and affect the angular distribution of the scattering intensities especially at low angles.

10 ml volumetric flasks were washed with the filtered methanol and dried using nitrogen. All of the samples taken during the degradation were made up to concentrations ranging between 1 and 10 mg/ml.

The light scattering cell was carefully rotated in the thermostatted bath until there was no deviation of the laser beam as it passed through the cell.

Before the solutions were placed in the cell, they were filtered three times using 0.2 μm Acrodiscs (Gelman Sciences Ltd).

When the solution was in the cell, it was left to equilibrate for 15 minutes before any measurements were taken. The temperature was controlled to ± 0.2°C.

The angles at which the scattering intensities were measured were 30°, 45°, 60°, 75°, 90°, 105°, 120°, 135° and 150°.

2.3.3 GPC Viscometry

The level of chain branching in those samples studied by light scattering (Section 2.3.2) was also calculated using GPC viscometry, the measurements being undertaken by Dr S. Holding at RAPRA.

The viscosity detector was employed in tandem with a differential refractometer and continuously measured the pressure drop across a capillary which is proportional to its specific viscosity. This was related to the level of branching in the sample by

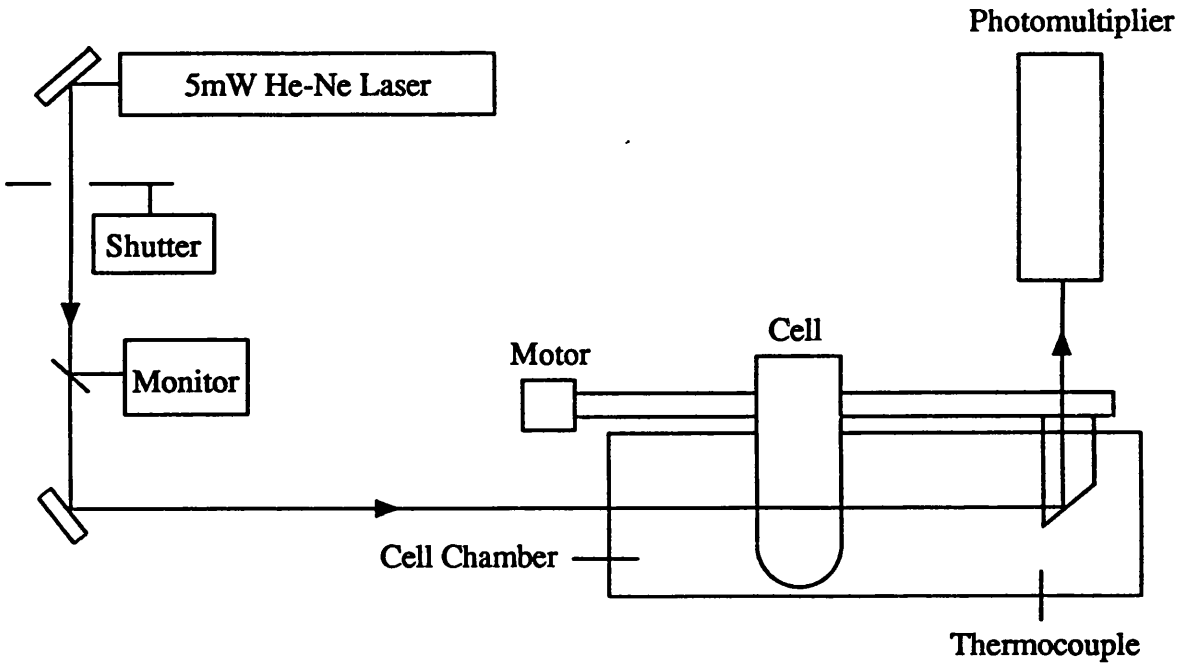

FIGURE 2.2. Light Scattering Photometer.

comparing the value for the polymer being analysed with that for a sample known to be a linear polystyrene as will be discussed in Section 3.8.2.

2.3.4 Molecular weight measurements using GPC

The Gel Permeation Chromatograph used was a Bruker LC41 system, fitted with Polymer Laboratories Ltd PLGel columns having exclusion limits of 10^4, 10^3 and 500 Å and was controlled from an EPSON QX16 data station.

All of the samples run had a concentration of 0.5% w/v to avoid any concentration effects. The eluent was pumped at 1 ml min^{-1} using a constant flow pump. A dual detector system of a Knauer ultraviolet spectrometer and differential refractometer was used for the polymer analysis.

Calibration of the GPC was undertaken using low polydispersity polystyrene standards supplied by Polymer Laboratories Ltd. The molecular weights of the standards were 2650000, 1030000, 675000, 465000, 127000, 68000, 30300, 9200, 2950, 1050.

2.3.5 Copolymer composition from Nuclear Magnetic Resonances spectroscopy

NMR spectra of the homopolymers and copolymers synthesised were recorded in $CDCl_3$on a JEOL GX270 FT-NMR spectrometer using TMS as an internal standard. Both ^{13}C and ^{1}H-spectra were recorded.

The ^{1}H NMR of the copolymer formed can give details on the ratio of component monomers. In the case of methyl methacrylate and styrene, this is calculated by examining the area of two peaks, one solely due to the styrene $C_6H_5^-$, and one due to the methyl methacrylate $-OCH_3$. These spectra are shown in Figure 2.3.

By dividing by the number of protons due to each peak a fraction can be calculated:

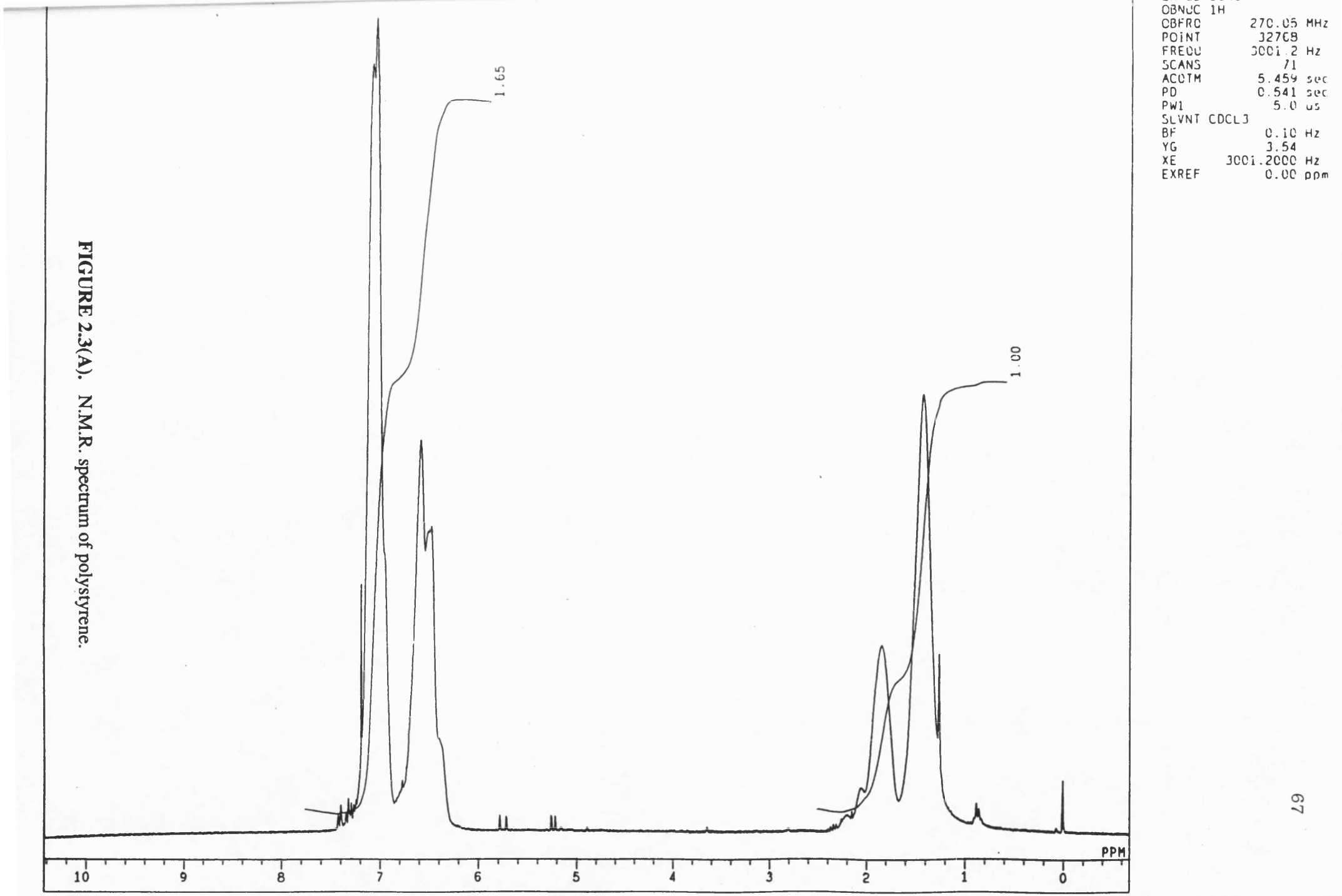

FIGURE 2.3(A). N.M.R. spectrum of polystyrene.

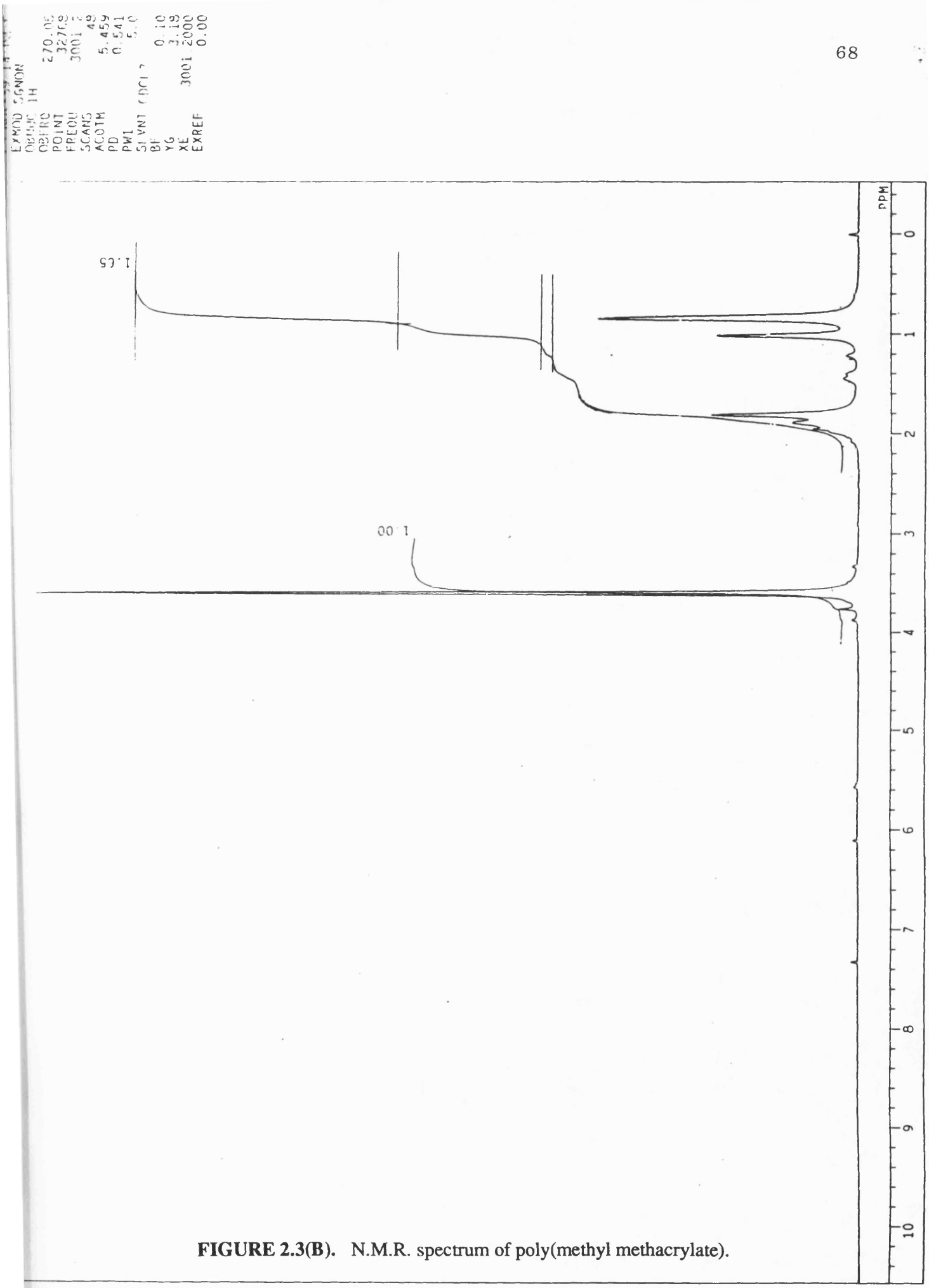

FIGURE 2.3(B). N.M.R. spectrum of poly(methyl methacrylate).

$$\text{Number of styrene units} = \frac{\text{Area } C_6H_5^-}{5}$$

$$\text{Number of methyl methacrylate units} = \frac{\text{Area } -OCH_3}{3}$$

$$\text{Fraction of styrene in copolymer} = \frac{\dfrac{\text{Area } C_6H_5^-}{5}}{\dfrac{\text{Area } C_6H_5^-}{5} + \dfrac{\text{Area } -OCH_3}{3}}$$

2.3.6 Estimation of errors in the results

The largest errors in the results arise from the calculation of the value for the limiting molecular weight. The error from the calculation of the molecular weight from the GPC chromatogram is approximately ± 5%. The error from the extrapolation of the degradation curves is estimated at ± 2000.

CHAPTER THREE

CONTROL OF POLYSTYRENE DEGRADATION

In order to prepare block copolymers with accurately known structure and properties, the factors that control the structure of the macroradical arising from polystyrene degradation, and hence the polystyrene block size, were examined.

The factors that influence the degradation include the starting molecular weight of the polymer, the nature and physical properties of the solvent and any gases dissolved in it, the concentration of the polymer and its conformation adopted in solution, the solution temperature and finally the intensity of the ultrasound.

The properties investigated were the variation of molecular weight with time, i.e. the rate of degradation and the polydispersity of the polymer. The final molecular weight reached during the process was of particular interest. Another factor of importance in the use of polymer materials is the extent of chain branching and the degree of this introduced during the degradation was studied using light scattering and GPC/viscometry.

Before discussing the various factors in detail, the treatment of results will be illustrated using one system.

3.1 Effect of Initial Polymer Molecular Weight

Figure 3.1 shows the effect of sonication of 0.5% solutions of four polystyrene calibration standards dissolved in toluene. As well as showing the effect of initial molecular weight, this figure serves to illustrate some general factors of the degradation described in Chapter One.

It can be seen that the reduction in M_n is faster at higher molecular weights but slows to give a limiting value (M_{LIM}) that is independent of the starting value. For this system, M_{LIM} was approximately 40000. To confirm that no degradation occurred at lower molecular weights, a polymer with molecular weight 30000 was processed under the same conditions but no change in M_n was found.

The standards used had polydispersities in the range 1.01 - 1.05. The preferential degradation of the high molecular weight material results in an initial increase in γ as shown in Figure 3.2 although at longer times, the value falls.

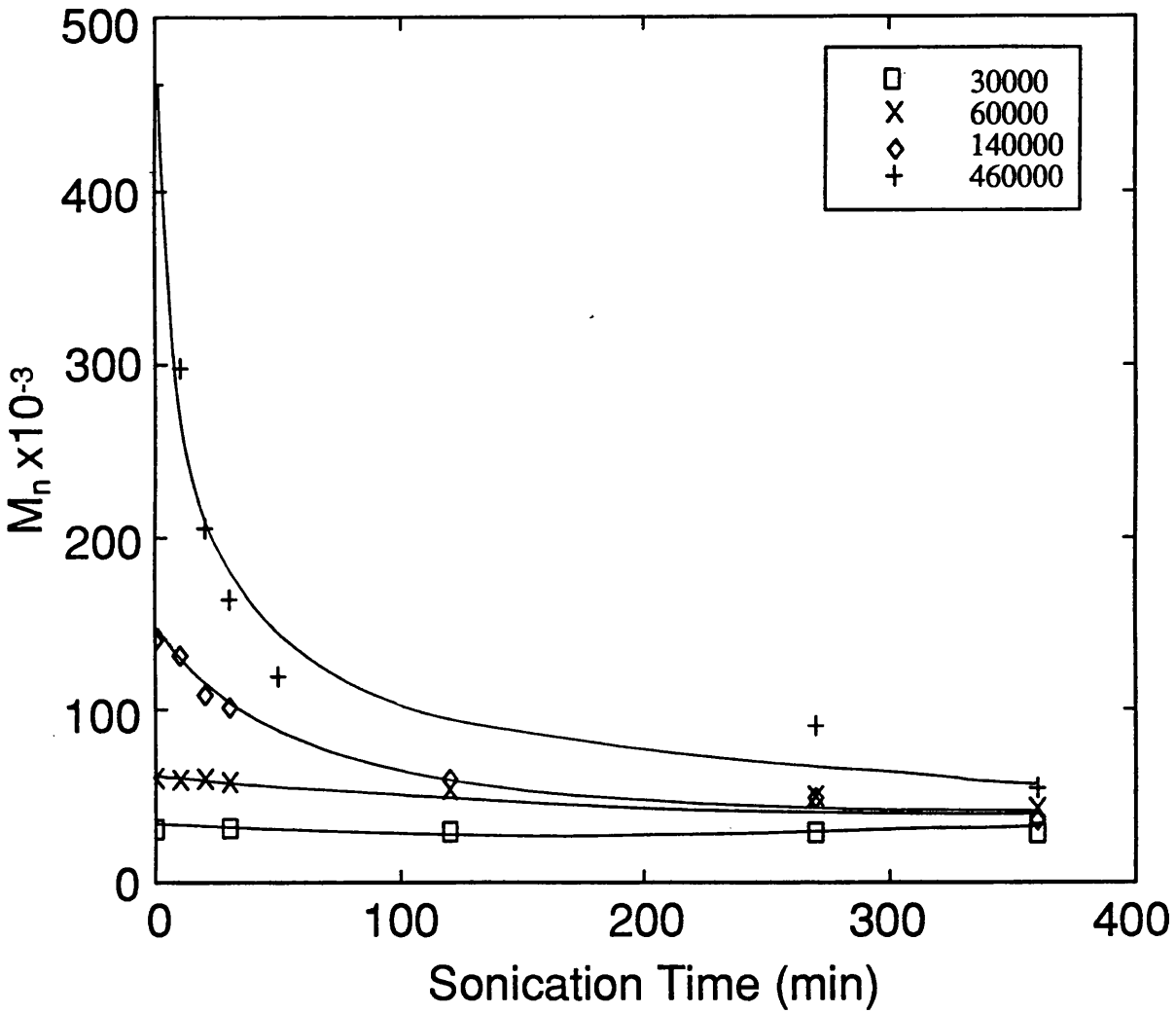

FIGURE 3.1. Variation of number average molecular weight during the sonication of 0.5%w/v polystyrene in toluene having various initial molecular weights.

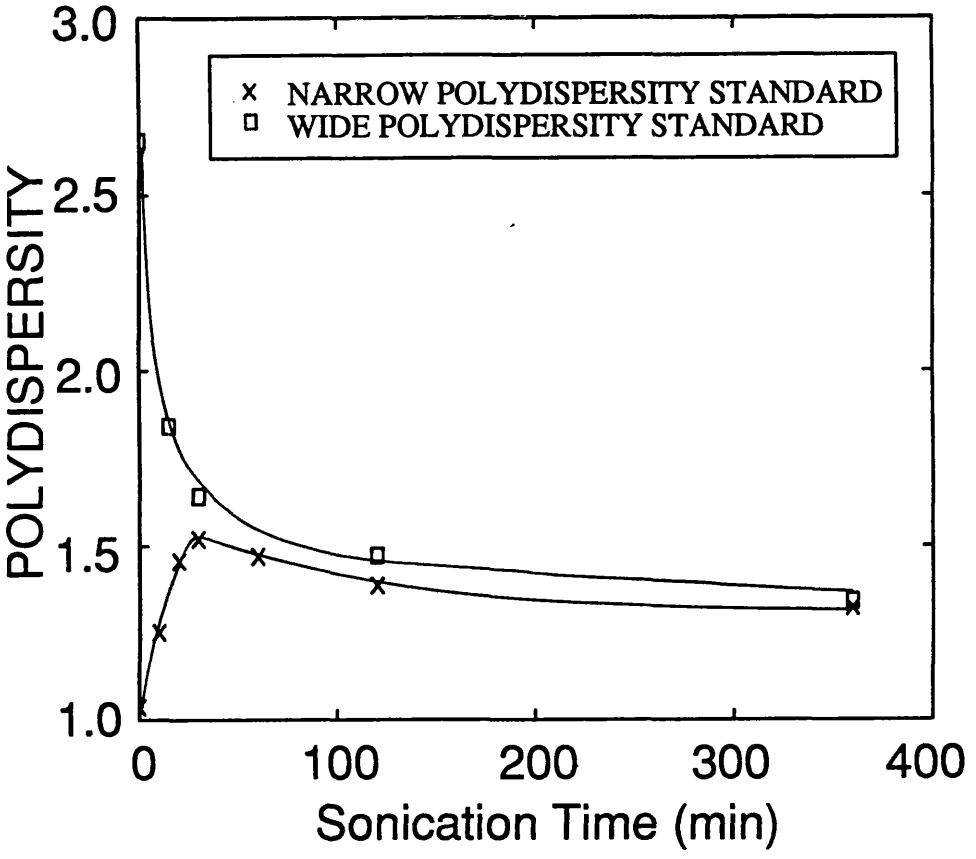

FIGURE 3.2. Variation of the polydispersity of a wide and narrow distribution polystyrene during the sonication of 0.5%w/v polystyrene in toluene.

The property of the high molecular weight polymer degrading more rapidly than low, has a dramatic effect on a polymer with a wide polydispersity. Also shown in Figure 3.2 is the variation in γ for a wide distribution polymer of starting molecular weight 140000.

Another factor affecting the polydispersity is the "centre cleavage" model described in Chapter One. The non random nature of the degradation is shown in Section 1.7.2. The effects described here can all be explained by considering the generally accepted mechanism of the process as outlined earlier.

Early workers suggested that the polymer chains themselves may be acting as cavitation nuclei and so the longer the chain, the more cavitation and hence the greater the degradation[82]. However, this seems unlikely since the total number of monomer units in solution for all of the molecular weights will be the same although the chain lengths are different due to the concentrations being prepared by weight. Therefore, the number of cavitation nuclei present in each sample will be the same.

The effect can be explained using the shock wave mechanism proposed by Thomas[85]. As a chain becomes longer, there will not only be a large velocity gradient between the side of the polymer coil near the cavity and the side away from the cavity, but also between both ends of the chain. One end of the chain may be at a distance far enough away from the cavity to be unaffected by its implosion whereas the other end may be moved very rapidly by the fast moving solvent molecules. As proposed by Thomas[85], this model indicates that there will be a linear dependence of the rate of degradation on the degree of polymerisation of the polymer from

$$\frac{1}{\eta_b} = \frac{dB}{dt} \times \frac{L}{F} \qquad 3.1$$

where η_b is the number concentration of polymer bonds, dB/dt is the rate of bond rupture, F is the force required to cleave the polymer chain and L is the extended polymer length.

3.2 Models for Ultrasonic Degradation Rates

In order to quantify the effect of the various factors, it is necessary to define a rate constant for the process. The nature of polymer molecules, with their distribution of chain lengths makes the exact definition of rate equations very difficult. The degradation process is essentially one of a series of compounds of varying molecular weight undergoing a series of parallel reactions and hence an exact treatment requires the solution of a large number of simultaneous equations.

A number of workers have attempted to define a rate equation for the degradation process. The aim of this section is to introduce these models and to apply each to a range of systems in order to select the most appropriate model. These will then be applied to the various factors described in the preceding section to characterise the effect of each on the degradation.

3.2.1 Rate models

A. Schmid Model[187]: This first attempt at a kinetic scheme considered a monodisperse polymer sample and assumed the rate of chain breakage, dx/dt could be represented by

$$dx/dt = k(P_t - P_{LIM}) \qquad 3.2$$

where P_t and P_{LIM} are the degrees of polymerisation at time t and at the end of the degradation, x is the number of chain breaks per unit volume and k is a rate constant.

Introducing the monomer molecular weight, M_o, and the solution concentration, C, in base moles dm^{-3}, Schmid showed that a rate equation could be derived including the polymer molecular weights at the start of the degradation, M_i, the limiting value, M_{LIM} and that at time t, M_t, that had the form

$$\frac{M_{LIM}}{M_t} + Ln(M_t - M_{LIM}) = \frac{kt}{C}\left(\frac{M_{LIM}}{M_o}\right)^2 + \left(\frac{M_{LIM}}{M_i}\right) + Ln(M_i - M_{LIM}) + Ln\left(\frac{M_t}{M_i}\right) \quad 3.3$$

Hence a plot of $[(M_{LIM}/M_t) + Ln(1 - M_{LIM}/M_t)]$ against t should yield a straight line with a slope of $k/C(M_{LIM}/M_o)^2$.

The main problem with this treatment is the assumption of an initially monodisperse polymer. However, despite this, the model has been found to give good linear fits for a range of systems[187,188].

The Schmid model has been the most extensively used for the calculation of ultrasonic rate constants. Workers such as Jellinek and White[23] and Mostafa[189] have attempted to improve this original model. However, owing to the great complexity and limited improvement using these models, they will not be discussed here.

B. Xu Rate Model: Xu and co-workers[190], studying the degradation of polybutadiene used a basic first order rate model,

$$Ln\left(\frac{M_t}{M_i}\right) = -kt \quad 3.4$$

and found that the initial degradation gave good linear fits.

C. Fujiwara Rate Model: Fujiwara *et al.*[121] derived a rate of mechanical degradation as:

$$\frac{1}{(P_t - P_{LIM})} = kt + \frac{1}{(P_i - P_{LIM})} \quad 3.5$$

where P_i, P_t and P_{LIM} are the degree of polymerisation of the polymer at time t=0, time t=t and the limiting degree of polymerisation respectively. It was

found that this gave very good linear fits to the degradation of polystyrene in cyclohexane.

D. El'tsefon and Berlin Rate Model[184]: El'tsefon and Berlin[184], studying polystyrene solutions of benzene, predicted that the degradation obeyed the equation

$$P_t = \frac{P_i}{\sqrt{1 + 2\beta P_i^2 kt}} \qquad 3.6$$

where β is a constant that takes into account the polydispersity of the polymer. The rate constant could be found as the slope of the straight line from plotting $(P_i/P_t)^2$-1 against t.

E. Sato and Nalepa Rate Model[191]: Sato and Nalepa[191], studying the ultrasonic degradation of cellulose obtained the degradation rate constant using a model derived by Jellinek[192] for a random degradation process. The relationship between the number average degree of polymerisation (P_t) and the time, t is given by

$$-\mathrm{Ln}\left(1 - \frac{1}{P_t}\right) = kt - \mathrm{Ln}\left(1 - \frac{1}{P_i}\right) \qquad 3.7$$

When P_n is large, equation 3.7 can be approximated by

$$1/P_t = 1/P_i + kt \qquad 3.8$$

The number average molecular weight, M_n, is given by

$$M_n = M_o P_n \qquad 3.9$$

where M_o is the average molecular weight of each monomer unit, hence equation 3.8 can be reduced to

$$1/M_t = 1/M_i + k't \qquad 3.10$$

where M_t and M_i are the number average molecular weights of the polymer at t=t and t=0 respectively and $k' = k/M_o$.

F. Shear Degradation Rate Model[193]: As described in Section 1.7.4, some mechanisms have considered the degradation to be due to shear effects. However, no rate models have been applied considering shear degradation and hence a pure shear kinetic model was applied to the results in this thesis. An overall reaction rate can be defined as

$$\frac{dB}{dt} = k(B_{LIM} - B_t) \qquad 3.11$$

and hence the rate is found from

$$\text{Ln}\ \frac{B_{LIM}}{B_{LIM} - B_t} = kt \qquad 3.12$$

where B_{LIM} and B_t are the number of bonds broken at the limiting molecular weight and time, t, respectively.

The number of bonds broken, B, is defined as

$$B = \frac{M_i}{M_t} - 1 \qquad 3.13$$

G. Ovenall Rate Model Henglein[13,14] was the first worker to measure the number of bonds broken in the polymer as a function of the degradation time. He proposed that the breakage of the covalent bond led to two macromolecular radicals which could be monitored by the use of a radical scavenger, 2,2-diphenylpicrylhydrazyl (DPPH).

Using these results, Ovenall *et al* produced a rate equation for the rate of bond breakage,

$$\frac{dB}{dt} = k\,Ln\left(\frac{P_t}{P_{LIM}}\right) \qquad 3.14$$

and from this a rate equation can be found:

$$Ln\left(\frac{1}{M_{LIM}} - \frac{1}{M_t}\right) = Ln\left(\frac{1}{M_{LIM}} - \frac{1}{M_i}\right) - k\,\frac{M_{LIM}}{CM_o}\,t \qquad 3.15$$

A plot of $Ln(1/M_{LIM} - 1/M_t)$ against t produces a straight line with a gradient of $-k/C(M_{LIM}/M_o)$.

H. Initial Rate Model: During the analysis of the results, it was found that the rate constants from some models did not correlate with the observed rate of degradation. To give a more qualitative idea of the rates, the change of M_n over the first 30 minutes sonication was calculated. This was taken to be the initial rate of the degradation.

3.2.2 Application to experimental systems

In order to decide which of the preceding models best describes the process in polystyrene solutions, each was applied to the results for the four different molecular weight standards. As part of the study degradations were also run in a number of

solvents and under various gases and the rate models were also applied to these. It is not the intention to fully discuss the various effects here, they will be dealt with more comprehensively in later sections. In this section, only the applicability of the various rate models will be examined.

Table 3.1 Molecular weight variation of rate constants for polystyrene in toluene

	RATE CONSTANTS / min^{-1}							
M_i	Schmid ($\times 10^{10}$)	Xu ($\times 10^3$)	Sato ($\times 10^6$)	Shear ($\times 10^3$)	Berlin ($\times 10^3$)	Fuji ($\times 10^3$)	Ovenall ($\times 10$)	Initial Rate (min^{-1})
60000	4.92	1.08	1.89	2.24	2.25	1.79	-	78
140000	13.50	11.10	12.50	8.61	53.30	4.34	-	1298
460000	4.66	26.60	13.10	6.86	285.0	2.22	-	9917

A. Schmid Model (Figs 3.3 - 3.5). In all of the studies good linear plots are obtained at short degradation times. Although marked deviations occur on longer processing However, from Table 3.1, it appears that the rate model does not account for any initial molecular weight variation. The degradation curves for the effect of the initial molecular weight on the degradation (Figure 3.1) show that the higher molecular weights have much faster initial rate of degradation than the lower molecular weights. This is not indicated by the Schmid model rate constants.

B. Xu Model (Figs 3.6 - 3.8). This model appears not to apply for the systems studied. In all of the systems, curves are produced contrary to that found by Xu *et al.*

Linear fits are only obtained for the degradation of polystyrene under CO_2 and for the degradation of a polystyrene standard of molecular weight 60000. In both of these systems only limited degradation was observed.

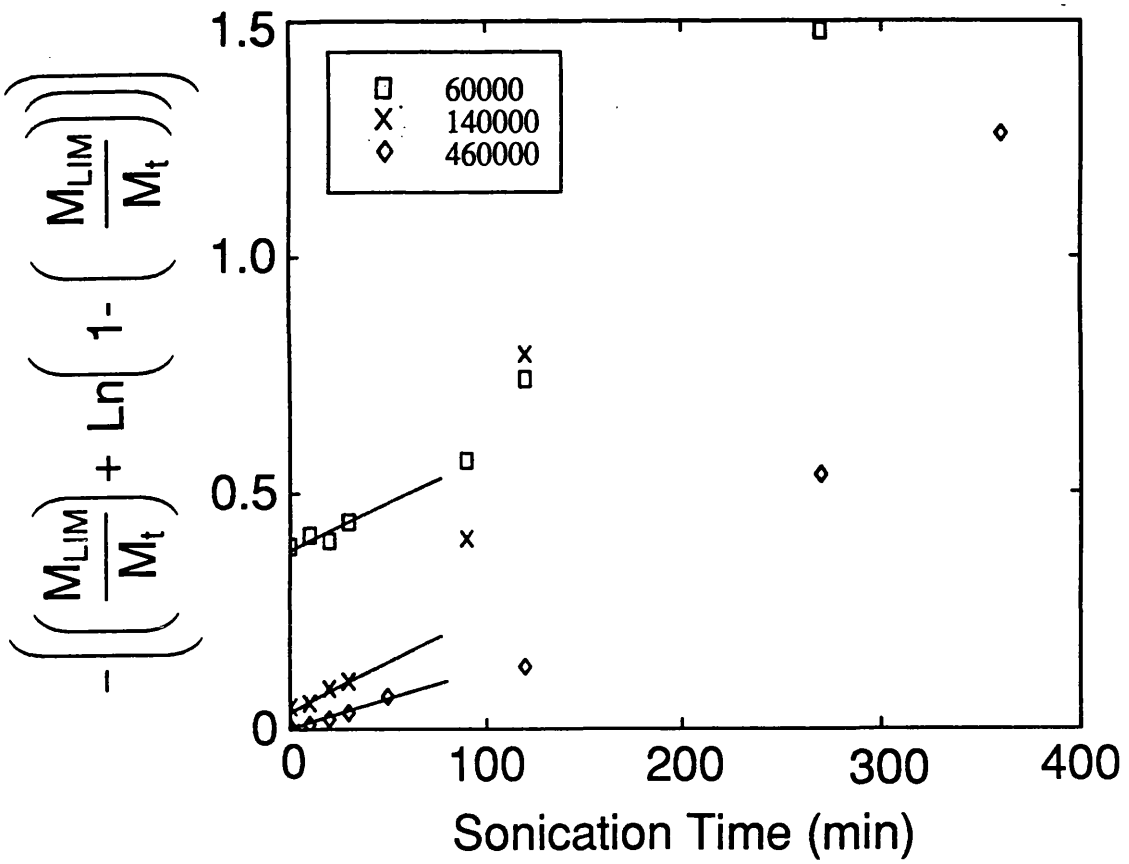

FIGURE 3.3. Schmid kinetic rate plot for the sonication of 0.5%w/v polystyrene in toluene having various initial molecular weights.

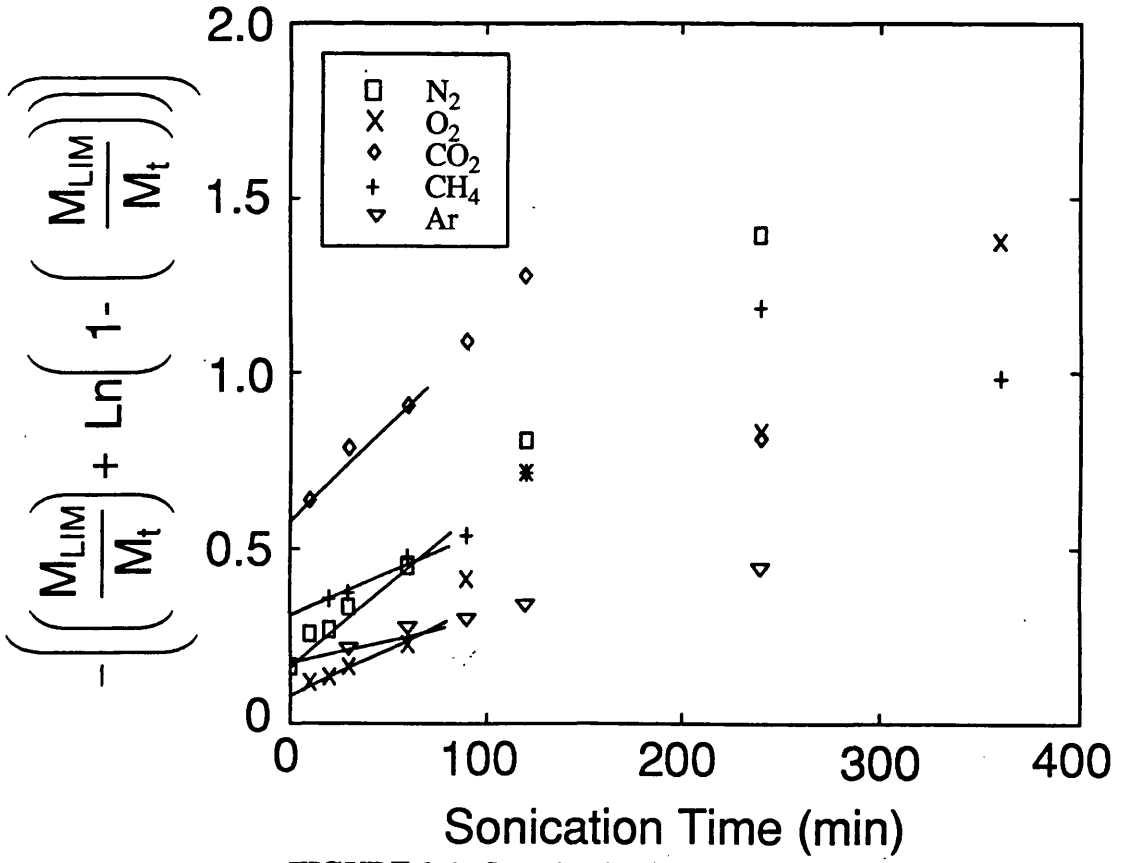

FIGURE 3.4. Schmid kinetic rate plot for the sonication of 0.5%w/v polystyrene in toluene under various gases.

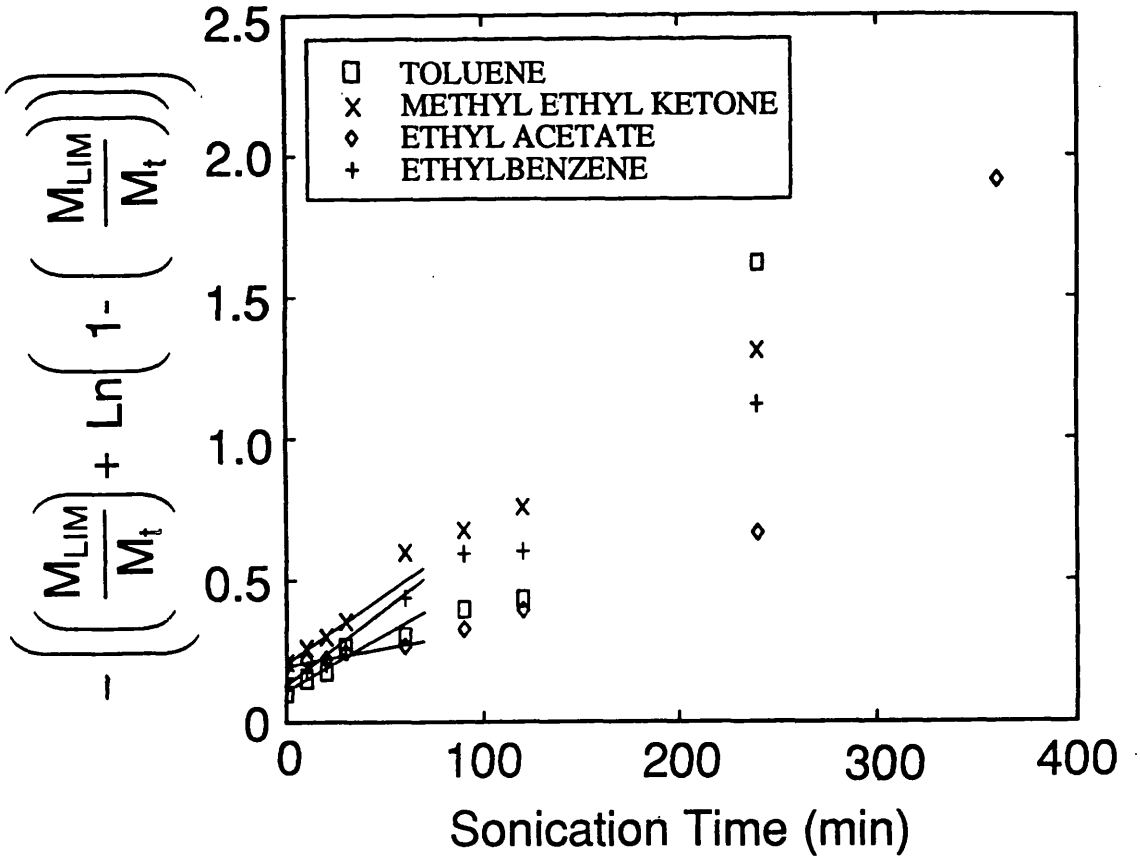

FIGURE 3.5. Schmid kinetic rate plot for the sonication of 0.5%w/v polystyrene in various solvents.

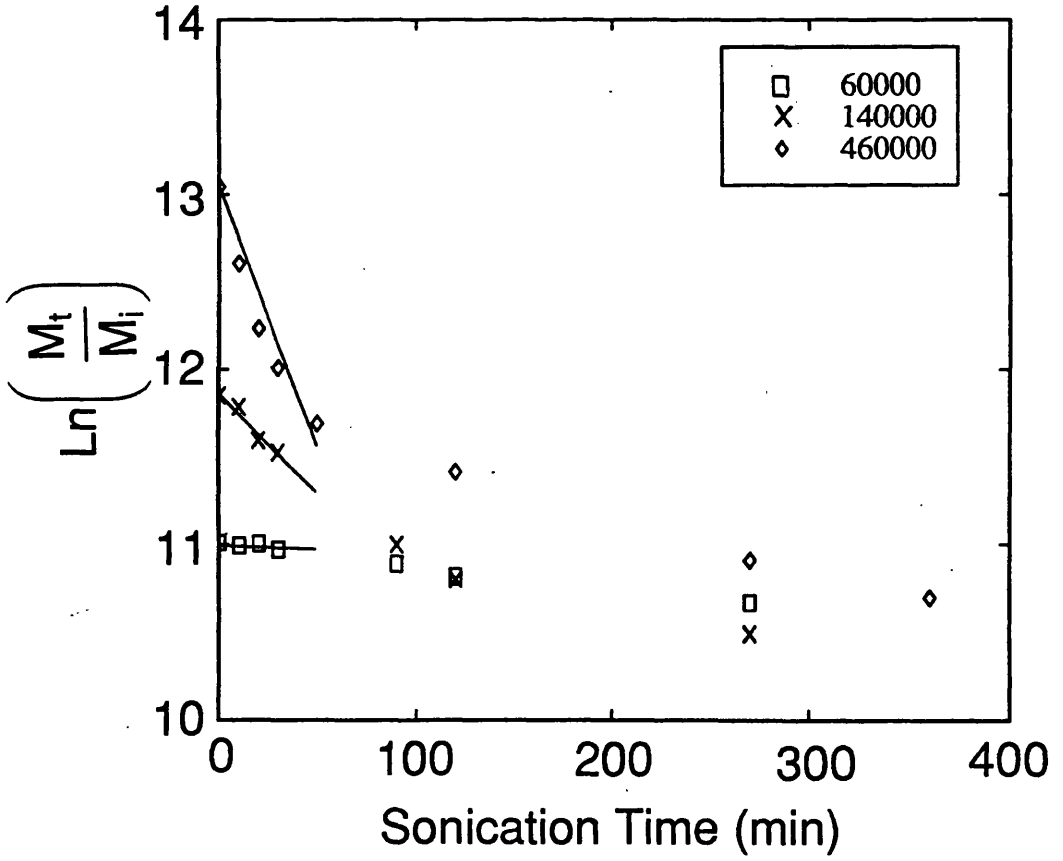

FIGURE 3.6. Xu kinetic rate plot for the sonication of 0.5%w/v polystyrene in toluene having various initial molecular weights.

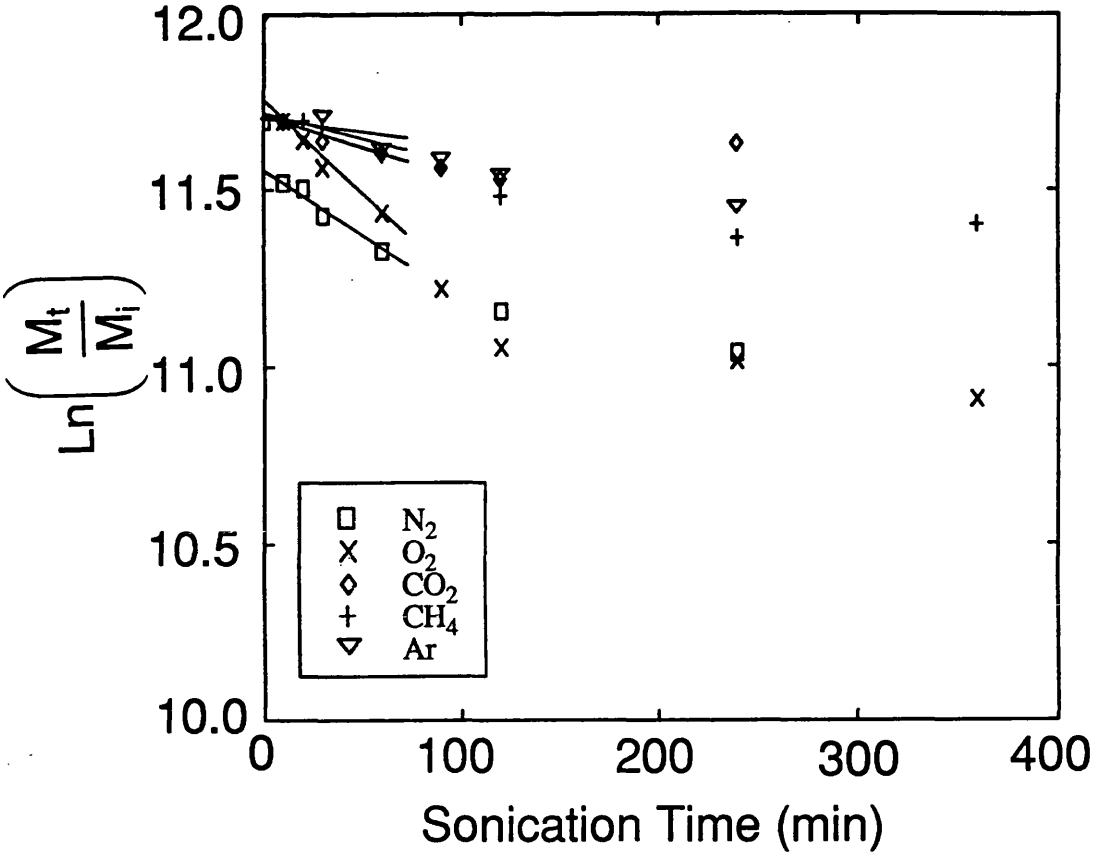

FIGURE 3.7. Xu kinetic rate plot for the sonication of 0.5%w/v polystyrene in toluene under various gases.

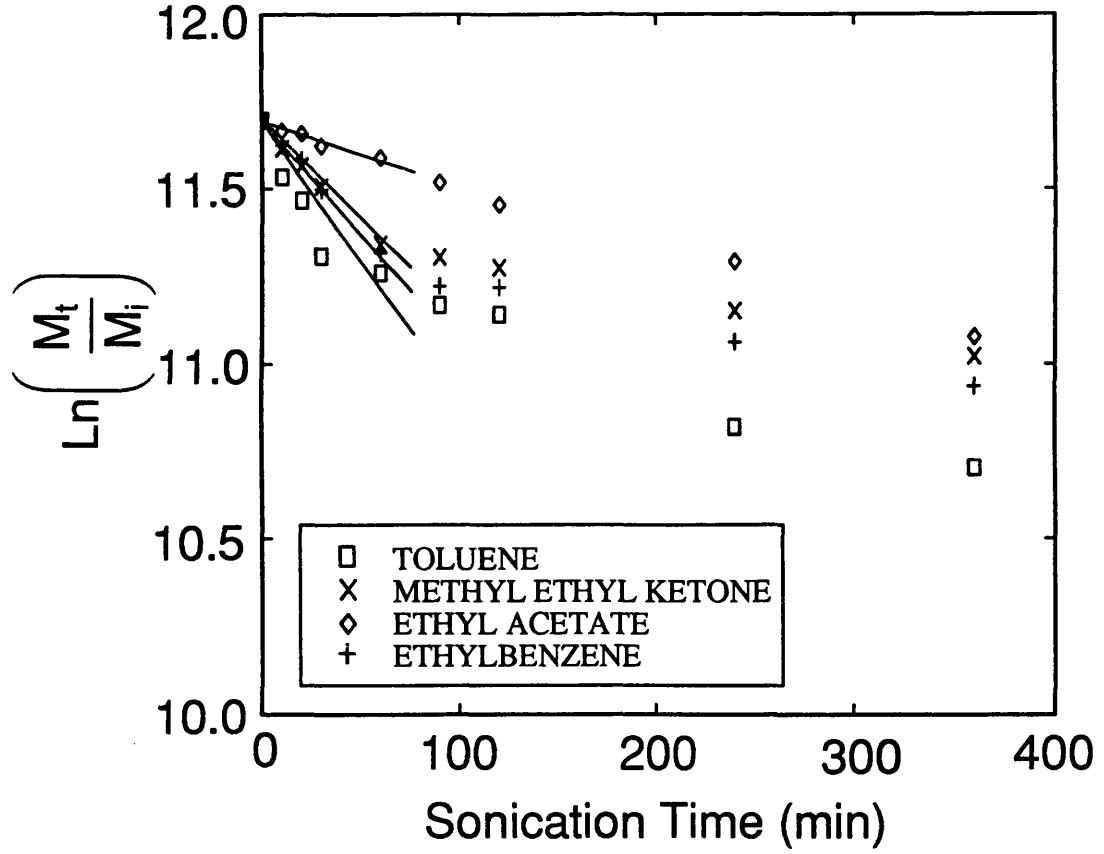

FIGURE 3.8. Xu kinetic rate plot for the sonication of 0.5%w/v polystyrene in various solvents.

C. Fujiwara Model (Figs 3.9 - 3.11). In the cases of the solvent and gas degradation studies, the Fujiwara model provides very good linear correlations for the initial 120 minutes of the degradation. After this time there is a marked deviation from linearity. However, the variation of initial molecular weights only produces a linear fit for the initial 90 minutes of the degradation, after this time there are also large deviations.

D. El'tsefon and Berlin Model (Figs 3.12 - 3.14). This model provides very good linear fits in all of the systems for approximately 200 minutes. The plot obtained for the ultrasonic degradation under an atmosphere of oxygen is only linear for the initial 100 minutes of the degradation.

The plot obtained for the effect of the initial molecular weights on the degradation provides the expected trend in rate constants, with the highest initial molecular weight producing the faster rate. This can be seen in Table 3.1

E. Sato and Nalepa Model (Figs 3.15 - 3.17). Contrary to that found by these authors, this random degradation model does not provide linear plots for any of the systems. This was expected because ultrasonic degradation is known to be a non-random process as discussed in Chapter One.

F. Shear Model (Figs 3.18 - 3.20). Although shear degradation mechanisms have been used to account for the characteristics obtained during ultrasonic degradation, the rate model derived does not appear to be valid for ultrasonic degradation. Linear fits are not produced in any of the systems studied. This indicates that ultrasonic degradation is not entirely produced by shear forces of the type considered in the model.

G. Ovenall Model (Figs 3.21 - 3.23). This model gives good linear correlations for approximately 200 minutes in the three systems examined.

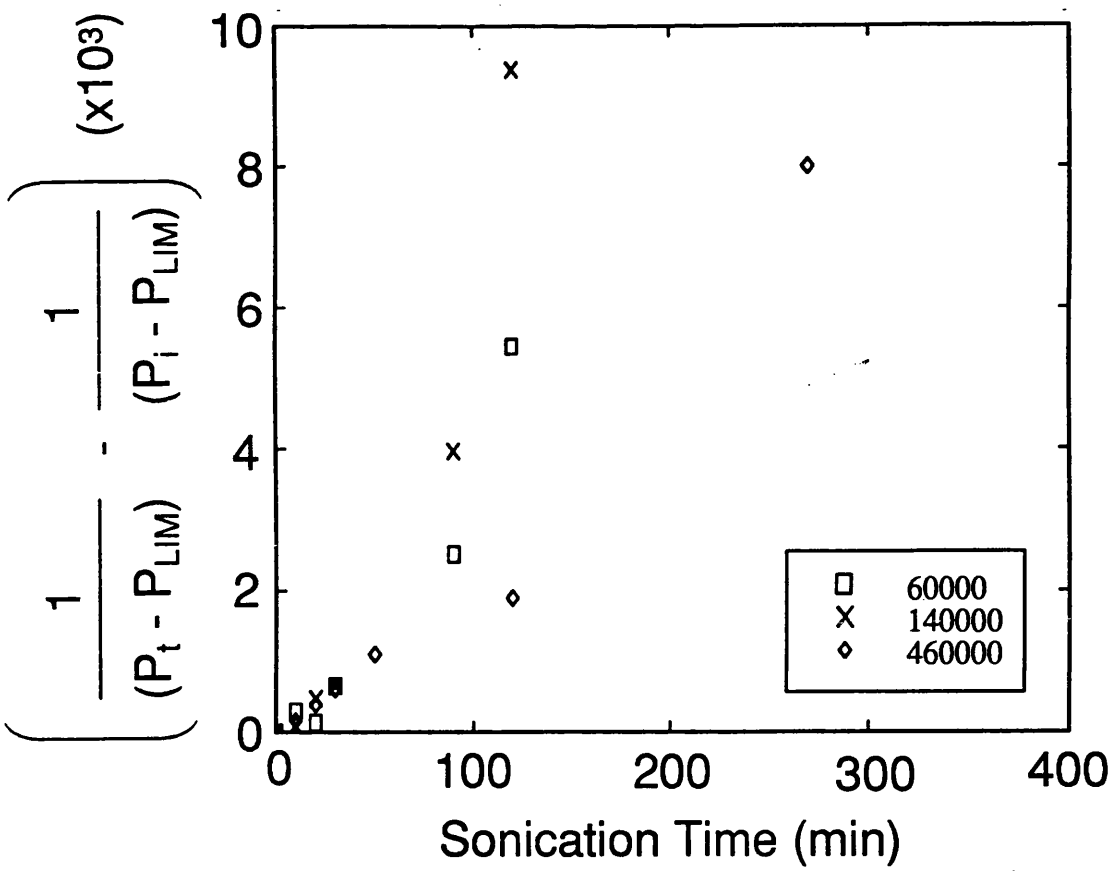

FIGURE 3.9. Fujiwara kinetic rate plot for the sonication of 0.5%w/v polystyrene in toluene having various initial molecular weights.

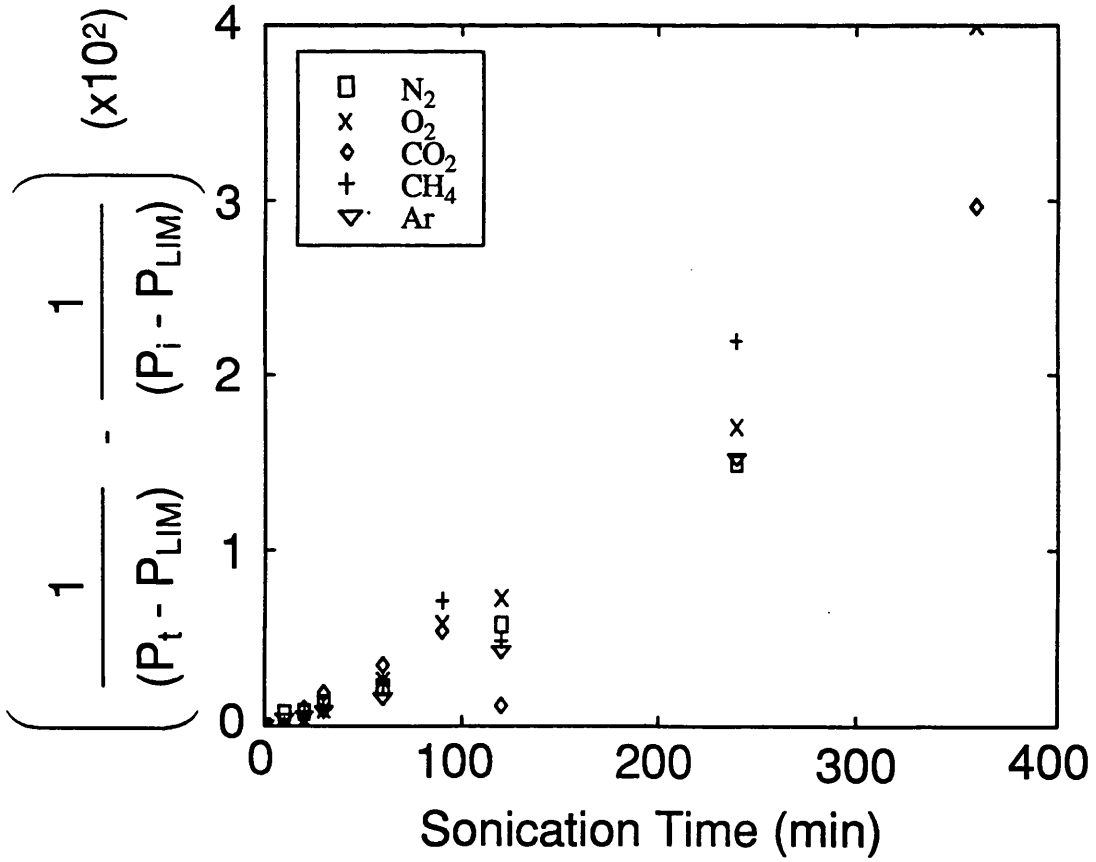

FIGURE 3.10. Fujiwara kinetic rate plot for the sonication of 0.5%w/v polystyrene in toluene under various gases.

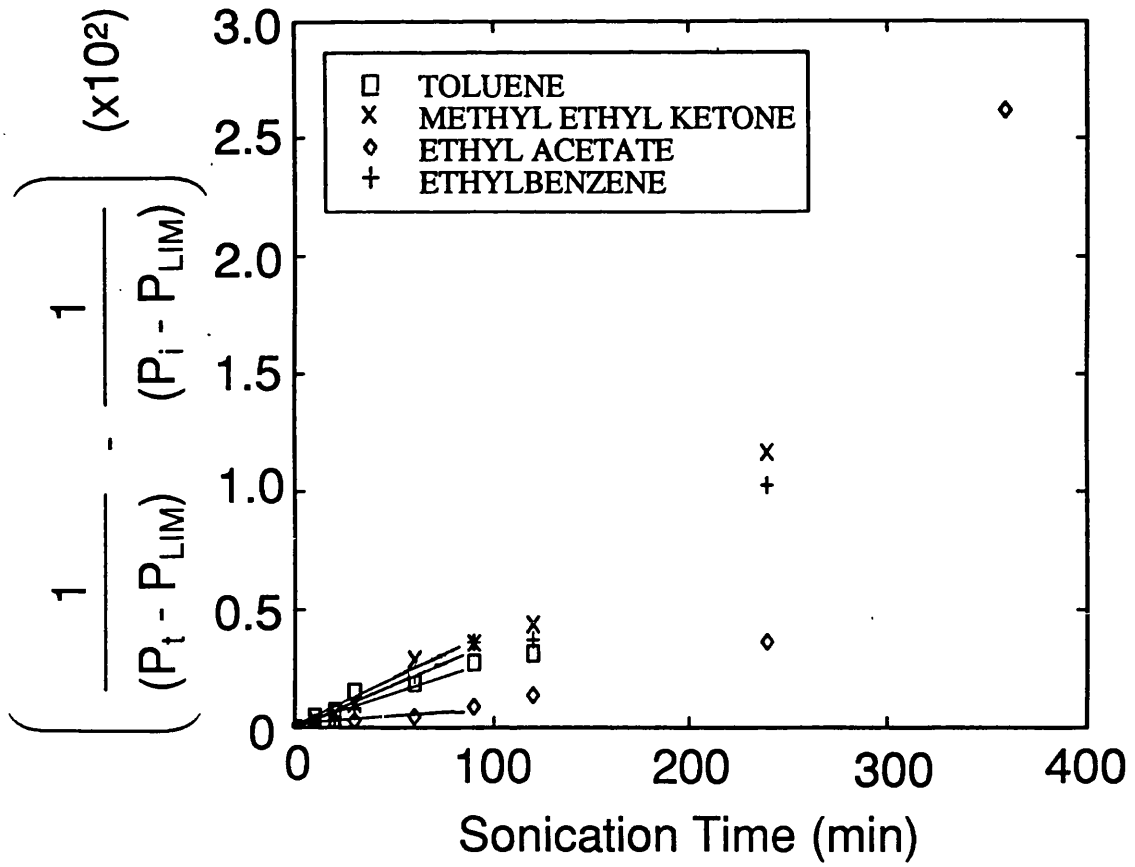

FIGURE 3.11. Fujiwara kinetic rate plot for the sonication of 0.5%w/v polystyrene in various solvents.

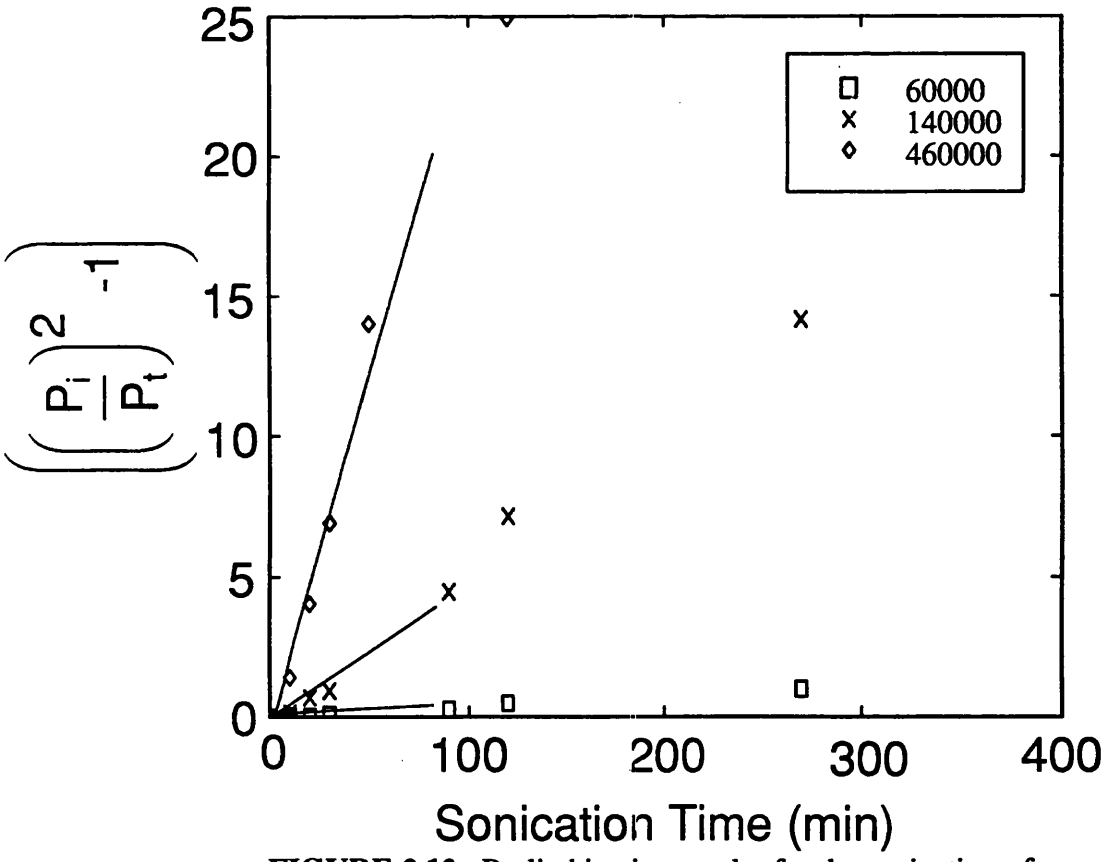

FIGURE 3.12. Berlin kinetic rate plot for the sonication of 0.5%w/v polystyrene in toluene having various initial molecular weights.

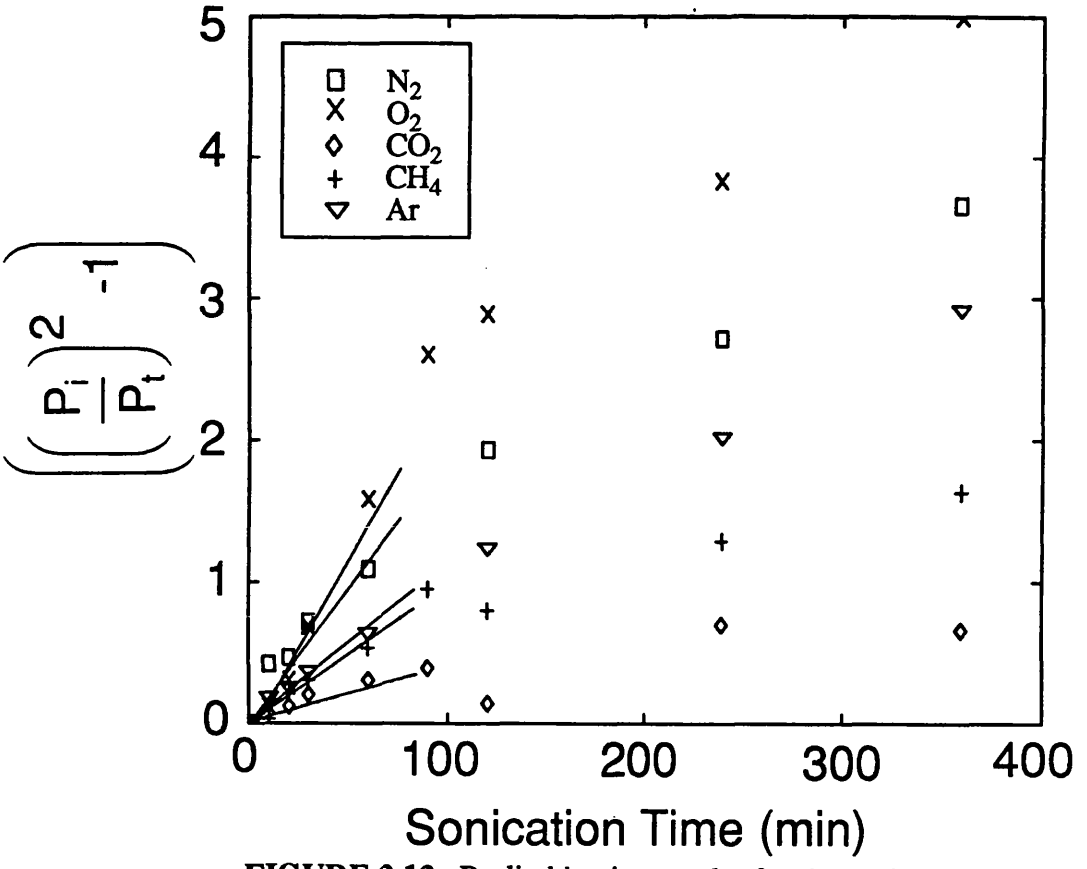

FIGURE 3.13. Berlin kinetic rate plot for the sonication of 0.5%w/v polystyrene in toluene under various gases.

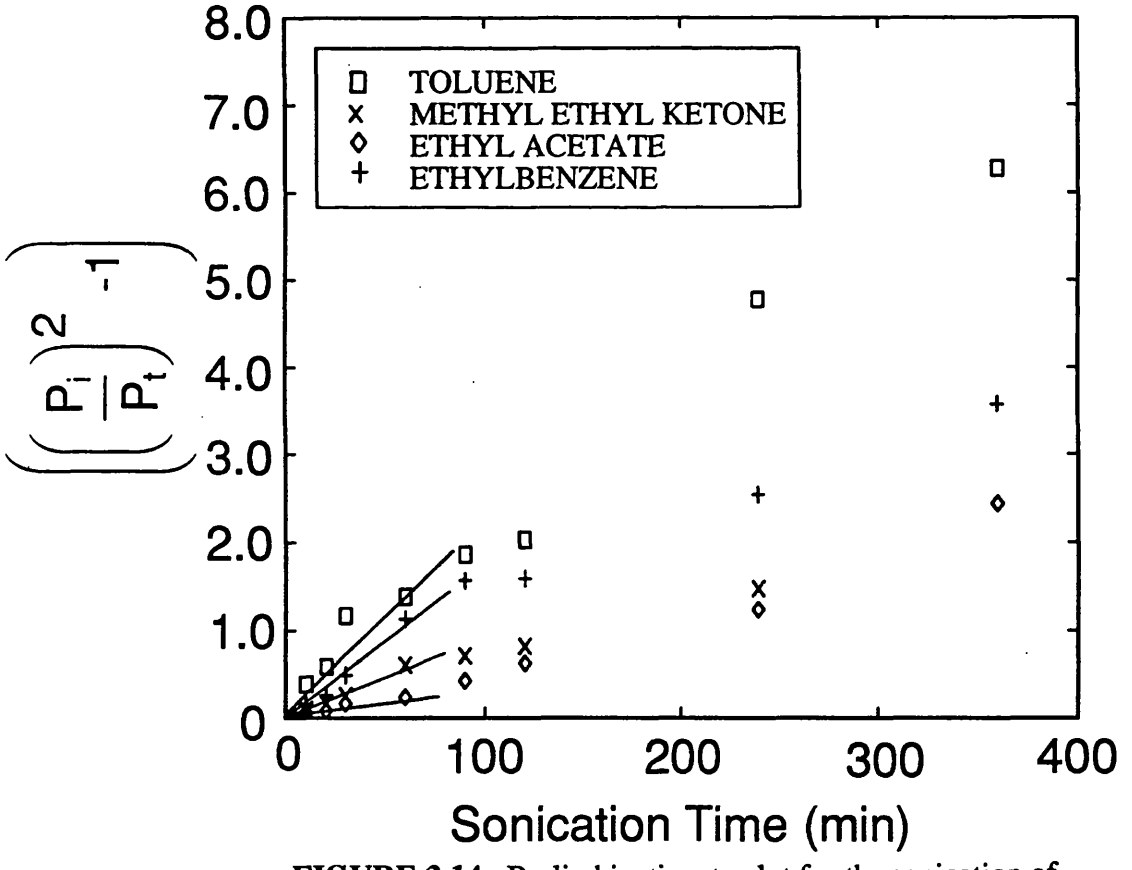

FIGURE 3.14. Berlin kinetic rate plot for the sonication of 0.5%w/v polystyrene in a range of solvents.

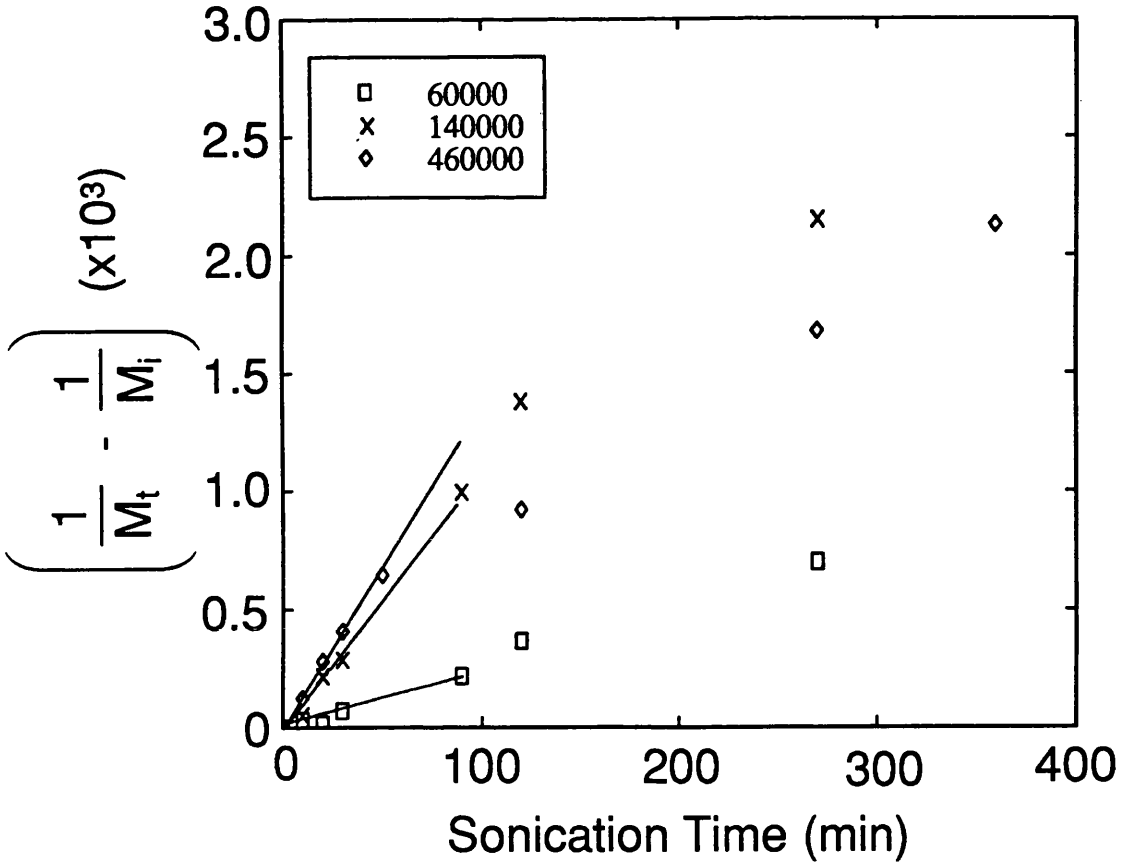

FIGURE 3.15. Sato kinetic rate plot for the sonication of 0.5%w/v polystyrene in toluene having various initial molecular weights.

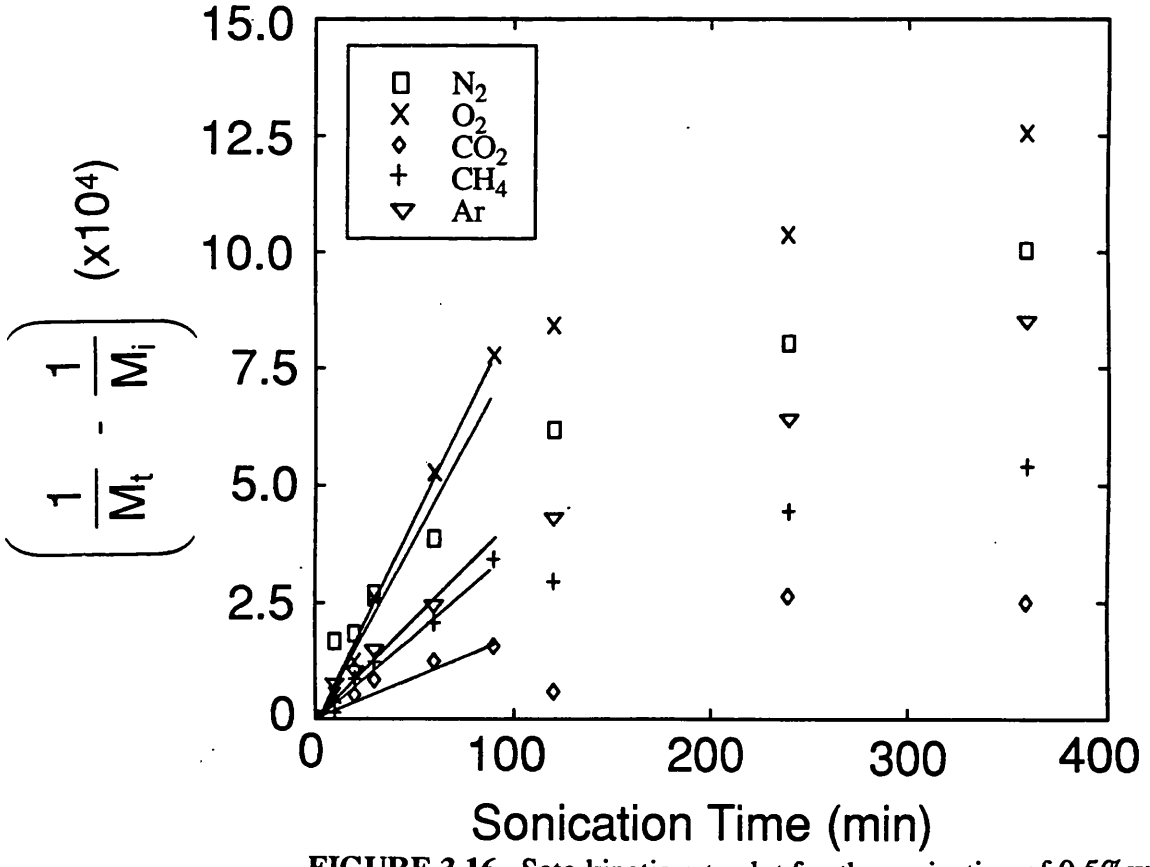

FIGURE 3.16. Sato kinetic rate plot for the sonication of 0.5%w/v polystyrene in toluene under various gases.

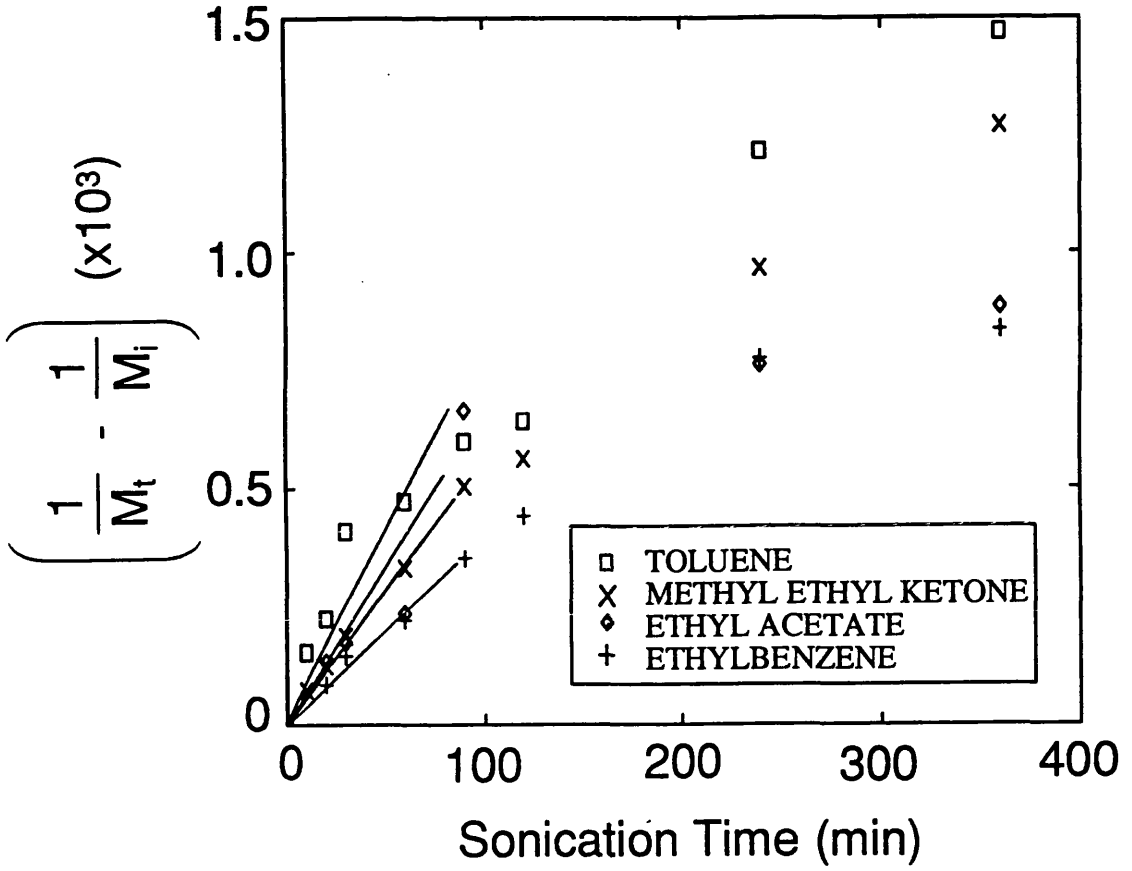

FIGURE 3.17. Sato kinetic rate plot for the sonication of 0.5%w/v polystyrene in various solvents.

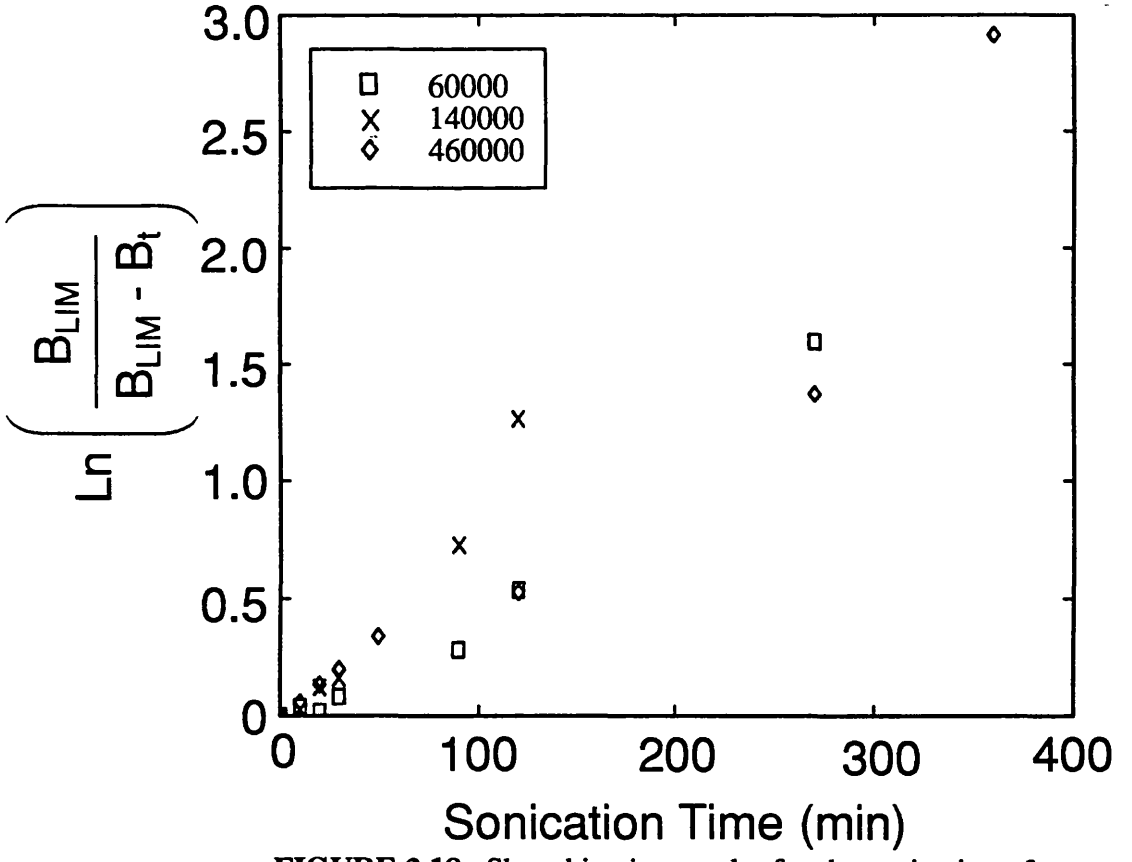

FIGURE 3.18. Shear kinetic rate plot for the sonication of 0.5%w/v polystyrene in toluene having various initial molecular weights.

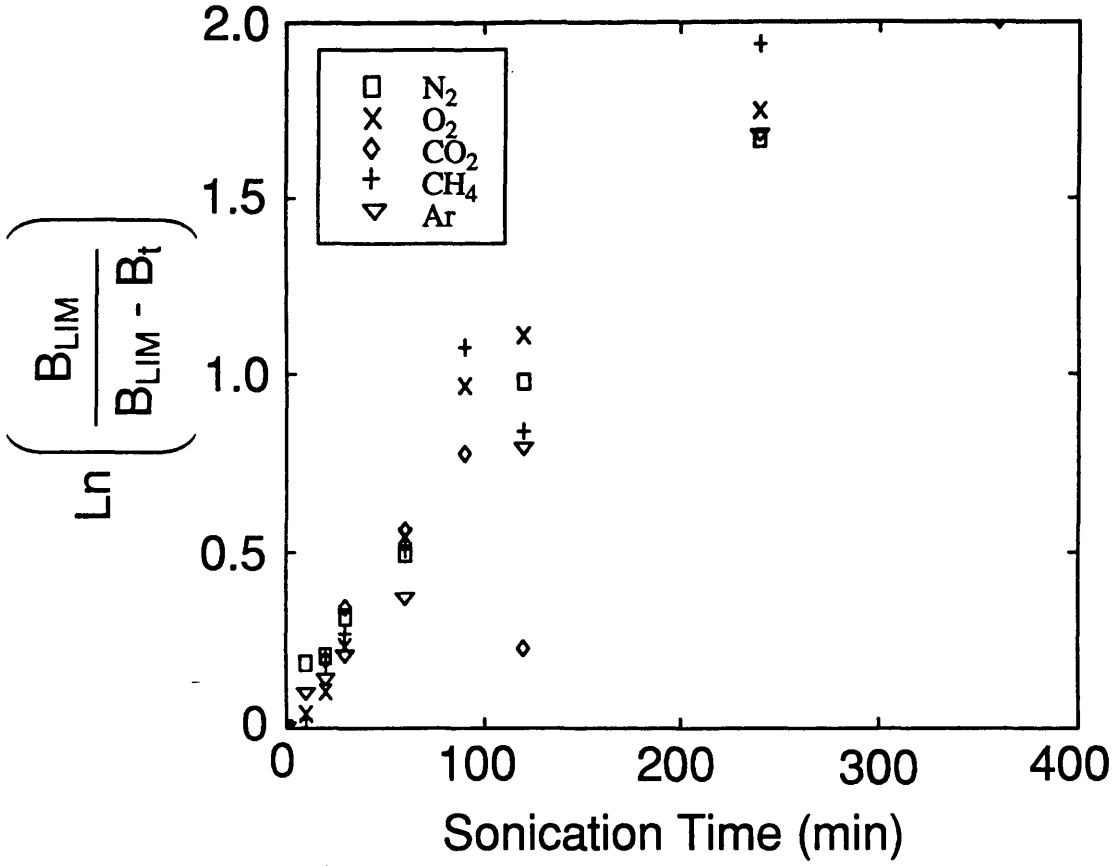

FIGURE 3.19. Shear kinetic rate plot for the sonication of 0.5%w/v polystyrene in toluene under various gases.

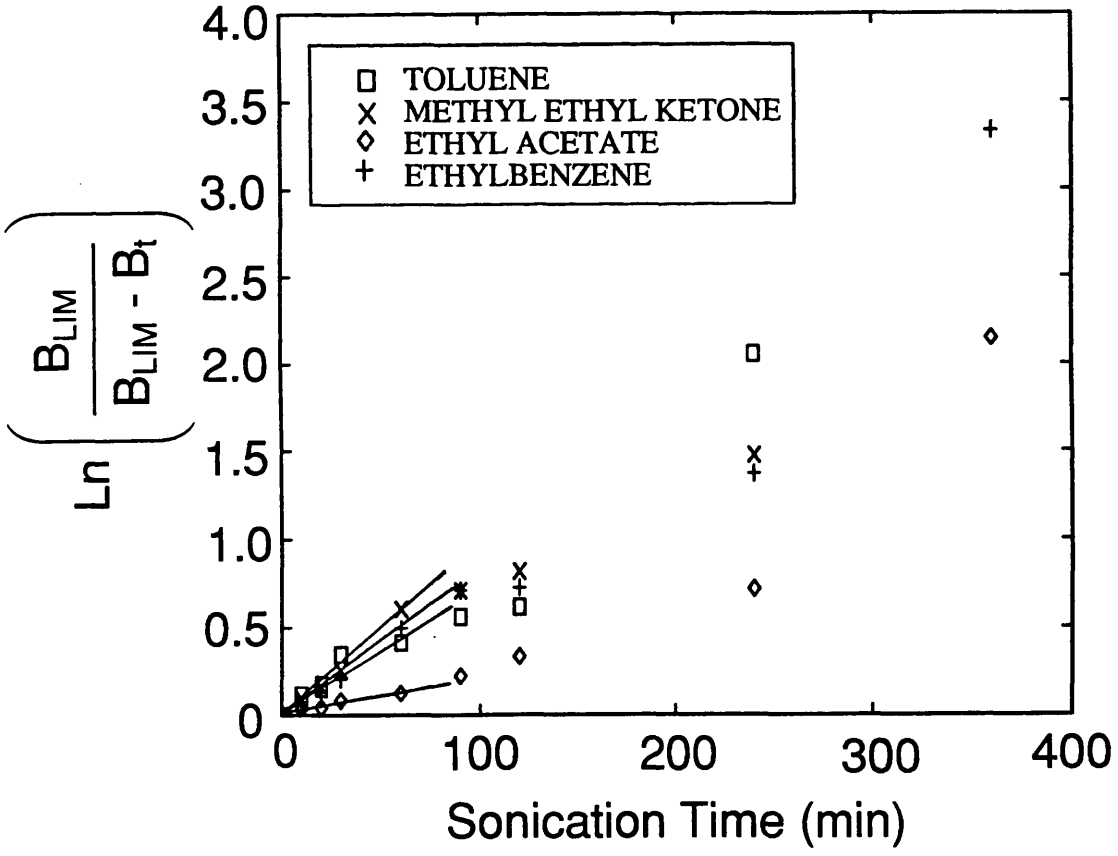

FIGURE 3.20. Shear kinetic rate plot for the sonication of 0.5%w/v polystyrene in various solvents.

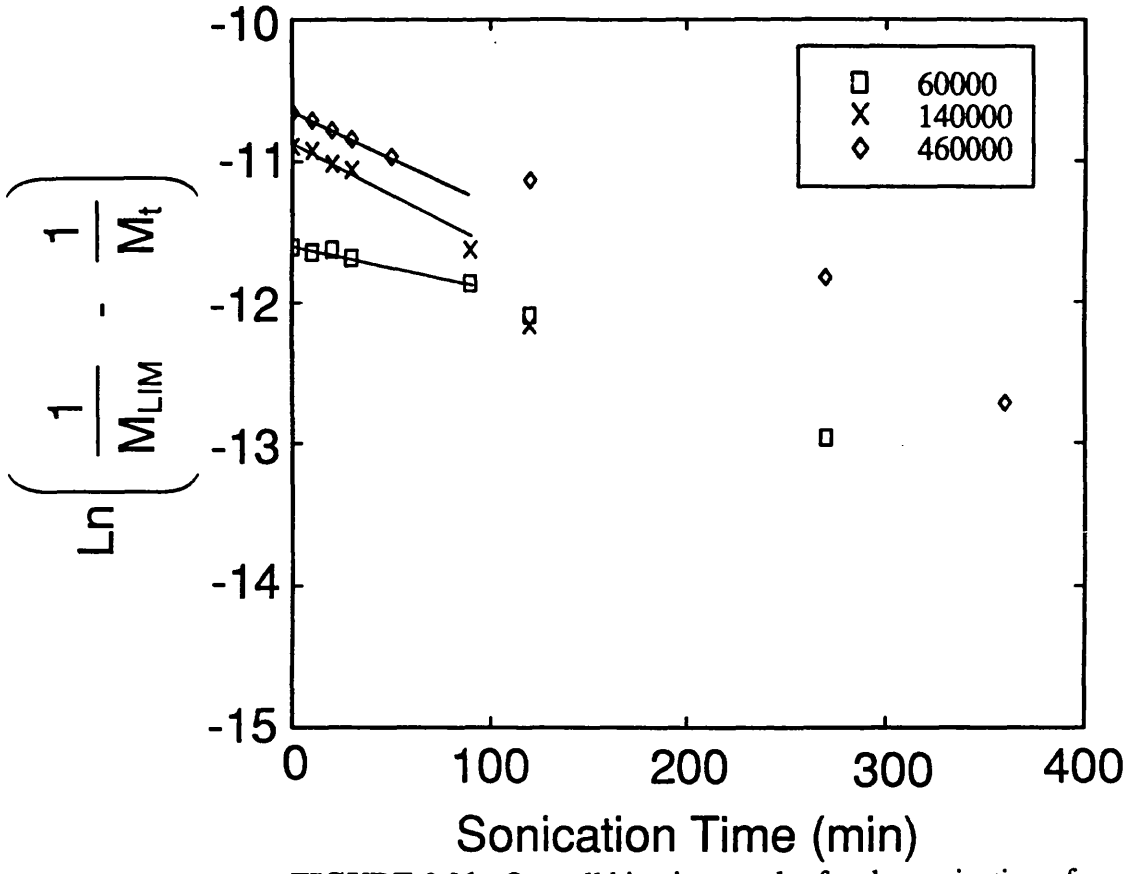

FIGURE 3.21. Ovenall kinetic rate plot for the sonication of 0.5%w/v polystyrene in toluene having various initial molecular weights.

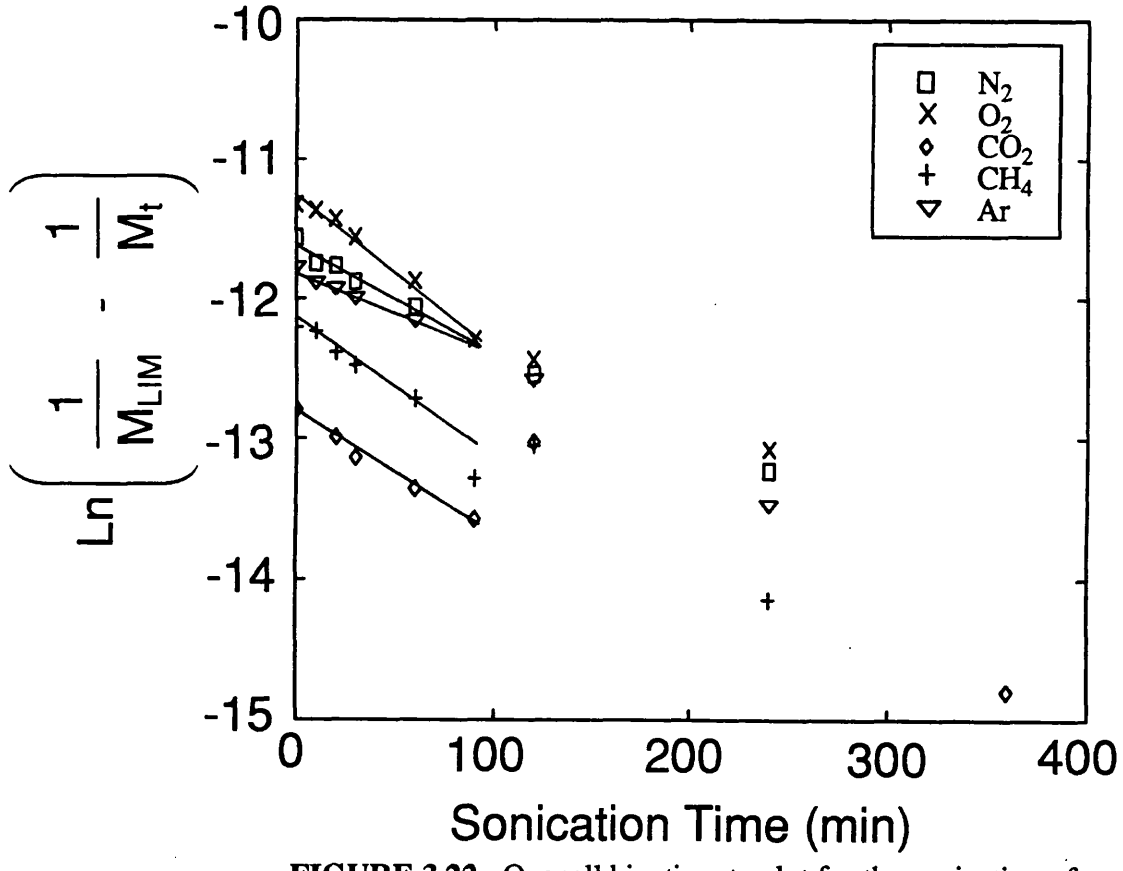

FIGURE 3.22. Ovenall kinetic rate plot for the sonication of 0.5%w/v polystyrene in toluene under various gases.

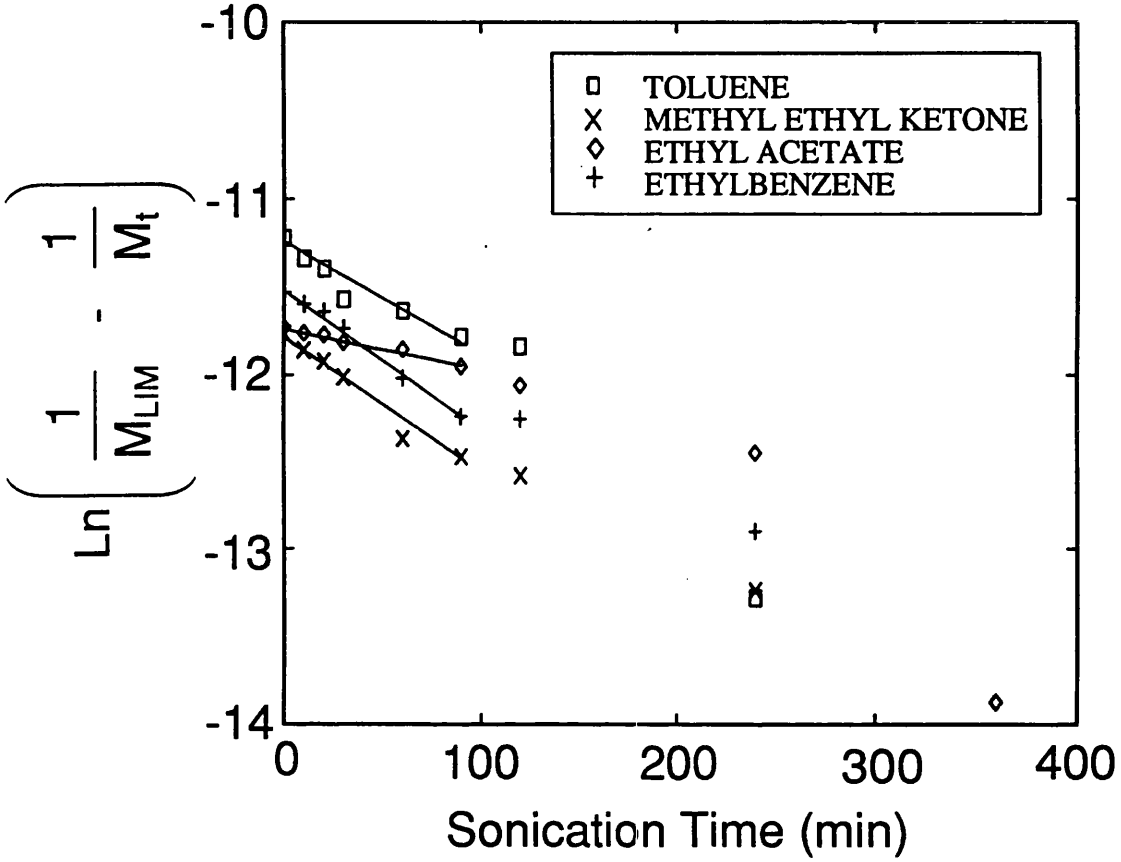

FIGURE 3.23. Ovenall kinetic rate plot for the sonication of 0.5%w/v polystyrene in a range of solvents.

3.2.3 Choice of rate models

From the analysis described above, it was decided to apply the Schmid, Fujiwara, El'tsefon and Berlin and the Ovenall rate models to each of the systems studied in this thesis, owing to these providing the best linear correlations for the degradations. The Sato and Nalepa, shear degradation and Xu models did not fit the experimental data sufficiently to be used.

3.3 Effect of the Ultrasound Intensity on the Degradation

In order to examine the effect of intensity on the degradation a Sonic Systems VC600 ultrasonic probe was used. This provided a larger range of intensities than those obtained with the VC50 used in the other studies. The intensities were calibrated as discussed in Section 3.2.2 and the intensities obtained are shown in Table 3.2 (the area of the probe tip was 0.7853 cm^2).

Table 3.2 Calibration of Ultrasonic Intensity of VC600

Nominal Output	$\Delta\theta$	Time (s)	Heat Capacity of apparatus ($J K^{-1}$)	Intensity $W cm^{-2}$
2.5	7.3	180	947.88	48.9
5.0	13.4	180		89.8
7.5	21.5	180		144.1
10.0	27.4	180		183.7

Figure 3.24 shows the variation of the number average molecular weight with sonication time for the various intensities, studying 0.5% w/v solutions of polystyrene in toluene.

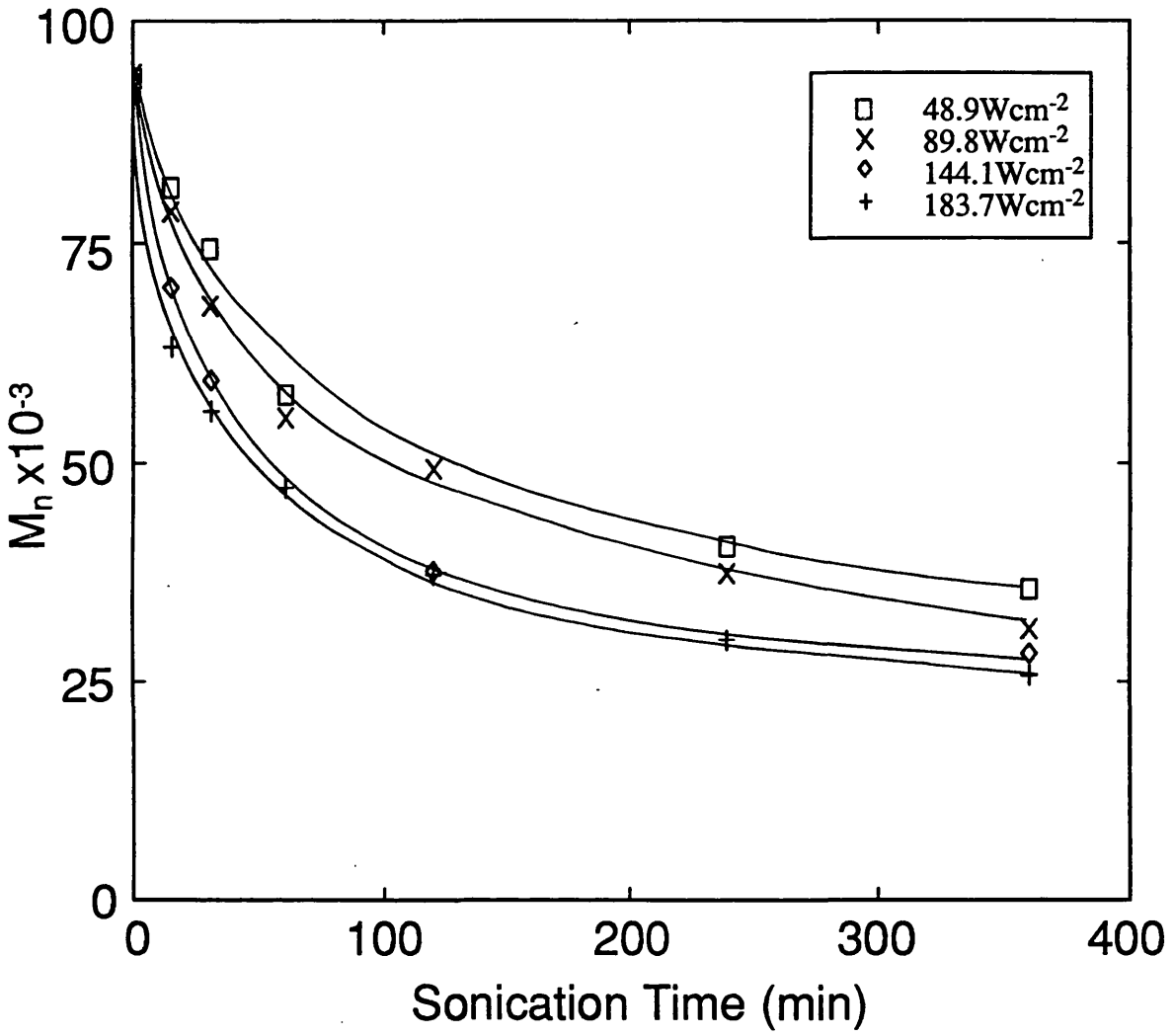

FIGURE 3.24. Variation of number average molecular weight during the sonication of 0.5%w/v polystyrene in toluene using various intensities.

As would be expected, the degradation is faster and proceeds further at higher intensities. The limiting molecular weight reached falls with increasing intensity in an almost linear fashion. This is shown in Figure 3.25, linear regression yielding the relation with correlation coefficient -0.996.

$$M_{LIM} = 35700 - 68.2 \times \text{Intensity} \qquad 3.16$$

This effect is also reflected in the variation of polydispersity with time, as shown in Figure 3.26. As may be seen, at the highest intensity the resulting polymer has a polydispersity of 1.13, comparable with that of a calibration standard.

Figures 3.27 - 3.30 show the effect of intensity on the degradation rate constants. Jellinek[71], using a rate model very similar to the Schmid rate model, showed that the degradation rate constant was a linear function of intensity for the degradation of polystyrene in benzene. Mostafa[73], using a theory derived by Jellinek and White[25], also found a linear relationship between the rate constant and ultrasonic intensity for the degradation of polystyrene in benzene. There was a very good agreement between the two sets of results.

The range of intensities used by Mostafa and Jellinek was small, between 5 and 15 W cm^{-2}. The range of intensities used in this study was much wider, ranging from 48.9 W cm^{-2} to 183.7 W cm^{-2}. As can be seen in Figs 3.27 - 3.30 all of the models give an initial linear relationship between the rate constant and the intensity of sonication. All of the models show that above 144 W cm^{-2}, the rate of degradation decreases. The error in the Schmid and Ovenall rate models is approximately ± 10%, so that the reduction in the rate constant at 183.7 W cm^{-2} is well outside that expected by extrapolating the linear graph to this intensity.

The error in the Fujiwara rate constant, again considering the largest error to be in the limiting molecular weight is approximately ± 10.5%. The Berlin rate model is unaffected by the limiting molecular weight and the major error arises from the measurement of molecular weights from the GPC. The error is estimated to be

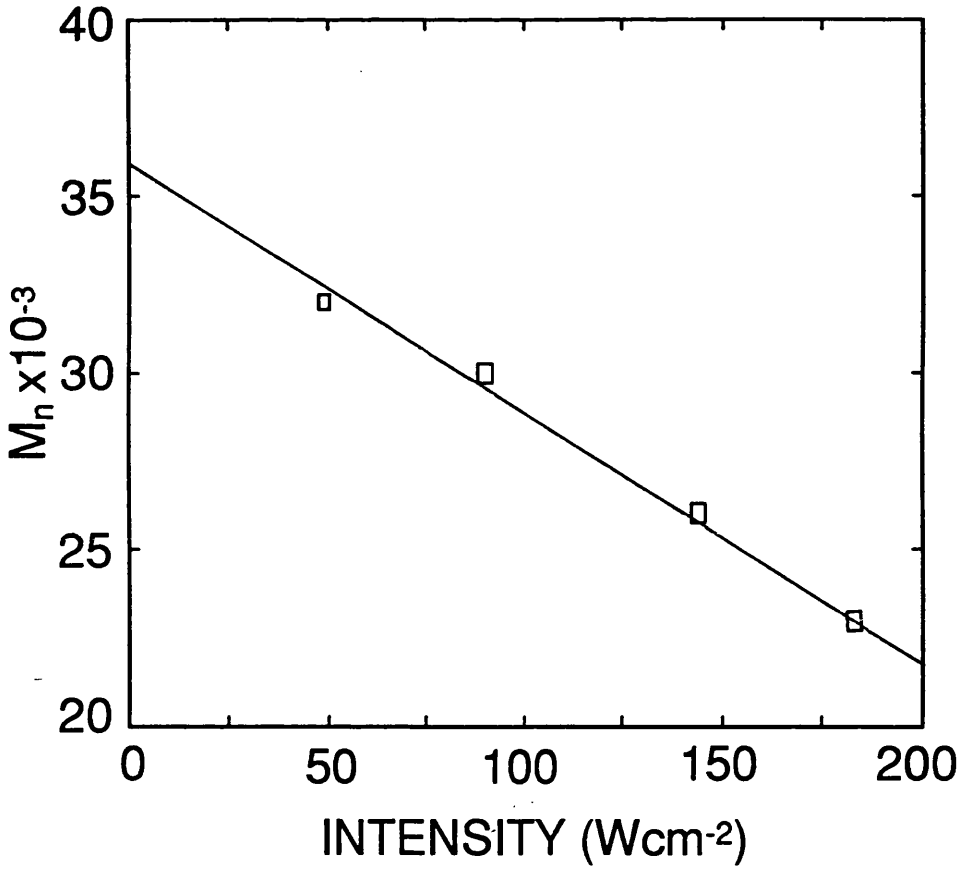

FIGURE 3.25. Effect of ultrasonic intensity on the limiting molecular weight of polystyrene for the sonication of a 0.5%w/v solution in toluene.

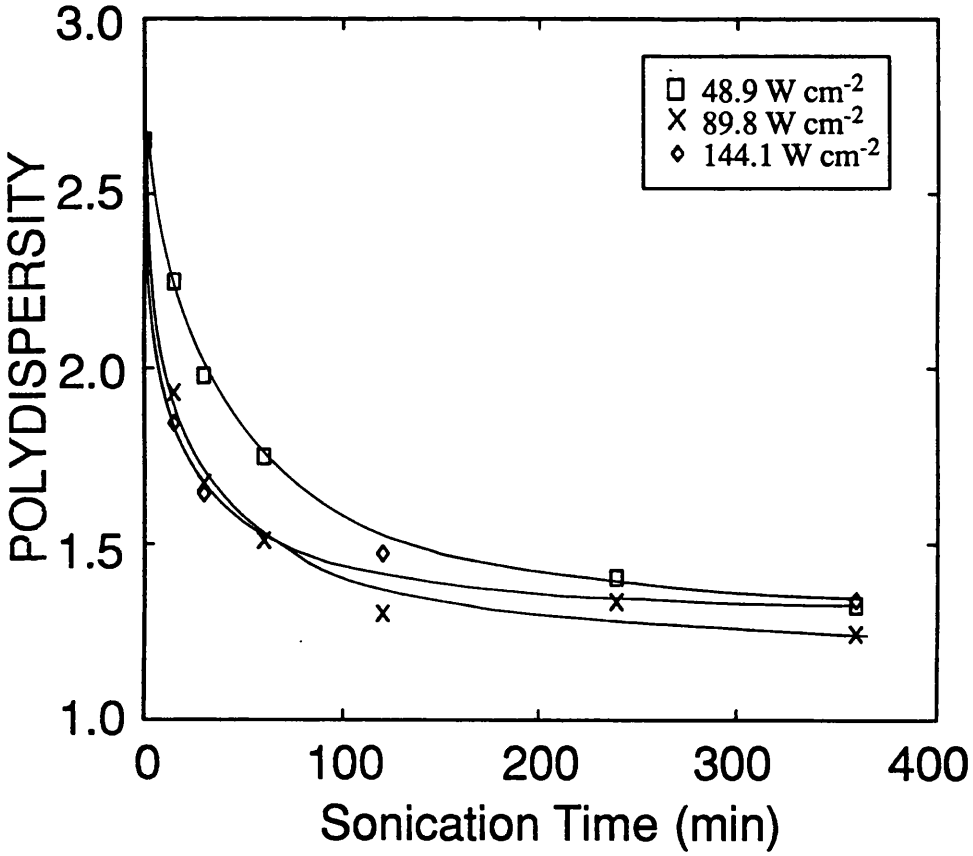

FIGURE 3.26. Variation of the polydispersity of the polystyrene during the sonication of 0.5%w/v polystyrene in toluene using various intensities.

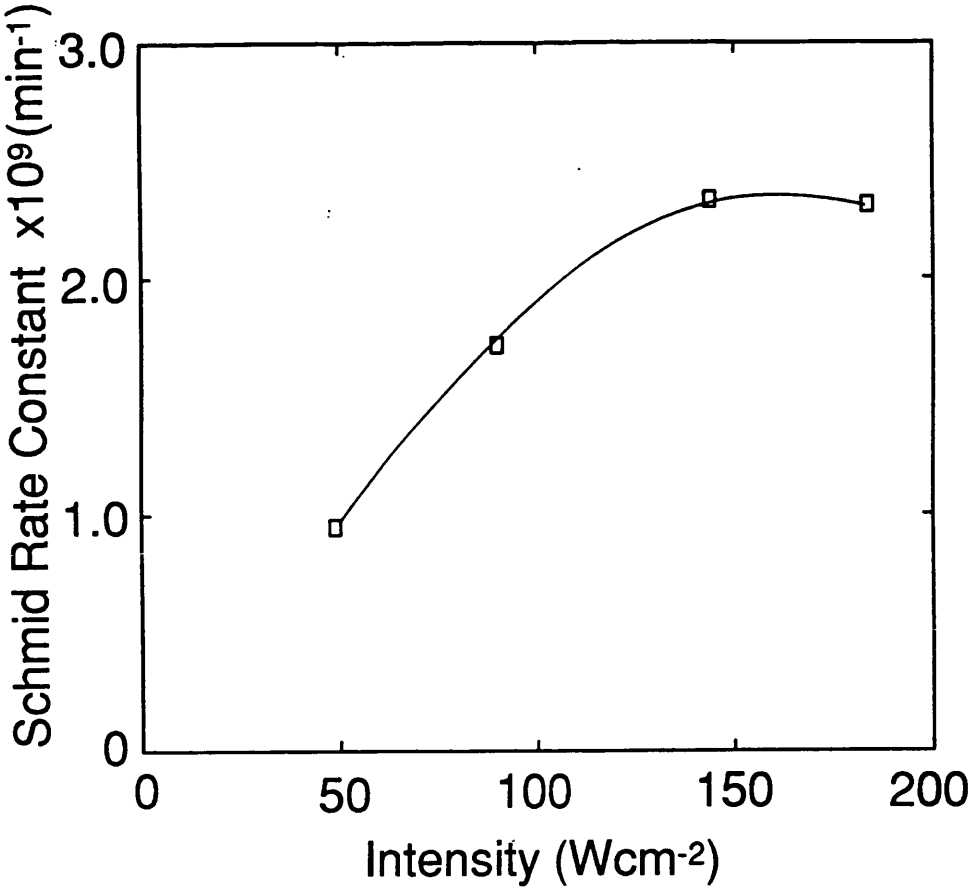

FIGURE 3.27. Effect of the ultrasonic intensity on the Schmid rate constant for the sonication of 0.5%w/v polystyrene in toluene.

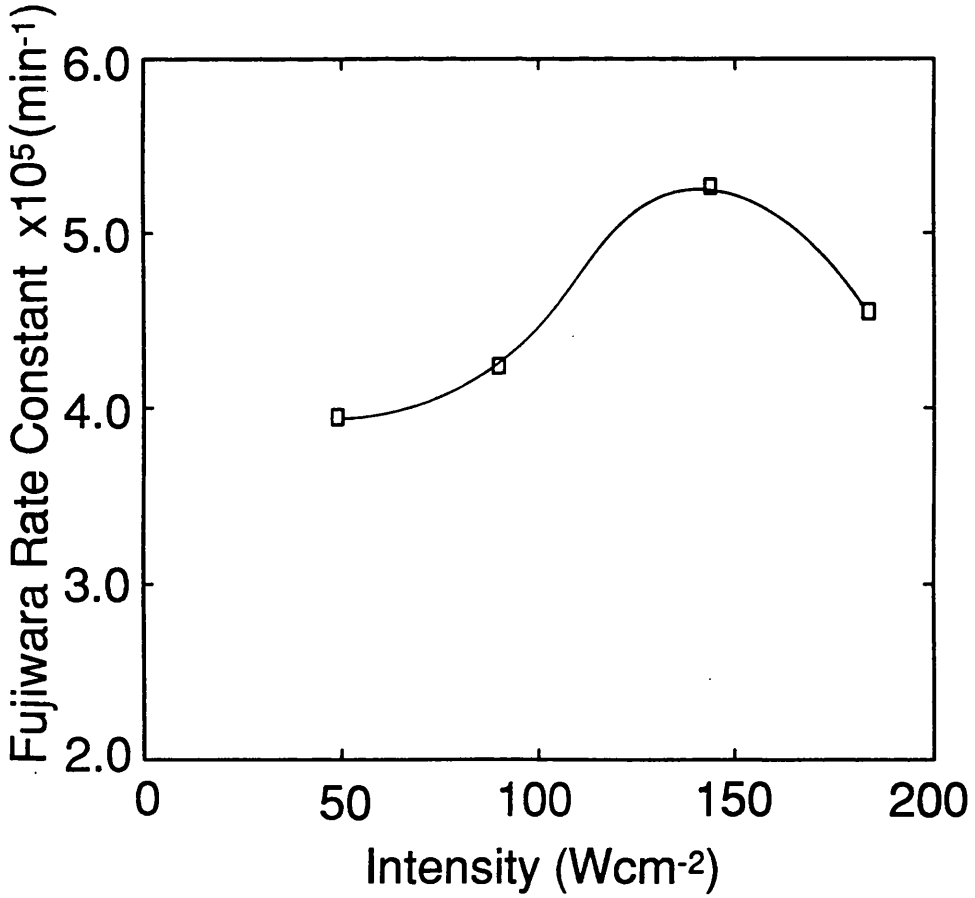

FIGURE 3.28. Effect of the ultrasonic intensity on the Fujiwara rate constant for the sonication of 0.5%w/v polystyrene in toluene.

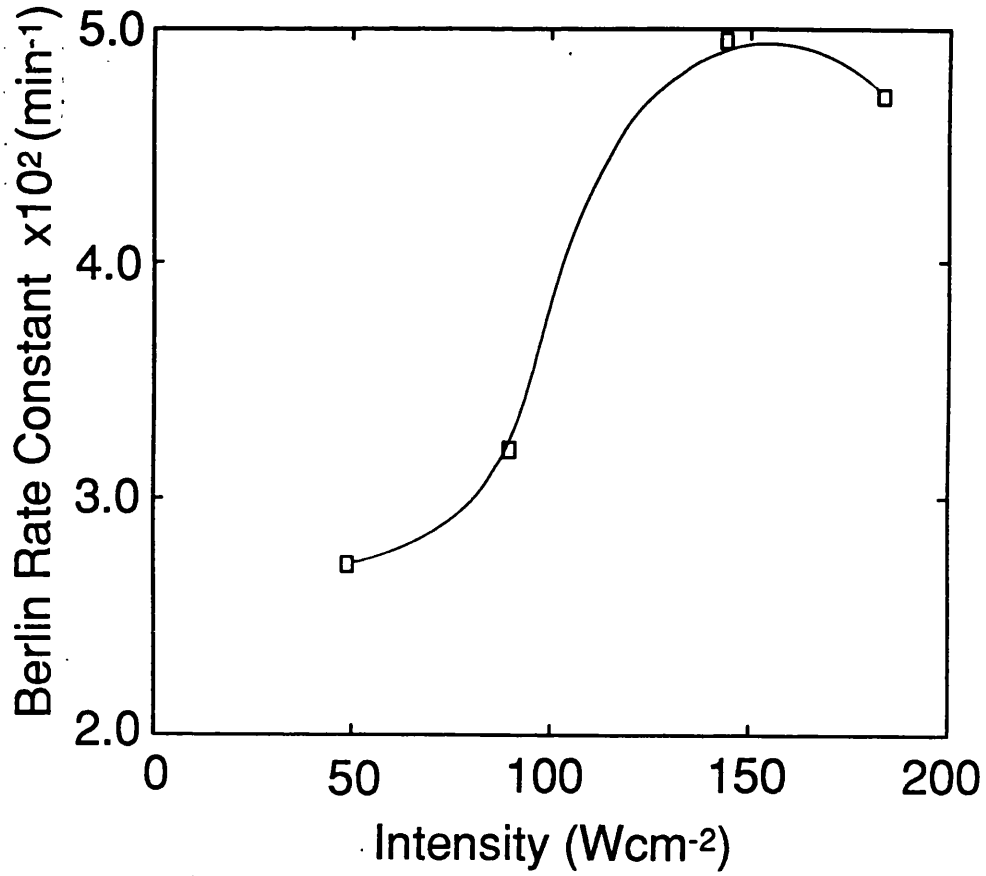

FIGURE 3.29. Effect of the ultrasonic intensity on the Berlin rate constant for the sonication of 0.5%w/v polystyrene in toluene .

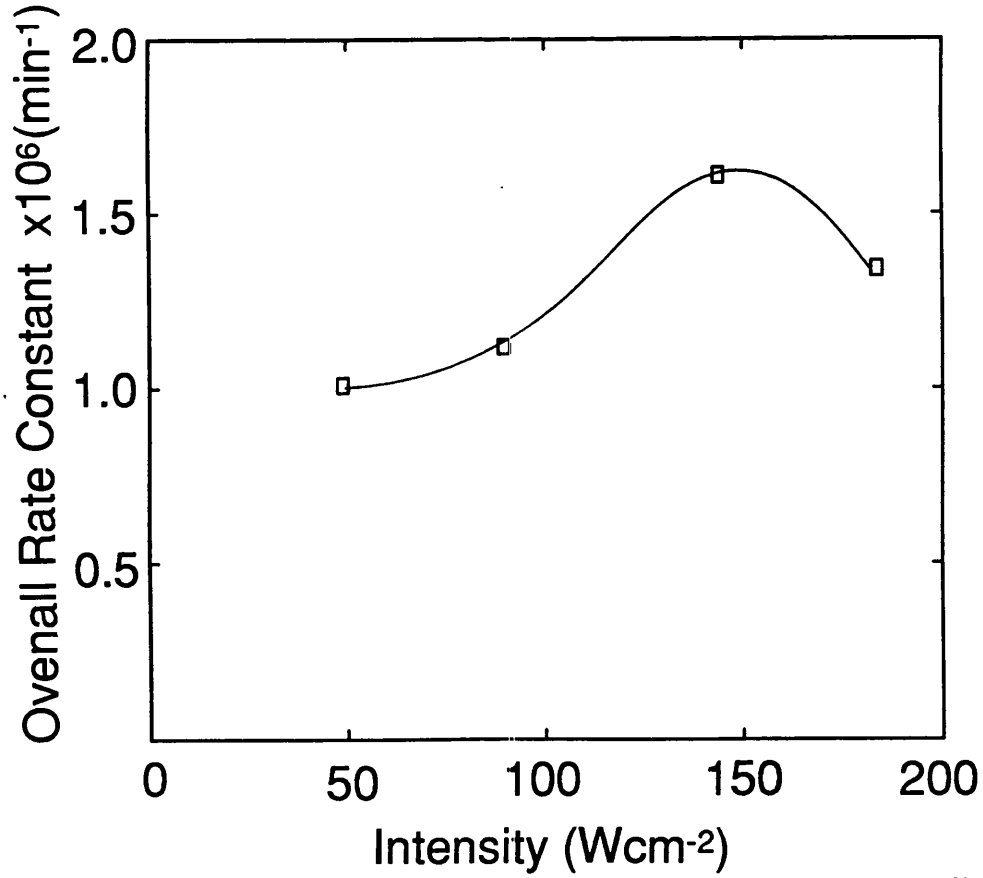

FIGURE 3.30. Effect of the ultrasonic intensity on the Ovenall rate constant for the sonication of 0.5%w/v polystyrene in toluene.

approximately ± 8%.

Hence in all of the these models, the fall in rate constant above 144 W cm^{-2} is outside the experimental error. The trend observed would be expected considering the ultrasonic theory of Noltingk and Neppiras[31]. They suggested that providing the intensity is kept inside the threshold values for cavitation, the maximum radius, R_m, reached by a cavity during its growth, is a function of its intensity,

$$R_m = f(I^{1/2}) \qquad 3.17$$

Therefore, an increase in intensity will increase the radius of the cavitation bubble so that there will be greater forces produced on the bubble collapse, enabling more polymer molecules to be broken.

However, if the intensity is increased beyond a certain level, the bubble radius will have increased to such a large extent that there would be insufficient time between acoustic cycles for a transient collapse, so that the rate should begin to decrease.

Thus, we may conclude that, while in general an increase in intensity further promotes the degradation process, an optimum value exists beyond which no further benefit can be gained.

3.4 Effect of Temperature on the Degradation

Altering the temperature of a solution can alter its physical properties, such as viscosity and saturated vapour pressure, hence changing its cavitational properties. Therefore it was important to examine how this affected the degradation of polystyrene.

The effect of the solution temperature on the degradation of 0.5% w/v polystyrene in toluene can be seen in Figure 3.31 and shows that the lower the solution temperature, the faster the rate of degradation and the lower the limiting molecular weight obtained. The effect of the temperature on the limiting molecular weight can be seen in Figure 3.32 and suggests a linear dependence of the form

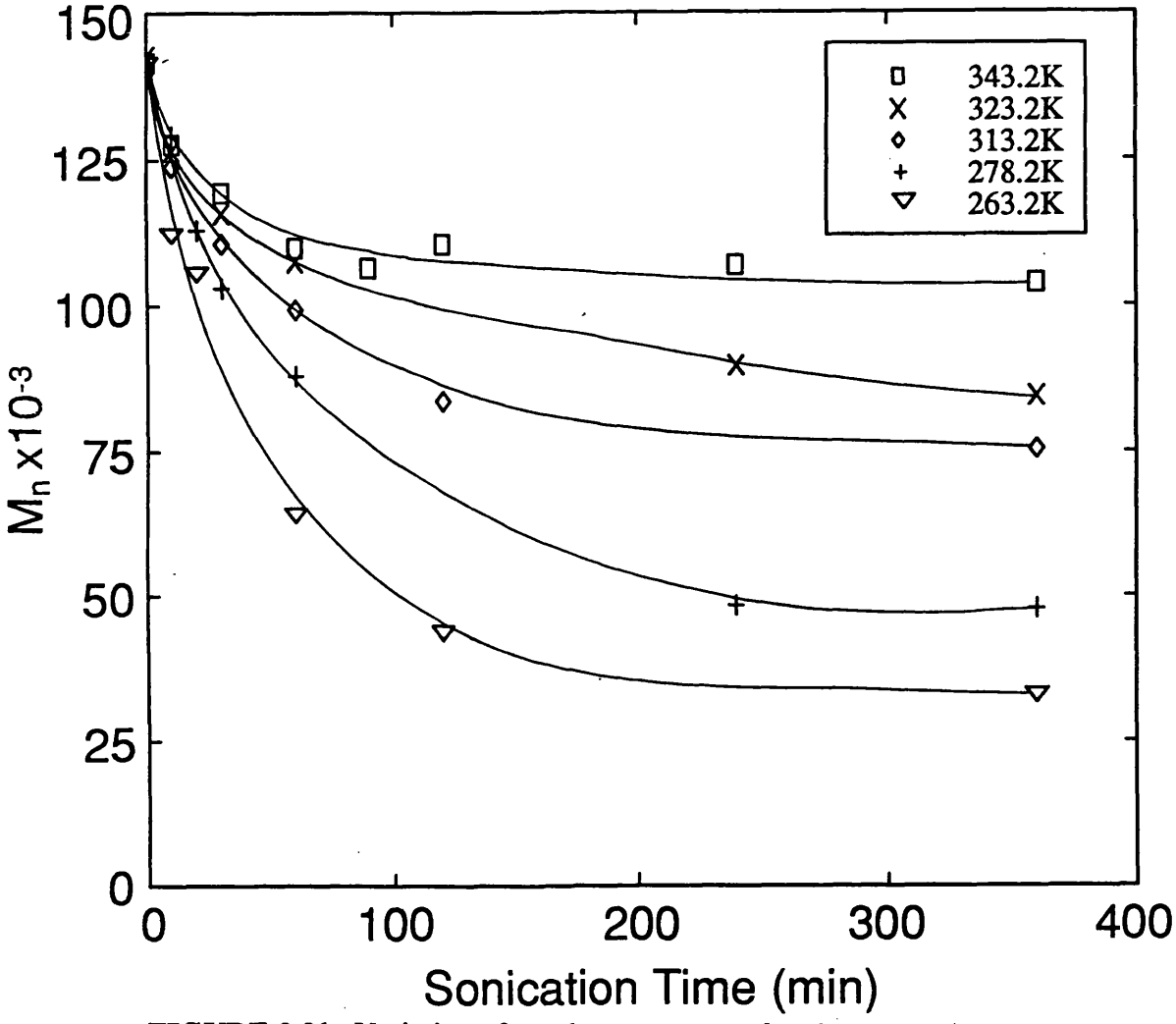

FIGURE 3.31. Variation of number average molecular weight during the sonication of 0.5%w/v polystyrene in toluene at various temperatures.

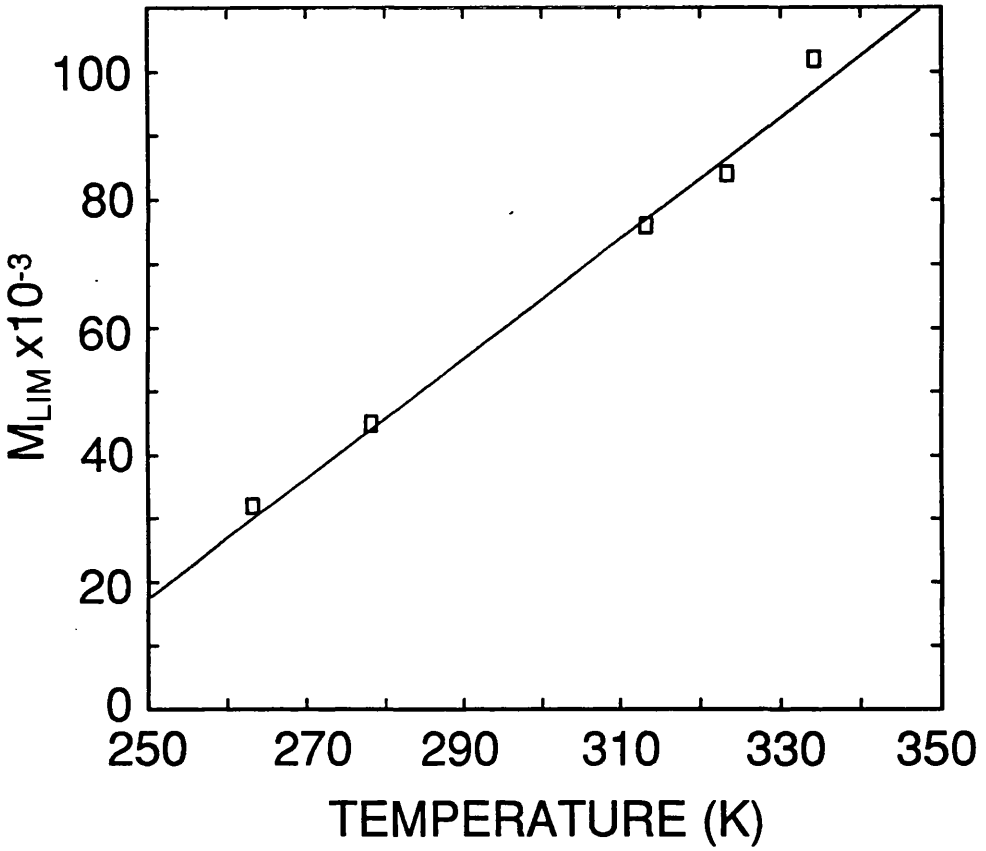

FIGURE 3.32. Effect of temperature on the limiting molecular weight of polystyrene for the sonication of a 0.5%w/v solution in toluene.

$$M_{LIM} = 40.0 + 1050 \times T/^{\circ}C$$

although it should be noted that the degradation at 61°C lies off the line.

These results are qualitatively similar to those found by Malhotra[63], who worked on a series of poly(alkyl methacrylates) in toluene and tetrahydrofuran. Increased degradation was found at -20°C. Schmid and Beuttenmuller[96] also investigated the effect of bulk temperature on the ultrasonic degradation of solutions of polystyrene in toluene over the range of 40-120°C. The results showed that the degradation was slower and produced higher limiting molecular weights at higher temperatures.

The effect may be explained by considering the cavitation process. At higher temperatures, the solvent will have a higher vapour pressure and hence more vapour will enter the cavitation bubble.

This can be seen from the Clausius-Clapeyron equation,

$$\text{Ln } P = \text{constant} - \frac{\Delta H_v}{RT} \qquad 3.18$$

where ΔH_v is the heat of vaporisation of the solvent, R is the molar gas constant, T is the absolute temperature of the solution and P is the saturated vapour pressure.

A higher temperature produces a higher vapour pressure and hence the cavitation bubbles will be cushioned on collapse, and the shock wave will be reduced. At lower temperatures the bubble will be less cushioned and so the shock waves will be more severe, hence causing more degradation.

Malhotra also suggested that lower temperatures cause higher viscosities and so there would be a much better transference of energy from the transducer to the solution.

The enhancement of the degradation process at lower temperatures also increases the reduction in polydispersity as may be seen in Figure 3.33

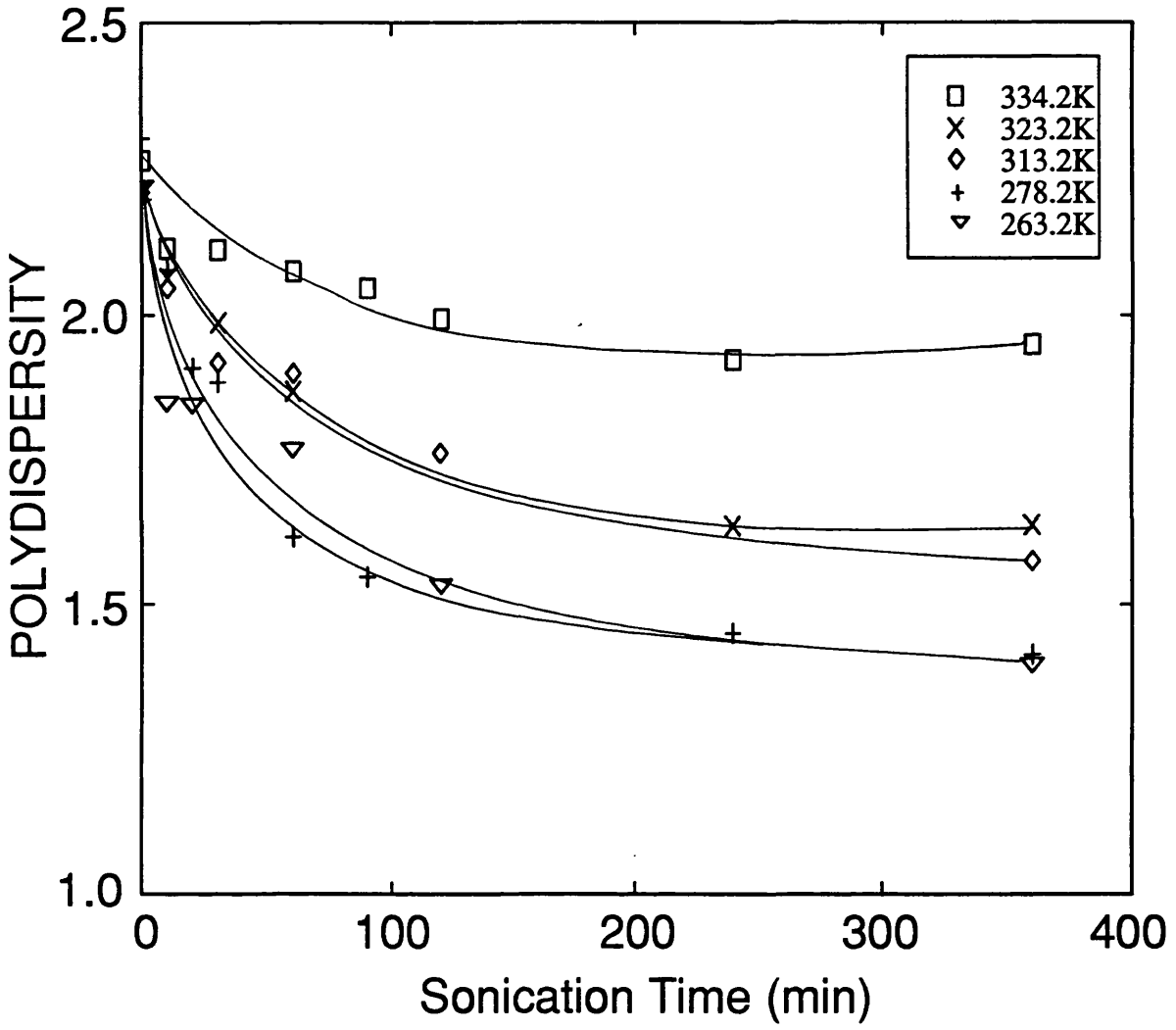

FIGURE 3.33. Variation of the polydispersity of the polystyrene during the sonication of 0.5%w/v polystyrene in toluene at various temperatures.

Table 3.3 shows the effect of temperature on the degradation rate constants calculated from models developed earlier.

Table 3.3 Degradation rate constants for polystyrene in toluene at various temperatures

Temperature K	RATE CONSTANTS / min^{-1}				Rate min^{-1}
	Berlin ($x10^2$)	Ovenall ($x10^7$)	Fujiwara ($x10^5$)	Schmid ($x10^{10}$)	
334.2	1.03	10.69	17.20	9.90	733
323.2	1.20	5.97	4.20	5.17	833
313.2	1.59	7.11	4.66	6.43	1000
283.2	2.64	6.26	2.28	6.02	1200
263.2	6.55	11.36	3.89	14.60	1833

From the previous discussion it would be expected that low temperatures would produce the fastest degradation rate constant. However, this only occurs when using the El'tsefon and Berlin rate model and calculating the rate of change of molecular weight for the first 30 minutes. The Schmid and Ovenall models do produce the fastest rate constant at 263 K, however the rates produced at higher temperatures do not follow any trend. The degradation curves obtained show that the rate is faster at lower temperatures and hence it can be concluded that although the Ovenall, Fujiwara and Schmid models do produce good linear correlations to obtain the rate constants, the values obtained do not correlate with the observed trends.

However, the El'tsefon and Berlin rate model does produce increasing rate constants with decreasing temperature. Using this model, rate constants can be used in the Arrhenius equation[194].

$$\text{Ln}\, k = \text{Ln}\, A - \frac{E_a}{RT} \qquad 3.19$$

where k is the rate constant at the absolute temperature, T, E_a is the activation energy, R is the molar gas constant and A is the pre-exponential factor (which is temperature independent), an activation energy for the degradation can be calculated. This can be seen in Figure 3.34. The activation energy, E_a, is the minimum amount of energy required for the reaction to occur.

The activation energy for a reaction is normally positive, due to the rate of most reactions increasing with an increase in temperature. However, in the case of ultrasonic degradation, lower temperatures increase the rate and hence an apparently negative activation energy is produced. This feature has been noted previously by researchers studying various types of mechanochemical degradation[195]. The activation energy obtained from the Berlin rate plot is -17.3 kJ mol^{-1}. This is considerably below that found for the thermal degradation of polystyrene[193] (M_w = 430000, γ = 3.1) of 167.4 kJ mol^{-1}.

3.5 Effect of Concentration on the Degradation

Concentration studies were carried out in two solvents, toluene and methyl butyrate. Methyl butyrate was used because of its physical properties being very similar to those of methyl methacrylate, as shown previously in Table 2.1. It can be seen that the degradations in both solvents have similar characteristics (Figures 3.35, 3.36). The degradation is much faster and the limiting molecular weight lower in the less concentrated solutions. In both solvents, degradation is suppressed when the concentration reaches 20% w/v.

The effect of concentration on the limiting molecular weight can be seen in Figures 3.37 and 3.38. Both systems show a very large increase in the value for M_{LIM} in the concentration range 1-5% w/v and begin to reach an upper limiting molecular weight at 10% w/v.

Previous work has also found a decrease in degradation at high concentrations[57,58]. This can be explained by considering the mechanism of Thomas[85] which considered the effect of flow fields produced by cavitation in solutions where

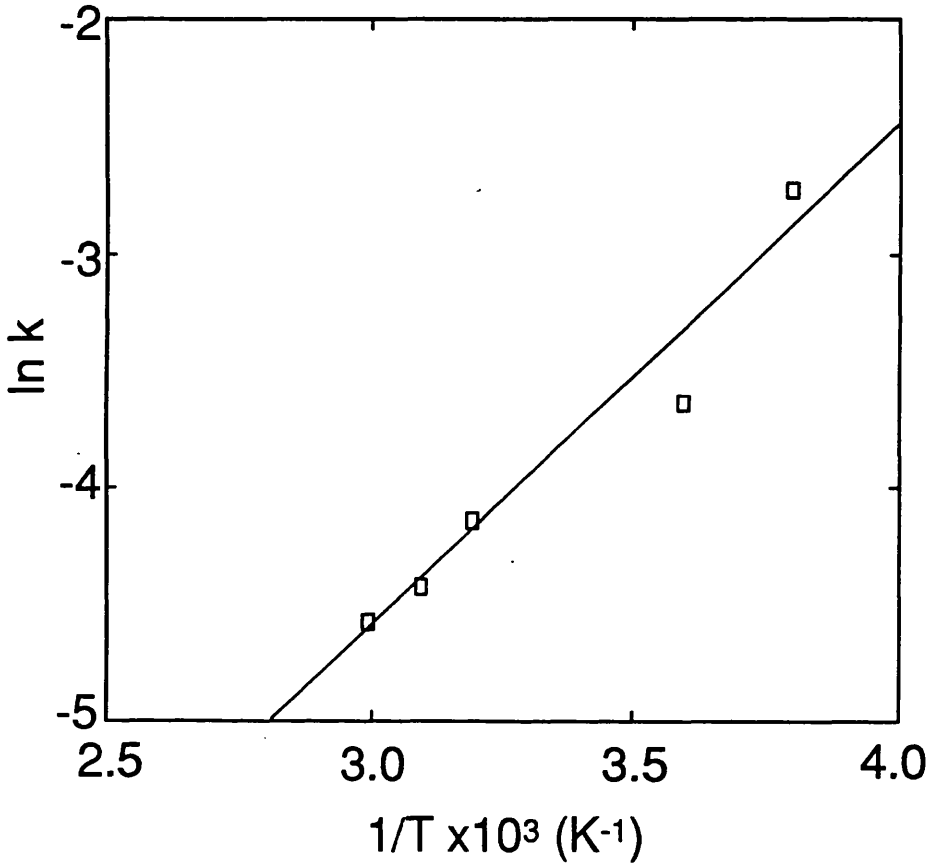

FIGURE 3.34. Calculation of the activation energy for the degradation of 0.5%w/v polystyrene in toluene using the Berlin rate constants.

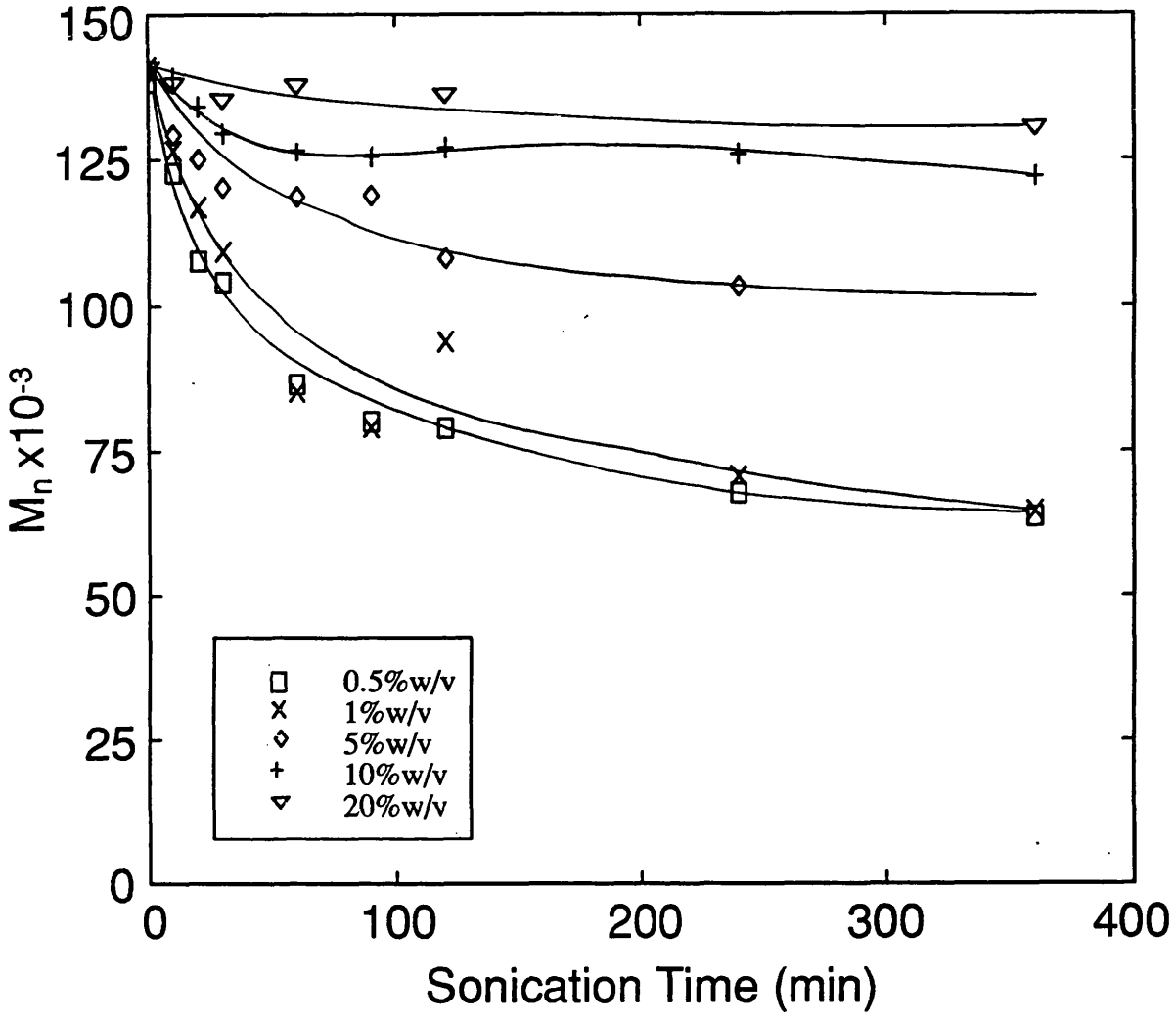

FIGURE 3.35. Variation of number average molecular weight during the sonication of polystyrene in methyl butyrate at various concentrations.

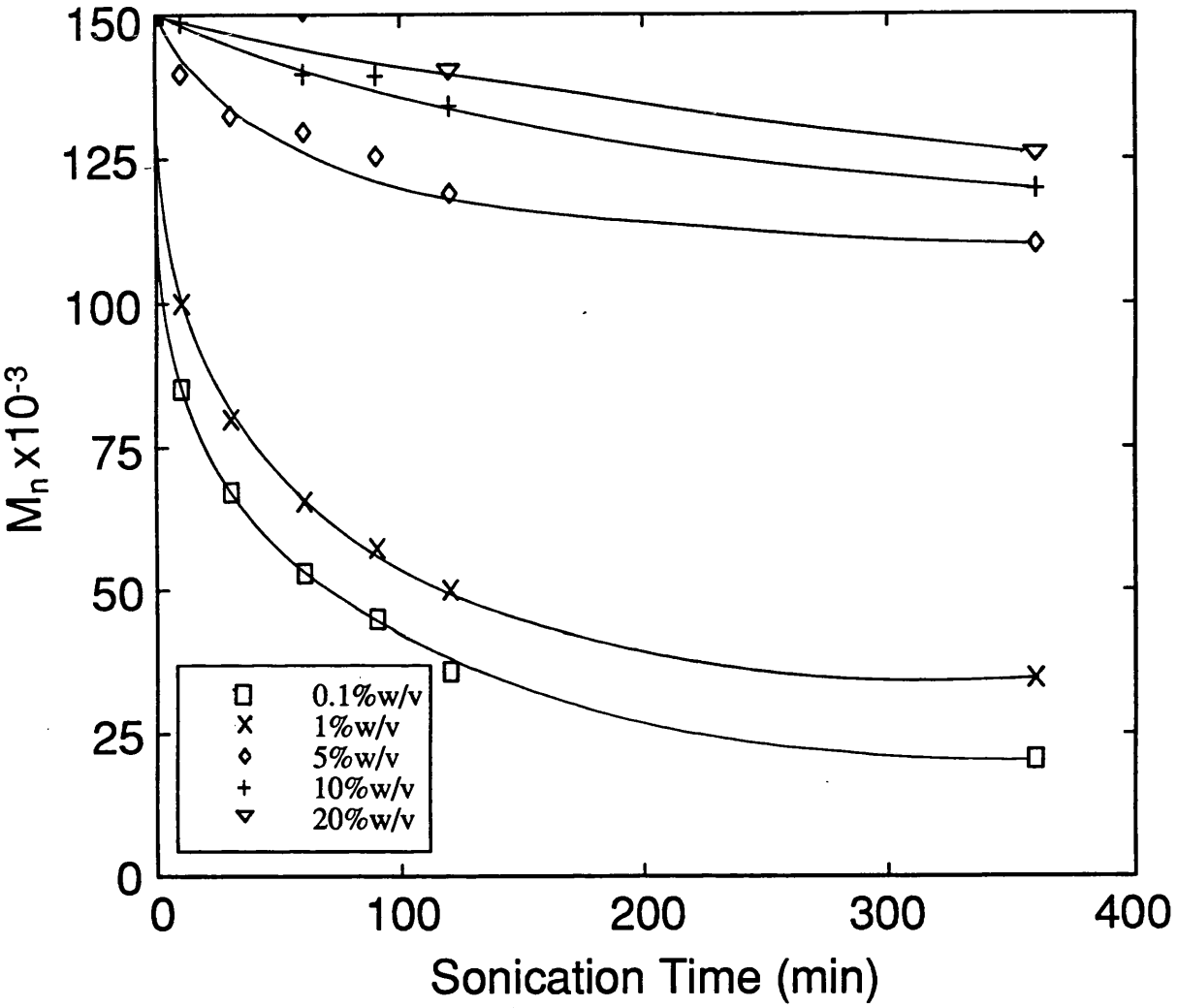

FIGURE 3.36. Variation of number average molecular weight during the sonication of polystyrene in toluene at various concentrations .

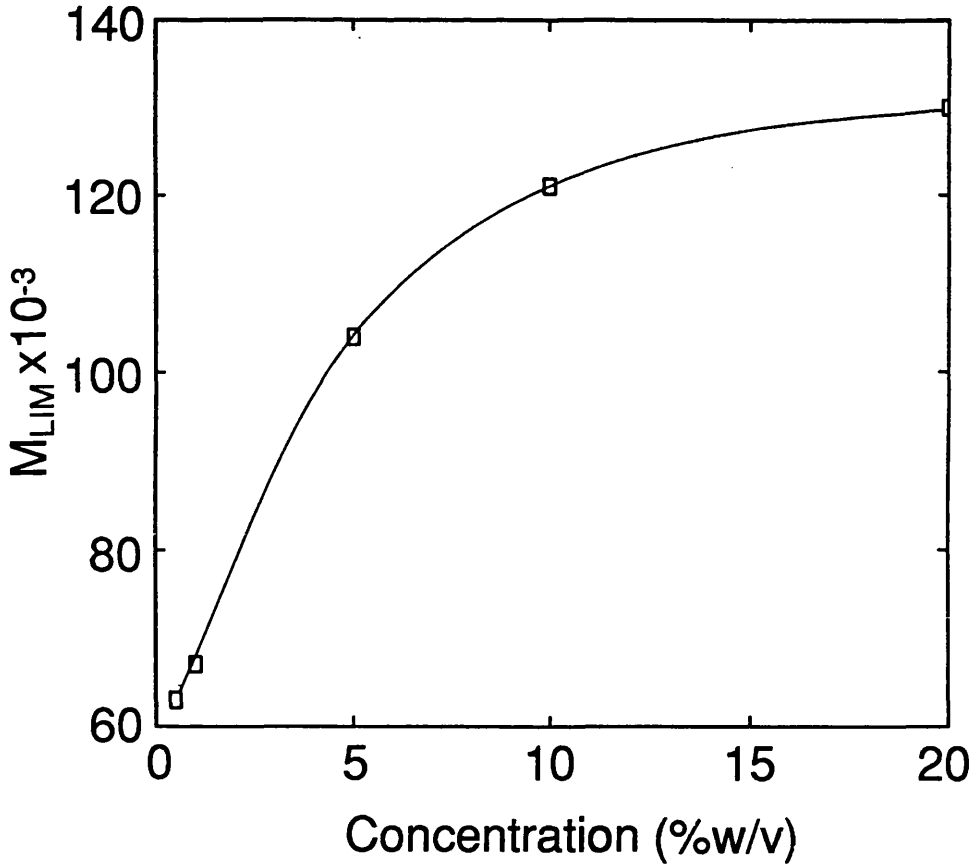

FIGURE 3.37. Effect of solution concentration on the limiting molecular weight of polystyrene for the sonication of polystyrene in toluene.

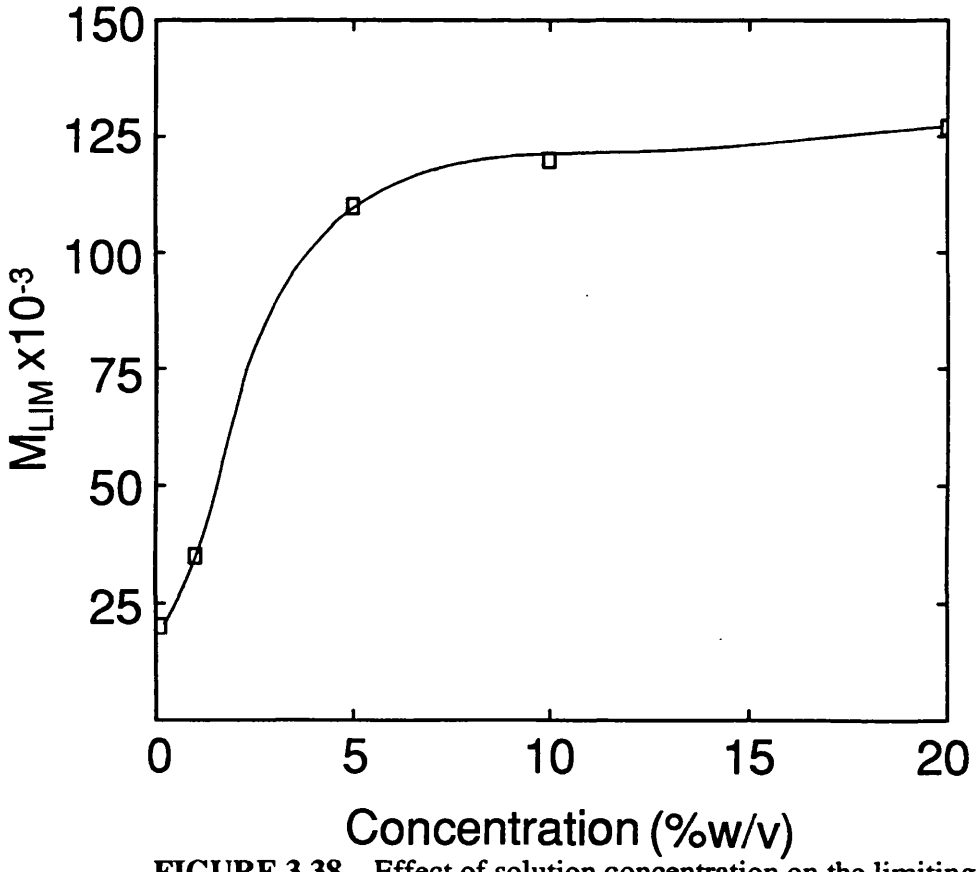

FIGURE 3.38. Effect of solution concentration on the limiting molecular weight of polystyrene for the sonication of polystyrene in methyl butyrate.

there was no association of polymer molecules (in very dilute solutions). As the cavitation bubble collapses, very large pressures and velocity gradients in the surrounding liquid are produced. As a polymer molecule occupies a relatively large volume, with sufficiently large velocity gradients, the side of the polymer coil near a collapsing cavity will move at a higher velocity than the side away from the collapsing cavity. Stresses are then produced on the polymer chain due to the relative motion of the polymer segments and solvents.

As the concentration increases it is felt that the flow field effect will become less important due to the larger number of polymer chains breaking the flow and hence lessening its effect. Although the polymer molecules in the vicinity of the collapsing bubble may still be affected, the number of molecules at a greater distance from the bubble still affected will be small.

This however, does not explain the large difference between degrading 1% w/v and 5% w/v polystyrene in both toluene and methyl butyrate. In order to explain this the critical overlap concentration, C*, must be incorporated. This is the concentration at which chains begin to entangle as shown in Figure 3.39. For polystyrene, C* can be calculated according to the formula[196]

$$C^* = 620\, M_w^{-0.78} \qquad 3.20$$

for good solvents, where M_w is the weight average molecular weight. Considering in these experiments, M_w = 448000, this gives a critical overlap concentration of 0.024 g/ml or 2.4% w/v. This coincides with the large difference between degrading 1% w/v and 5% w/v solutions. As the chains begin to overlap, there is both more restriction to their movement and on cleavage, a greater chance of the chains recombining. Hence the amount of degradation is reduced, and the limiting molecular weight increases.

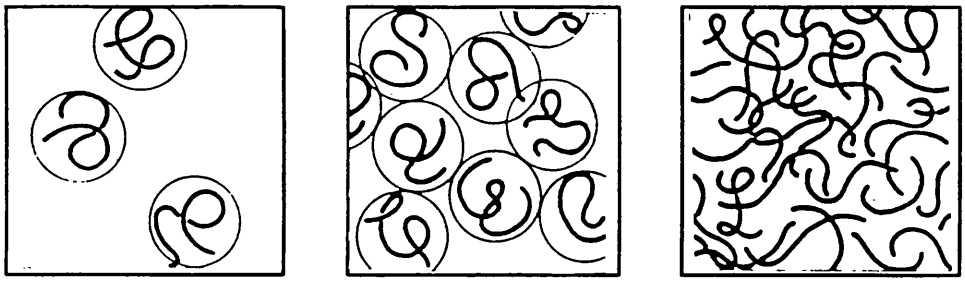

C<C* C=C* C>C*

FIGURE 3.39. Conformations of chains in solution showing the critical overlap concentration, C*.

As might be expected from the discussion in preceding sections, the greatest change in polydispersity occurs in the conditions where maximum reduction in molecular weight takes place, i.e. at low concentrations as shown in Figure 3.40.

The effect of concentration on the degradation rate constants can be seen in Figures 3.41 - 3.44. All of the models produce very different effects. Previous workers have studied the effect of concentration on the rate of degradation of polystyrene in benzene[25,57,58]. A maximum in the rate was displayed in the region of 0.01 - 0.03% w/v and fell at higher concentrations. This decrease in rate was attributed to a reduction in the cavitation efficiency as the polymer chains begin to overlap. The concentration range studied by these workers was very small, ranging from 0.005% w/v to 1% w/v. The rates were obtained by measuring the fractional change in the average chain length after 15 minutes sonication.

In this study the range of concentrations used was much larger. The Schmid model shows an increase in the rate constants with concentration, with a maximum in the methyl butyrate system at around 10% w/v.

From the degradation curves, (Figs 3.35 and 3.36) it can be seen that the degradation rate obviously decreases with increasing concentration and hence although the Schmid model gives good linear correlations, it does not give rates that correlate with the observed results.

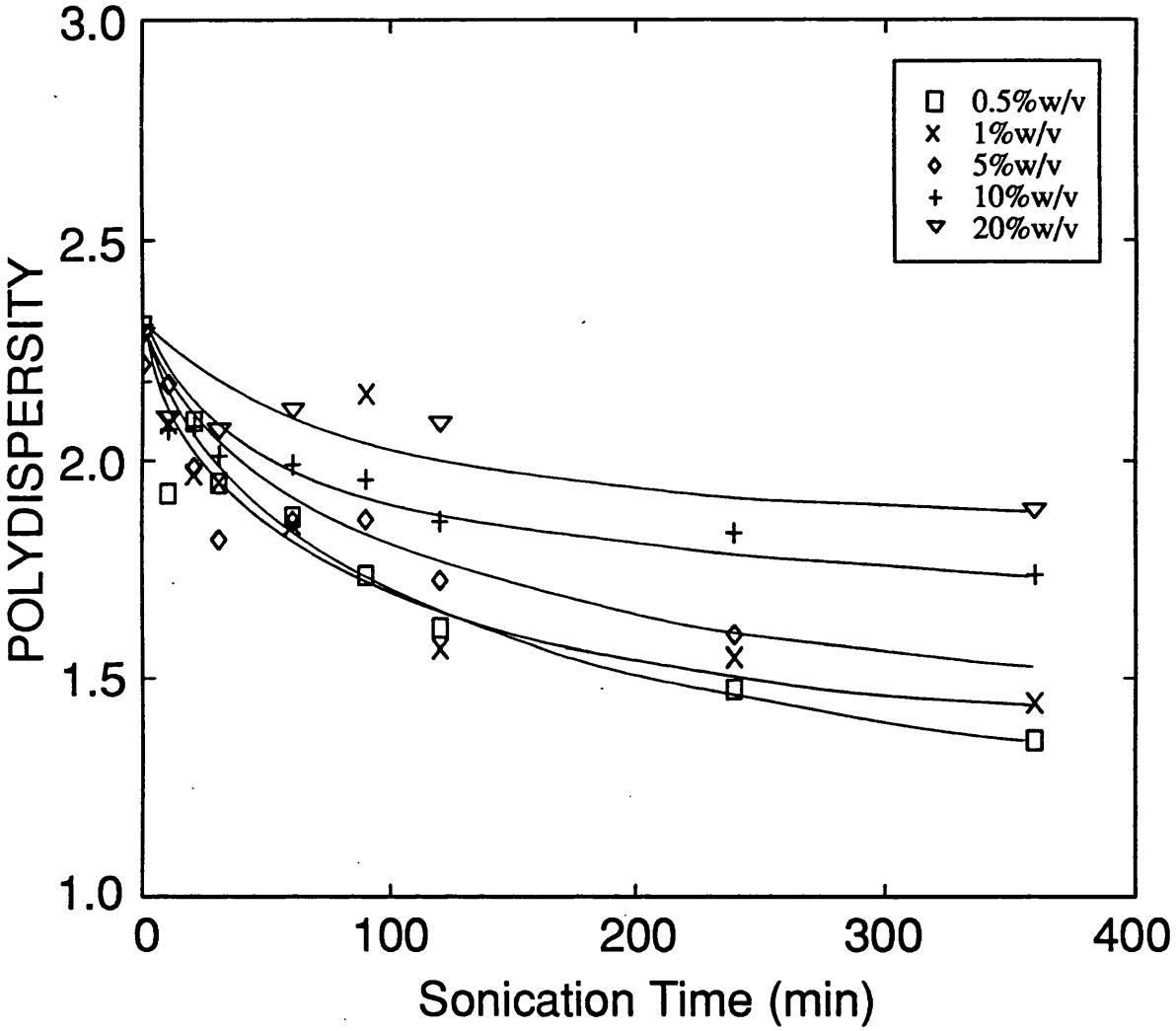

FIGURE 3.40. Variation of the polydispersity of the polystyrene during the sonication of polystyrene in methyl butyrate at various concentrations.

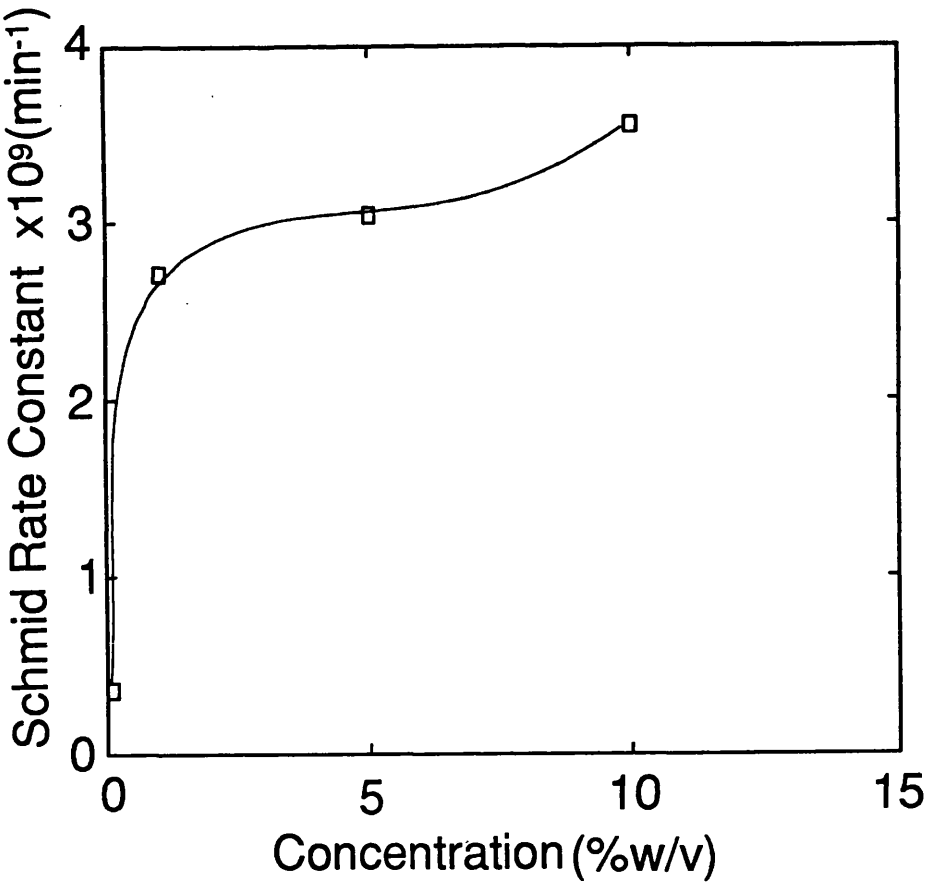

FIGURE 3.41(A). Effect of the polystyrene concentration on the Schmid rate constant for the sonication of polystyrene in toluene.

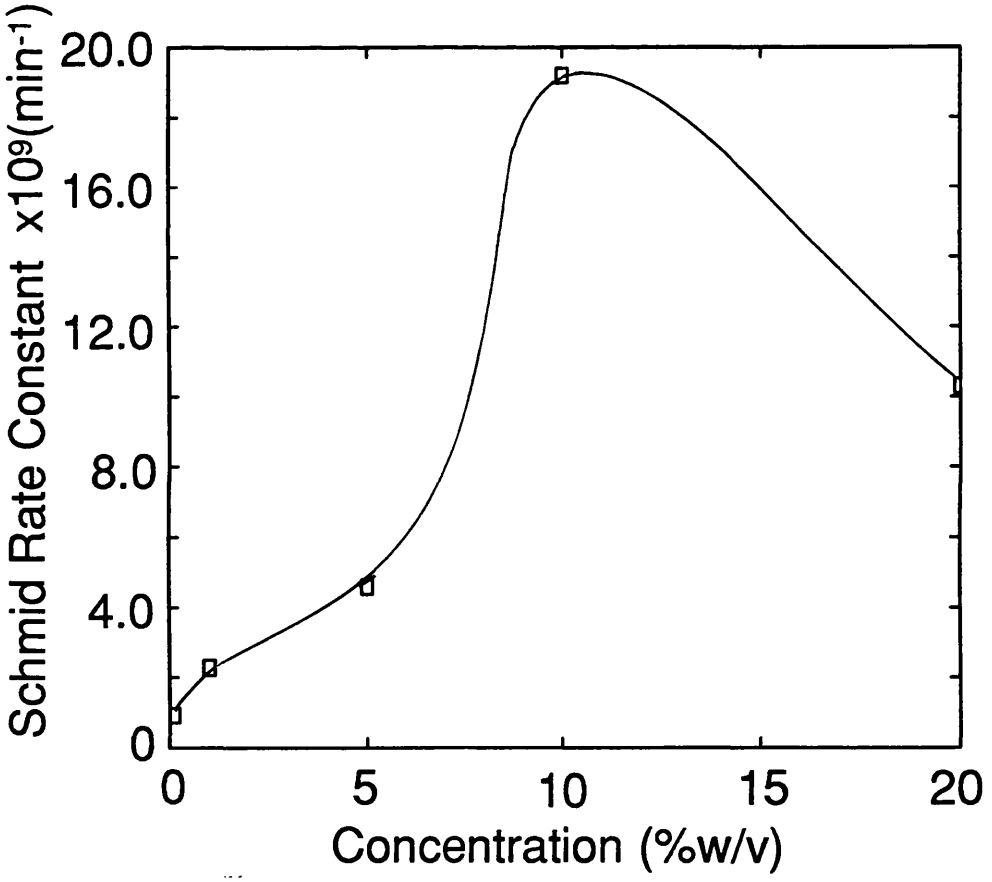

FIGURE 3.41(B). Effect of the polystyrene concentration on the Schmid rate constant for the sonication of polystyrene in methyl butyrate.

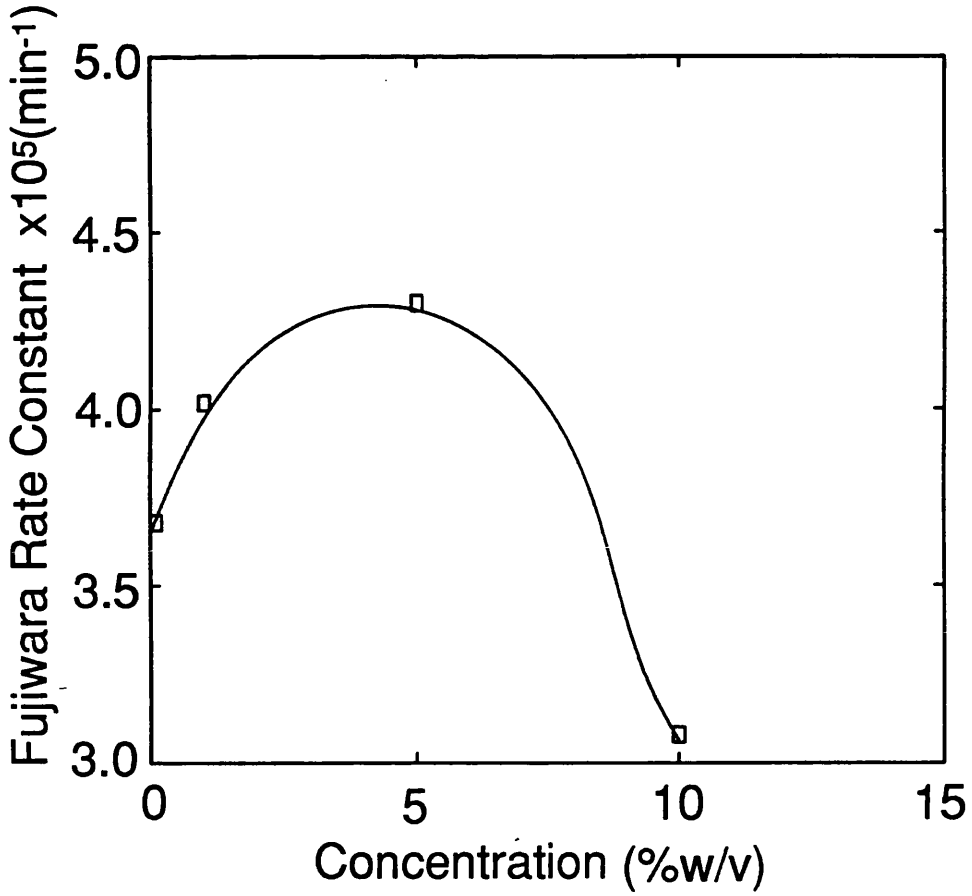

FIGURE 3.42(A). Effect of the polystyrene concentration on the Fujiwara rate constant for the sonication of polystyrene in toluene.

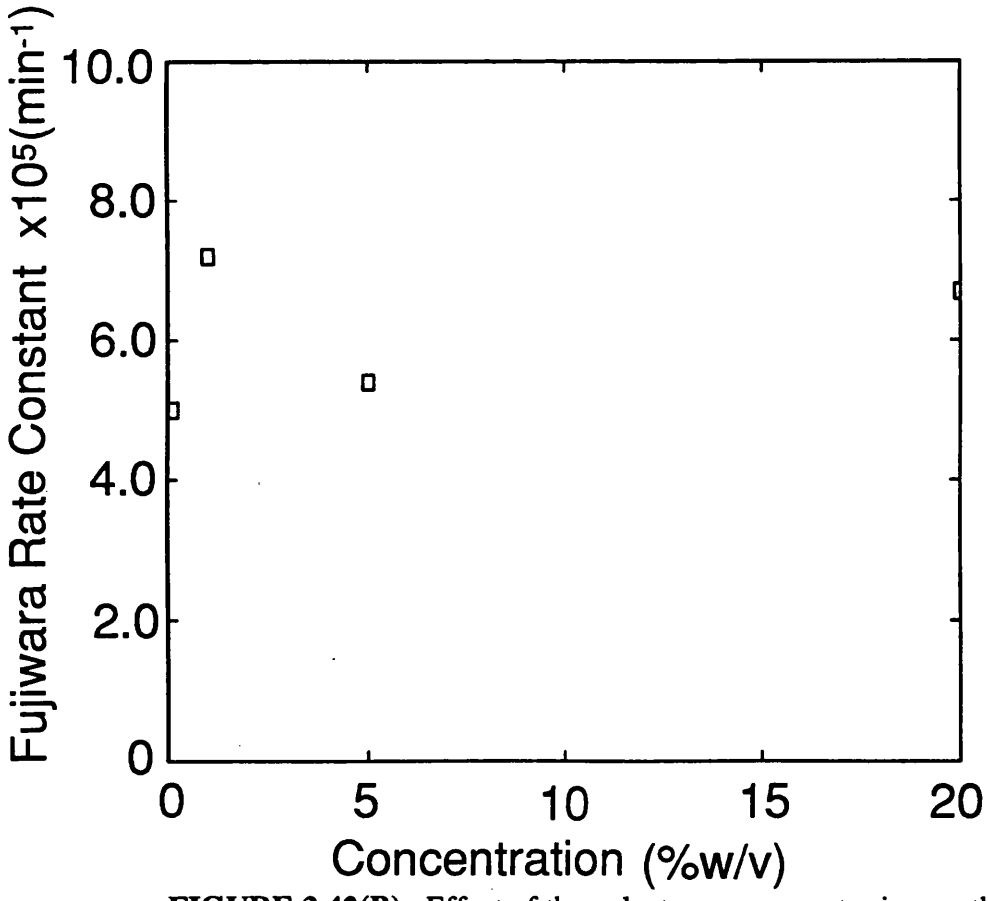

FIGURE 3.42(B). Effect of the polystyrene concentration on the Fujiwara rate constant for the sonication of polystyrene in methyl butyrate.

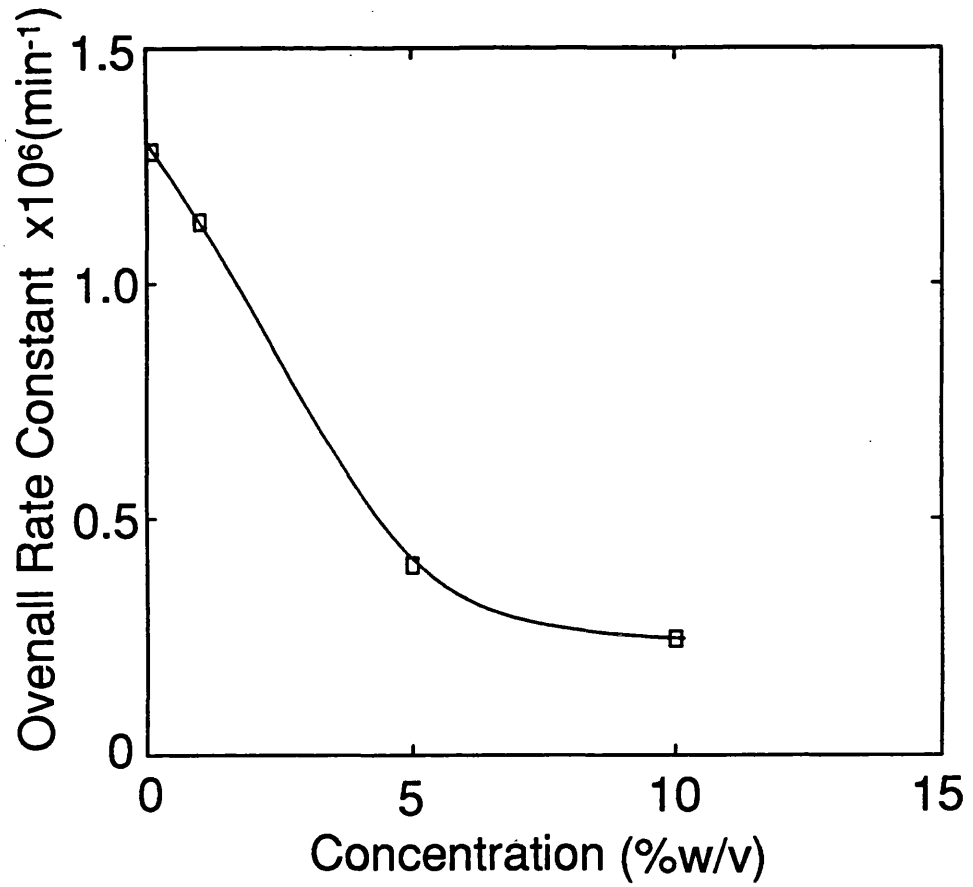

FIGURE 3.43(A). Effect of the polystyrene concentration on the Ovenall rate constant for the sonication of polystyrene in toluene.

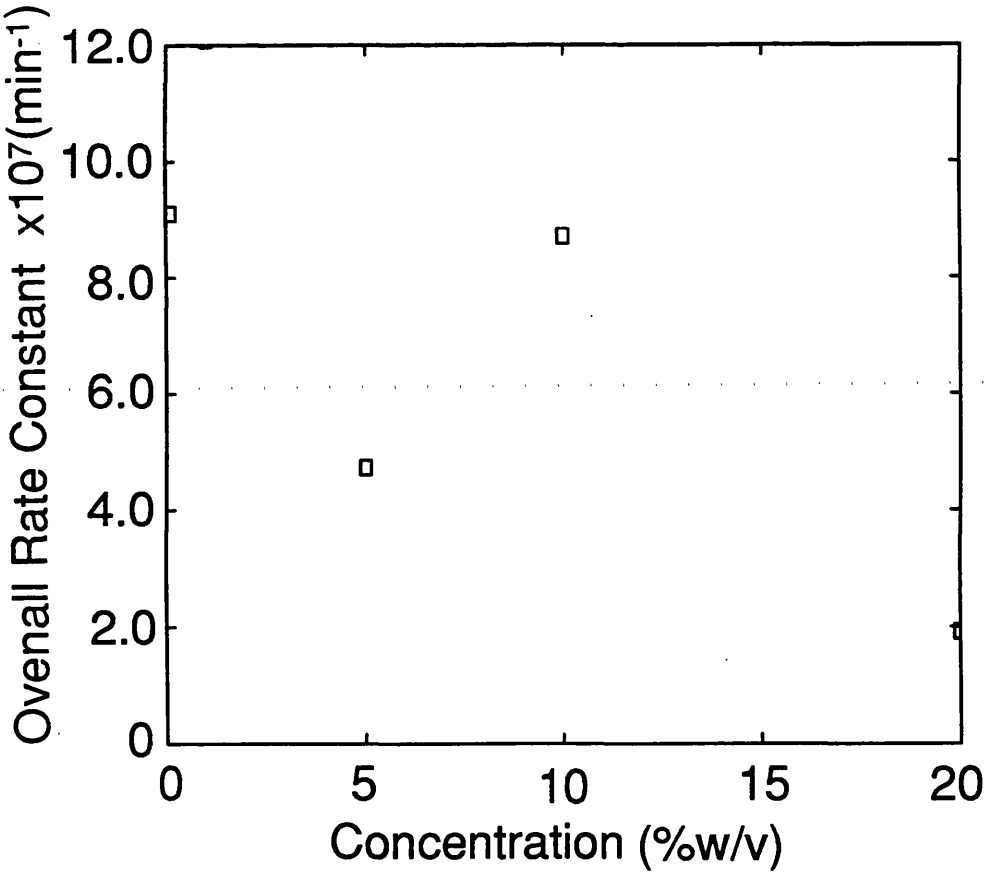

FIGURE 3.43(B). Effect of the polystyrene concentration on the Ovenall rate constant for the sonication of polystyrene in methyl butyrate.

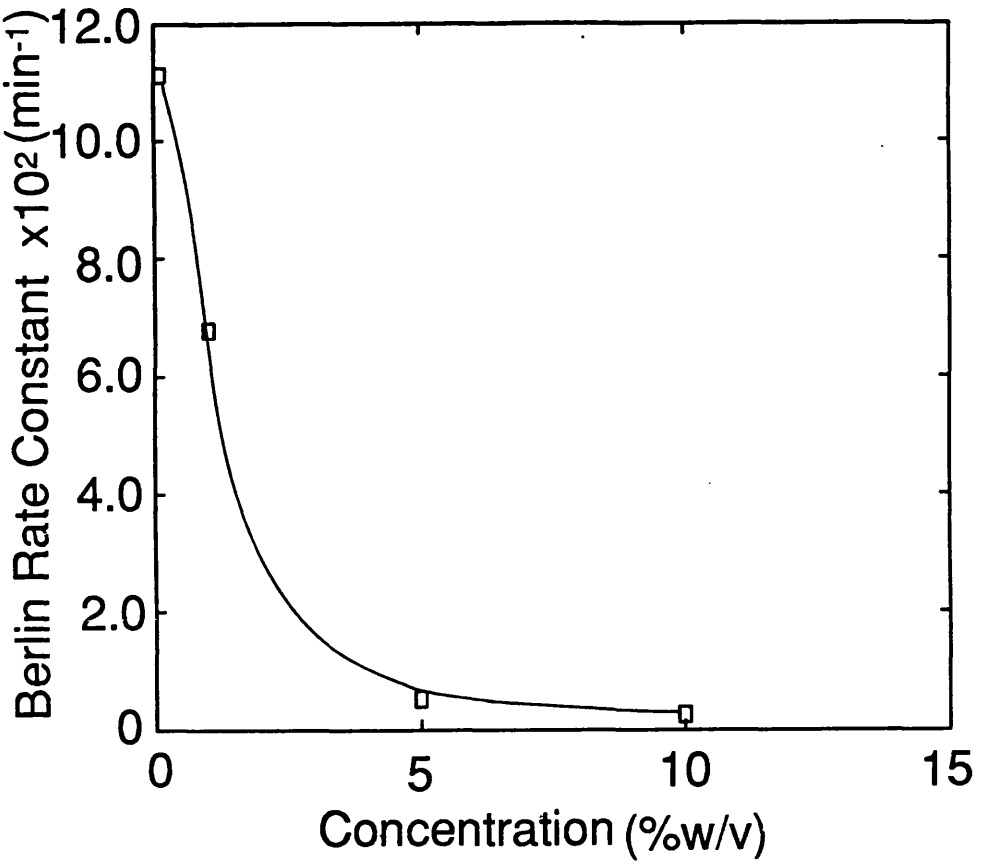

FIGURE 3.44(A). Effect of the polystyrene concentration on the Berlin rate constant for the sonication of polystyrene in toluene .

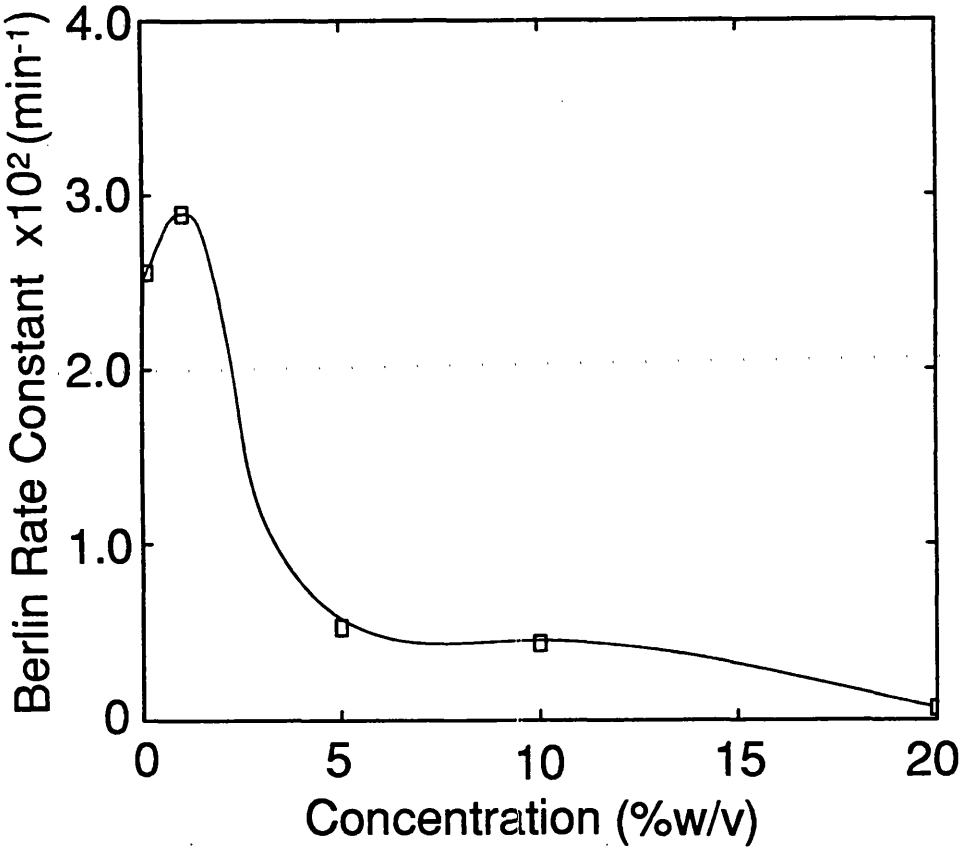

FIGURE 3.44(B). Effect of the polystyrene concentration on the Berlin rate constant for the sonication of polystyrene in methyl butyrate.

The Ovenall and El'tsefon and Berlin models both show a decrease in the rate constants with increasing concentration. However, in the case of the degradation in methyl butyrate, both of these models show that the 1% w/v solution degrades faster than the 0.5% w/v solution. However, this increase in the rate constant is within the experimental error described earlier.

The Berlin rate model shows that the largest decrease in rate occurs between 1% and 5% w/v, coinciding with the value of the critical overlap concentration calculated earlier in this section. Hence as the chains begin to overlap, the flow field effect is reduced and there is a greater chance of the chains recombining after breaking.

3.6 Effect of Dissolved Gases on the Degradation

As discussed in Chapter One, the nature of the gas present affects the cavitation process. However, its effects on the degradation have not been thoroughly examined.

The effect of the dissolved gas on the degradation was examined by saturating the system before sonication and blanketing the solution with gas during the reaction. The gases studied were argon, nitrogen, oxygen, methane and carbon dioxide. These were chosen because they gave a good range of properties[197]. This can be seen in Table 3.4 overleaf.

Table 3.4 Physical properties of dissolved gases

Gas	Solubility (X_A) x 10^3	Thermal Conductivity x 10^2($Wm^{-1}K^{-1}$)	C_p/C_v	M_{LIM}
CO_2	9.1 (benzene)	1.37	1.30	90000
CH_4	2.09 (benzene)			75000
Ar	0.88 (toluene)	1.58	1.67	63000
N_2	0.57 (toluene)	2.28	1.40	56000
O_2	0.92 (toluene)	2.33	1.40	50000

The value for the solubility of the gases is quoted as the mole fraction of the gas in the solvent,

$$X_A = \frac{N_A}{1 + N_A} \qquad 3.21$$

where N_A is the number of moles of A absorbed per mole of the solvent at 1 atmosphere pressure and 25°C. A large value of X_A indicates a high solubility[197]. All of the degradations were carried out in toluene but the solubilities were not all available for this solvent. In these cases the gas solubility in benzene was used.

The degradation curves can be seen in Figure 3.45 These gave the well known basic shapes and are very dependent on the gas present in solution. A wide range of limiting molecular weights was reached and these are tabulated in Table 3.4.

A graph of the effect of the solubility on the limiting molecular weight can be seen in Figure 3.46. As the solubility of the gas increases, the limiting molecular weight increases. The anomaly in the results is oxygen, which has a lower M_{LIM} than expected from consideration of solubility alone.

Figures 3.47 and 3.48 show the effect of the gas and gas solubility on the

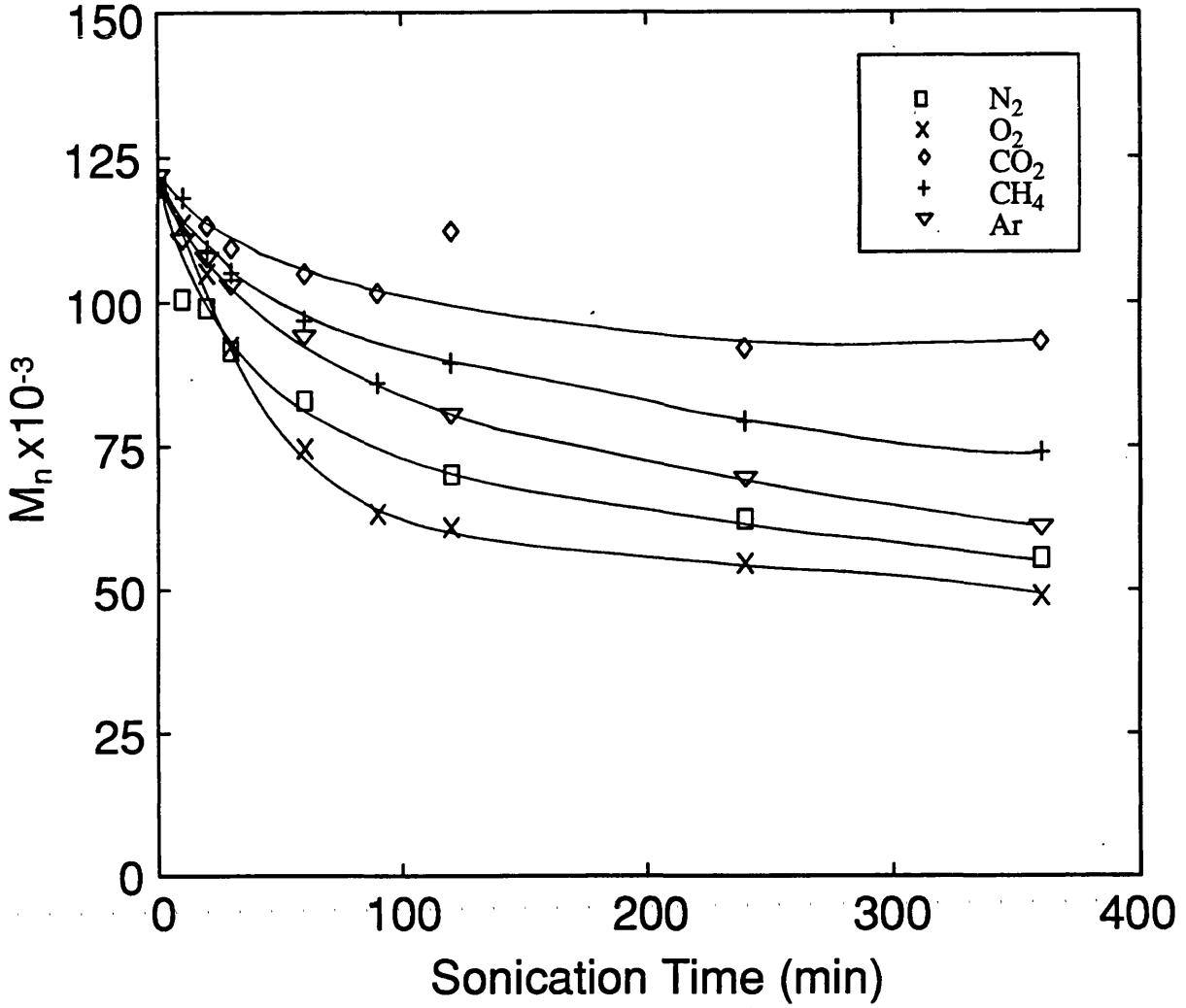

FIGURE 3.45. Variation of number average molecular weight during the sonication of 0.5%w/v polystyrene in toluene in the presence of various gases.

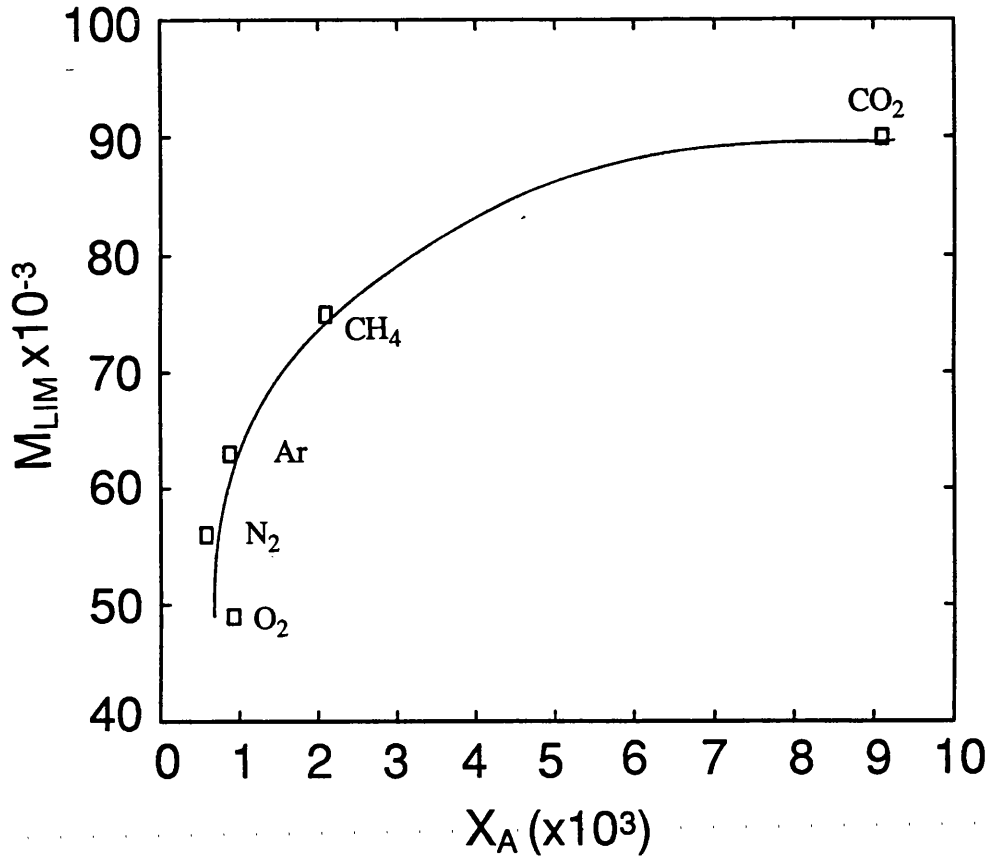

FIGURE 3.46. Effect of gas solubility on the limiting molecular weight of polystyrene for the sonication of a 0.5%w/v solution.

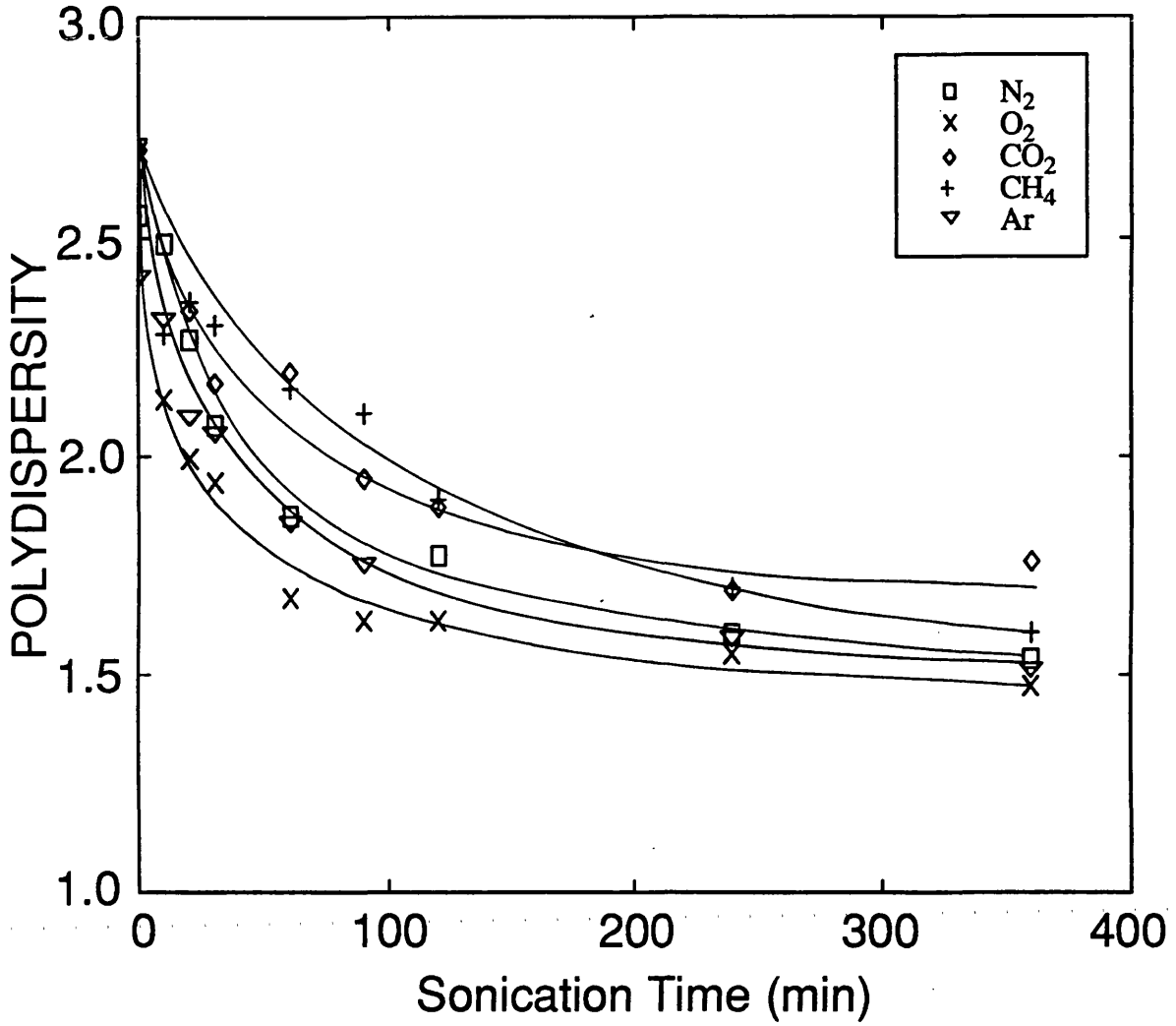

FIGURE 3.47. Variation of the polydispersity of the polystyrene during the sonication of 0.5%w/v polystyrene in toluene in the presence of various gases.

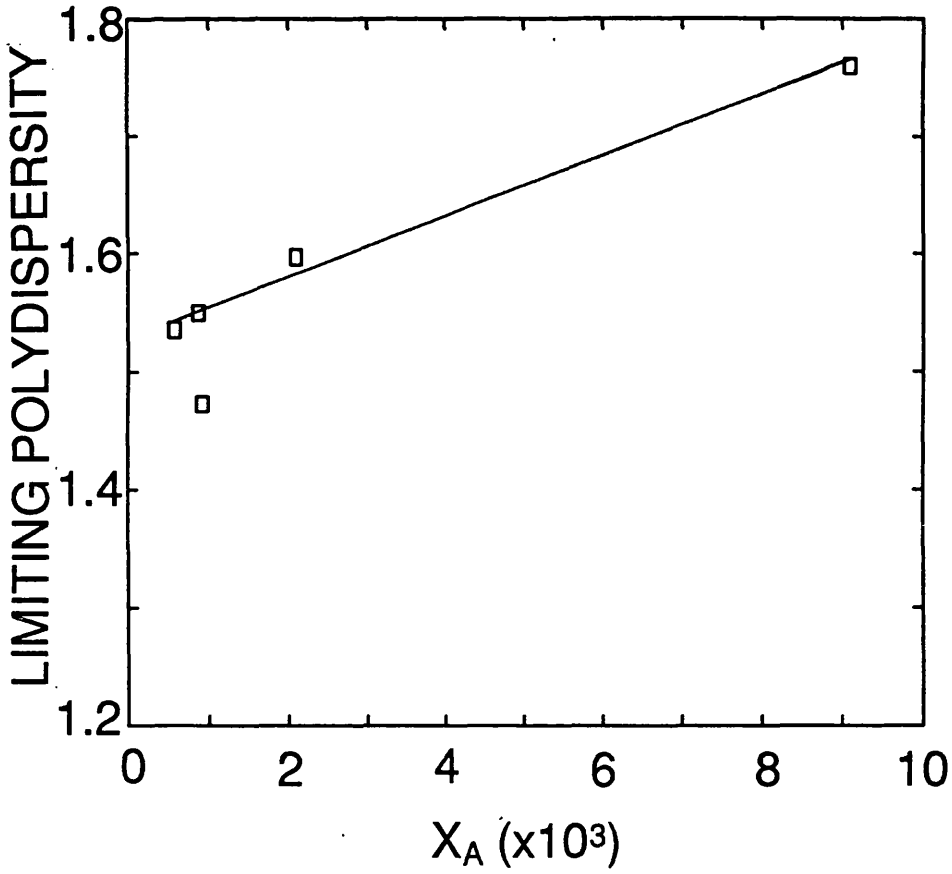

FIGURE 3.48. Effect of gas solubility on the limiting polydispersity of polystyrene for the sonication of a 0.5%w/v solution.

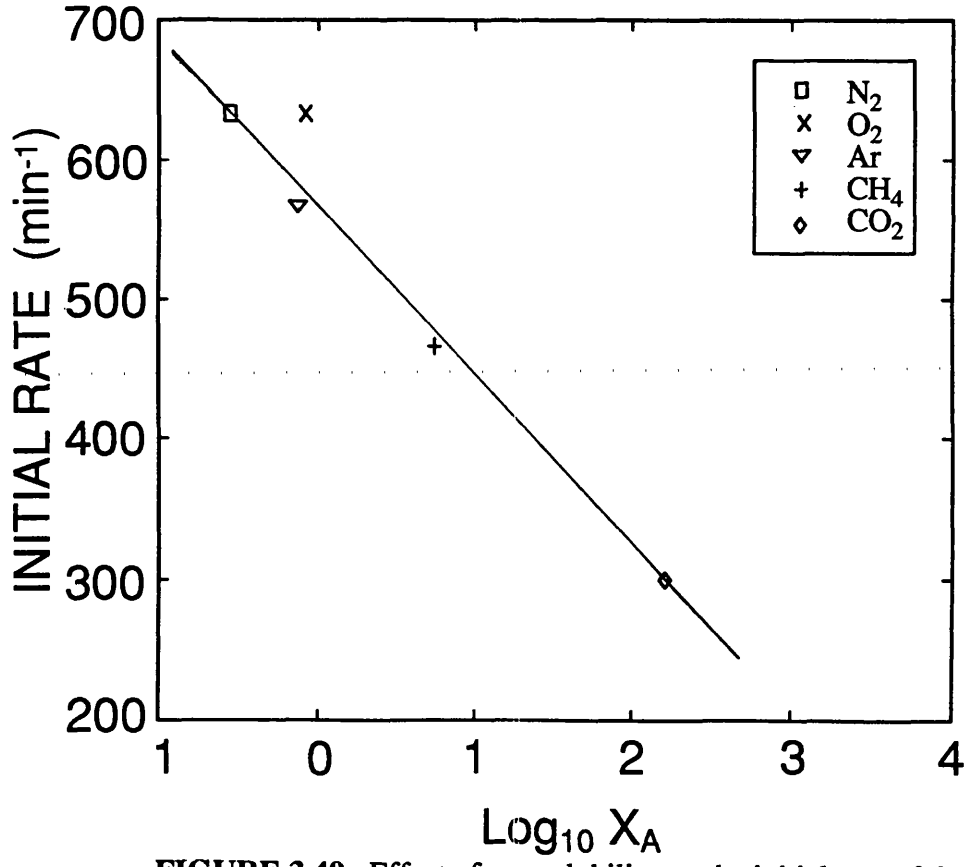

FIGURE 3.49. Effect of gas solubility on the initial rate of degradation of polystyrene for the sonication of a 0.5%w/v solution.

polydispersity of the polymer during sonication. Gases with lower solubilities produce polymers with lower polydispersities. The polydispersity obtained when oxygen is used is much lower than expected from solubility data alone. With the exception of oxygen, there appears to be a linear relationship between the limiting polydispersity and the gas solubility.

As explained in Section 1.5.1, increasing the gas content of the solvent reduces the pressure P_{MAX} produced on bubble collapse, due to more gas diffusing into the cavitation bubble and cushioning the collapse. This would affect the shock wave mechanism. Owing to the cushioning effect, the shock wave produced would be much reduced, so producing less force on the polymer chain. Considering the model of Thomas[85], the speed of the collapse would be reduced owing to the greater gas content of the bubble and hence the difference in force on either side of the polymer chain would also be reduced.

Shorter polymer chains require a larger force to break them and so owing to the force from the cavitation bubble collapse being reduced as the solubility of the gas is increased, the limiting molecular weight also increases. The M_{LIM} produced from the degradation of the polystyrene in an oxygen saturated solution is approximately 15000 lower than expected from solubility data alone. This could be due to the oxygen combining with the radicals formed on the polymer chain end during the degradation and preventing any recombination of the degraded polymer chains.

The effect of the gas solubility on the degradation rate constants can be seen in Table 3.5 overleaf.

Table 3.5 Effect of dissolved gases on rate constants for degradation of polystyrene in toluene

Gas	Solubility ($X_A \times 10^3$)	RATE CONSTANTS / min^{-1} Schmid ($\times 10^{10}$)	Ovenall ($\times 10^7$)	Berlin ($\times 10^3$)	Fujiwara ($\times 10^5$)	Rate (min^{-1})
CO_2	9.1 (benzene)	7.74	56.3	5.10	5.87	300
CH_4	2.09 (benzene)	8.22	5.92	9.35	4.28	466
Ar	0.88 (toluene)	4.78	4.8	10.10	2.50	566
N_2	0.57 (toluene)	10.40	6.88	16.9	3.54	633
O_2	0.92 (toluene)	11.90	9.44	27.6	4.51	633

From the explanation of the effect of gases on the degradation, it would be expected that a gas with a high solubility would produce a very slow degradation rate due to the cushioned bubble collapse. However, the rate models of Schmid, Ovenall, Berlin and Fujiwara produce rate constants that are independent of gas solubility. This is despite the models having good linear correlation coefficients. However, the initial rate model does show a logarithmic relationship with gas solubility, as shown in Figure 3.49 with the exception of oxygen.

3.7 Effect of the Solvent on Polymer Degradation

In order to measure the effect of solvents on the degradation, a series was chosen that gave a good range of heats of vaporisation, saturated vapour pressures, viscosities and Flory-Huggins interaction parameters. The solvents chosen were those listed earlier. All of the solutions were sonicated at an intensity of 17 W cm^{-2} and at a concentration of 0.5% w/v as described in Section 2.2.7.

Graphs showing the variation of the number average molecular weight with sonication time can be seen in Figures 3.50 - 3.52.

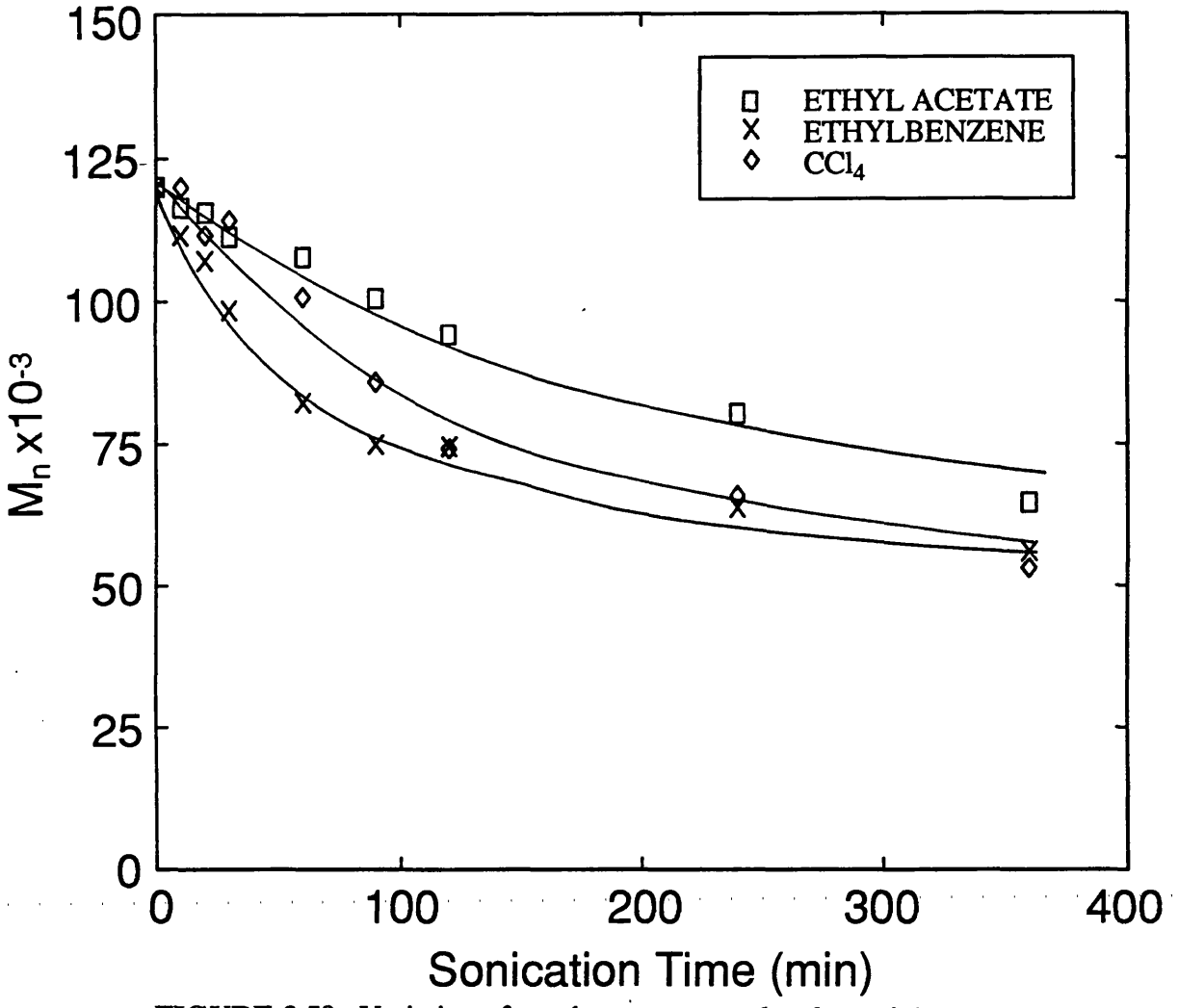

FIGURE 3.50. Variation of number average molecular weight during the sonication of 0.5%w/v polystyrene in various solvents.

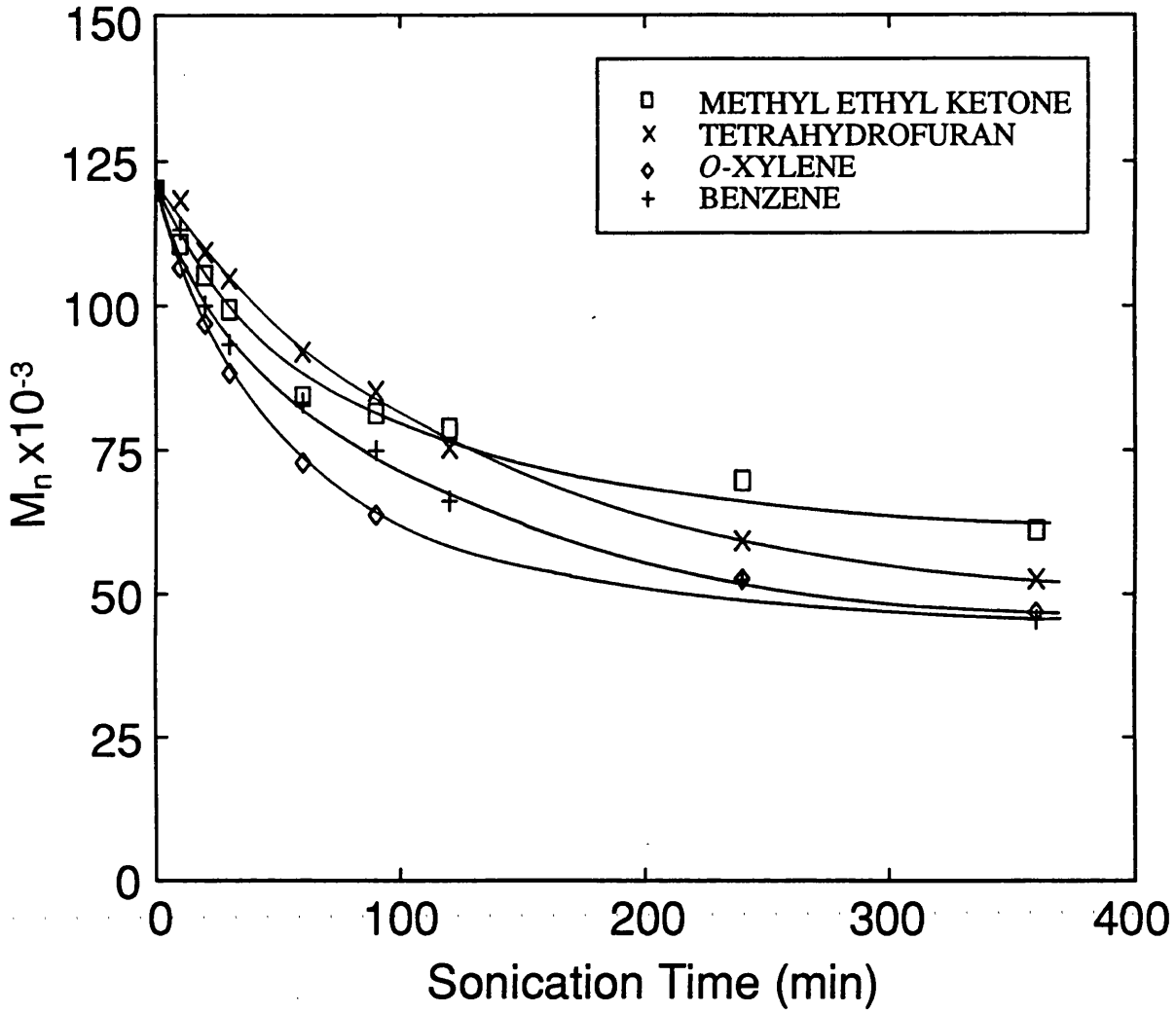

FIGURE 3.51. Variation of number average molecular weight during the sonication of 0.5%w/v polystyrene in various solvents.

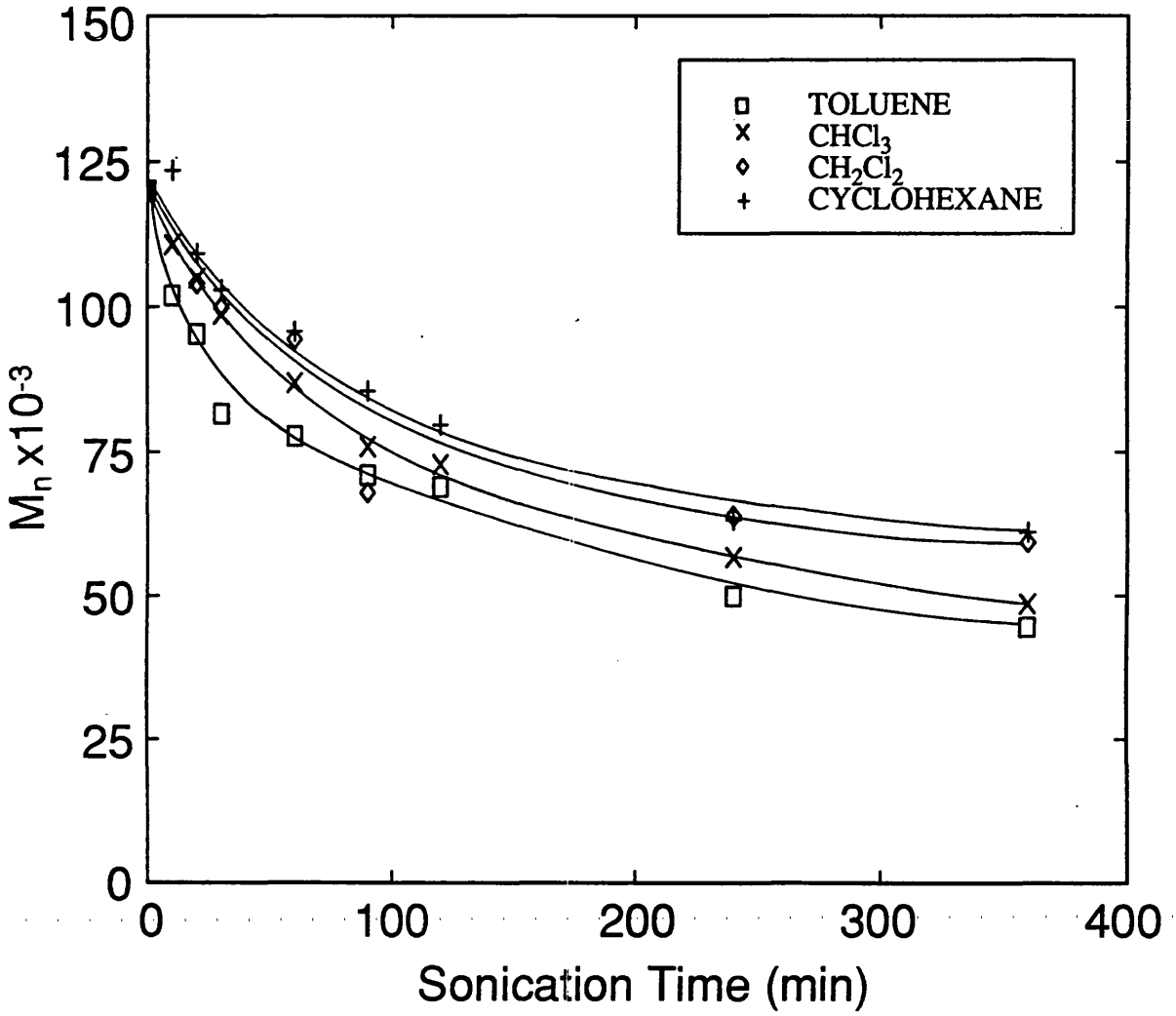

FIGURE 3.52. Variation of number average molecular weight during the sonication of 0.5%w/v polystyrene in various solvents.

All of the degradations show the same basic characteristics described previously.

3.7.1 Correlation of the degradation with the solvent viscosity

Since it is necessary for the negative pressure in the rarefaction cycle to overcome the cohesive forces in the liquid to form a cavitation bubble, an increase in viscosity should affect the cavitation process, although the increase in viscosity raises the cavitational threshold, if cavitation does occur, it has been found that the pressures exerted are more severe[37].

A calibrated Ubbelohde viscometer enabled the absolute viscosities of the solvents in centipoise to be calculated. Figure 3.53 shows the effect of the viscosity on the limiting molecular weight.

There appears to be no relationship between the viscosity of the solvent and the limiting molecular weight obtained.

3.7.2 Correlation of the degradation with the heat of vaporisation of the solvent

As described in Section 1.5.1, when the volatility of the solvent is high, the amount of vapour entering the cavitation bubbles is also high, hence causing a cushioning effect when the bubbles collapse. Therefore, if cavitation is involved in the degradation process, the heat of vaporisation should affect the degradation.

Figure 3.54 shows the effect of the heat of vaporisation on the limiting molecular weight of the polystyrene. The graph has a linear correlation of only 0.092, showing there to be very little, if any, relationship between the two parameters.

Figures 3.55 - 3.58 show the effect of the heat of vaporisation of the solvent on the degradation rate constants.

All of the graphs show the same trend of a high heat of vaporisation producing a fast rate. The effect of the heat of vaporisation on degradation rate was studied by Basedow and Ebert looking at the degradation of dextran in various solvents[9]. These workers obtained a much wider range of values for ΔH_v, spanning from 40 kJ mol^{-1} to

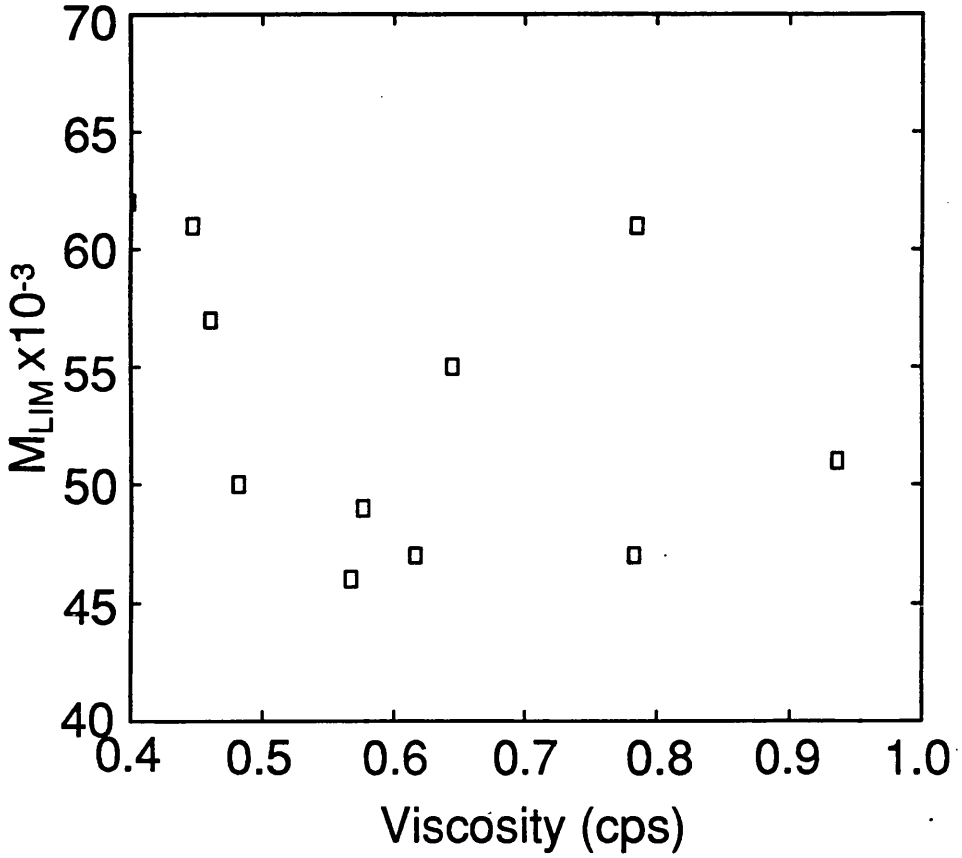

FIGURE 3.53. Effect of viscosity on the limiting molecular weight of polystyrene for the sonication of a 0.5%w/v solution.

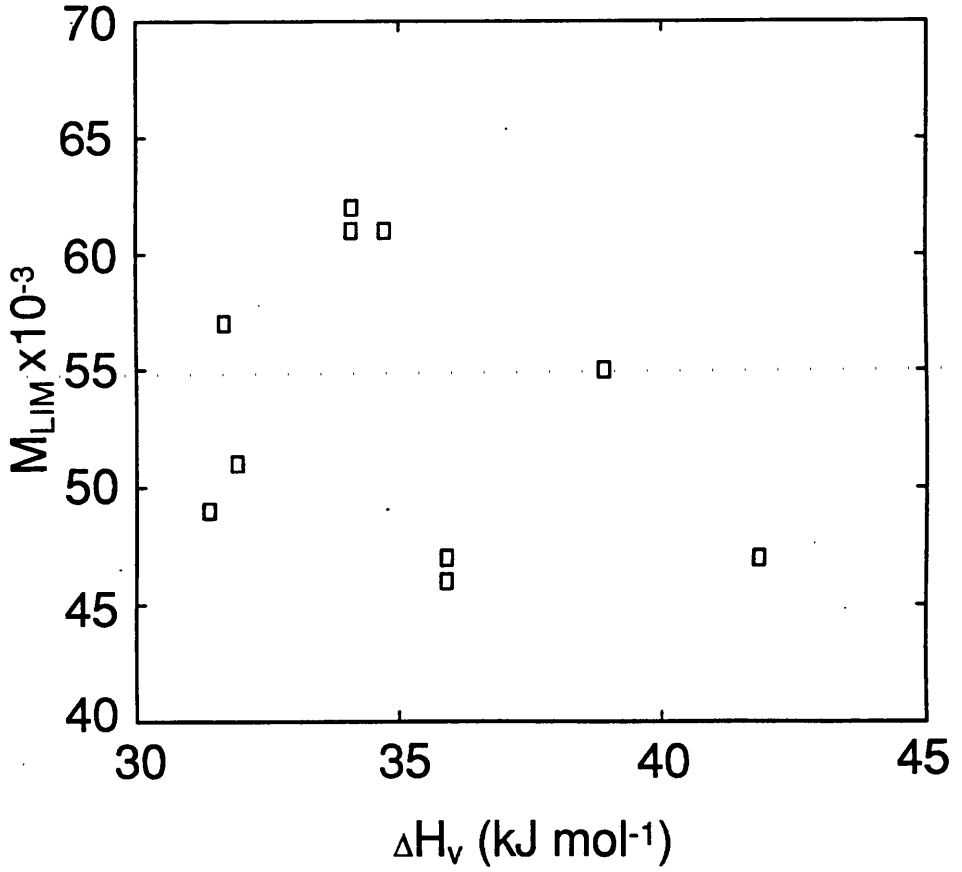

FIGURE 3.54. Effect of the heat of vaporisation on the limiting molecular weight of polystyrene for the sonication of a 0.5%w/v solution.

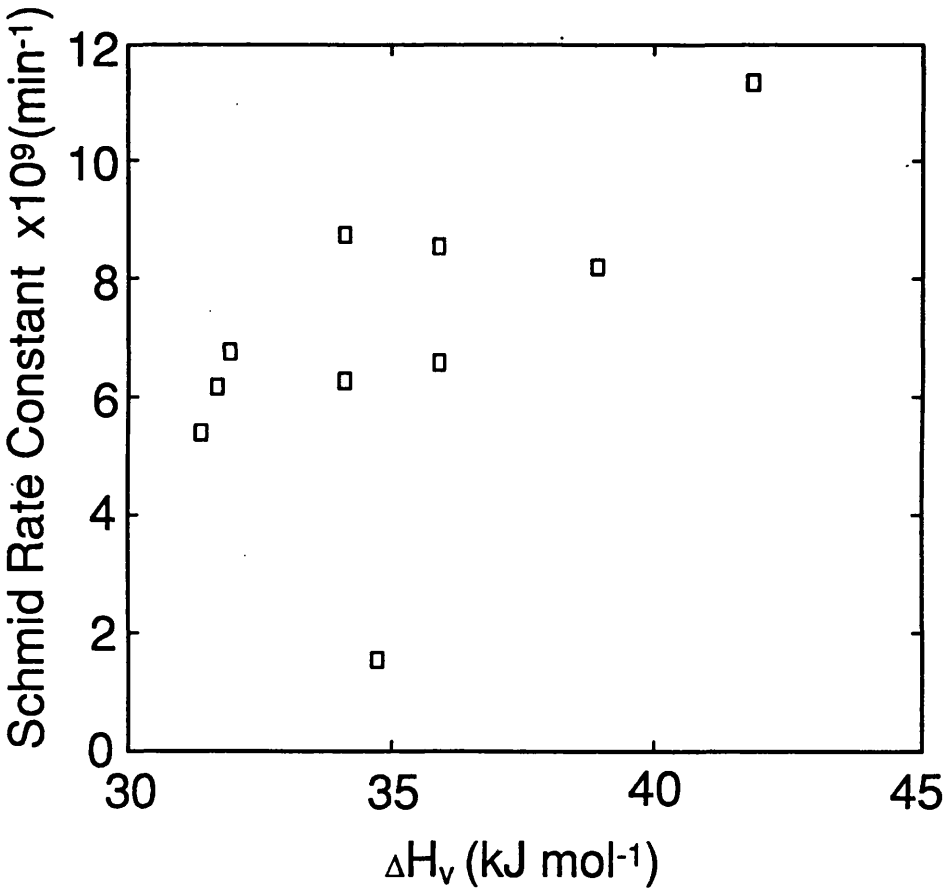

FIGURE 3.55. Effect of the heat of vaporisation of the sovent on the Schmid rate constant for the sonication of 0.5%w/v polystyrene in a range of solvents.

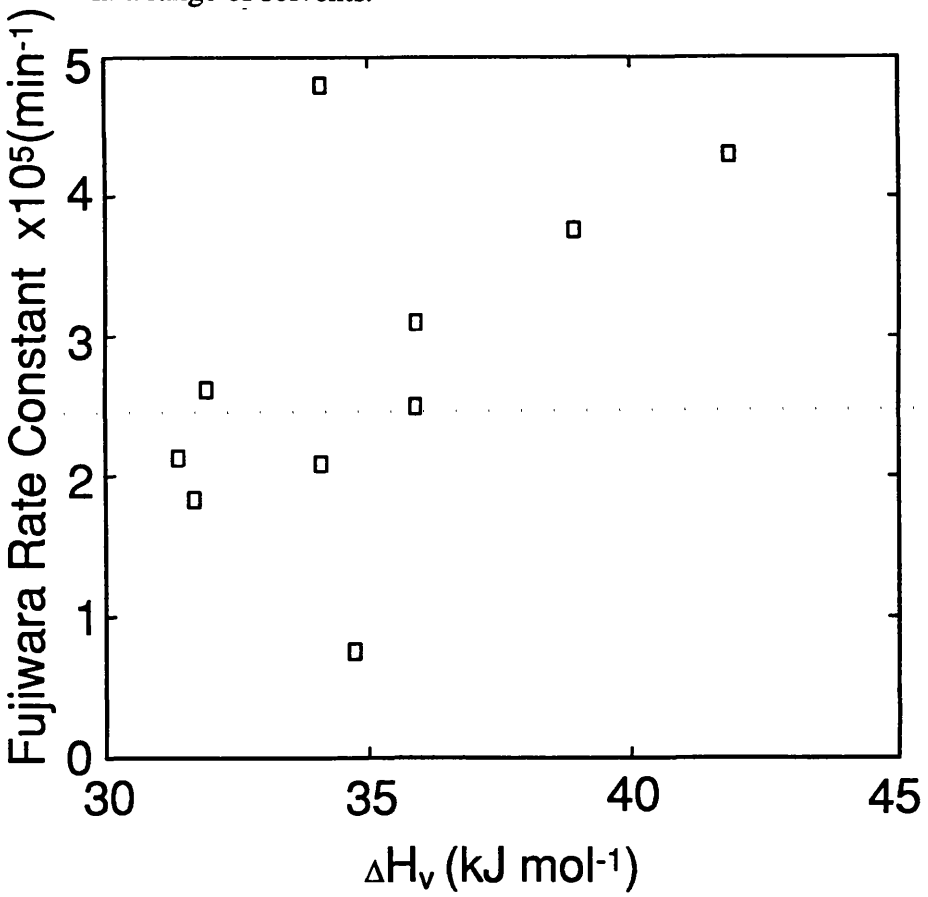

FIGURE 3.56. Effect of the heat of vaporisation of the solvent on the Fujiwara rate constant for the sonication of 0.5%w/v polystyrene in a range of solvents.

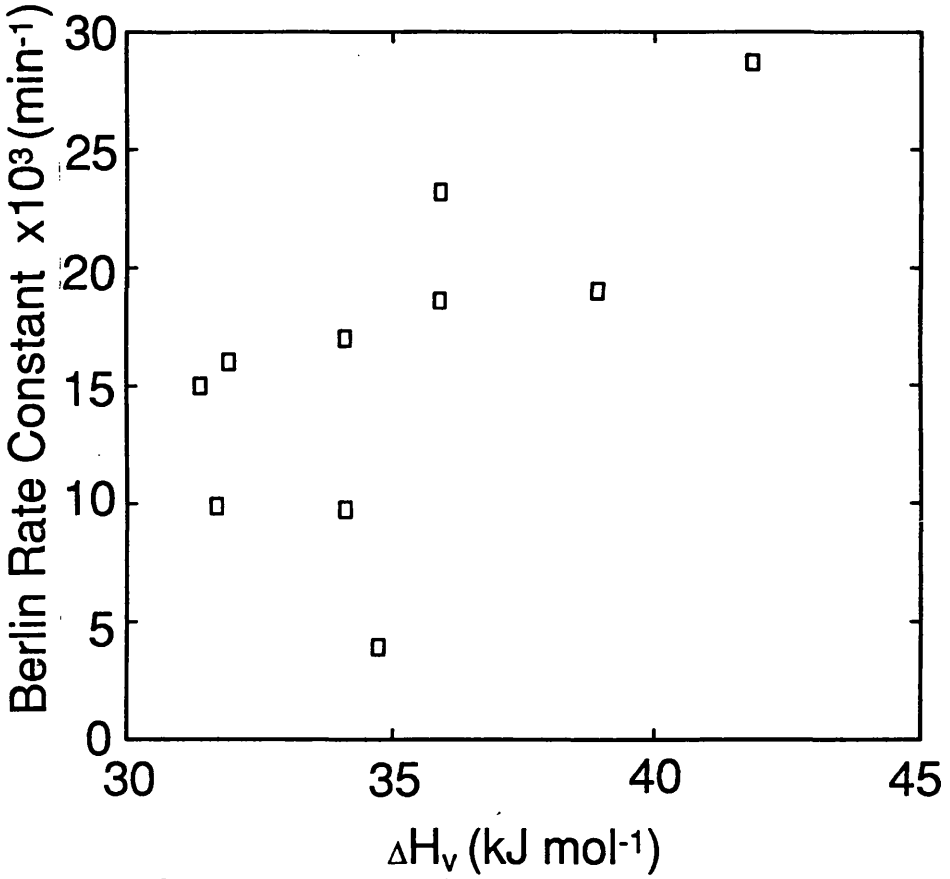

FIGURE 3.57. Effect of the heat of vaporisation of the solvent on the Berlin rate constant for the sonication of 0.5%w/v polystyrene in a range of solvents.

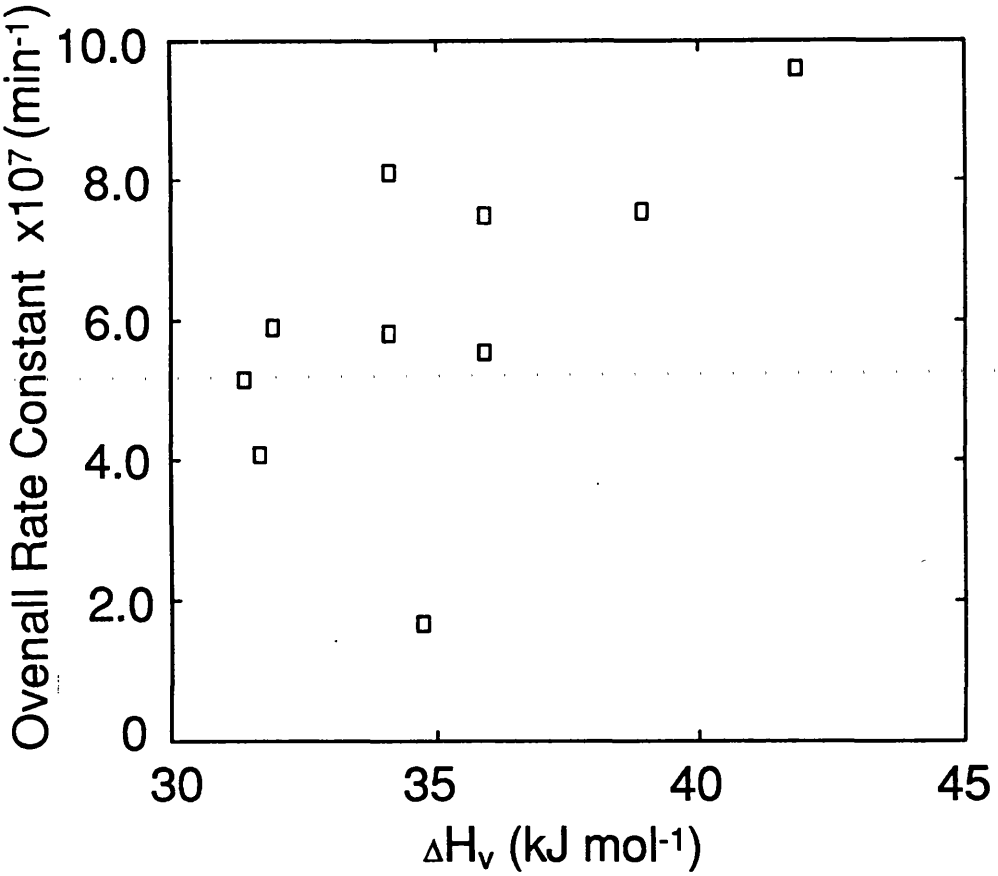

FIGURE 3.58. Effect of the heat of vaporisation of the solvent on the Ovenall rate constant for the sonication of 0.5%w/v polystyrene in a range of solvents.

62 kJ mol^{-1}. The rate constants were calculated using the Schmid rate model. The range of ΔH_v obtained in this study was much smaller, ranging from 31 to 41 kJ mol^{-1}. The Schmid rates obtained show the same trend as that obtained previously with the solvent with the highest ΔH_v, *o*-xylene, giving the faster rate. Where the heats of vaporisation are very similar, for chloroform, dichloromethane, carbon tetrachloride and cyclohexane, there is a scatter of values for the rate constant. This scatter of rate constants can also be observed in the results of Basedow and Ebert where the solvents have very similar heats of vaporisation, in the region of 40 k J mol^{-1}.

Considering the error in the limiting molecular weight to be the largest error and estimating this to be ± 2000, this produces an error of approximately ± 8% in the final rate constant obtained. Hence the spread of rates obtained is within experimental error. Where there is a large difference in the heats of vaporisation, for example between o-xylene and chloroform, a large difference between rates is seen which cannot be attributed to experimental error.

All of the rate plots show the same trend as the Schmid results. In all of the figures, the rate value obtained for the degradation of polystyrene in ethyl acetate lies considerably further from the line than accounted for by experimental error alone.

The lower the heat of vaporisation the higher the volatility of the solvent and the more vapour will enter the cavitation bubble. Hence the bubble collapse will be more cushioned in solvents with low heats of vaporisation and therefore reduce the force on bubble collapse. The results obtained exhibit this trend provided that there is a significant difference between the heats of vaporisation of the solvents. All of the graphs show some scatter of the points indicating that when the heats of vaporisation of the solvents are very similar other factors control the rate of degradation.

These results show that the heat of vaporisation of the solvent does not affect the extent of degradation but does affect the rate at which the polymer degrades although it is clearly not the only factor in operation.

3.7.3 Correlation of the degradation with the Flory-Huggins interaction parameter

In order to examine the parameters controlling the extent of the polymer degradation, values for the Flory-Huggins interaction parameters for polystyrene in each of the solvents were obtained. This parameter describes the conformation of the polymer in solution and was explained in section 1.8.

The Flory-Huggins interaction parameter, χ, was calculated using viscometric measurements discussed in section 1.8.2.

Owing to the time consuming nature of the measurement of the intrinsic viscosity, the values obtained using the conventional extrapolation method were compared with two 'single-point' methods, those of Soloman-Ciuta[162] and Rudin[169], in order to test the accuracy of the single-point methods. Graphs showing the extrapolated intrinsic viscosities can be seen in Figures 3.59 and 3.60.

In order to calculate the single point intrinsic viscosities, the relative viscosity from the lowest concentration was used for both methods. Table 3.6 (overleaf) shows a comparison of the extrapolated intrinsic viscosity with the single point values.

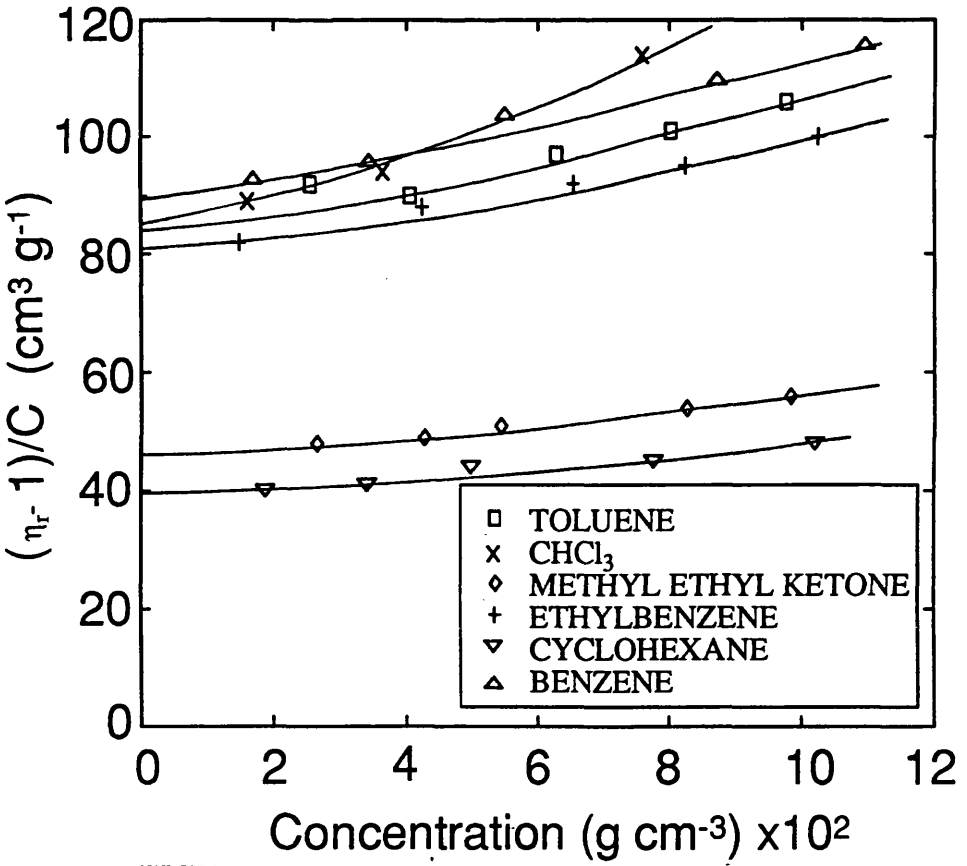

FIGURE 3.59. Calculation of intrinsic viscosities of polystyrene solutions.

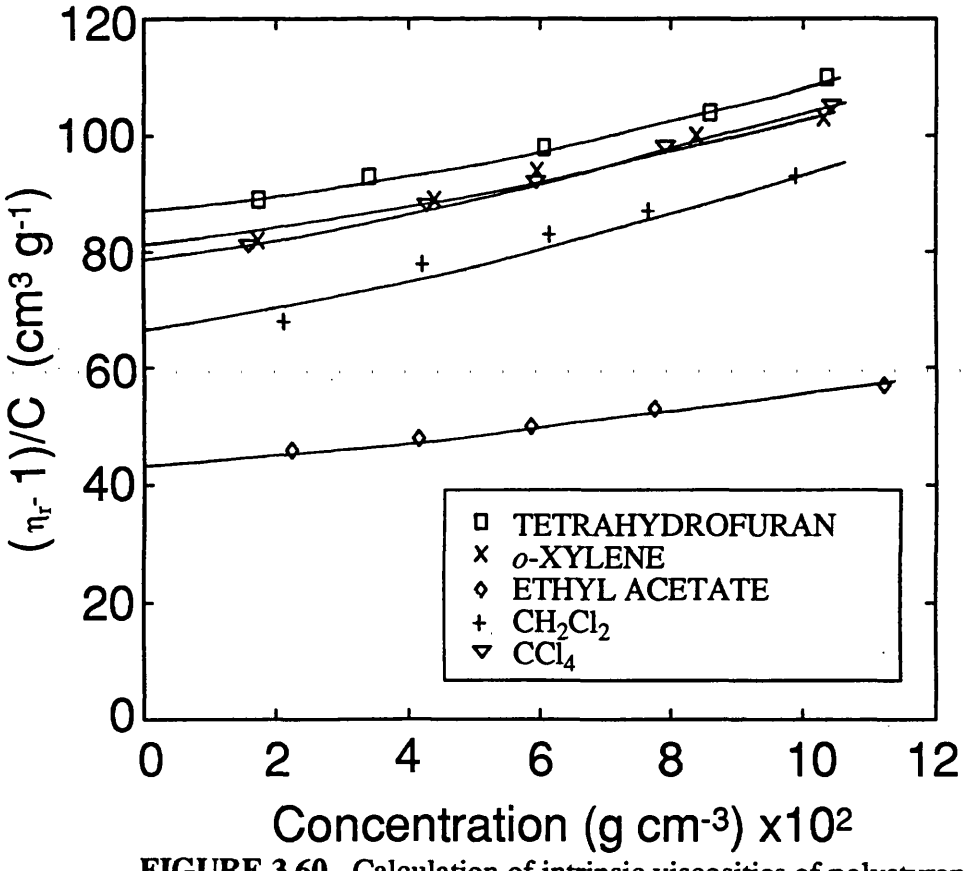

FIGURE 3.60. Calculation of intrinsic viscosities of polystyrene solutions.

Table 3.6 Single point determinations of Intrinsic Viscosities

Solvent	Extrapolated [η], $cm^3\ g^{-1}$	Soloman-Ciuta [η]	Soloman-Ciuta Δ/%[a]	Rudin [η]	Rudin Δ/%[a]
Toluene	85.8	85.8	0.0	86.9	1.3
Benzene	89.4	88.6	0.9	89.4	0.0
Cyclohexane*	39.1	39.4	0.8	39.5	0.1
o-xylene	80.8	78.6	2.7	79.2	2.0
Ethyl benzene	80.2	79.3	1.1	79.9	0.4
Dichloromethane	69.1	70.8	2.5	71.9	4.0
Chloroform	85.6	84.6	1.2	85.3	0.4
Tetrachloromethane	78.8	79.0	1.0	78.6	0.3
Ethyl Acetate	44.4	44.1	0.7	44.3	0.4
Butan-2-one	46.4	46.6	0.3	46.8	0.9
Tetrahydrofuran	87.0	84.5	2.9	85.3	2.0

* at 34°C

[a] Δ/ is the percentage difference between the extrapolated and single-point values of [η].

Both methods give a very good prediction of [η], the average percentage difference from the extrapolated values being 1.3% for the Soloman-Ciuta method and 1.1% for the Rudin method, well within the experimental error introduced by the extrapolation of the concentration series results. Thus, for polystyrene, both 'single-point' methods are suitable for the calculation of [η].

The intrinsic viscosity was measured in order that the Flory-Huggins interaction parameter could be calculated. The theory for this is discussed in section 1.8.2. Both of the single-point measurements of [η] and the extrapolated values of [η] were used to calculate χ. The equations used were those derived by Kok and Rudin[153-155] (Eqns. 1.31 - 1.34) and by Tseng and Lloyd[172] (Eqns. 1.34 and 1.35).

Table 3.7 shows the values of χ employing the three equations on the extrapolated and single-point intrinsic viscosities. It can be seen that all three equations give very similar results, with the values from equation 1.34 being the closest to the literature values quoted. It must be noted that there is a spread of χ values in the literature, depending on the method used to calculate them and hence those quoted in Table 3.7 (overleaf) can only be taken as a guide.

The aim of using the single-point measurements was to measure the interaction parameter as rapidly as possible with no loss of accuracy. From Table 3.7 it can be seen that comparison of the interaction parameter calculated by a single-point method with those from the time consuming extrapolation method in most cases gave differences of only 0.001 - 0.002. In only one case was the difference greater than 0.004. This is considerably less than the spread of literature results and so it is felt that the use of 'single-point' intrinsic viscosities to calculate interaction parameters was justified.

Since the χ values using the extrapolated $[\eta]$ values and equation 1.34 give values closest to literature values it is these that will be used to examine the effect of polymer conformation on the degradation. A graph of the effect of χ on the limiting molecular weight can be seen in Figure 3.61.

It can be seen in Figure 3.61 that a decrease in the value of χ, or the more open the conformation adopted in solution, then the lower the limiting molecular weight obtained. The only exception was that of ethylbenzene.

The effect of the polymer conformation in solution on the limiting molecular weight has not previously been studied for solutions of polystyrene. The effect observed can be explained by consideration of the shock wave mechanism described in section 1.7.4.

A chain that is uncoiled in solution will experience a greater force across it as it is pulled towards the collapsing bubble than a chain of the same length that is coiled. Hence those polymers in good solvents will be degraded more than those in poor solvents.

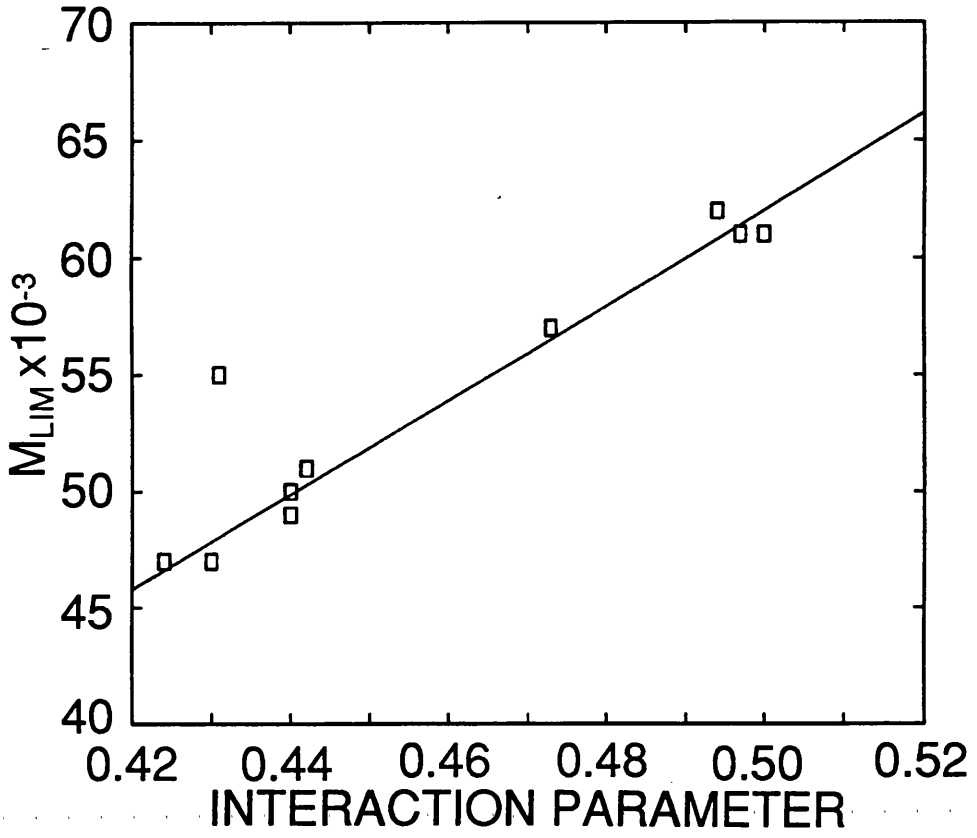

FIGURE 3.61. Effect of the interaction parameter on the limiting molecular weight of polystyrene for the sonication of a 0.5%w/v solution.

Table 3.7 Interaction Parameters Calculated from the Extrapolated and Single-Point Intrinsic Viscosities

	RUDIN Eqn.1.32			LLOYD Eqn.1.34			LLOYD Eqn.1.35				
	EXTRAP [η]	SOLOMAN [η]	RUDIN [η]	EXTRAP [η]	SOLOMAN [η]	RUDIN [η]	EXTRAP [η]	SOLOMAN [η]	RUDIN [η]	Lit	Ref
Toluene	0.435	0.435	0.434	0.448	0.448	0.466	0.417	0.417	0.414	0.44	a
Benzene	0.442	0.443	0.442	0.451	0.452	0.451	0.422	0.424	0.422	0.455	a
Cyclohexane*	0.495	0.494	0.494	0.500	0.500	0.500	0.500	0.500	0.527	0.50	a
o-xylene	0.434	0.436	0.436	0.450	0.454	0.453	0.423	0.430	0.428	0.41	a
Ethylbenzene	0.432	0.434	0.433	0.450	0.451	0.450	0.422	0.431	0.430	0.45	a
DCM	0.473	0.471	0.471	0.484	0.482	0.481	0.476	0.474	0.471	0.42	a
Chloroform	0.450	0.452	0.451	0.458	0.462	0.461	0.433	0.440	0.438	0.43	a
CCl_4	0.448	0.448	0.448	0.462	0.462	0.463	0.459	0.442	0.443	0.46	a
Ethyl Acetate	0.488	0.488	0.488	0.497	0.497	0.497	0.496	0.497	0.496	0.49	a
MEK	0.484	0.483	0.483	0.495	0.495	0.495	0.494	0.494	0.493	0.49	a
THF	0.449	0.457	0.451	0.459	0.462	0.461	0.434	0.440	0.438	-	

* at 34°C

a Reference 160

Figures 3.62 - 3.64 show the effect of the solvent on the polydispersity of the polystyrene. In all cases, the polydispersity initially falls rapidly from a value of 3.2 and at longer sonication times reaches a limiting polydispersity, γ_{LIM}. This value varies according to the solvent used.

Figures 3.65 - 3.68 show the effect of the χ value on the degradation rate constants. The same trend is seen in all of the models. The higher rate constants are observed in solvents possessing low χ values. The nearer the solvent becomes to being a theta solvent, the slower the rate. Methyl ethyl ketone does not obey this trend in any of the models, having a rate constant much higher than expected.

Where the solvents have very similar χ values, as in the case of o-xylene, toluene and benzene the calculated rates are very different indicating that other factors are influencing the rate of degradation.

Golubev[92] and Malhotra[93] have attempted to correlate the degradation rate with the polymer conformation in solution, indicated by the Huggins constant derived from solution viscometry. The higher the value of the Huggins constant, the more uncoiled the polymer chain. It was found that for hydroxypropyl cellulose dissolved in water, ethanol and tetrahydrofuran and solutions of alkyl methacrylates, the rate accelerated as the chain became more uncoiled. These previous results correlate very well with the results obtained in this study.

The results obtained are those expected on consideration of the shear and shock wave mechanisms discussed in section 1.7.4. These mechanisms predict that the more uncoiled the polymer in solution, the greater the degradation. This is most easily visualised in the case of the shock wave mechanism. A highly coiled polymer such as the polystyrene in ethyl acetate will be pulled towards the collapsing bubble in its tight configuration. However, a polymer that is uncoiled, such as polystyrene in o-xylene, will have the solvent molecules on one side of the polymer chain being pulled towards the collapsing bubble very violently, whereas the solvent molecules on the side away from the cavity will not experience such a large effect. Hence this differential pull on either side of the polymer chain will cause chain cleavage.

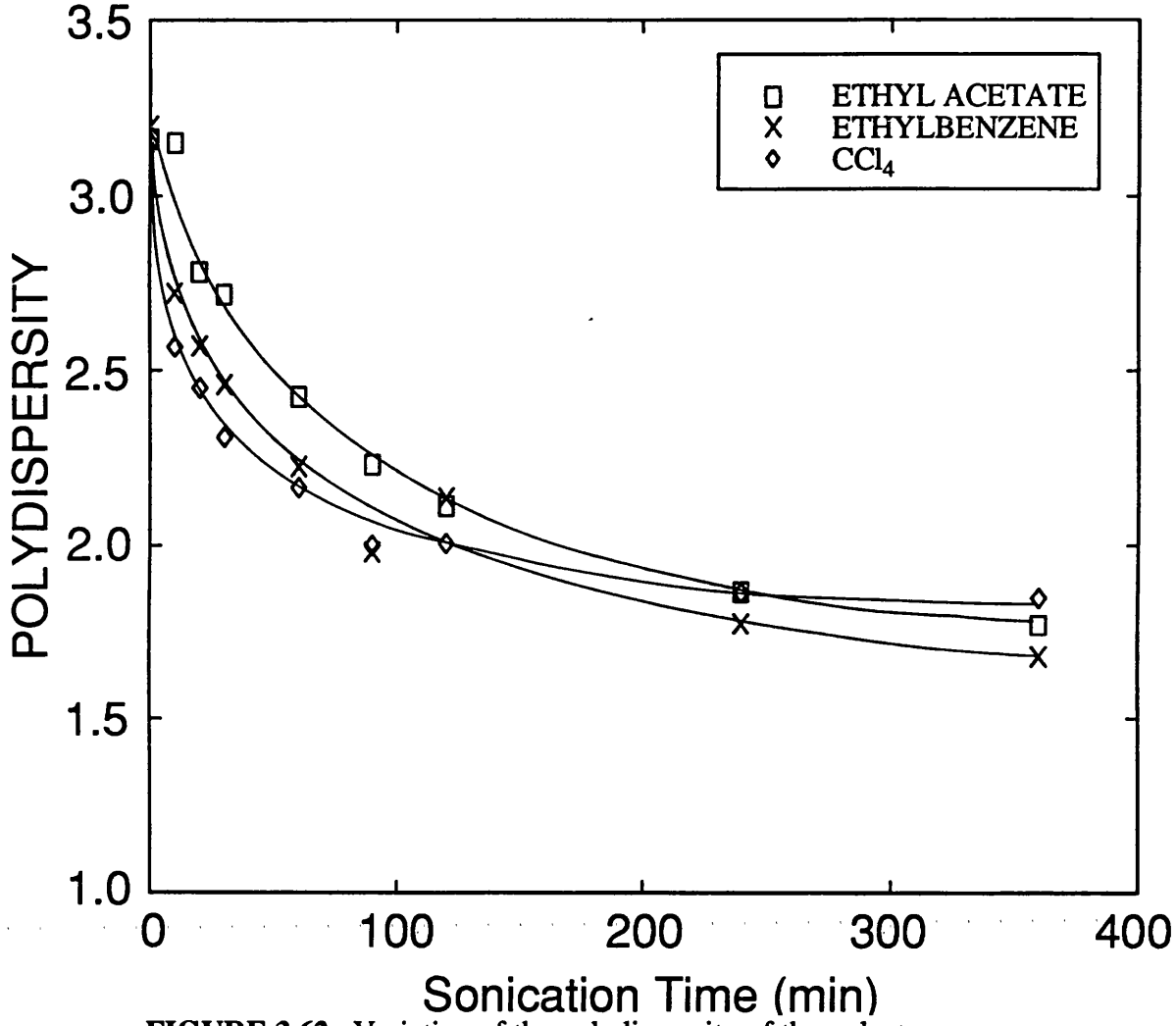

FIGURE 3.62. Variation of the polydispersity of the polystyrene during the sonication of 0.5%w/v polystyrene in various solvents.

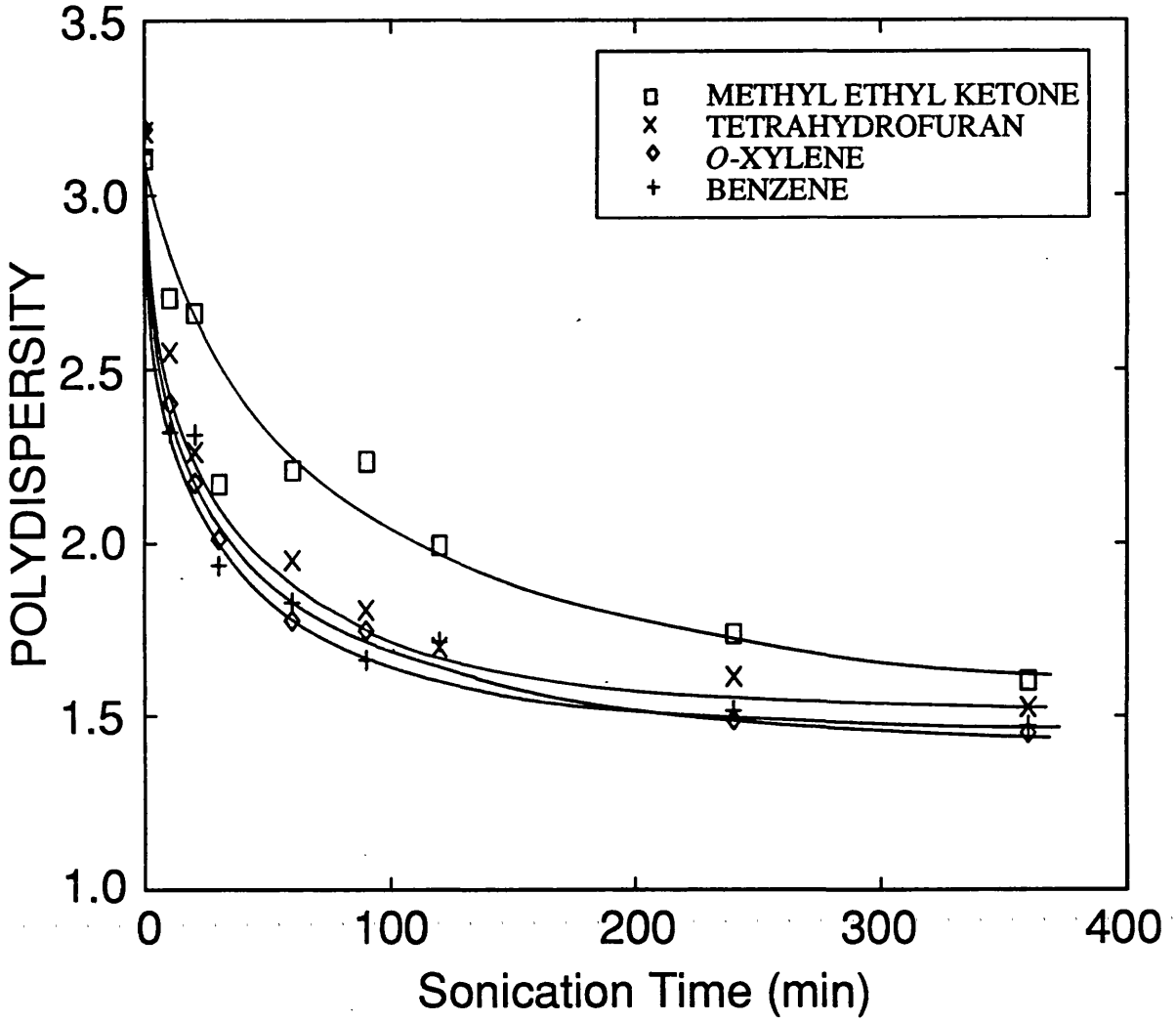

FIGURE 3.63. Variation of the polydispersity of the polystyrene during the sonication of 0.5%w/v polystyrene in various solvents.

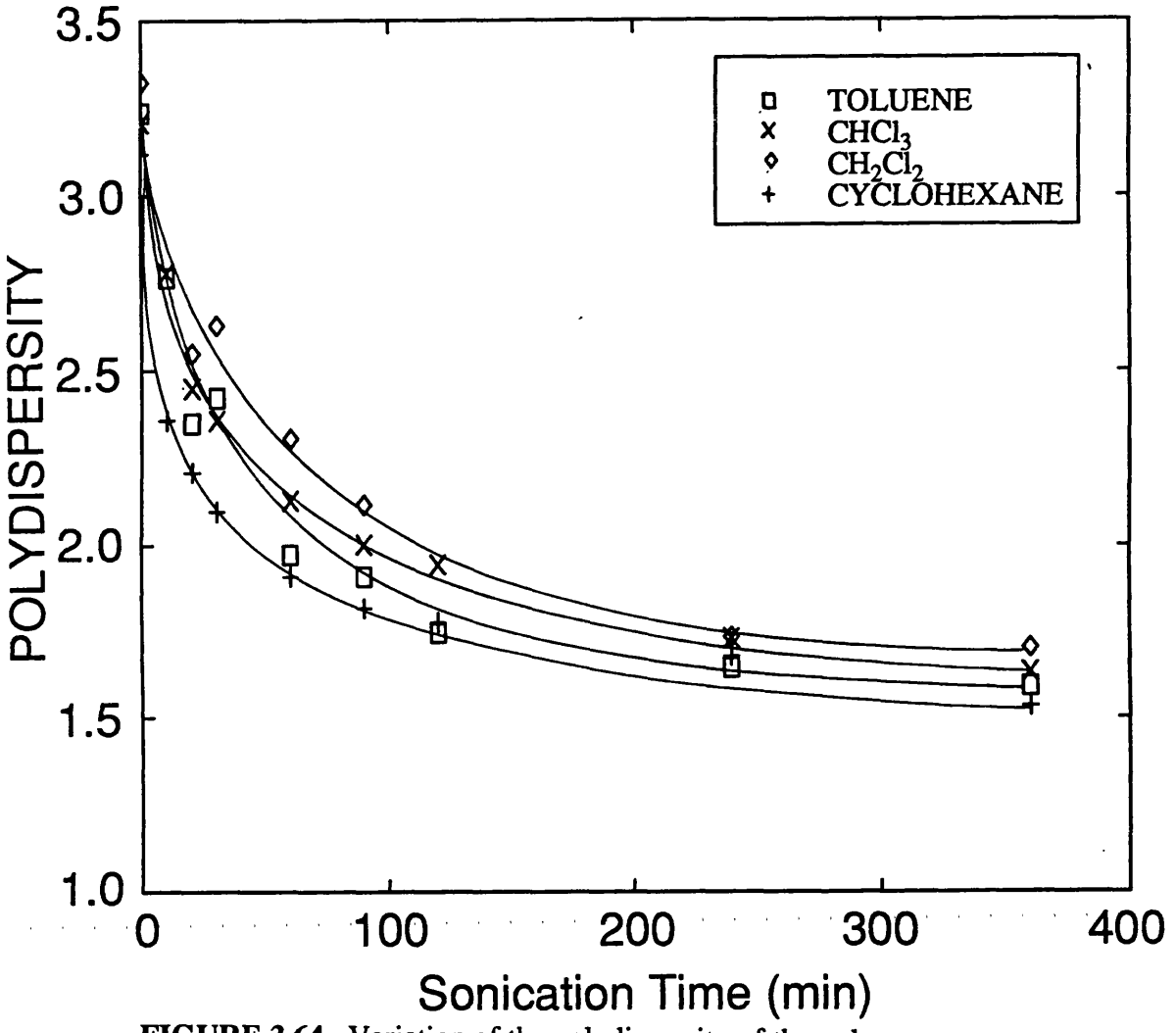

FIGURE 3.64. Variation of the polydispersity of the polystyrene during the sonication of 0.5%w/v polystyrene in various solvents.

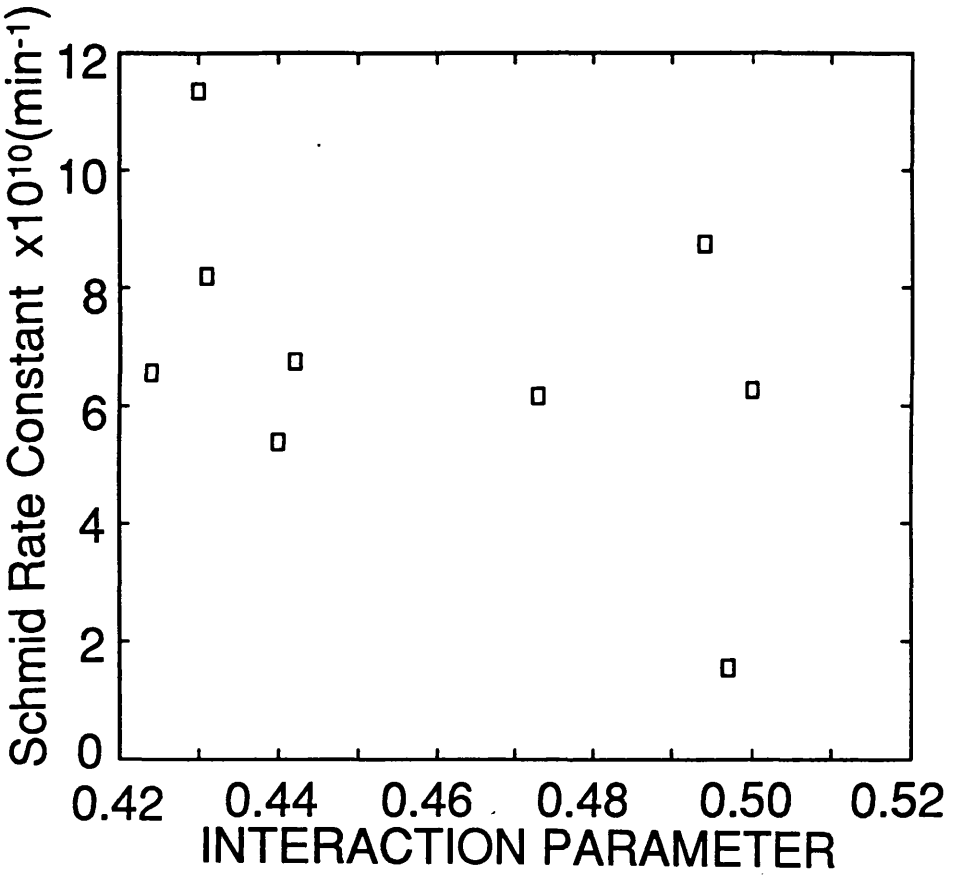

FIGURE 3.65. Effect of the interaction parameter on the Schmid rate constant for the sonication of 0.5%w/v polystyrene in a range of solvents.

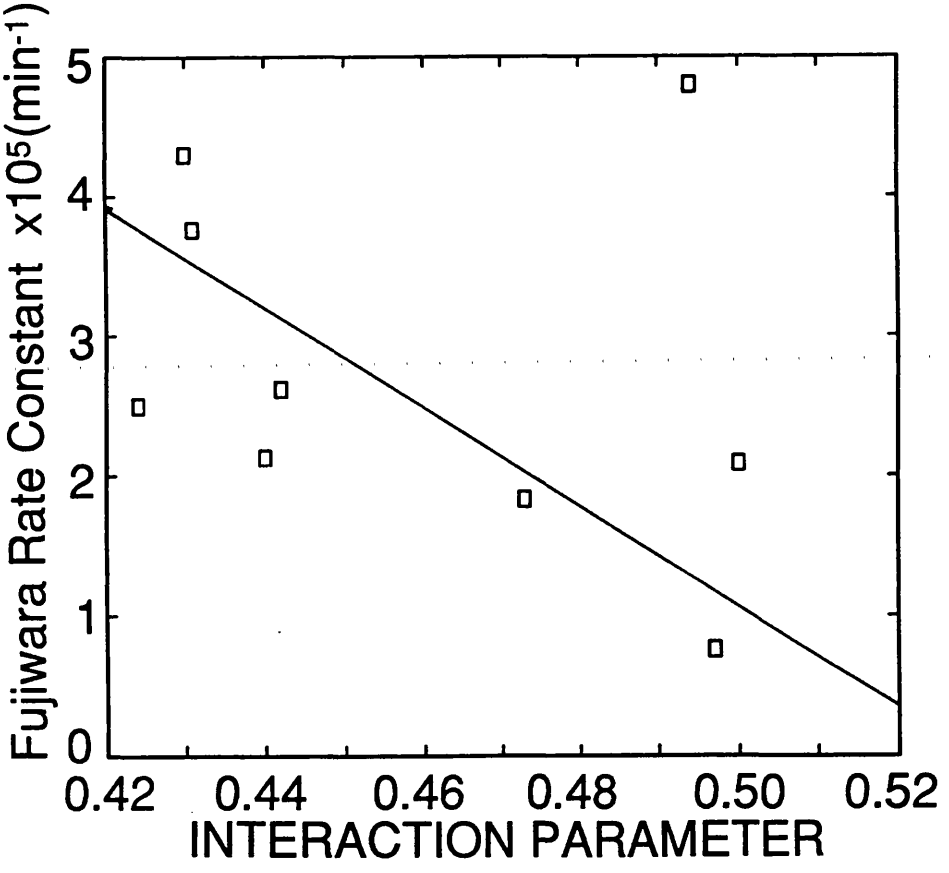

FIGURE 3.66. Effect of the interaction parameter on the Fujiwara rate constant for the sonication of 0.5%w/v polystyrene in a range of solvents.

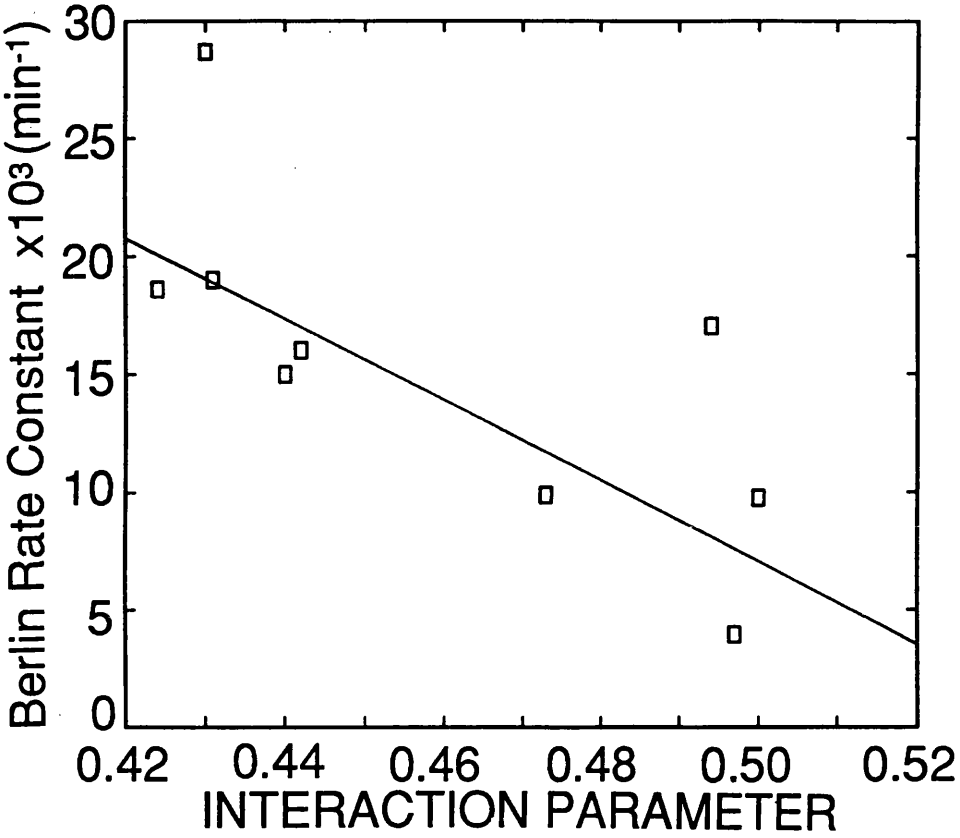

FIGURE 3.67. Effect of the interaction parameter on the Berlin rate constant for the sonication of 0.5%w/v polystyrene in a range of solvents.

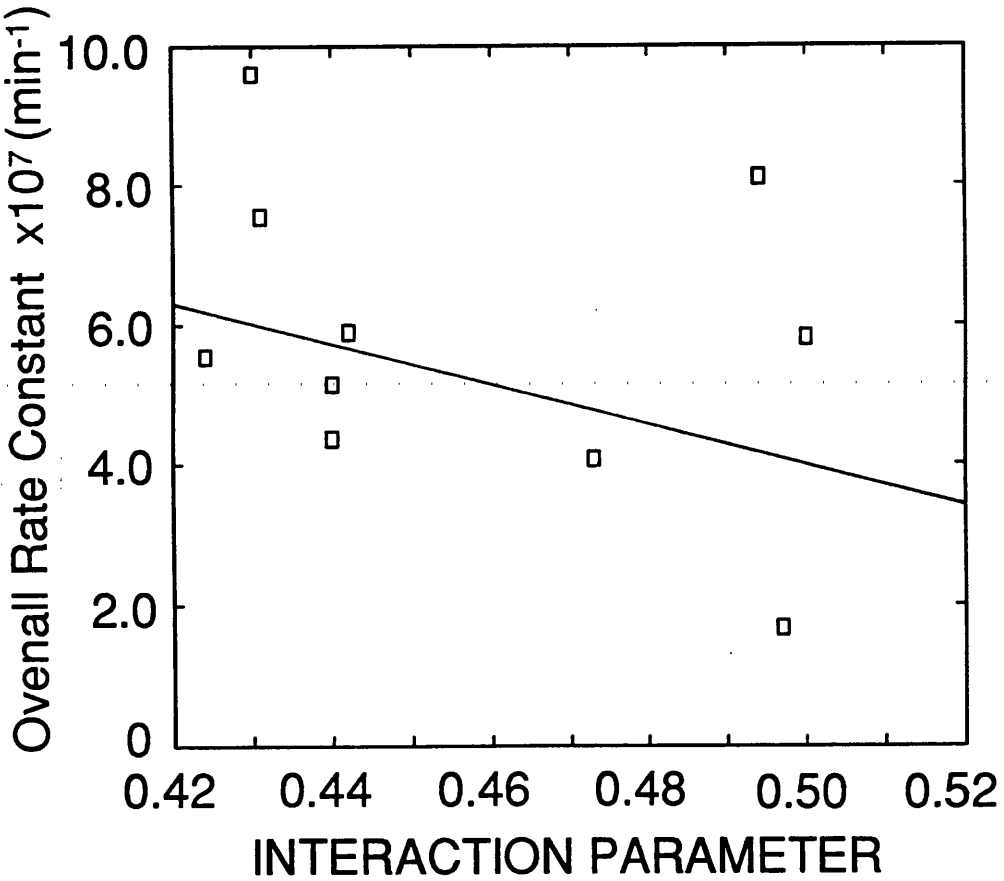

FIGURE 3.68. Effect of the interaction parameter on the Ovenall rate constant for the sonication of 0.5%w/v polystyrene in a range of solvents.

The rate of degradation of polystyrene in o-xylene is higher than that of polystyrene in toluene and benzene despite the χ values differing by only 0.003. Examination of the ΔH_v values of these solvents shows that o-xylene has a much higher heat of vaporisation than toluene or benzene, and hence the bubble collapse in this solvent will be less cushioned and therefore more violent, as described in section 3.7.2.

3.8 Effect of the Degradation on Chain Branching

Branching is normally caused by transfer reactions within the polymer molecules. The tendency for the transfer depends on the reactivity of the active centre, and hence branching is more common in polymers produced by free radical reactions. Long chain branches greatly affect the rheological properties and also mechanical properties of polymers by affecting the ability of a polymer molecule to crystallise[4].

Owing to the ultrasonic degradation producing radicals on the chain ends due to the homolytic cleavage, it was felt necessary to examine whether branching of the polymers occurred during the sonication and whether a concentrated solution produced more branching due to the close proximity of the polymer chains. If polymer chains were in close contact, inter-, as well as intramolecular transfer could occur, hence producing more branching in a more concentrated solution.

The extent of chain branching was examined using two techniques; static light scattering and GPC-viscometry. The results from the GPC-viscometry were provided by RAPRA.

Two degradation experiments were carried out as described in Section 2.2.5, degradation of 15% w/v and of 1% w/v solutions of polystyrene in toluene. Samples were taken during the sonication and these were analysed for chain branching.

3.8.1 Static light scattering

The experimental details were described in Section 2.3.3. The use of static light scattering to measure the extent of chain branching has been examined by Murayama *et al*[198] who studied solutions of polystyrene in toluene, branched polystyrenes being

prepared by copolymerising styrene and p-divinylbenzene. It was found that linear polystyrenes had higher second virial coefficients, A_2, than the branched materials as shown in Figure 3.69.

Second virial coefficients were calculated for the samples removed during the sonications and they are also shown in Figure 3.69. The values cannot be directly compared with those of Murayama since their polystyrenes had polydispersities in the range 1.03 - 1.19, considerably lower than the polymers used in this study. However, the trends observed in the Murayama results can be extended to the degradation study.

The A_2 for the polymers sonicated in dilute solution (1%) initially rise as expected with the reduction in molecular weight. However, on longer treatment times, the values fall dramatically and end up on a line extrapolated from the branched polymers of Murayama, suggesting that branching is introduced into the polymers at long sonication times. It must be noted that the sample taken from the dilute solution at 360 minutes sonication time had a polydispersity of approximately 1.3, much closer to the polydispersities of the samples used by Murayama and hence the A_2 value for this sample lies on the extrapolated line from Murayama's results. In contrast, sonication of the concentrated (15%) solutions results in a rapid lowering of A_2 suggesting that branching is introduced immediately.

Hence the light scattering results suggest that branching is indeed being introduced into the materials. However, this evidence is not conclusive so that a second technique was also employed.

3.8.2 GPC-viscometry

Solution viscometry is recognised as the primary method for determining the extent of long chain branching in polymers. The intrinsic viscosity of a polymer depends upon its size in solution and this in turn depends on its degree of branching.

Zimm and Stockmayer[199] proposed a theory of chain branching which led to the relation

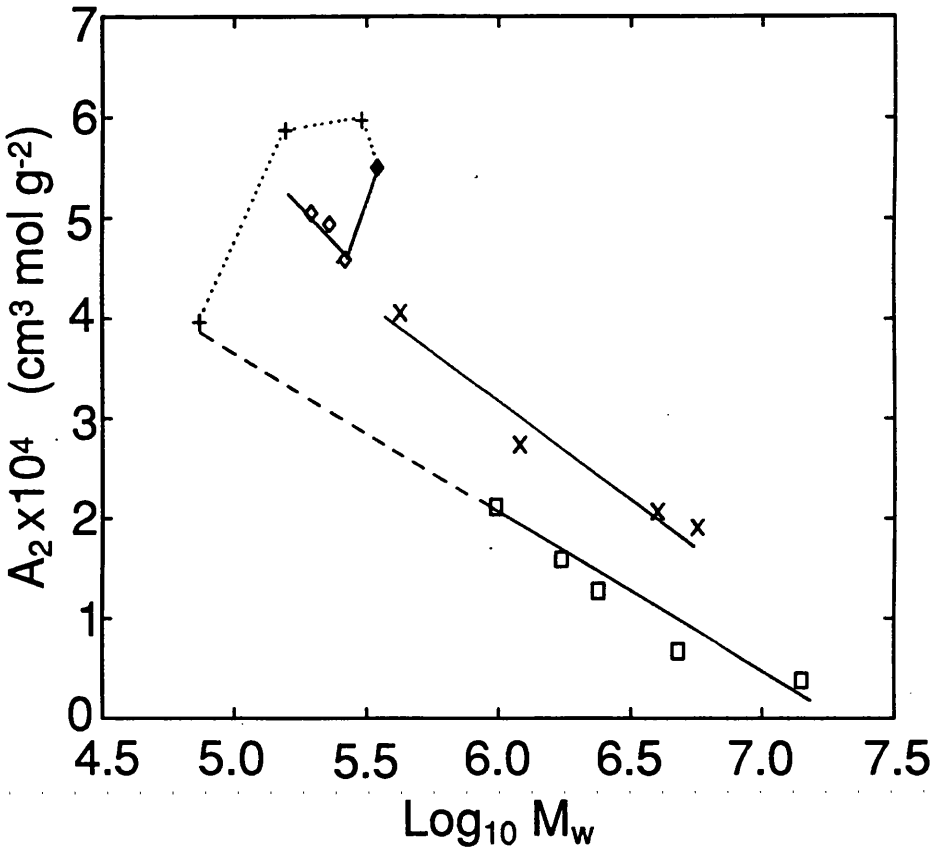

FIGURE 3.69. Variation of the second virial coefficient of polystyrene sonicated in a concentrated and dilute toluene solution. (□ =Murayama branched polystyrene, x =Murayama linear polystyrene, ◊ =sonication of 15%w/v polystyrene, + = sonication of 1%w/v polystyrene.)

$$g = \left[\frac{[\eta]_b}{[\eta]_l} \right] \qquad 3.22$$

where $[\eta]_b$ and $[\eta]_l$ are the intrinsic viscosities of the branched and linear polymers respectively. A ratio of unperturbed radii of branched and linear polymers was derived

$$g_o = \frac{\langle r_g^2 \rangle_b^{1/2}}{\langle r_g^2 \rangle_l^{1/2}} \qquad 3.23$$

where $\langle r_g^2 \rangle_l$ and $\langle r_g^2 \rangle_b$ are the radii of gyration of the linear and branched polymers respectively. The relation between g and g_o is given by

$$g = g_o^k \qquad 3.24$$

where k is an arbitrary constant with a value between 0.5 and 1.5. In this study, the value used for k was 0.78.

The number of branches per molecule, n, is calculated from

$$g_o = \left((1 + \frac{n}{7})^{1/2} + \frac{4n}{9n} \right)^{-1/2} \qquad 3.25$$

The branching frequency, λ, the number of branches per molecule per repeat unit of molecular weight, M is given by

$$\lambda = \frac{Rn}{M} \qquad 3.26$$

where R is the molecular weight of a repeat unit.

The results obtained can be seen in Figure 3.70 show the effect of sonication on the 1% w/v solution of polystyrene in toluene. The results suggest that the level of

FIGURE 3.70. Frequency of chain branching obtained from the sonication of a 1%w/v solution of polystyrene in toluene.

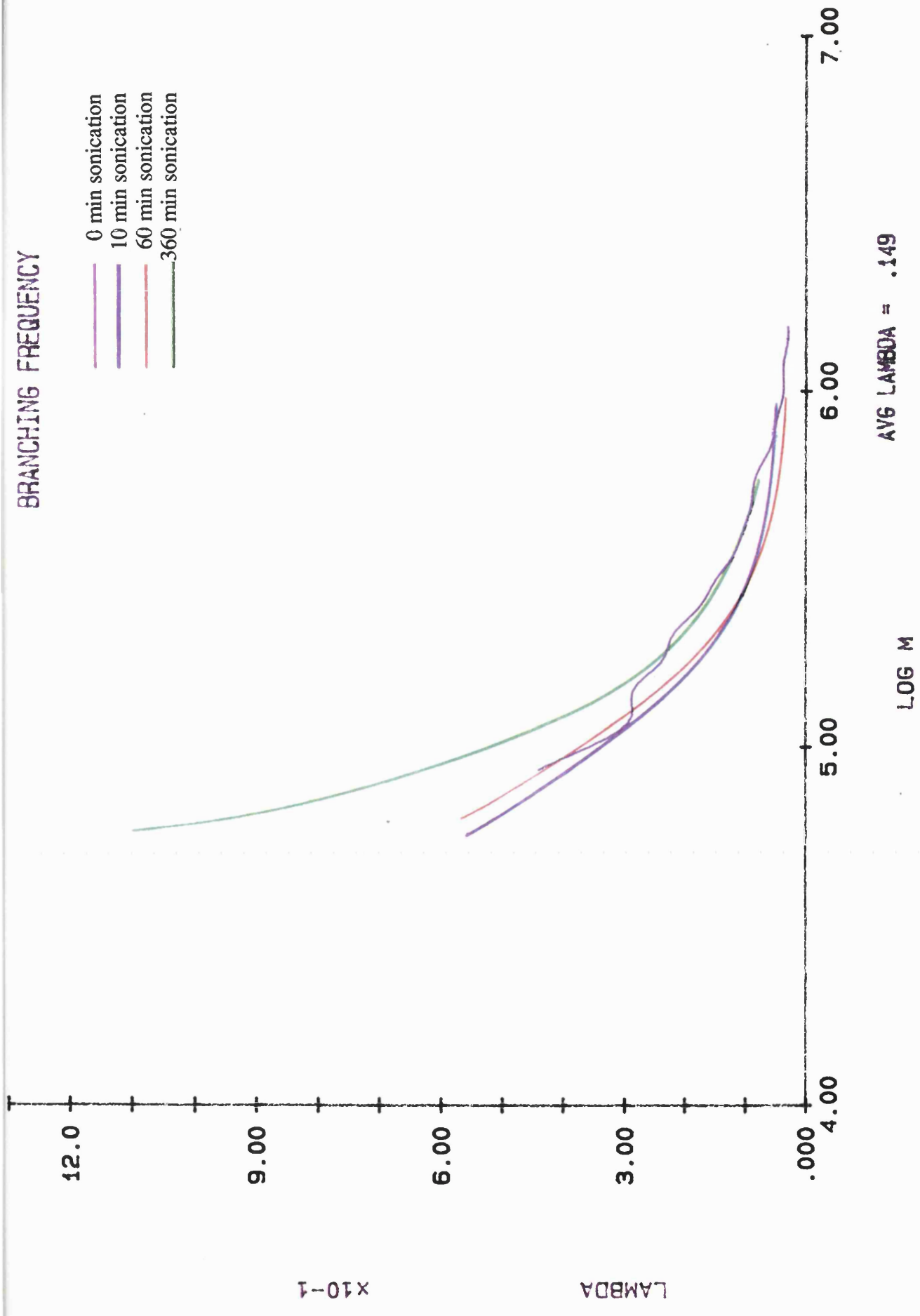

branching increases very slightly over the first 60 minutes sonication. However, after 360 minutes sonication, the branching frequency had increased significantly. The average λ over the polymer sample increased from 0.149 to 0.456 after 360 minutes sonication. The branching frequency increases most in the lower molecular weight section of the polymer.

Figure 3.71 shows the effect of sonication on the 15% w/v solution of polystyrene in toluene. The branching increases considerably in the first 60 minutes sonication, the average λ increasing from 0.149 to 0.256. However, after 360 minutes, the average λ obtained of 0.271 is less than that observed after 360 minutes sonication of the 1% w/v solution. As in the case of the 1% w/v solution, the branching frequency increases in the low molecular weight section of the polymer.

3.8.3 Discussion of branching results

The light scattering and GPC-viscometry results both suggest that branching increases with sonication and the extent of branching is greater in the concentrated 15% w/v solution. Both sets of results also indicate that the dilute 1% w/v sample after 360 minutes sonication is the most branched sample.

It would be expected that the 15% w/v samples will be the most highly branched due to the close proximity of the chains and hence making hydrogen abstraction along the chain by the radical on the chain end more probable.

This intermolecular chain transfer is less likely to occur in the 1% w/v solution due to the chains being further apart (as discussed in section 3.5, 1% w/v is below the critical overlap concentration).

However, after 360 minutes sonication the 1% w/v sample is more branched than the 15% w/v sample. This is indicated by both static light scattering and GPC-viscometry. The probable reason for this being that there are considerably more chain breaks occurring in the 1% w/v sample than in the 15% w/v as shown by the concentration studies in Section 3.5. This makes the chance of either intra or intermolecular transfer much more probable.

FIGURE 3.71. Frequency of chain branching obtained from the sonication of a 15%w/v solution of polystyrene in toluene.

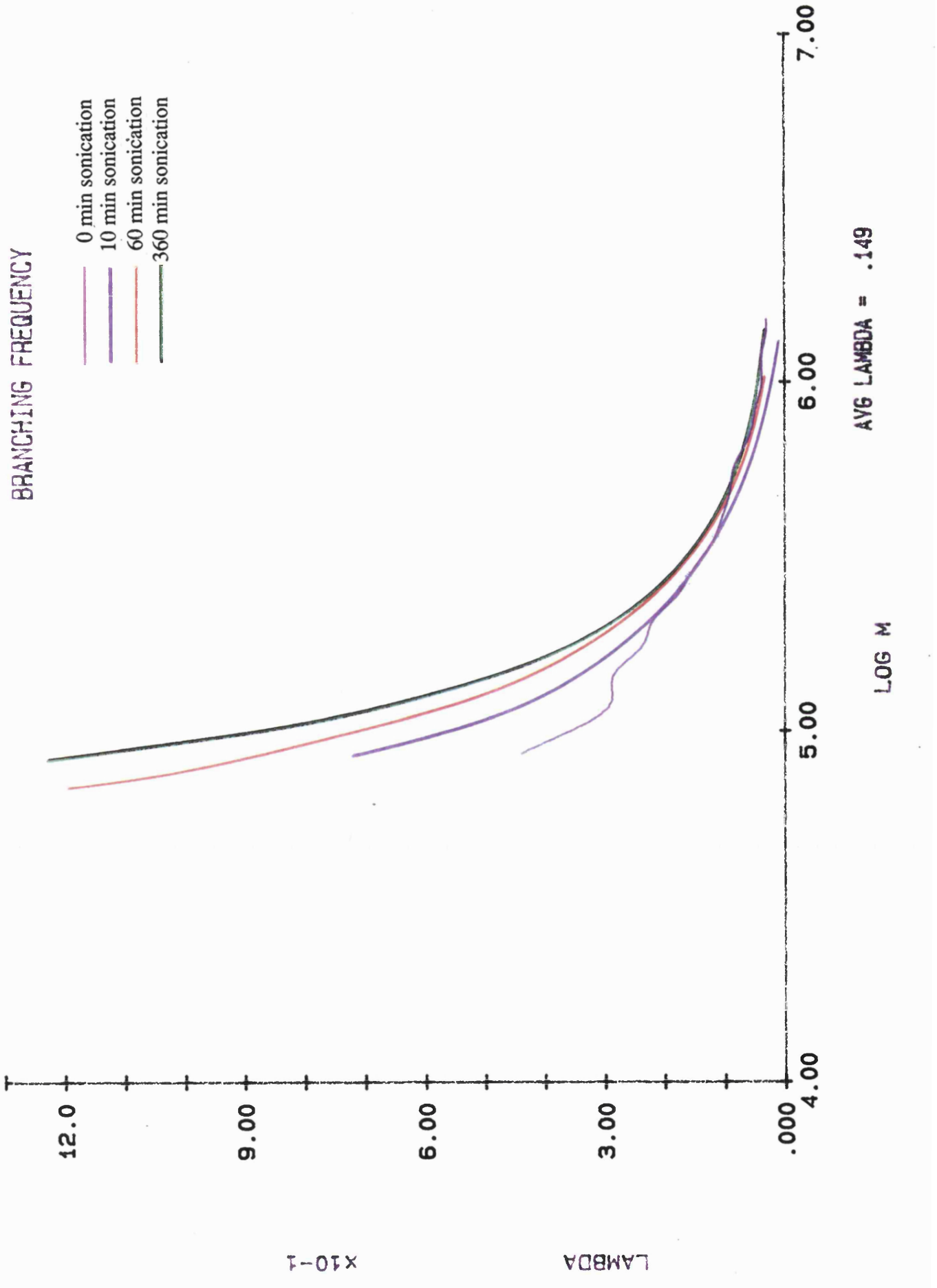

Although independently neither of the results are conclusive, taken together they indicate the same trend and show an increase in the level of branching with sonication time.

3.9 Discussion

The general trends found throughout the degradation studies are similar to those found by previous workers[9]. However, the work described here is a more comprehensive study of a single system than has appeared previously and we have characterised all the possible processes in the degradation of polystyrene solutions. The only omission was the sound frequency, due to the unavailability of commercial apparatus. The decrease in the molecular weight during the sonication was relatively fast initially, slowing at later stages in the degradation and reaching a limiting molecular weight. The value of M_{LIM} was found to vary with all of the parameters studied, with the exception of the initial molecular weight used. Sonication of a polymer with a molecular weight below that of the limiting molecular weight produced very little degradation. The very slight amount observed can be attributed to the polymer consisting of a distribution of molecular weights, and although the average molecular weight was below the M_{LIM} value, some polymer chains still had molecular weights above M_{LIM} and hence were degraded causing a slight decrease in the number average molecular weight.

It was found that the value of M_{LIM} could be varied by altering the solubility of gas present in the solution, the temperature of the bulk solution, the intensity of the sonication, the concentration of the solution and the solvents used. All of these results were explained by considering their effect on cavitation and by considering the degradation mechanism proposed by Thomas[89].

In all of the systems, a reduction in polydispersity of the polymer was observed. This is indicative of a non-random degradation and preferential removal of high molecular weight material was noted. This non-random cleavage is illustrated in Figure 3.72. The production of non-random cleavage showed that the degradation was

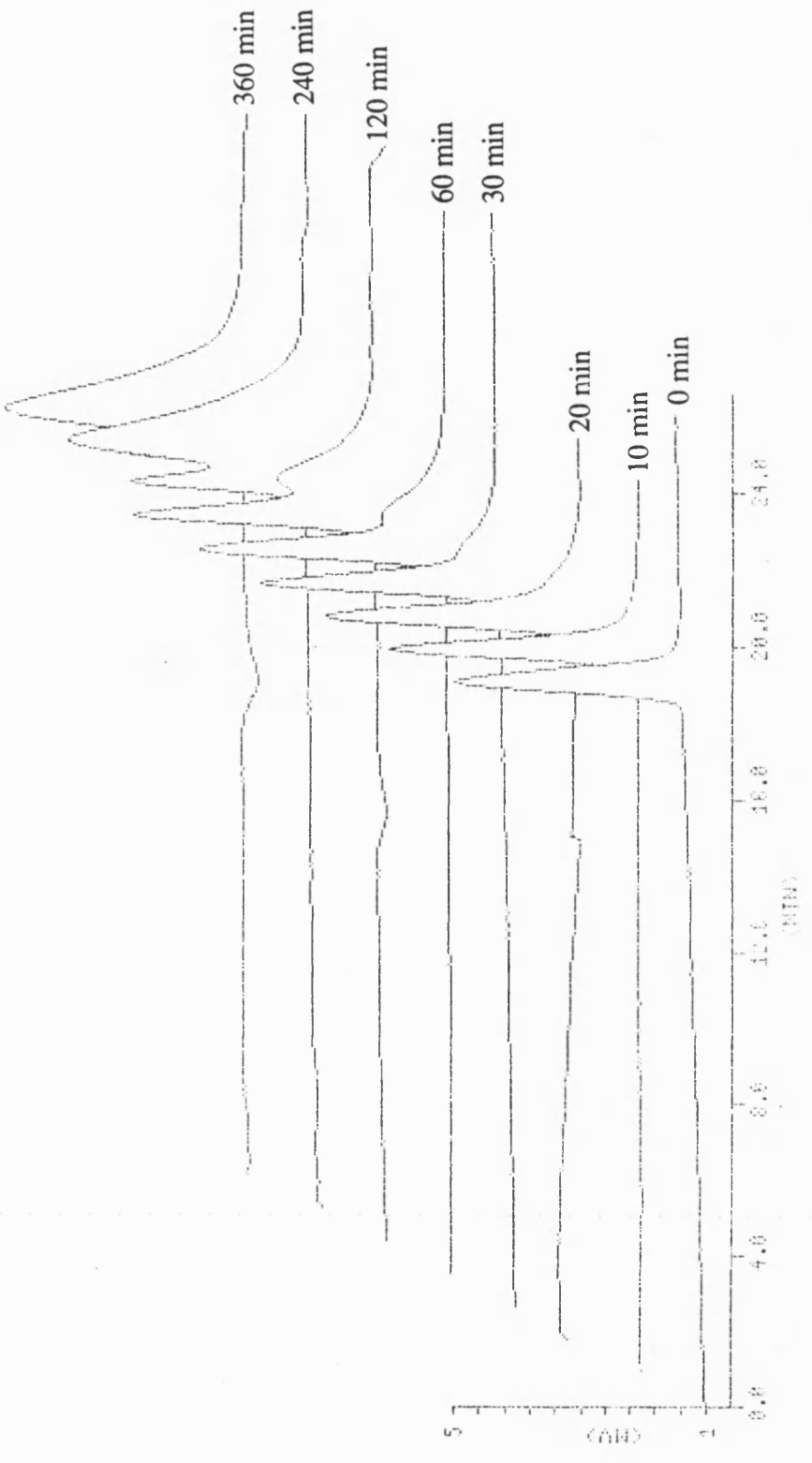

FIGURE 3.72. Gel Permeation Chromatograms showing centre cleavage.

not produced through the thermal effects of the cavitation bubbles. As explained in Chapter One, the collapse of cavitation bubbles produces very high localised temperatures, above 1000 K[31]. Thermal degradation of polystyrene is a random process, and produces styrene. Further evidence of the degradation not being of thermal origin was provided by analysing the degradation products for traces of styrene. A 1% w/v solution of polystyrene in tetrahydrofuran was sonicated at an intensity of 183.7 W cm^{-2}, samples removed at regular intervals and analysed using a Pye gas chromatograph with a Flame-Ionization-Detector and 5% OV101 on chromosorb column (Injector temperature, 300^{O}C, oven temperature, 90^{O}C). The solution was sonicated for 12 hours but no styrene was detected.

A range of kinetic studies was examined in order to find a rate model that accurately fitted ultrasonic degradation. All of the rate models applied with the exception of the shear degradation, random degradation and the Xu models gave linear kinetic plots. However, despite this, the rate constants obtained did not correlate with the observed results, with the exception of the model derived by El'tsefon and Berlin. In all of the kinetic plots there were wide deviations from linearity at long sonication times. The failure to obtain linear plots from the random degradation model again corroborates the fact that the degradation is not produced through thermal effects.

The models of Schmid, Ovenall and Fujiwara all depend on the value of M_{LIM} which was obtained by extrapolation beyond the last data point. Due to the errors in the measurement of the M_n value and introduced by the extrapolation procedure, the cumulative error in the rate constants was in the range of 8-10%. The rate obtained from the El'tsefon and Berlin model was not dependent on the value for M_{LIM}.

Another factor that could affect the measurement of rate constants was the introduction of chain branching during the sonication. This had not previously been examined by other workers. The results obtained from light scattering and GPC-viscometry studies indicate that branching was introduced at long sonication times in dilute solutions and throughout the sonication in concentrated solutions. This will cause errors in the calculation of molecular weights using GPC and hence

introduce more errors into the measured rate constants. Since the level of branching is highest at long sonication times, the limiting molecular weight obtained will be incorrect and hence the Schmid, Fujiwara and Ovenall models will be affected by this.

The results obtained from ultrasonic degradation are analogous to those obtained using shear degradation[200]. Pure shear degradation of polystyrene solutions was studied by Odell and Keller[201]. In pure shear degradation, the polymer chain is extended fully in solution using an elongational flow. For solutions of polystyrene, poly(ethylene oxide) and DNA, centre cleavage has been noted and a limiting molecular weight was obtained. It was observed that the rate of shear degradation was highest at low temperatures[200] thus producing an apparent negative activation energy as found in the ultrasonic process.

The effect of concentration on shear degradation has been examined by several workers[201,202], however there is disagreement on the results. Odell and Keller observed an increase in the rate of chain scission in more concentrated solutions. This was rationalised in terms of the increased entanglement effects causing greater forces on the chain. However, it was noted that the concentration effects were too small to draw any definite conclusions and further concentrations were to be studied.

When turbulence is involved with the shear degradation, increasing the concentration of the solution reduces and delays the onset of turbulence and hence the degradation rate is reduced[203]. Thus it can be seen that ultrasonic degradation correlates better with a turbulent shear than a pure shear degradation. This could be the reason why the pure shear rate model used in the kinetic studies did not produce linear relationships.

Ultrasonic degradation of polymers is a very complex system. Altering one parameter alters many of the solutions properties and hence it is almost impossible to study the effect of a single parameter on the degradation. This is well demonstrated by considering the effect of temperature on the degradation. The temperature not only affects the saturated vapour pressure of the solution but also affects the Flory-Huggins interaction parameter. This can be seen in equation 3.27,

$$\chi = \frac{a - b}{T} \qquad 3.27$$

Hence a decrease in the temperature will cause the polymer to coil in solution and reduce the degradation.

However, despite this it is possible to predict the molecular weight and polydispersity of a polymer degraded under a certain set of conditions. This could have applications in polymer processing. For example a high molecular weight component in a material can cause high melt viscosity, low solubility and so give process problems. Inclusion of a sonication step after manufacture can reduce this and so reduce these problems. Some initial studies have been performed using rubber type polymers and the method has been found to be potentially useful[204].

The following chapter will describe another potential use of the high degree of structural control offered by ultrasonic degradation in the production of functionalised polystyrene materials.

CHAPTER FOUR

SYNTHESIS OF FUNCTIONALISED POLYMERS

The previous chapter examined the ability to control the polystyrene chain length by varying the conditions of ultrasonic degradation. The work described in this chapter shows how this may be used to produce functionalised polystyrenes with known structures.

The initial product on chain cleavage in polystyrene is a pair of "macroradicals" as described in Chapter One. This gives a reactive site which can be used to join other reagents to the chain. Using the results from Chapter Three allows a large degree of control of the resulting structure. Two examples of the approach will be discussed; production of telechelic polystyrene and of polystyrene block copolymers.

4.1 Production of Telechelic Polystyrenes

A telechelic polymer is a polymer having two reactive end groups[205]. These terminal functional groups are then capable of further reactions, such as coupling to form block copolymers[206]. Bamford[207] prepared the first telechelic polymer from polystyrene and demonstrated the functionality by coupling reactions to form block copolymers.

Telechelic materials have been obtained by cleavage of a polymer, which can be carried out by oxidation, reduction and irradiation with light. The disadvantage of these methods is that the degradation is random so that the polydispersity of the functionalised polymers will be high, and therefore the properties of the resulting materials will be less defined.

The structural control offered by the non-random ultrasonic degradation with the production of radicals presumably at the chain ends[53] offers the possibility of producing telechelic polymers with well defined chain lengths, making them more suitable for further usage. This technique has not, to our knowledge, previously been examined.

The presence of two functional groups in a polymer of a molecular weight 100000 would be very difficult to detect using normal analytical techniques. Hence, a functional group attached to a highly U.V. active molecule was used, and presence of

the functional group was indicated by U.V. absorbance. Two chromophoric groups were used, naphthalene and anthracene. To promote reactivity, bromo substituted compounds were used as these are known to be susceptible to radical attack.

Figure 4.1 shows the U.V. absorbance spectra of 9-bromoanthracene, 1-amino-4-bromonaphthalene and polystyrene. It should be noted that polystyrene has no absorbance above 300 nm while the other two absorb strongly in this region. Figure 4.2 shows the spectra of polystyrene sonicated in THF containing excesses of the two chromophores. The polymers were extensively purified to remove unattached chromophore and it can clearly be seen that the polymers are functionalised. This was further confirmed by recording GPC chromatograms using both refractive index and U.V. detection at 360 nm as shown in Figure 4.3. The RI trace corresponds to the whole polymer sample while the U.V. responds only to the anthracene group. The correspondence of the peaks clearly shows that the anthracene is attached to the polymer.

In order to obtain an approximate capping efficiency, the extinction coefficient of 9-bromoanthracene at 370 nm in tetrahydrofuran was measured. The value obtained was 7714 mol^{-1} dm^3 cm^{-1}.

A known concentration of the capped polymer was prepared in a 10 ml volumetric flask and its U.V. spectrum recorded. The capping efficiency was calculated as follows, using the anthracene as an example:

Concentration of capped polymer solution = 0.1357 g in 10 ml

Absorption at 370 nm = 0.18

Using the Beer-Lambert law, $A = \epsilon Cl$

Where A is the absorption, ϵ is the extinction coefficient, C is the concentration of the absorbing species and l is the path length, the concentration of the anthracene is

$$\frac{0.18}{7714} = 2.33 \times 10^{-5} \text{ mol dm}^{-3}$$

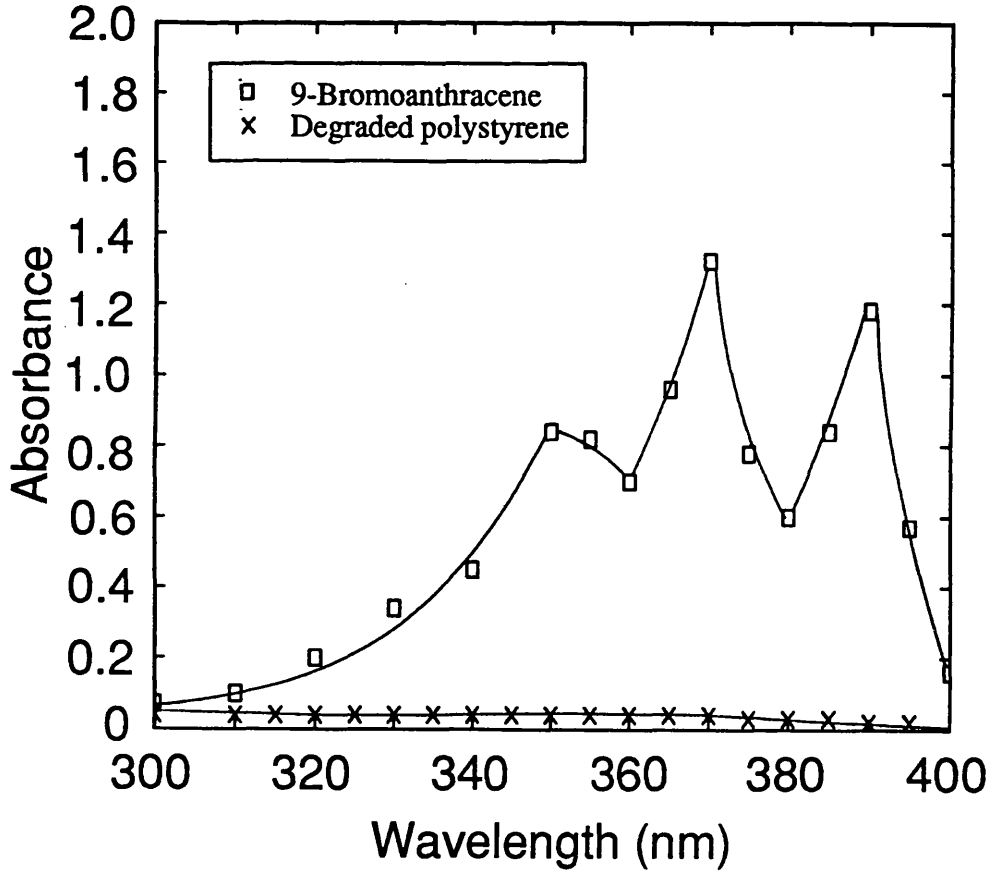

FIGURE 4.1(A). U.V. spectra of 9-bromoanthracene and ultrasonically degraded polystyrene in tetrahydrofuran.

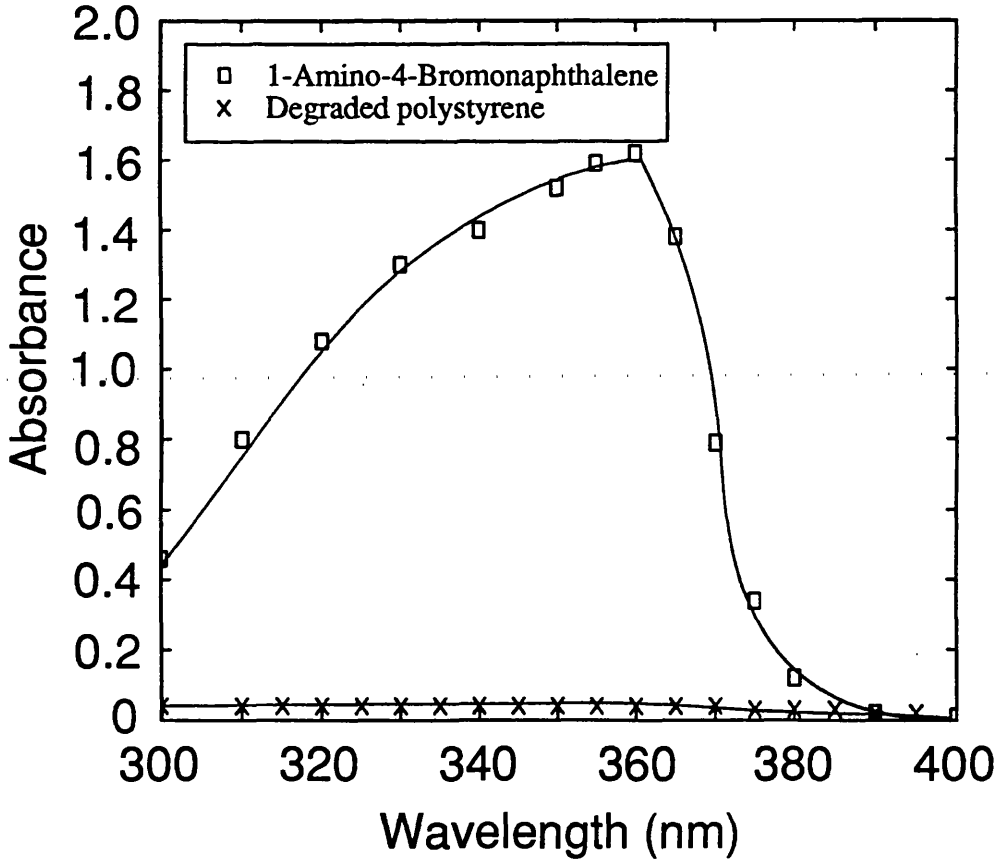

FIGURE 4.1(B). U.V. spectra of 1-amino-4-bromonaphthalene and ultrasonically degraded polystyrene in tetrahydrofuran.

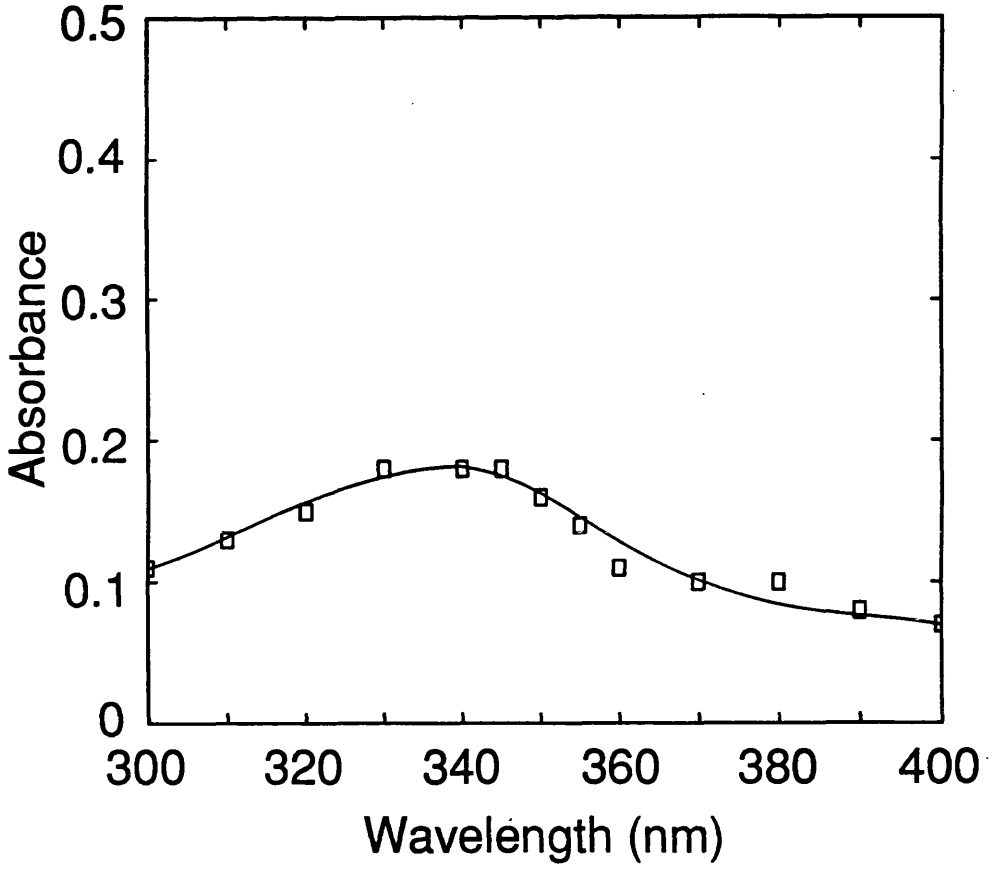

FIGURE 4.2(A). U.V. spectra of polystyrene sonicated in a solution of 9-bromoanthracene in tetrahydrofuran.

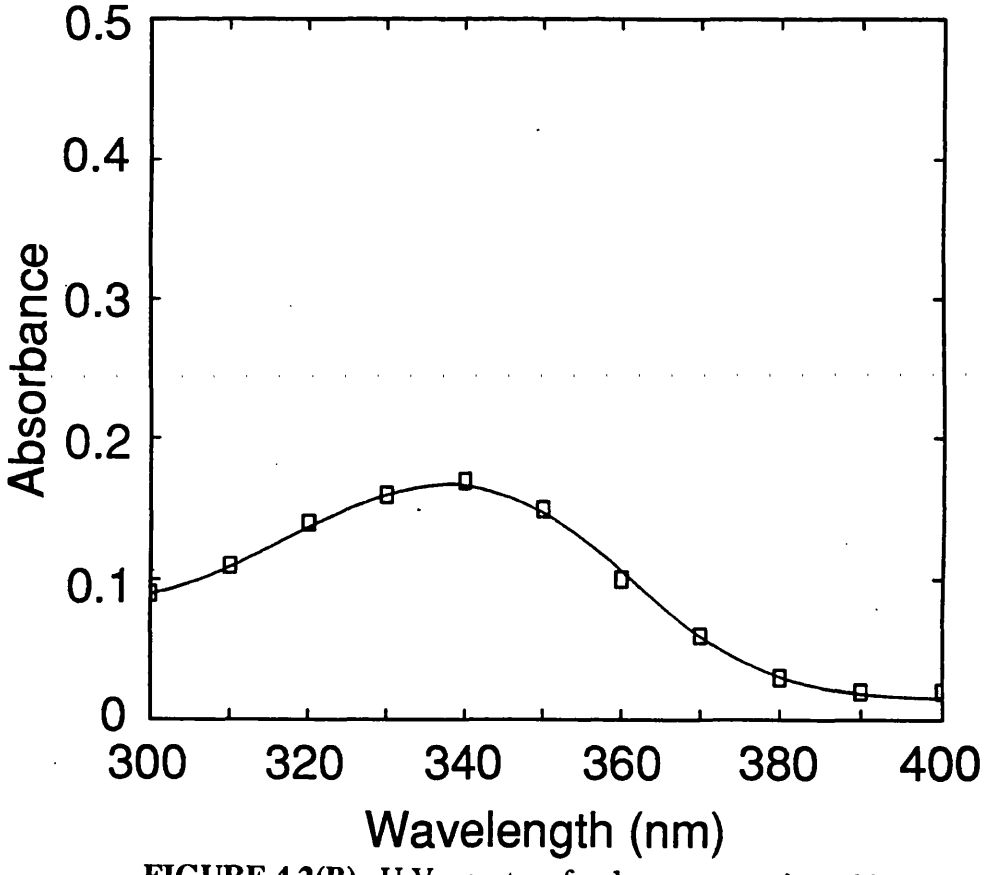

FIGURE 4.2(B). U.V. spectra of polystyrene sonicated in a solution of 1-amino-4-bromonaphthalene in tetrahydrofuran.

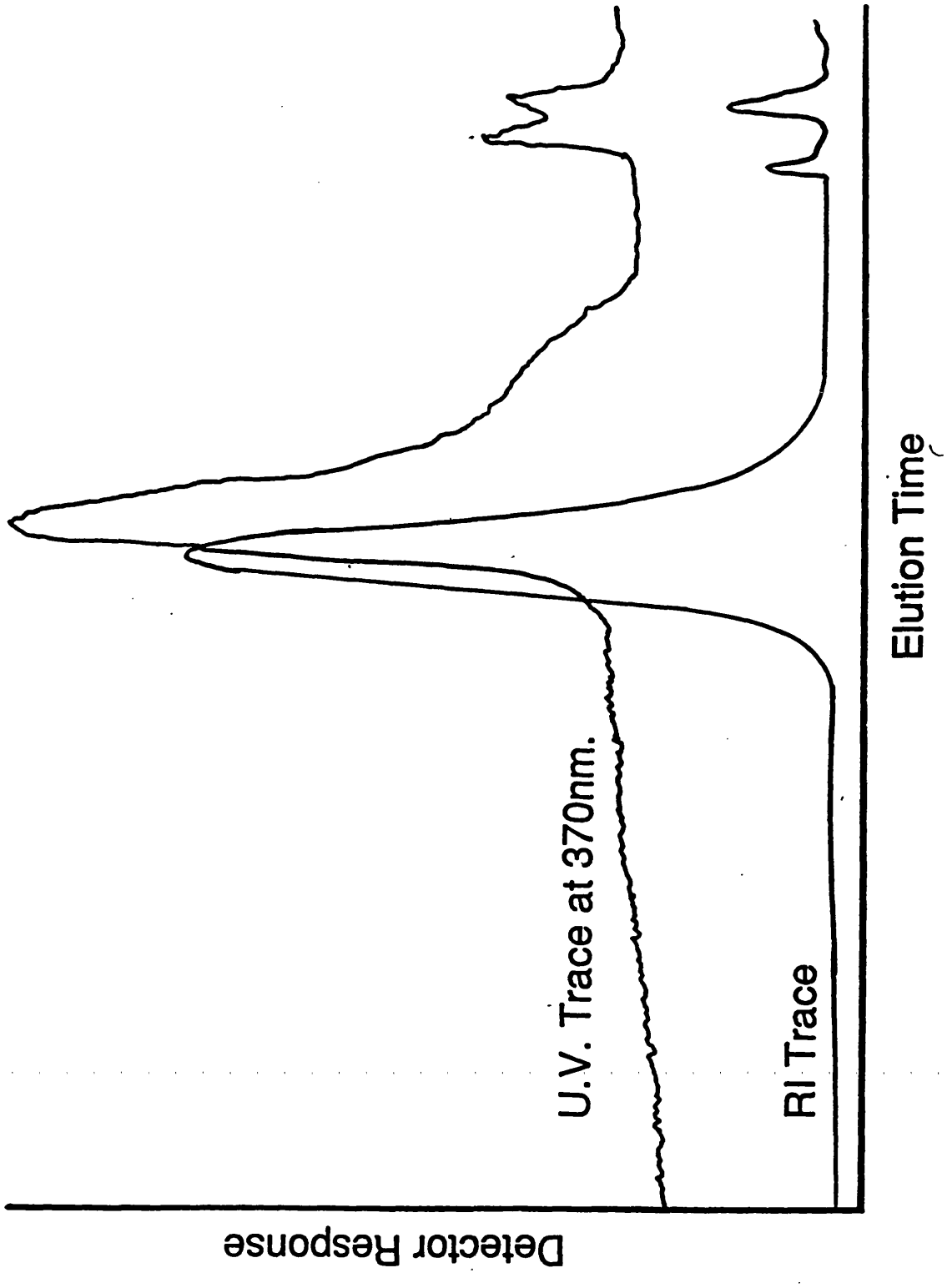

FIGURE 4.3. G.P.C. dual detector trace of polystyrene sonicated in 1-amino-4-bromonaphthalene.

Considering one cap per polymer

$$13.57 \text{ g dm}^{-3} = 2.33 \times 10^{-5} \text{ mol dm}^{-3}$$

and hence the molecular weight of the polymer is 582000.

However, the molecular weight of the polymer measured from GPC was only 55000 and hence there is approximately only 1 anthracene on every 10 polymer chains.

The extinction coefficient of 1-amino-4-bromonapthalene in tetrahydrofuran at 370 nm was measured as 875 mol^{-1} dm^3 cm^{-1}. Applying the method used to calculate the capping in the 9-bromoanthracene system, a molecular weight of 44200 was obtained. Considering the molecular weight obtained from GPC to be approximately 55000, this indicates that there are 1.2 caps per polymer chain.

4.2 Production of Polystyrene Block Copolymers

Methods of synthesis of copolymers containing long sequences of monomers (block copolymers) are of great interest, since they may lead to polymers with properties widely different from those of either homopolymers or random copolymers. The preceding chapter demonstrated the ability to control the polystyrene block length using ultrasonic degradation. However, in order to predict the properties of the copolymer, the addition of the second monomer must also be controlled. For this study methyl methacrylate was chosen as a model because it is a very well characterised system, and the copolymer composition could be easily followed using NMR as described in Section 2.3.5.

Control of the methyl methacrylate block length was examined by degrading polystyrene in methyl methacrylate monomer, varying the concentration of the polystyrene and the monomer. Previous workers have sonicated mixtures of polystyrene and poly(methyl methacrylate) in a common solvent[111]; however, with both polymers degrading under the ultrasound, the copolymer composition was very difficult to control.

4.2.1 Effect of varying the polystyrene concentration

Varying concentrations of polystyrene from 0.5% w/v to 20% w/v were degraded in pure methyl methacrylate as described in Section 2.2.3.

Figure 4.4 shows the yield of poly(methyl methacrylate) produced during the degradation. The highest yield is produced by degrading 1% w/v polystyrene in methyl methacrylate, above this concentration the percentage yield drops significantly.

Analysis of the resulting purified copolymer by NMR showed that degradation of 1% w/v polystyrene in the monomer also produced the highest proportion of methyl methacrylate in the copolymer. An example of a spectrum given by a copolymer is shown in Figure 4.5. Increasing the polystyrene concentration above 1% w/v resulted in a decrease of the methyl methacrylate in the resulting copolymers. This can be seen in Figure 4.6.

In order to examine the variation in the composition of the copolymers during the sonication, a 0.5% w/v solution of polystyrene in methyl methacrylate was sonicated as described previously for various times and the polymers obtained were purified and analysed using NMR.

The change in the copolymer composition can be seen in Figure 4.7. The percentage of poly(methyl methacrylate) in the copolymer increases to 90% in 4 hours, but decreases after 6 hours to 51%.

The degradation of polystyrene in methyl butyrate found in Section 3.5, showed that a 1% and a 0.5% w/v solution degrade to approximately the same extent. However, degradation of a 1% w/v solution produces a greater number of chain breaks than a 0.5% w/v solution in the same time, due to the greater number of chains in solution. Hence more radicals are produced and the probability of methyl methacrylate polymerising is greater than in the 0.5% w/v solution. This is shown by the higher percentage conversion obtained in the 1% w/v solution. The percentage methyl methacrylate conversion in the 0.5% w/v solution is the same as that obtained from ultrasonic polymerisation of pure methyl methacrylate with no added polystyrene. This

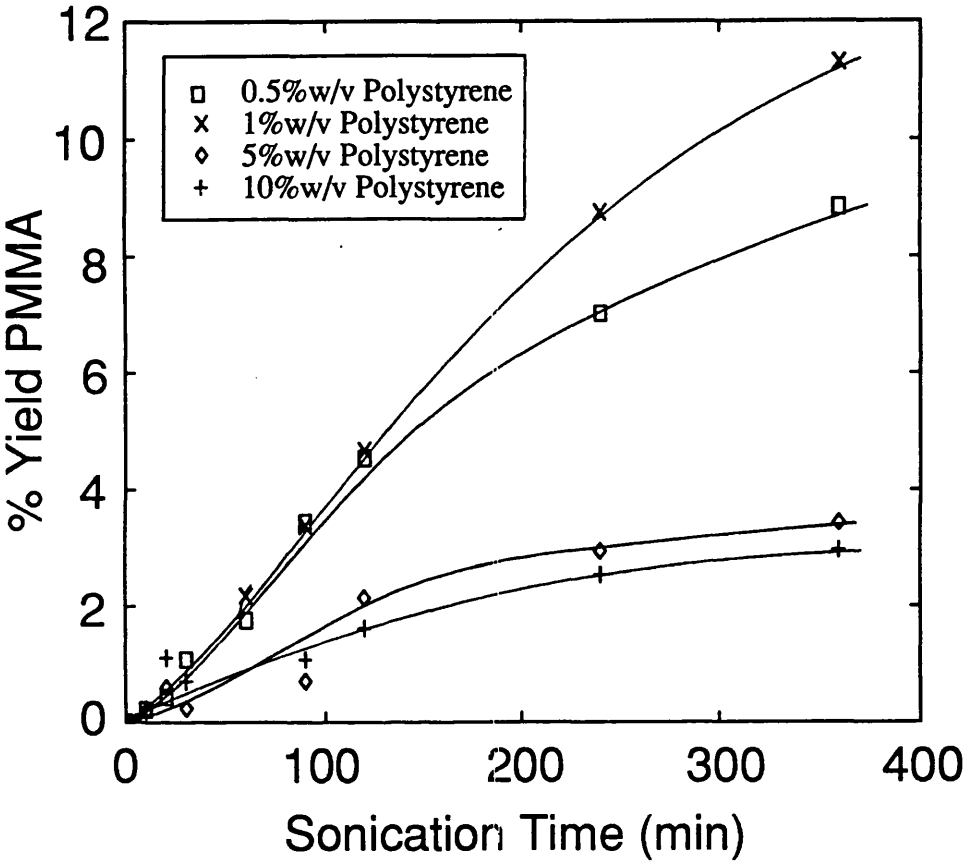

FIGURE 4.4. Percentage yield of poly(methyl methacrylate) obtained from the sonication of solutions of polystyrene in methyl methacrylate.

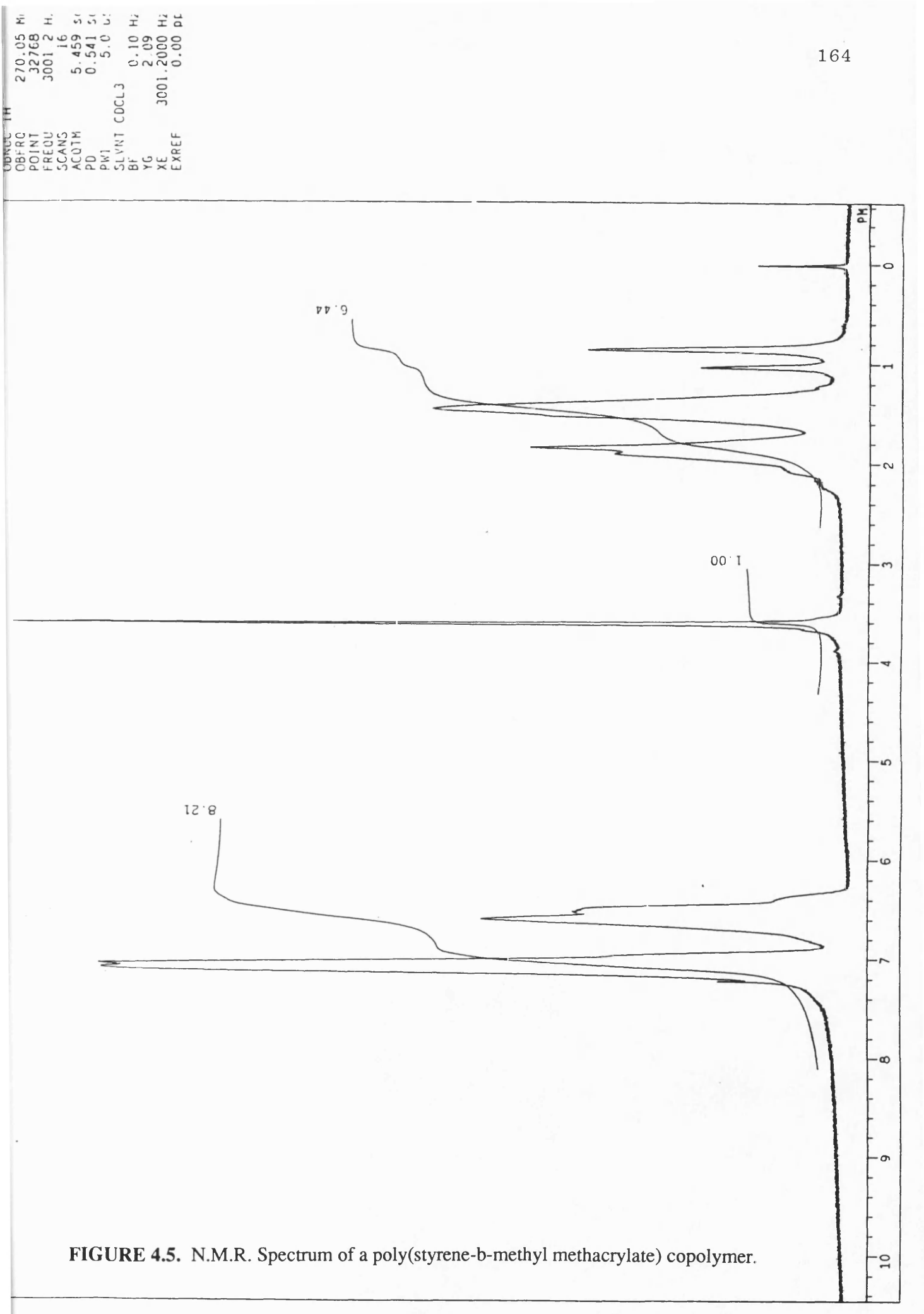

FIGURE 4.5. N.M.R. Spectrum of a poly(styrene-b-methyl methacrylate) copolymer.

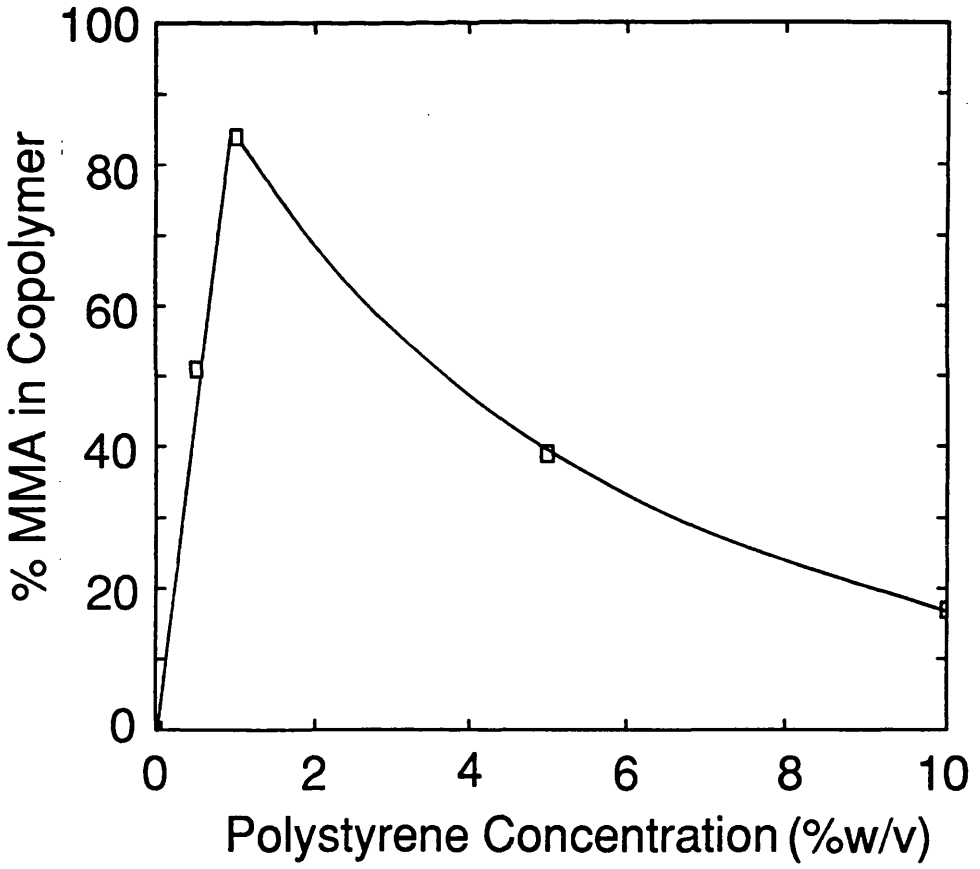

FIGURE 4.6. Copolymer composition obtained from the sonication of various concentrations of polystyrene in methyl methacrylate.

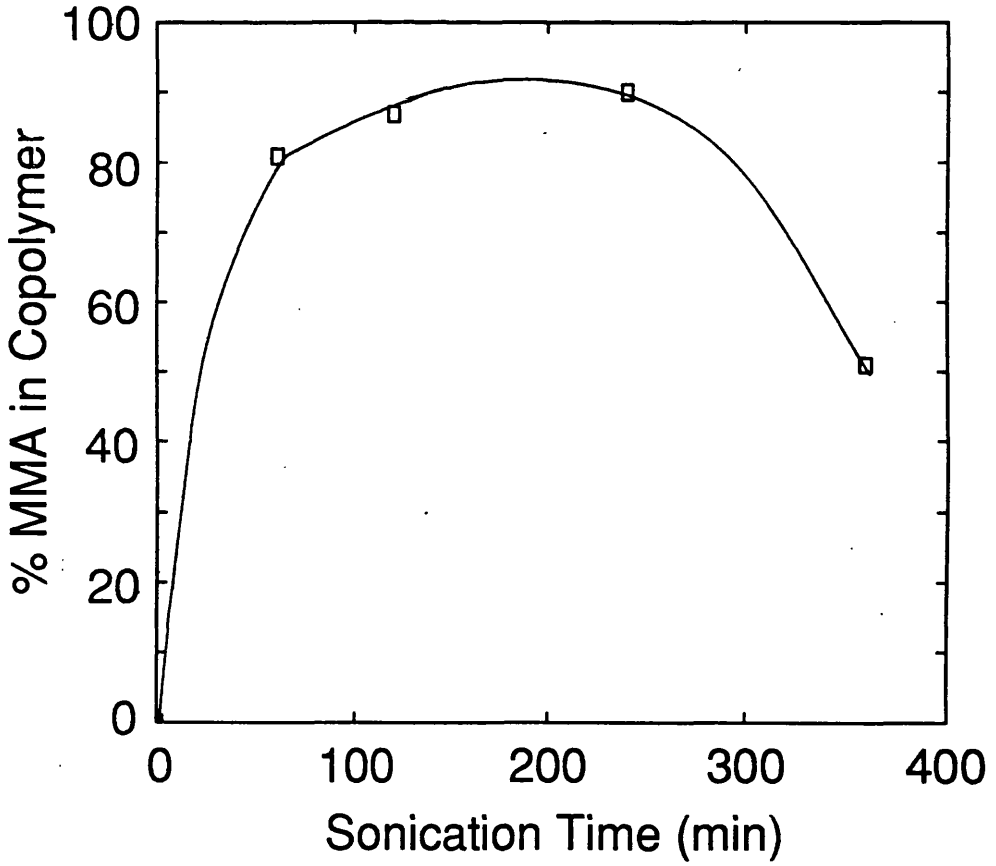

FIGURE 4.7. Variation of the copolymer composition during the sonication of 0.5%w/v polystyrene in methyl methacrylate.

indicates that the presence of polymer chains is not of primary importance for the generation of radicals in the monomer. However, above a concentration of 0.5% w/v polystyrene, the increased number of chain breaks does cause a signficant increase in the monomer polymerisation.

An increase in the solution concentration from 1% w/v to 5% w/v causes a significant decrease in the percentage monomer conversion. As shown in Section 3.5 the critical overlap concentration, C*, is 2.4% w/v and hence this decrease in monomer conversion does correspond with the point at which chains begin to overlap and entangle. The percentage monomer conversion at 5 and 10% w/v polystyrene is less than half that obtained from the polymerisation of the pure monomer with no added polystyrene. Hence it appears that increasing the concentration decreases the radical formation in the monomer as well as the amount of chain breaks in the polymer. The decrease in the radical formation could be due to the increased viscosity of the solution, raising the cavitational threshold as described in Section 1.5.1.

The percentage monomer conversions for the 10% w/v solution are almost identical to those of the 5% w/v solution and this may be due to experimental error. The 1 cm^3 samples removed from the 10% w/v solution were very viscous and removal of all of the unreacted methyl methacrylate was very difficult. Hence the weights obtained may be higher than expected due to residual methyl methacrylate monomer.

The percentage of methyl methacrylate in the resulting copolymers correlates well with the percentage monomer conversion curves found in Figure 4.4. The 5% and 10% w/v solutions which had the lowest monomer conversion also have the lowest amount of methyl methacrylate in the copolymer.

The copolymer obtained from the 1% w/v solution contained over 80% methyl methacrylate. This seemed exceptionally high considering that the solution already contained the polystyrene blocks. However, it can be explained considering the degradation process. As the monomer polymerises and forms a copolymer with the polystyrene, the copolymer is immediately broken in half by the sonication. If only a small quantity of monomer had joined the chain, this would result in the chain breaking

in the polystyrene section, hence the resulting copolymer would consist of a small section of polystyrene and a larger section of methyl methacrylate. This can be seen below:

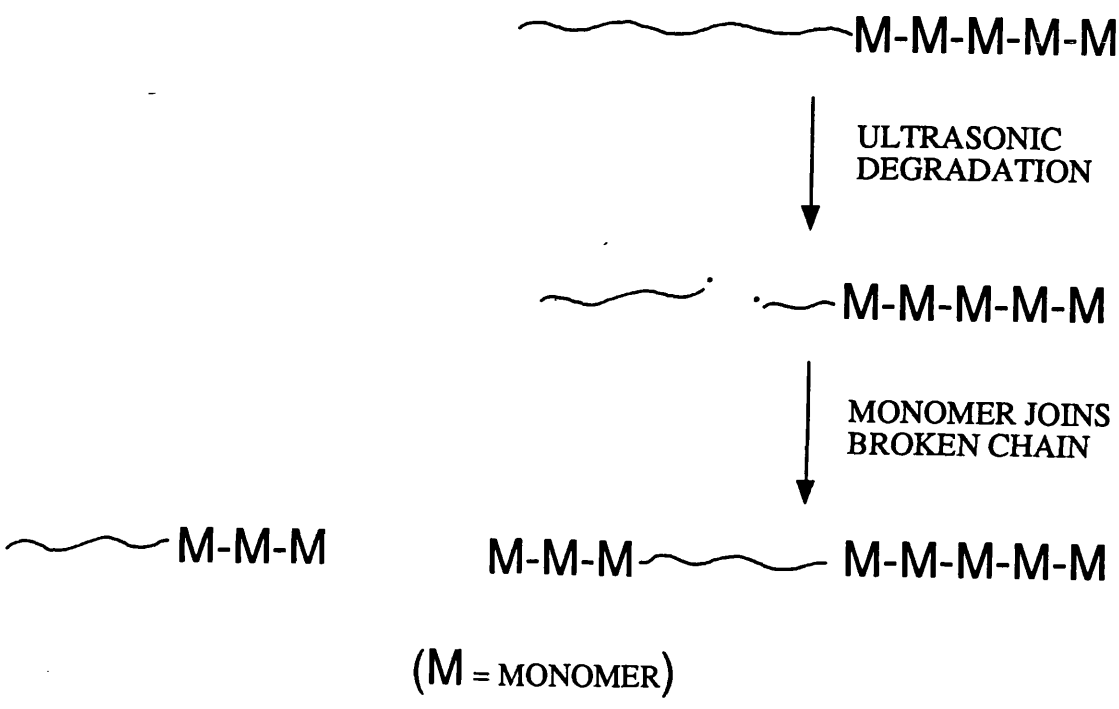

As can be seen from the illustration, after the chain has broken, since it is surrounded by monomer, the monomer can add to the radical on the chain end producing a copolymer with poly(methyl methacrylate) on either end of the copolymer and polystyrene in the centre. Every time the copolymer breaks, methyl methacrylate will join the chain since there is little chance of polystyrene recombining due to

1% w/v being below the critical overlap concentration for the solution. In this fashion, the percentage of methyl methacrylate in the copolymer will increase.

The variation of the copolymer composition during the sonication of a 0.5% w/v solution of polystyrene in methyl methacrylate can be seen in Table 4.1:

Table 4.1 Variation of copolymer composition during the sonication of 0.5% w/v polystyrene in methyl methacrylate

Sonication time (min)	% Styrene	% Methyl methacrylate
60	19	81
120	13	87
240	10	90
360	49	51

It can be seen that the percentage methyl methacrylate increased for 240 minutes but after 360 minutes the methyl methacrylate content had decreased to 51%. This experiment was repeated and identical copolymer ratios obtained, indicating that the decrease was not due to experimental error even though the result appears to be anomalous.

4.2.2 Effect of varying the monomer concentration

The concentration of the methyl methacrylate in the reaction was varied by the addition of methyl butyrate. As was shown in Table 2.1 this has physical properties very similar to that of methyl methacrylate. Hence this would mimic the cavitational properties of methyl methacrylate without itself undergoing polymerisation. While varying the methyl methacrylate:methyl butyrate ratio, the polystyrene concentration in the solution was kept constant at 0.5% w/v, i.e. isolating the effect of the methyl methacrylate concentration, all other factors remaining constant.

The percentage monomer conversion during the sonication for the various methyl methacrylate concentrations can be seen in Figure 4.8. The figure shows that the highest conversions are obtained with the 75% and 50% methyl methacrylate. The initial rate of polymerisation is fastest for the pure methyl methacrylate and 75% solution. This would be expected considering free radical polymerisation kinetics. The rate of polymerisation is given by

$$-\frac{d[M]}{dt} = k_R[M]$$

where k_R is a composite rate constant, consisting of the rate constants of initiation, propagation and termination, [M] is the monomer concentration and t is the time. Hence the rate should be linearly dependent on the monomer concentration. As shown in Figure 4.9 this is not apparent from these results with a deviation from linearity at high concentrations. This may be due to degradation of the poly(methyl methacrylate) giving rise to an increase in the number of radical species subsequently inducing further polymerisation.

However, as the process continues, the polymerisation of the 100% methyl methacrylate slows and reaches the value of 8.7% after 360 minutes, whereas the 50% and 75% methyl methacrylate solutions have increased conversions at 10.7%. The added methyl butyrate reduces the viscosity of the solutions and enables the polymerisation to continue to higher conversions. However, addition of 75% methyl butyrate reduces the monomer concentration to such an extent that the polymerisation is impaired.

The change in composition of the copolymer with monomer concentration can be seen in Table 4.2 overleaf:

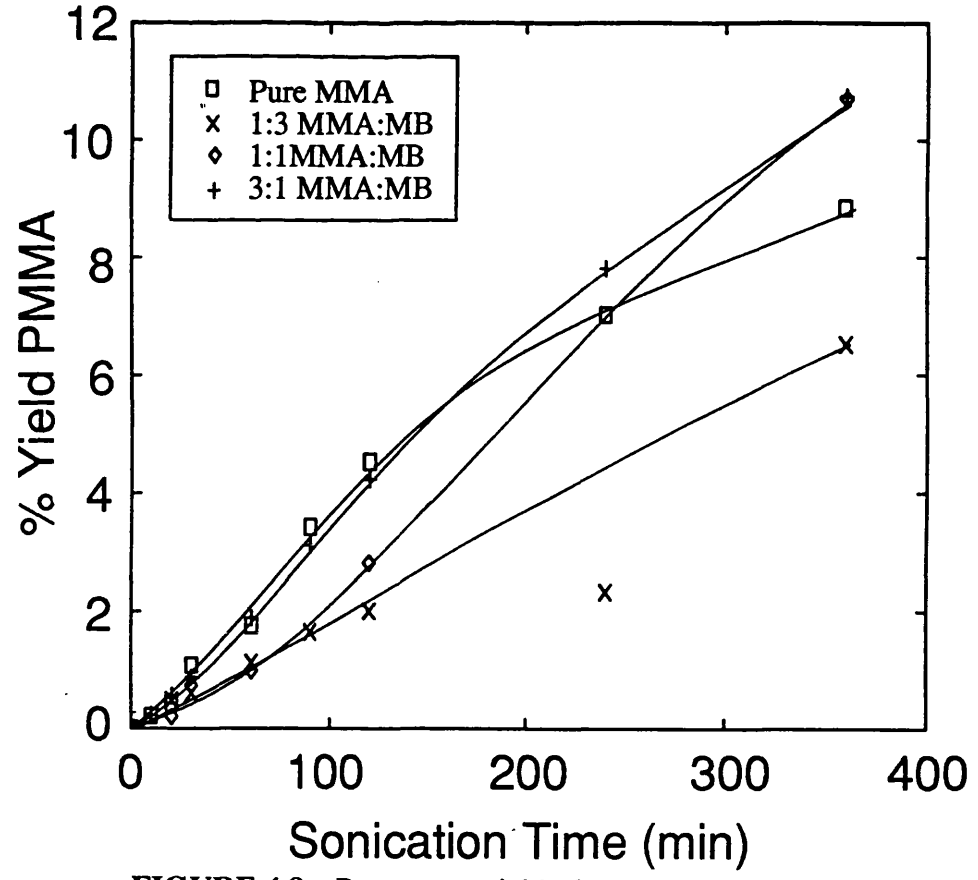

FIGURE 4.8. Percentage yield of poly(methyl methacrylate) obtained from the sonication of solutions of polystyrene in methyl methacrylate with varying volumes of methyl butyrate.

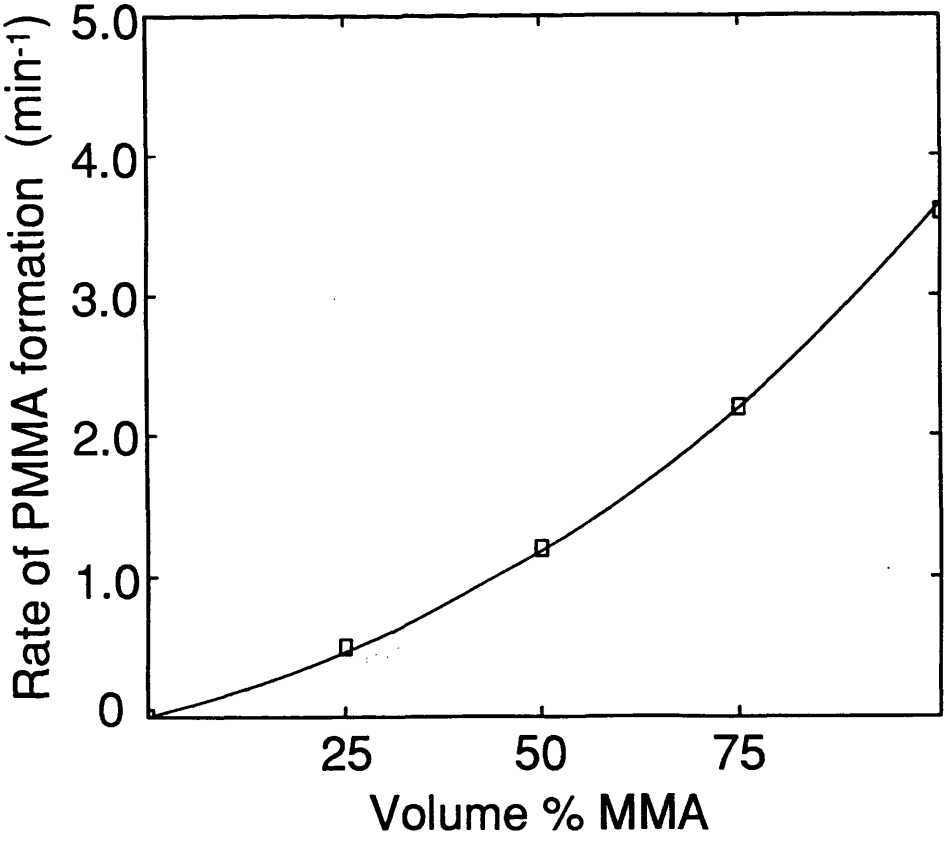

FIGURE 4.9. Effect of the methyl methacrylate concentration on the rate of formation of poly(methyl methacrylate).

Table 4.2 Variation of copolymer composition with varying monnomer concentration

% Methyl methacrylate	Sonication time (min)	% Styrene	% Methyl methacrylate
100	360	49	51
75	360	8	92
50	360	13	87
25	360	27	73

The percentage methyl methacrylate in the copolymer follows the percentage methyl methacrylate yields obtained as shown in Figure 4.8, with the exception of 100% methyl methacrylate with 0.5% w/v polystyrene. As the percentage monomer in the solution increases, there is a greater probability of the monomer polymerising and joining the polystyrene chain. However, the lower than expected methyl methacrylate composition of the copolymer from the 100% methyl methacrylate feed cannot be explained by the above discussion and other factors must be involved.

In order to examine the composition of the copolymers during the sonication, a 50:50 methyl methacrylate: methyl butyrate solution containing 0.5% w/v polystyrene was sonicated for 1, 2, 4 and 6 hours. The copolymer compositions can be seen in Table 4.3:

Table 4.3 Variation of copolymer composition during the sonication of 0.5% w/v polystyrene in 50:50 methyl methacrylate:methyl butyrate

Sonication time (min)	% Styrene	% Methyl methacrylate
60	35	65
120	27	73
240	12	88
360	13	87

Table 4.4 Molecular weights of polymers

SYSTEM	SONICATION TIME (hr)	% MMA	Mn ($\times 10^{-3}$)	γ
0.5% PS in 3:1 MMA:MB	6	92	149	1.9
0.5% PS in 1:1 MMA:MB	6	87	126	1.6
0.5% PS in 1:3 MMA:MB	6	73		
0.5% PS in MMA	6	51	123	2.1
0.5% PS in MMA	4	90	195	1.9
0.5% PS in MMA	2	87	145	2.0
0.5% PS in MMA	1	81	219	2.2
0.5% PS in 1:1 MMA:MB	4	88	150	1.8
0.5% PS in 1:1 MMA:MB	2	73	145	1.9
0.5% PS in 1:1 MMA:MB	1	65		
1% PS in MMA	6	84	179	1.7
5% PS in MMA	6	39	160	2.0
10% PS in MMA	6	17	192	1.7
20% PS in MMA	6	0	117	2.1
0.5% PS + 0.5% PMMA in THF	6		75	1.7

PS = Polystyrene $M_o = 145000$ $\gamma_o = 3.2$

MMA = Methyl methacrylate monomer

MB = methyl butyrate

PMMA = poly(methyl methacrylate) $M_o = 245000$ $\gamma_o = 3.1$

The percentage of methyl methacrylate in the copolymer increases for 240 minutes and then stays constant. The increase in the methyl methacrylate content can be explained by the mechanism described in Section 4.3.1. However it appears that there is a maximum in methyl methacrylate content at approximately 88%. This could be the point at which at equilibrium is reached between the amount of methyl methacrylate polymerising and joining the chain and the amount being lost by ultrasonic degradation.

4.2.3 Molecular weights

Molecular weights of the copolymers were measured by GPC, these were also run at RAPRA. Calibrations for copolymers are usually taken as an average of those for the component homopolymers but in this case calibrations using the homopolymers gave results agreeing within experimental error, so that only those from the polystyrene calibration will be discussed here. Table 4.4 (overleaf) shows the molecular weights for all of the copolymers prepared.

Unfortunately there is no pattern within each group of experiments. From the results in Chapter 3, the limiting molecular weight for polystyrene degraded in methyl butyrate for 6 hours was 67000. The fact that the copolymer molecular weights are considerably above this shows that methyl methacrylate is adding to the ends of the macroradical. Clearly, the copolymers, once formed, are also subject to degradation under the conditions used here leading to a complex dependence of molecular weight on sonication conditions.

4.3 Discussion

4.3.1 Telechelic polymers

The results obtained indicate that functional groups can be attached to a polymer chain using ultrasound. However, there appears to be a large difference between the number of caps attached when using 9-bromoanthracene compared to using 1-amino-4-bromonaphthalene.

There are uncertainties in the calculation of the capping efficiency. In both cases the extinction coefficients used to calculate the concentration of functional groups are those from the original compound. However, when the cap is present on the chain, the halogen has been removed and replaced by an alkyl group, hence a more accurate result would be obtained if the extinction coefficient for a compound of similar structure to that of the cap was used, although in related naphthalene compounds, the difference was small[208]. Clearly more work is needed to characterise the process. One approach would be to arrange the conditions so that only one chain break occurred, producing materials with one cap per chain.

Other methods for producing these materials include anionic[209,210], cationic[211] and radical polymerisation[212]. However, these methods are restrictive in that the anionic mechanism needs a high level of purity, a cationic chain-end is prone to undergo inter- or intramolecular transfer[205] and the radical polymerisation produces high polydispersity products. The method discussed here does offer considerable control over the structure and gives the possibility of obtaining a chain capped at both ends with a low polydispersity. However, much more work is needed before the full potential of the method can be realised.

4.3.2 Preparation of copolymers

The results described in Chapter Three showed that the block length of the major component could be controlled by modifying the sonication conditions. This chapter has illustrated the possibility of control of the block size of the second component. This is not as straightforward as hoped and this preliminary study has shown some of the problems of the technique. There are fewer parameters available to influence this aspect without changing the degradation, the concentration of components being the only readily available variable, although this changes throughout the reaction as monomer adds to the growing chain.

This method of copolymer formation does not appear to offer the levels of control obtained through use of anionic and Ziegler-Natta block copolymer synthesis[1].

Degradation of the copolymer after its formation limits the level of control of the copolymer block lengths, however more work is needed on the addition of the monomer before the method's applicability can be fully appreciated.

REFERENCES

1. Ceresa, R.J., 'Block and Graft Copolymers', Butterworths, London, 1962.
2. Bolland, J.L., Melville, H.W., *Proc. First Rubber Technol. Conf.*, London, **239**, 1938.
3. Szwarc, M., *Nature*, **178**, 1168, 1956.
4. Young, R.J., 'Introduction to Polymers', Chapman and Hall, London, 1986.
5. Dawkins, J.V., 'Steric Exclusion in Liquid Chromatography of Polymers', ed. J. Janca. New York, 1984.
6. Grubisic, Z., Rempp, P., Benoit, H., *J. Polym. Sci., Polym. Lett. Ed.*, **5**, 753, 1967.
7. Henglein, A., *Ultrasonics*, **25**, 6, 1987.
8. Flynn, H.G., *Physical Acoustics*, **1(B)**, 57, 1964, Academic Press, New York.
9. Basedow, A.M., Ebert, K.H., *Adv. Polym. Sci.*, **22**, 83, 1977.
10. Kirchoff, G., *Ann. Phys.*, **134**, 177, 1868.
11. Margulis, M.A., *Ultrasonics*, 157, 1985.
12. Crumm, L.A., IEEE, Ultrasound Symposium, **1**, 1982.
13. Crumm, L.A., *Nature*, **278**, 148, 1979.
14. Apfel, R.E., *J. Acoust. Soc. Am.*, **48**, 1179, 1970.
15. Greenspan, M., Tschiegg, C.E., *J. Res. Nat. Bur. Std.*, **C71**, 229, 1967.
16. Willard, G.W., *J. Acoust. Soc. Am.*, **25**, 669, 1953.
17. Galloway, W.J., *J. Acoust. Soc. Am.*, **26**, 849, 1954.
18. Noltingk, B.E., Neppiras, E.A., *Proc. Phys. Soc.*, **63B**, 674, 1950.
19. Neppiras, E.A., *Phys. Rep.*, **61**, 160, 1980.
20. Fitzgerald, M.E., Griffing, V., Sullivan, J., *J. Chem. Phys.*, **25**, 926, 1956.
21. Smith, F.D., *Philos. Mag.*, **19**, 1147, 1935.
22. Weissler, A., *J. Appl. Phys.*, **21**, 171, 1950.
23. Jellinek, H.H.G., White, G., *J. Polym. Sci.*, **6**, 745, 1951.
24. Jellinek, H.H.G., White, G., *J. Polym. Sci.*, **6**, 757, 1951.
25. Jellinek, H.H.G., White, G., *J. Polym. Sci.*, **7**, 33, 1951.
26. Bergmann, L., 'Ultrasonics', G. Bell and Sons, N.Y., 1964.

27. Jellinek, H.H.G., *J. Polym. Sci.*, **22**, 149, 1956.

28. Diedrich, G.K., Kruus, P., Rachlis, L.M., *Can. J. Chem.*, **50**, 1743, 1972.

29. Gaertner, W., *J. Acoust. Soc. Am.*, **26**, 977, 1954.

30. Eyring, H.J., *J. Chem. Phys.*, **4**, 283, 1936.

31. Neppiras, E.A., Noltingk, B.E., *Proc. Phys. Soc.*, **64B**, 1032, 1951.

32. Brett, A.W., Jellinek, H.H.G., *J. Polym. Sci.* **13**, 441, 1954.

33. Crumm, L.A., *Appl. Sci. Res.*, **38**, 101, 1982.

34. Curie, J., Curie, P., *Compt. Rend.*, **91**, 294, 1880.

35. Curie, J., Curie, P., *Compt. Rend.*, **93**, 1137, 1881.

36. Galton, F., 'Inquiries into Human Faculty and Development', Macmillan, 1883.

37. Mason, T.J., Lorimer, J.P., 'Sonochemistry', Ellis Horwood Ltd., 1988.

38. Flosdorf, E.W., Chambers, L.A., *J. Amer. Chem. Soc.*, **55**, 3051, 1933.

39. Gyorgi, A.S., *Nature*, **131**, 279, 1933.

40. Szalay, A., *Z. Phys. Chem.*, **A164**, 234, 1933.

41. Freundlich, H., Gillings, J., *Trans. Faraday Soc.*, **34**, 649, 1938.

42. Heyman, E., *Trans. Faraday Soc.*, **31**, 846, 1935.

43. Freundlich, H., *J. Physic. Chem.*, **41**, 1151, 1937.

44. Brohult, F., *Nature*, **140**, 805, 1937.

45. Schmid, G., Rommel, O., *Z. Elektrochem.*, **45**, 659, 1936.

46. Schmid, G., *Phys. Z.*, **41**, 326, 1940.

47. Jellinek, H.H.G., *J. Polym. Sci.*, **37**, 485, 1959.

48. Jellinek, H.H.G., Brett, H.W., *J. Polym. Sci.*, **21**, 535, 1956.

49. Henglein, A., *Makromol. Chem.*, **14**, 15, 1954.

50. Henglein, A., *Makromol. Chem.*, **15**, 188, 1955.

51. Melville, H.W., Murray, A.J., *Trans Faraday Soc.*, **46**, 996, 1950.

52. Tabata, M., Miyazawa, T., Sohma, J., *Proc. 3rd Yamada Conference on Free Radicals*, Yamadi Sci. Found., Osaka, 243, 1979.

53. Tabata, M., Miyazawa, T., Sohma, J., Kobayashi, O., *Chem. Phys. Lett.*, **73**, 178, 1980.

54. Thomas, J.R., de Vries, D.L., *J. Phys. Chem.*, **63**, 254, 1959.

55. Gooberman, G., *J. Polym. Sci.*, **47**, 329, 1960.

56. Schmid, G., Schneider, C., Henglein, A., *Kolloid Z.*, **148**, 73, 1956.

57. Gooberman, G., Lamb, J., *J. Polym. Sci.*, **42**, 35, 1960.

58. Gooberman, G., Lamb, J., *J. Polym. Sci.*, **47**, 229, 1960.

59. Moore, J.C., *J. Polym. Sci.*, **A2**, 835, 1964.

60. Porter, R.S., Cantow, M.J., Johnson, J.F., *J. Appl. Polym. Sci.*, **11**, 335, 1967.

61. Niezette, J., Linkens, A., *Polymer*, **19**, 939, 1978.

62. Shaw, M.T., Rodriguez, F., *J. Appl. Polym. Sci.*, **11**, 991, 1967.

63. Malhotra, S.L., *J. Macromol. Sci. Chem.*, **A23**, 729, 1986.

64. Wu, C.F., Sheth, P.J., Johnson, J.F., *Polymer*, **18**, 822, 1977.

65. Smith, W.B., Temple, H.W., *J. Phys. Chem.*, **72**, 4613, 1968.

66. Glynn, P.A.R., Van der Hoff, B.M.E., Reilly, P.M., *J. Macromol. Sci. Chem.*, **A6**, 1653, 1972.

67. Glynn, P.A.R., Van der Hoff, B.M.E., Reilly, P.M., *J. Macromol. Sci. Chem.*, **A7**, 1695, 1973.

68. Van der Hoff, B.M.E., Glynn, P.A.R., *J. Macromol. Sci. Chem.*, **A8**, 429, 1974.

69. Banwell, C.N., 'Fundamentals of Molecular Spectroscopy', McGraw-Hill, 1983.

70. Mostafa, M.A.K., *J. Polym. Sci.*, **33**, 311, 1958.

71. Jellinek, H.H.G., *J. Polym. Sci.*, **37**, 485, 1959.

72. Schmid, G., Poppe, W., *Z. Elektrochem.*, **53**, 28, 1949.

73. Mostafa, M.A.K., *J. Polym. Sci.*, **28**, 519, 1958.

74. Wade, E., Nakane, H., *J. Sci. Research Inst.*, **1**, 45, 1951.

75. Keqiang, C., Ye, S., Hiulen, L., Xi, X., *J. Macromol. Sci. Chem.*, **A22**, 455, 1985.

76. Shaw, M.T., Rodriguez, F., *J. Appl. Polym. Sci.*, **11**, 991, 1967.

77. Cao, Z., Xu, X., *Huagong Xuebao*, **1**, 56, 1985 [CA103(20): 16096].

78. Okuyama, M., *Z. Elektrochem.*, **59**, 565, 1955.

79. Schoon, T.G., Rieber, G., *Angew. Makromol. Chem.*, **23**, 43, 1972.

80. Basedow, A.M., Ebert, K.H., *Makromol. Chem.*, **176**, 745, 1975.

81. Basedow, A.M., Ebert, K.H., *Angew. Chem. Int. Ed. Eng.*, **13**, 413, 1974.

82. Mostafa, M.A.K., *J. Polym. Sci.*, **33**, 295, 1958.

83. Schoon, T.G., Rieber, G., *Angew. Makromol. Chem.*, **23**, 43, 1972.

84. Schoon, T.G., Rieber, G., *Angew. Makromol. Chem.*, **15**, 263, 1971.

85. Thomas, G.R., *J. Phys. Chem.*, **63**, 1725, 1959.

86. Grassie, N., Melville, H.W., *Proc. Roy. Soc.*, **A.199**, 39, 1946.

87. Encina, M.V., Lissi, E., Sarasua, M., Gargallo, L., Radic, D., *J. Polym. Sci. Polym. Lett.*, **18**, 757, 1980.

88. Schmid, G., Beutenmuller, E., *Z. Elektrochem.*, **49**, 325, 1943.

89. Thomas, B.B., Alexander, W.J., *J. Polym. Sci.*, **25**, 285, 1957.

90. Nelkenbaum, Y.Y., Prokofiev, I.K., Sangalov, Y.A., *Vyskomol. Soedin. Ser. A*, **28**, 1058, 1986. [CA 106(20):156965].

91. Price, G J., Smith, P.F., *Polymer Int.*, **24**, 159, 1991.

92. Golubev, S.V., Tikhonova, Z.A., Semchikov, Y.D., Trubina, I.V., *Vyskomol. Soedin. Ser. A*, **29**, 2393 [CA 108(4):22407].

93. Malhotra, S.L., *J. Macromol. Sci. Chem.*, **A17**, 601, 1982.

94. Basedow, A.M., Ebert, K.H., Fosshag, E., *Makromol. Chem.*, **179**, 2565, 1978.

95. Malhotra, S.L., Breton, M., Gauthier, J.M., *J. Macromol. Sci. Chem.*, **A18**, 1151, 1982.

96. Schmid, G., Beutenmuller, E., *Z. Elektrochem.*, **50**, 209, 1940.

97. Schmid, G., Rommel, O., *Z. Phys. Chem.*, **185**, 97, 1939.

98. Thomas, B.B., Alexander, W., *J. Polym. Sci.*, **15**, 361, 1955.

99. Kawase, S., Doi, H., Kakurai, T., *Kobunshi Ronbunshu*, **35**, 109, 1978 [CA 88(24): 170690].

100. Fujiwara, H., Tsunoda, M., Goto, K., *Kobunshi Ronbunshu,* **32**, 106, 1975 [CA 82(24): 156918].

101. de Boer, J.H., *Trans. Faraday Soc.,* **32**, 10, 1936.

102. Jellinek, H.H.G., White, G., *J. Polym. Sci.,* **7**, 21, 1951.

103. Thieme, A., *Physik, Z.,* **39**, 384, 1938.

104. Flory, P.J., 'Principles of Polymer Chemistry', Cornell University Press, New York, 602, 1953.

105. Okuyama, M., Hirose, T.J., *J. Appl. Polym. Sci.,* **7**, 591, 1963.

106. Gooberman, G., *J. Polym. Sci.,* **42**, 25, 1960.

107. Alexander, P., Fox, M., *J. Polym. Sci.,* **12**, 533, 1954.

108. Schoon, T.G., Rieber, T., *Angew. Makromol. Chem.,* **49**, 23, 1976.

109. Odell, J.A., Keller, A., . *Polym. Sci., Polymer Phys. Ed.,* **24**, 1889, 1986.

110. Harrington, R.E., Zimm, B.H., *J. Phys. Chem.,* **69**, 161, 1965.

111. Pritchard, N.J., Hughes, D.E., Peacocke, A.R., *Biopolymers,* **4**, 259, 1966.

112. Pritchard, N.J., Peacocke, A.R., *Biopolymers,* **6**, 605, 1968.

113. Hughes, D.E., Nyborg, N.L., *Science,* **138**, 108, 1962.

114. O'Driscoll, K.F., Sridharan, A.H., *Appl. Polym. Symp.,* **26**, 135, 1975.

115. Henglein, A., *Makromol. Chem.,* **18**, 37, 1956.

116. Malhotra, S.L., *J. Macromol. Sci. Chem.,* **A18**, 1055, 1981.

117. Melville, H.W., *Trans. J. Plastics Inst.,* **23**, 146, 1955.

118. Allen, P.E.M., Downer, J.M., Hastings, G.W., Melville, H.W., Molyneux, P., Urwin, J.R., *Nature,* **117**, 910, 1956.

119. Fujiwara, H., Sasaki, K., Hochi, K., Goto, K., *Nippon Gomu Kyokaishi,* **52**, 247, 1979. [CA 91(2): 5525].

120. Fujiwara, H., Kimura, K., Mori, H., Goto, K., *Polym. J.,* **13(10)**, 927, 1981.

121. Fujiwara, H., Goto, K., *Polymer Bulletin,* **23**, 27, 1990.

122. Fujiwara, H., Goto, K., *Embi to Porima,* **21(4)**, 9, 1981.

123. Nakagawa, K., Kawase, S., Kakwai, T., *Kobunshi Ronbunshu,* **33**, 339, 1976 [CA 85(16): 109319].

124. Malhotra, S.L., Gauthier, J.M., *J. Macromol. Sci. Chem.*, **A18**, 783, 1982.

125. Fukotomi, T., Ishizu, K., Ooba, K., Kakwai, T., *Kobunshu Ronbunshu,* **40**, 719, 1983 [CA 100(12): 86193].

126. Chen, K., Shen, Y., Li, H., Xu, X., *Gaofenzi Tongxun,* **6**, 401, 1985 [CA 105(10): 79473].

127. Gong, X., Chen, K., Xu, X., *Huagong Xuebao,* **3**, 318, 1987.

128. Hu, X., Xu, X., *Huagong Xuebao,* **4**, 319, 1982 [CA 99(12): 88684].

129. Sakurai, M., Torika, Y., Negishi, K., *Seisan Kenkyu,* **23**, 272, 1971 [CA 76(10): 46568].

130. El'Piner, I.E., 'Ultrasound: Physical, Chemical and Biological Effects', Consultants Bureau, NY, 1964.

131. Lindstrom, O., Lamm, O., *J. Phys & Colloid Chem.*, , **55**, 1139, 1951.

132. Berlin, A.A., El'tsefon, B.S., *Khim. Nauka. Prom.*, **2**, 667, 1957.

133. Kruus, P., *Ultrasonics*, **21**, 201, 1983.

134. Kruus, P., Dupond, L.A., Patraboy, T.J., *Ultrasonics International,* 502, 1983.

135. Price, G.J., Daw, M.R., Newcombe, N.J., Smith, P.F., *British Polymer J.*, **23**, 63, 1990.

136. Price, G.J., Smith, P.F., West, P.J., *Ultrasonics,* **29**, 166, 1991.

137. Kopina, I.V., Korneeva, D.G., Kononenko, G.G., Malkes, L., *Deposited Doc., spstl khp-081,* 1981 [CA: 97: 145370].

138. Kopecy, K.R., Hall, M.C., *Can. J. Chem.*, **59**, 3090, 1981.

139. Miyata, T., Nakashio, F., *J. Chem. Eng. Jpn.*, **8**, 463, 1975.

140. Kruus, P., Patraboy, T.J., *J. Phys. Chem.*, **89**, 3379, 1985.

141. Donaldson, D.J., Farrington, M.D., Kruus, P., *J. Phys. Chem.*, **83**, 3130, 1979.

142. Billmeyer, F.W., 'Textbook of Polymer Science', John Wiley & Sons, 1984.

143. Flory, P.J., *J. Chem. Phys.*, **9**, 660, 1941.

144. Flory, P.J., *J. Chem. Phys.*, **10**, 51, 1942.

145. Huggins, M.L., *Ind. Eng. Chem.*, **35**, 216, 1943.

146. Huggins, M.L., *J. Am. Chem. Soc.*, **64**, 1712, 1942.

147. Bonner, D.C., *J. Macromol. Sci., Rev. Macromol. Chem.*, **C13**, 263, 1975.

148. Smidsrod, O., Guillet, J.E., *Macromolecules*, **2**, 272, 1969.

149. Patterson, D., Tewari, Y.B., Schreiber, H.P., Guillet, J.E., *Macromolecules*, **4**, 356, 1971.

150. Flory, P.J., *J. Chem. Phys.*, **17**, 223, 1949.

151. Krigbaum, W.R., Flory, P.J., *J. Am. Chem. Soc.*, **75**, 1775, 1953.

152. Flory, P.J., Krigbaum, W.R., *J. Chem. Phys.*, **18**, 1086, 1950.

153. Kok, C.M., Rudin, A., *J. Appl. Polym. Sci.*, **26**, 3575, 1981.

154. Kok, C.M., Rudin, A., *J. Appl. Polym. Sci.*, **26**, 3583, 1981.

155. Kok, C.M., Rudin, A., *J. Appl. Polym. Sci.*, **27**, 353, 1982.

156. Staudinger, H., Heuer, W., *Ber. Deutsch., Chem. Ges.*, **B63**, 222, 1930.

157. Huggins, M.L., *J. Am. Chem. Soc.*, **64**, 2716, 1942.

158. Alfrey, T., Justice, J.D., Nelson, S.J., *Trans. Faraday Soc.*, **B42**, 50, 1946.

159. Eirich, F., Riseman, J., *J. Polym. Sci.*, **4**, 417, 1949.

160. Streeter, D.J., Boyer, R.F., *Ind. & Eng. Chem.*, **43**, 1979, 1951.

161. Debye, P., Bueche, A.M., *J. Chem. Phys.*, **16**, 573, 1948.

162. Soloman, O.F., Ciuta, I.Z., *J. Appl. Polym. Sci.*, **6**, 683, 1962.

163. Palit, S.R., Kar, I., *J. Polym. Sci., A1*, **5**, 2629, 1967.

164. Deb, P.C., Chatterjee, S.R., *Makromol. Chem.*, **125**, 283, 1969.

165. Elliot, J.H., Horowitz, K.H., Hoodock, T., *J. Appl. Polym. Sci.*, **14**, 2947, 1970.

166. Rudin, A., Wagner, R.A., *J. Appl. Polym. Sci.*, **19**, 3361, 1975.

167. Rudin, A., Strathdee, G.B., *J. Paint. Technol.*, **46**, 33, 1974.

168. Kraemer, E.O., *Ind. Eng. Chem.*, 30, 1200, 1938.

169. Rudin, A., *J. Appl. Polym. Sci.*, **19**, 619, 1975.

170. Brandrup, J., Immergut, E.H., 'Polymer Handbook', Wiley Interscience, NY, 1975.

171. Tseng, H.S., Lloyd, D.R., *Polymer*, **25**, 670, 1984.

172. Fox, T.G., Flory, P.J., *J. Am. Chem. Soc.*, **73**, 1904, 1951.

173. Fox, T.G., Flory, P.J., *J. Phys. Chem.*, **46**, 151, 1942.

174. Kurata, M., Stockmayer, W.H., Riog, A., *J. Chem. Phys.*, **33**, 151, 1960.

175. Chee, K.K., *Polymer Commun.*, **27**, 135, 1986.

176. Chee, K.K., *Polymer*, **28**, 977, 1987.

177. Van Krevelen, D.W., 'Properties of Polymers', Elsevier, 1990.

178. Murayama, M., Okada, M., Fukutomi, T., Nose, T., *Makromol. Chem.*, **188**, 829, 1987.

179. Debye, P., *J. Phys. Coll. Chem.*, **51**, 18, 1947.

180. Zimm, B.H., *J. Chem. Phys.*, **16**, 1099, 1948.

181. Bauer, N., Leurin, S.Z., 'Physical Methods of Organic Chem.', **1(2)**, 1211, Interscience Pub. NY

182. Huglin, M.B., 'Light Scattering from Polymer Solutions', Academic Press, NY, 1972.

183. El'tsefon, B.S., Berlin, A.A., *Vyskomol Soedin*, **4**, 1033, 1962.

184. El'tsefon, B.S., Berlin, A.A., *Polym. Sci., U.S.S.R.*, **5**, 668, 1964.

185. Allen, G., Bevington, J.C., (Eds) Comprehensive Polymer Science, Pergamon Press, **1**, 175, 1989.

186. Barr, G., 'A Monograph on Viscometry', Oxford Univ. Press, London, 1931.

187. Schmid, G., *Z. Phys. Chem.*, **186**, 113, 1940.

188. Ovenall, D.W., Hastings, G.W., Allen, P.E.M., *J. Polym. Sci.*, **33**, 207, 1958.

189. Mostafa, M.A.K., *J. Polym. Sci.*, **22**, 535, 1956.

190. Chen, K., Chen, S., Xu, X., 33rd IUPAC International Symposium on Macromolecules, Conf. Proc., 1990.

191. Sato, T., Nalepa, D.E., *J. Appl., Polym., Sci.*, **22**, 865, 1978.

192. Jellinek, H.H.G., Degradation of Vinyl Polymers, Academic Press, NY, 1955.

193. Ballauff, M., Wolf, B.A., *Adv. Polym. Sci.*, **85**, 1989.

194. Atkins, P.W., Physical Chemistry, Oxford Univ. Press, 1982.

195. Casale, A., *J. Appl. Polym. Sci.*, **19**, 1461, 1975.

196. Adam, M., *J. Non-Crystalline Solids*, **131**, 773, 1991.

197. Gerrard, W., 'Gas Solubilities', Pergamon Press, 1980.

198. Murayama, M., Okada, M., Fukutomi, T., Nose, T., *Makromol. Chem.*, **188**, 829, 1987.

199. Zimm, B.H., Stockmayer, W.H., *J. Chem. Phys.*, **17**, 1301, 1949.

200. Casale, A., *J. Appl. Polym., Sci.*, **19**, 1461, 1975.

201. Odell, J.A., Keller, A., *J. Polym. Sci. Polym. Phys. Ed.*, **24**, 1889, 1986.

202. Nguyen, T.Q., Kausch, H.H., *Macromolecules*, **23**, 5137, 1990.

203. Odell, J.A., Muller, A.H., Narh, A., Keller, A., *Macromolecules*, **23**, 3092, 1990.

204. Price, G.J., Smith, P.F., Unpublished work, 1991.

205. Ebdon, J.R., 'New Methods of Polymer Synthesis', Chapman and Hall, 162, 1991.

206. Bamford, C.H., Jenkins, A.D., *Nature (London)*, **176**, 78, 1955.

207. Bamford, C.H., Jenkins, A.D., Wayne, R.P., *Trans. Faraday Soc.*, **56**, 932, 1960.

208. D.M.S. U.V. Atlas of Organic Compounds, Butterworths, 1971.

209. Burgess, F.J., Richards, D.H., *Polymer*, **17**, 1020, 1976.

210. Luston, J., Vass, S., *Adv. Polym. Sci.*, **56**, 91, 1984.

211. Franta, E., Reibel, L., Lehmann, J., Penczek, S., *J. Polym. Sci., Polym. Symp.*, **56**, 139, 1976.

212. Joyce, R.M., Handford, W.E., Harmon, J., *J. Am. Chem. Soc.*, **72**, 2213, 1950.